

Strain Rate Dependent Properties of Younger Human Cervical Spine Ligaments

by

Stephen Mattucci

A thesis

presented to the University of Waterloo

in fulfillment of the

thesis requirement for the degree of

Master of Applied Science

in

Mechanical Engineering

Waterloo, Ontario, Canada, 2011

©Stephen Mattucci 2011

AUTHOR'S DECLARATION

I hereby declare that I am the sole author of this thesis. This is a true copy of the thesis, including any required final revisions, as accepted by my examiners.

I understand that my thesis may be made electronically available to the public.

Stephen Frank Ernesto Mattucci

Abstract

The cervical spine ligaments play an essential role in limiting the physiological ranges of motion in the neck; however, traumatic loading such as that experienced in automotive crash scenarios can lead to ligament damage and result in neck injury. The development of detailed finite element models for injury simulation requires accurate ligament mechanical properties at relevant loading rates.

The objective of this research was to provide detailed mechanical properties for the cervical spine ligaments, by performing tensile tests at elongation rates relevant to automobile crash scenarios, using younger specimens (less than 50 years old), and to provide a comprehensive investigation of spinal level and gender effects.

The five primary ligaments (present between C2-T1) investigated were: the anterior longitudinal ligament, posterior longitudinal ligament, capsular ligament, ligamentum flavum, and interspinous ligament. The craniovertebral ligaments (Skull/C0-C2) investigated were the tectorial membrane/vertical cruciate/apical/alar ligament complex, transverse ligament, anterior atlanto-occipital membrane, posterior atlanto-occipital membrane, anterior atlanto-axial membrane, and posterior atlanto-axial membrane. Tests were performed within an environmental chamber designed to mimic *in vivo* temperature and humidity conditions, and specimens were preconditioned for 20 cycles at 10% strain prior to testing to failure. Ligaments were tested at quasi-static (0.5s^{-1}), medium (20s^{-1}) and high ($150\text{-}250\text{s}^{-1}$). These strain rates were predicted by an existing cervical spine finite element model under typical crash scenarios.

Two hundred sixty-one total primary ligament tests were performed, with approximately even distribution within elongation rate, spinal level, and gender. Another forty-four craniovertebral ligaments were tested. Results were plotted as force-displacement curves and the response characteristics determined from the curves were: failure force, failure elongation, stiffness of the linear region, toe region elongation, failure stress, failure strain, modulus and toe region strain. The measured force-displacement data followed expected trends when compared with previous studies. The younger ligaments had less scatter, and were both stiffer and stronger than the older specimens that were reported in previous studies at both quasi-static and comparable higher elongation rates.

Statistical analysis was performed on the results to establish significant effects. Strain rate effects were most significant whereas spinal level effects were not found. In general, gender effects were not found to be significantly different, but consistent trends were identified with male ligaments having a higher stiffness and failure force than female ligaments. The post-ultimate load region of the curves was reported to offer insight into the ligament failure mechanism.

The characteristic values obtained were used to develop average curves for each ligament, with the intention to eventually be directly integrated into finite element models to better represent the ligament structures. Curves were developed to incorporate the strain rate, spinal level and gender effects for each ligament based on the statistical analyses. Post-failure response was incorporated into these curves because this region has been shown to have an effect on neck behaviour in mathematical models.

Recommendations for future studies include measuring accurate cross sectional areas of ligaments during tensile testing to obtain true stress and true strain measurements to better understand if differences in mechanical properties are structural or material. Other possible improvements would be further testing of young cervical spine ligaments with larger sample sizes to further explore spinal level and gender effects. Additional testing performed under identical testing conditions as the current study would allow for pooling of the results effectively increasing the sample size.

Acknowledgements

There are several people I would like to thank who played a role in my life during my time at the University of Waterloo working on my masters, both at school and in my life outside of school (however non-existent it seemed at times).

I would like to thank my supervisors; Dr. Duane Cronin and Dr. Naveen Chandrashekar for their knowledge and guidance. They have introduced me to academic research and the entire process from identifying the problem to interpreting results, and shown me what it takes to produce valuable work.

I am happy to thank the Global Human Body Model Consortium (GHBMC) for providing the motivation and funding behind this project. This research would not have been possible without their support. Specifically I would like to thank Dr. Yibing Shi and Dr. Zine Ben Aoun for providing a valuable external opinion and helping to bridge the gap between industry and academia.

I would also like to thank my family; my parents, Kathy and Domenic, and sister Aly. Your unwavering support and unconditional love has always provided me with the extra push in times of need. My grandparents; Frank Ridler, and Theresa and Ernesto Mattucci. Your accomplishments in life have provided me with the opportunities I have had, and for that I am truly grateful.

Dedication

I would like to dedicate this work to my sister Aly Mattucci. The challenges you overcome on a daily basis make me believe that anything is possible. You provide me with more inspiration and motivation than you could ever know.

Table of Contents

AUTHOR'S DECLARATION	ii
Abstract	iii
Acknowledgements	v
Dedication	vi
Table of Contents	vii
List of Figures	xii
List of Tables	xv
Chapter 1 Introduction	1
1.1 Motivation for Research	1
1.2 Research Objectives and Approach.....	3
1.3 Thesis Outline.....	4
Chapter 2 Anatomy and Physiology	6
2.1 Anatomical Terminology.....	6
2.1.1 Anatomical Directions.....	6
2.1.2 Anatomical Sections and Planes.....	8
2.2 Vertebrae	9
2.2.1 Cervical Vertebrae.....	11

2.2.2 C1 Vertebra (Atlas)	15
2.2.3 C2 Vertebra (Axis)	16
2.3 Facet Joints	19
2.4 Intervertebral Disc	20
2.5 Cervical Spine Ligaments.....	24
2.5.1 Primary Cervical Spine Ligaments.....	25
2.5.2 Craniovertebral Ligaments	31
Chapter 3 Tissue Mechanics.....	36
3.1.1 Mechanical Properties	38
3.1.2 Ligament Mechanical Properties	42
Chapter 4 Literature Review: Mechanical Properties of Cervical Spine Ligaments.....	47
4.1 General Methodology.....	47
4.2 Quasi-Static Studies	49
4.3 High Deformation Rate Studies.....	54
4.4 Craniovertebral Ligament Studies.....	58
4.5 Limitations of Previous Isolated Ligament Studies.....	61
4.5.1 Age Limitations	62
4.5.2 Testing Conditions Limitations	63

4.5.3 Uninvestigated Effects.....	64
4.6 Relevant Findings from Segment and Whole-Spine Studies.....	66
4.6.1 Level Effects.....	66
4.6.2 Gender Effects.....	67
4.6.3 Craniovertebral Segment Studies	67
Chapter 5 Methods.....	70
5.1 Cadaver Morphology.....	70
5.2 Ligament Isolation and Preparation.....	71
5.2.1 Primary Cervical Spine Ligament Isolation	73
5.2.2 Craniovertebral Ligament Isolation.....	76
5.2.3 Ligament Preparation for Testing.....	78
5.3 Testing Methods.....	80
5.4 Data Processing	86
5.5 Statistical Analysis	90
5.5.1 Statistical Background.....	91
Chapter 6 Results of Younger Ligament Testing	97
6.1 Loading Rate Effects	98
6.2 Spinal Level Effects	102

6.3 Gender Effects	104
6.4 Craniovertebral Ligament Results	106
Chapter 7 Discussion of Ligament Testing	110
7.1 Rate Effects	112
7.2 Spinal Level and Gender Effects	112
7.3 Comparison with Previous Studies	114
7.4 Confounding Differences when Comparing with Previous Studies	119
7.5 Discussion of Craniovertebral Ligament Study	120
Chapter 8 Development of Average Curves	126
8.1 Average Curves for Rate Effects	127
8.2 Incorporating Spinal Level and Gender Effects into Average Curves	134
8.3 Addition of Post-Failure Response Region to Average Curves	140
8.4 Validation of Average Curve Development	142
8.5 Craniovertebral Average Curves	143
Chapter 9 Conclusions and Recommendations	148
9.1 Conclusions	148
9.2 Recommendations	150
Appendix A Raw Data Ligament Values	152

Appendix B Ligament Curves	172
References	194

List of Figures

Figure 2-1: Anatomical Directions	7
Figure 2-2: Anatomical Depth Terminology	7
Figure 2-3: Neck Movement	8
Figure 2-4: Anatomical Planes	9
Figure 2-5: Labeled Sections of Whole Spine.....	10
Figure 2-6: Typical Cervical Vertebra	12
Figure 2-7: Superior View of Cervical Spine Vertebrae	14
Figure 2-8: C1 (Atlas) superior view.....	15
Figure 2-9: C2 (Axis)	16
Figure 2-10: Anterior view of atlas, axis connection	17
Figure 2-11: Atlas rotating about the axis	18
Figure 2-12: Facet joints as seen from right medial view of cervical spine section.....	19
Figure 2-13: Facet joint cross section view	20
Figure 2-14: Intervertebral discs from lateral view of spinal column	21
Figure 2-15: Intervertebral disc	21
Figure 2-16: Compressive loading on intervertebral disc	22
Figure 2-17: Bending load on intervertebral disc.....	23
Figure 2-18: Primary cervical spine ligaments.....	25
Figure 2-19: Primary cervical spine ligaments (cross section sagittal view)	26
Figure 2-20: Posterior view of vertebral bodies and posterior longitudinal ligament	28
Figure 2-21: Nuchal and supraspinous ligaments, sagittal view	30
Figure 2-22: Craniovertebral ligaments, sectioned view from posterior	31
Figure 2-23: Craniovertebral ligaments, sectioned sagittal view	32
Figure 2-24: Transverse ligament attached to atlas, superior view	33
Figure 3-1: Ligament hierarchy structure.....	37
Figure 3-2: Stress/strain vs. time curves for stress relaxation and creep.....	39
Figure 3-3: Hysteresis nonlinear loading response.....	40
Figure 3-4: Preconditioning of an ACL (Fung, 1993; Viidik, 1973).....	40

Figure 3-5: Mechanical models used to represent viscoelastic behaviour	41
Figure 3-6: Stiffening behaviour of viscoelastic material under increasing strain rates	42
Figure 3-7: Loading of a ligament mechanically modeled by incremental loading of spring elements	43
Figure 3-8: Complete mechanical model for ligament behaviour (Viidik, 1973)	44
Figure 3-9: Ligament force-elongation curve loading regions	45
Figure 3-10: Collagen fibres straightening as ligament is loaded	46
Figure 4-1: Ligament length definitions (Yoganandan et al., 2000)	52
Figure 4-2: Rate effects on failure force and stiffness for ALL and LF (Yoganandan et al., 1989)	54
Figure 4-3: Split Hopkinson bar fixture used for high rate testing (Shim et al., 2005)	55
Figure 4-4: Temperature-dependent viscoelasticity of porcine spinal ligaments (Bass et al., 2007) ...	64
Figure 4-5: Couple moment in craniovertebral joint causing fracture due to increased tension on dens	68
Figure 5-1: Functional spinal unit without soft tissues removed.....	72
Figure 5-2: Cervical spine sectioned into FSU's two different methods	72
Figure 5-3: FSU cuts to isolate ligaments	73
Figure 5-4: Isolated cervical spine bone-ligament-bone complexes	74
Figure 5-5: Skull-C2 segment with TM complex isolated. A - Anterior view, with fractured C1. B- Posterior view of TM	77
Figure 5-6: Ligaments secured with hardware before potting.....	79
Figure 5-7: Ligament specimens half potted	79
Figure 5-8: Stiffness of 3/8" steel bolt using resin and cup potting method	80
Figure 5-9: Ligament cooling time of ALL and ISL in 23.3°C ambient room temperature	81
Figure 5-10: Force-time and elongation-time preconditioning loading cycles for typical ALL	82
Figure 5-11: Quasi-static tensile fixture	83
Figure 5-12: Quasi-static fixture: zoomed view of specimen.....	83
Figure 5-13: High-speed electromagnetic fixture.....	85
Figure 5-14: High-speed fixture: zoomed view of specimen in environmental chamber	86
Figure 5-15: Polynomial fit to loading region raw quasi-static data to eliminate noise (ALL)	87

Figure 5-16: Start of ligament engagement at zero slope (PLL shown).....	88
Figure 5-17: Typical ligament response with distinctive points shown (PLL)	90
Figure 5-18: Bilinear fit to loading region to define toe region (PLL).....	90
Figure 5-19: Hierarchal nested design of the experiment.....	92
Figure 6-1: Rate effect shown by example curves for CL (female, middle level). The most characteristic shape curve from each rate was chosen, to illustrate rate effects.	98
Figure 6-2: Strain rate effect on stiffness for primary ligaments.....	101
Figure 7-1: Age compared to failure force and stiffness of current and previous cervical spine ALL and PLL studies	115
Figure 7-2: Graphical comparison of ligament force-deflection curves between current study (750- 2500 mm/s) results at high strain rate and Ivancic et al. (2007) (620-830 mm/s).....	118
Figure 7-3: Comparison of failure force data between studies at quasi-static rates	122
Figure 7-4: Comparison of stiffness data between studies at quasi-static rates	122
Figure 7-5: Stiffness comparison between studies on logarithmic rate scale.....	124
Figure 8-1: Characteristic points used to develop average rate curves (ALL shown).....	129
Figure 8-2: Average rate effect curves for ALL.....	130
Figure 8-3: Average rate effect curves for PLL, CL, LF, and ISL.....	131
Figure 8-4: Average quasi static ALL curve with spinal level and gender scaled curves.....	139
Figure 8-5: Combined gender and spinal level average curves for quasi-static ALL	140
Figure 8-6: Post-failure normalized curve response for primary ligaments	141
Figure 8-7: Average craniovertebral curves	144
Figure 8-8: Post-failure normalized curve response for primary ligaments	146

List of Tables

Table 4-1: Sample size matrix (Yoganandan et al., 1998)	53
Table 4-2: Combined results for previous quasi-static ligament tests	53
Table 4-3: Combined results from high rate ligament tests (force, elongation, stiffness).....	57
Table 4-4: Combined results from high rate ligament tests (stress, strain, and modulus).....	58
Table 4-5: Average age and testing conditions of previous studies	58
Table 4-6: Craniovertebral ligament property summary (Myklebust et al., 1988; Pintar, 1986)	59
Table 4-7: Alar, transverse ligament properties at quasi-static and high rates (Shim et al., 2005)	60
Table 4-8: Alar and transverse ligament property comparison (Panjabi et al., 1998; Shim et al., 2005)	61
Table 5-1: Cadaver spine statistics	71
Table 5-2: Isolated ligaments by spinal level matrix.....	75
Table 5-3: Ligament length measurements (mm) by spinal level	76
Table 5-4: Craniovertebral ligament quantity and dimensions.....	78
Table 5-5: Average force difference to zero for ligament curves.....	88
Table 5-6: Example procedure of ANOVA for effects on stiffness of ALL	96
Table 6-1: Quantity of ligaments tested by type, gender, rate and spinal level.....	97
Table 6-2: Loading rate effects for cervical spine ligaments	100
Table 6-3: Spinal level effects for cervical spine ligaments.....	103
Table 6-4: Gender effects for cervical spine ligaments	105
Table 6-5: Quantity of craniovertebral ligaments tested by type, gender and rate	106
Table 6-6: Tensile properties of AAAM and PAAM	107
Table 6-7: Loading rate effects for craniovertebral ligaments	108
Table 6-8: Gender effects for craniovertebral ligaments.....	109
Table 7-1: Comparison of data from current study to literature, grouped by comparable elongation rates	116
Table 7-2: Anticipated effects of experimental factors on results from current study contributing to a difference between previous studies.....	120
Table 7-3: Comparison of data from current study to literature, at quasi-static rates	121

Table 7-4: Comparison of data from current study to literature, at high rates	123
Table 8-1: Correction method for medium rate values outside quasi-static high rate bounds, shown for ISL (Toe Region).....	127
Table 8-2: Average values for toe region force and traumatic force ratio.....	128
Table 8-3: Average curve values for rate effects.....	132
Table 8-4: Spinal level effect ratios to average values	134
Table 8-5: Gender effect ratios to average values	135
Table 8-6: Average curve scaling factors for effects.....	136
Table 8-7: Spinal level and gender effect scaling factors for average curves	138
Table 8-8: Post-failure normalized values for primary ligaments	142
Table 8-9: Quantity of specific instance values to fall within standard deviations of raw data results	143
Table 8-10: Average curve values for craniovertebral ligaments.....	145
Table 8-11: Post-failure normalized values for craniovertebral ligaments	147

Chapter 1

Introduction

1.1 Motivation for Research

The cervical spine is the most frequently injured region of the spine during automobile crash events (Yoganandan et al., 1989). The ligaments of the cervical spine provide a significant contribution to the dynamic response of the neck in such vehicle crash scenarios (Yoganandan et al., 2001), where victims are predominantly young males with mean age of 37.8 years old (Robertson et al., 2002). Damage to these ligaments has been associated with injuries, such as neck strain (Webb et al., 1976; Harris et al., 1992) and whiplash associated disorders (Panjabi et al., 1998; Tominaga et al., 2006; Ito et al., 2004). The mechanical properties of the cervical spine ligaments are needed for a younger population, at relevant strain rates, for more accurate predictions of head/neck kinematic response and the prediction of injury using detailed finite element models. Dynamic response and injury predictors in such models are sensitive to material property changes of the soft tissues (Kumaresan et al., 1999), stressing the importance of accurate ligament properties for this application.

Soft tissues, including the ligaments, have been shown to exhibit viscoelastic or rate-dependent properties (Frisen et al., 1969; Viidik, 1973; Yoganandan et al., 2001; Troyer et al., 2011). The material properties used in finite model applications must be representative of the appropriate ligament deformation rate. Therefore, experimental tests must be performed at appropriate test speeds to measure relevant data.

Cervical spine ligaments can be subjected to deformations greater than the physiological range of motion in frontal impacts as low as 4g (Panjabi et al., 2004); where a 4g impact approximately corresponds to an impact velocity of 12 km/h (Cappon et al., 2003). Soft tissue injury threshold, as defined by a significant increase in flexibility (neutral zone range of motion), was found to occur at 8g frontal impacts (Pearson et al., 2005). Injury threshold has been identified as even lower for rear impacts, where significant increase in flexibility was seen at 5g accelerations on whole cervical spine specimens tested with muscle force replication (Ito et al., 2004).

A number of studies have been conducted on isolated cervical spine ligaments to identify tensile behaviours ranging from quasi-static strain rates (Myklebust et al., 1988; Chazal et al., 1985; Przybylski et al., 1996; Yoganandan et al., 1998; Yoganandan et al., 2000) to high strain rates (Yoganandan et al., 1989; Ivancic et al., 2007; Bass et al., 2007; Shim et al., 2005). This data has provided an excellent background on cervical spine ligament behavior. However, it has been shown that mechanical properties of the spine deteriorate with increasing age (Pintar et al., 1998; Cowin et al., 2007; Neumann et al., 1992; Neumann et al., 1994; Iida et al., 2002; Tkaczuk, 1968; Nachemson et al., 1968), and existing ligament data has only been reported from cadaver specimens ranging from the youngest of 55 ± 5 years (Chazal et al., 1985) to the oldest of 81 ± 11 years (Ivancic et al., 2007). It was also noted that the range of strain rates in the literature did not fully capture the range of strain rates anticipated in automotive crash scenarios. Furthermore, Bass et al. (2007) have shown that simulating *in vivo* conditions can have a significant influence on ligament response. Importantly, post-ultimate load response has never been reported prior to the present study, and is of interest as post ultimate load response has been shown to have a significant influence on cervical spine segment response in mathematical models (DeWit et al., 2010).

The ligaments of the craniovertebral joint have very specific functions, and complex anatomy. Data values for determining material properties of these ligaments are very limited, because very few studies have tested isolated craniovertebral ligaments (Myklebust et al., 1988; Panjabi et al., 1998; Shim et al., 2005). These material properties are important because the craniovertebral regions of the spine are the most common sites of trauma in fatal spinal injuries occurring from motor vehicle accidents (Yoganandan et al., 1989). Previous finite element model studies have also noted that improvements are needed for ligament properties in the craniovertebral region (Panzer, 2006).

Due to relatively small sample sizes in previous studies, a comprehensive investigation of gender and spinal level effects at strain rates applicable to automotive crash scenarios has also not been possible. One study compared gender and spinal level and found no significant effects (Bass et al., 2007), but sample sizes were relatively small. Yoganandan et al. (1998, 2000) evaluated the effect of spinal level but the results were limited to two regions (middle and lower), rather than individual level effects. Numerical models have shown that under loading cases, the distractions and forces seen at

each spinal level vary (Stemper et al., 2006), and this suggests the importance that ligaments at each spinal level are modeled accurately. Several segment and whole cervical spine studies have reported gender (Pintar et al., 1995; Ferrario et al., 2002; Stemper et al., 2003; Pintar et al., 1998; Nightingale et al., 2007) and spinal level differences (Shea et al., 1991; Nightingale et al., 2002), or recommended further investigation in those areas (Pintar, 1986; Van Ee et al., 2000).

1.2 Research Objectives and Approach

The objective of this research was to provide a more complete and accurate data set for determining the mechanical properties of cervical spine and craniovertebral ligaments. This data set was taken from a younger population, and would examine the significance, of deformation rate, spinal level, and gender, thus supporting the development of detailed cervical spine models. As part of the Global Human Body Model Consortium (GHBMC), the data obtained will be used to develop a biofidelically advanced finite element model of the human body.

A specific experimental testing approach was implemented in order to obtain the required data. Initially, existing finite element models were used to determine the deformation rates observed in the ligaments under external loading representative of vehicle crash events. By developing a complete set of data from one laboratory, variations due experimental procedure are reduced (Pintar et al., 1992). This variation is difficult to represent when combining or comparing data from different studies without reducing the fidelity of the modelling. Each ligament was tested at three different loading rates that encompass the range of rates seen in the model.

Cadaver specimens under the age of 50 years old were procured in order to provide data for a younger population. An upper limit of 50 years old was placed on cadaver spines used in the present study as osteoporosis has been shown to occur more often at the age of 50 and above (Kanis et al., 1994; Vernon-Roberts et al., 1973), and ligament properties have been shown to be correlated with bone mineral content (Neumann et al., 1994). This range also ensured a sufficient quantity of spines, as uninjured cervical spines are more difficult to acquire from the tissue banks under the age of 40.

Ligaments were carefully isolated from the spines with bone attachment points intact, into bone-ligament-bone complexes to be tested *in situ*, and kept moist throughout the procedure using saline spray. Bone segments were potted using a casting resin into plastic cups which were compatible with testing fixture gripping mechanisms. Specimens were tested in tension in an environmental chamber to mimic *in vivo* conditions. Ligaments were preconditioned before testing to failure. Force-deflection plots were produced for each test.

Characteristic points from each ligament force-deflection curve, such as failure force, failure elongation, stiffness, and the end of the toe region, were measured and compiled. A statistical analysis was performed on the data to determine if any rate, spinal level or gender effects were present.

Average curves were developed for each ligament for each using the characteristic points measured. Scaling factors were developed to be applied to each average curve based on specific spinal level and gender effects. The scaling factors were based on the different mean values and weighted by significance of the effect. The post-failure response region was also included in the average curves to provide a complete set of mechanical properties to be included in cervical spine finite element models.

1.3 Thesis Outline

The second chapter provides a brief background to the anatomy and physiology of the neck. The chapter examines the structures of the vertebrae, facet joints, intervertebral discs and ligaments, and the role they play in normal physiological function of the cervical spine.

The third chapter focuses on biological properties, including soft tissue mechanics and characteristics and analogous mechanical models. The behaviour and mechanical properties of ligaments are introduced, including viscoelastic effects.

Chapter four provides a detailed literature review of previous cervical spine studies. The methodology of previous studies performed on isolated cervical spine ligaments at both quasi-static and high strain rates is investigated. Limitations of other studies were outlined as they were

imperative in providing the direction of this research. Lastly, relevant findings from previous studies on whole and segment cervical spine studies were highlighted as possible areas of interest for isolated ligament tests that had not been explored in enough detail prior to this study.

The methodology of this research is found in chapter five. Detailed information is provided on the cadaver dissection and ligament preparation for testing, as well as the experimental methods used. This chapter also includes the data processing and statistical analysis procedure.

The detailed results are presented in chapter six. Results from the tests are categorized into loading rate, spinal level, and gender effects. Trends are highlighted in colour and statistical significance values are presented.

The seventh chapter includes the discussion of the results found in the current study and which factors had an effect on the ligament properties. Results from the current study were also compared to results from previous studies in this chapter.

Chapter eight presents the detailed procedure of how the characteristic values from the results were used to develop average curves. Average curves are shown for all ligaments with rate effects, and incorporation of spinal level and gender effects where applicable. The post-failure response region of the curve was formatted to be added to each average curve.

The ninth and final chapter provides a summary of the research and conclusions of the findings. Recommendations for improvement on future isolated cervical spine ligament studies are also shown here.

Chapter 2

Anatomy and Physiology

Before injury mechanisms of the cervical spine can be investigated, one must have a sufficient understanding of the anatomy and physiology of the proper functioning neck. Anatomy is the study of the structure and layout of biological tissue within the body, and physiology is the study of the normal functioning of the components of the human body (Silverthorn, 2010). In order to understand the cervical spine, the separate components must be understood and how they interact and function together as a system.

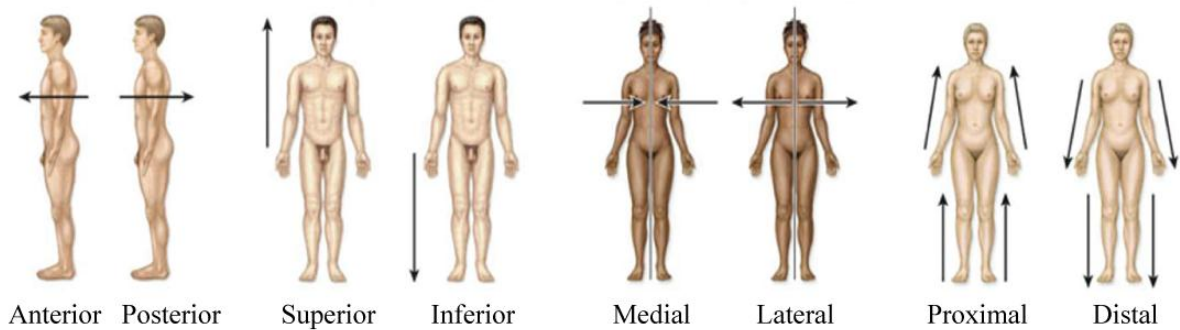
The components of the cervical spine that are relevant to this research are the vertebrae, intervertebral discs, facet joints, and ligaments. The vertebrae are the hard tissue structures (bone) of the neck, and the intervertebral discs provide a direct connection between the vertebral bodies to form the vertebral or spinal column (McKinley et al., 2008). The ligaments and facet joints restrict movement of the spine to prevent injury, and allow the spine to perform as a structural support for the human body.

2.1 Anatomical Terminology

There are specific terms used to describe orientations and directions when discussing human anatomy. These terms prevent confusion and provide easy communication of descriptions and ideas. These terms are preferred to describe positions and orientation of each body part relative to another without having to use terms that depend on orientation or view (McKinley et al., 2008). Terms such as ‘up’ and ‘down’ or ‘front’ and ‘back’ rely entirely on the orientation of the viewer.

2.1.1 Anatomical Directions

The directions when describing orientations of body components are universal and describe directions away and toward the body (Figure 2-1).



Adapted from McKinley, et al.(2008)

Figure 2-1: Anatomical Directions

Relative to the front (chest) or rear (back), anterior is toward the front surface, and posterior is toward the back surface. For example the heart is located anterior to the spine. Relative to the top (head) and bottom (feet), superior is toward the top and inferior is toward the bottom. An example is the knees are inferior to the stomach. Relative to the centerline of the body (through the nose and belly button), medial is towards the center and lateral is away from the center. For example, the shoulders are located laterally from the heart. When describing extremities such as the arms and legs, proximal is towards the body and distal is away from the body. For example the fingers are distal to the elbow.

There are specific terms to describe depth relative to the surface (Figure 2-2). Superficial is on the surface, deep is in the center and intermediate is in the middle.

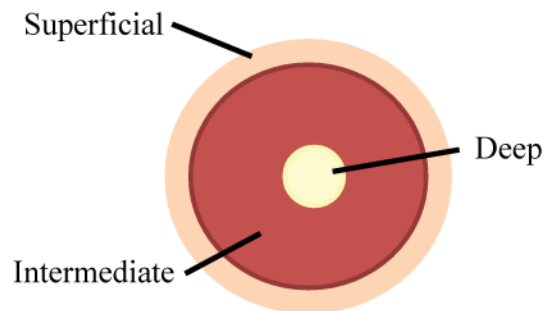


Figure 2-2: Anatomical Depth Terminology

Specific terminology is also used to describe neck movement as well. Flexion is looking downward, extension is looking upward, lateral bending is tilting the head to one side and axial rotation is twisting or looking to one side.

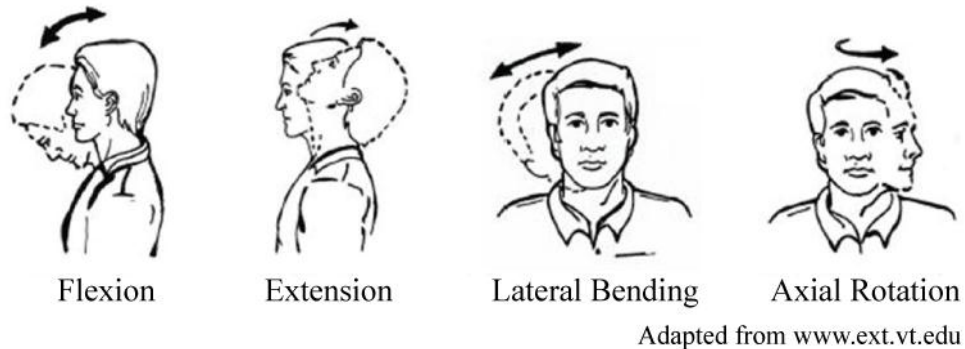
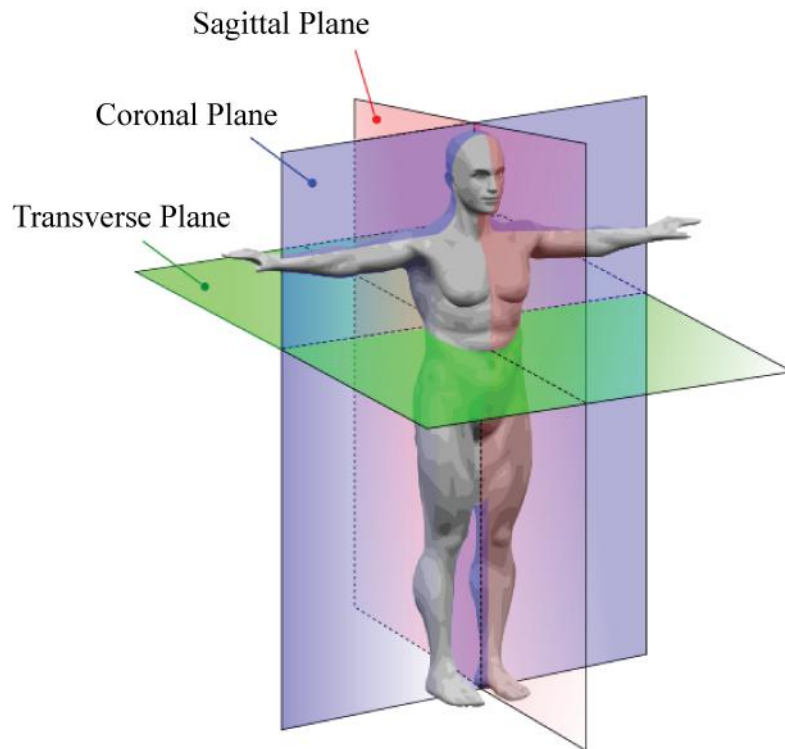


Figure 2-3: Neck Movement

2.1.2 Anatomical Sections and Planes

The body can be sectioned into three different planes for ease of description (Figure 2-4). The planes define the orientation or the section of body. These planes are known as the sagittal (or medial), coronal, and transverse. The sagittal plane divides the body into left and right sections, the coronal plane divides the body into anterior and posterior sections, and the transverse plane divides the body into superior and inferior sections. It is often most useful to view vertebrae in the transverse plane to see differences between each vertebral body at each level. The planes are not restricted to pass through the center of the body in each case, but when they do they are known as a mid-plane, such as midsagittal plane for example.



Adapted from www.makehuman.org

Figure 2-4: Anatomical Planes

2.2 Vertebrae

The vertebrae are the bony structures that make up the spine, comprised of 24 vertebrae, plus the sacrum. The spine is divided into 4 distinct regions; cervical, thoracic, lumbar and sacral (Figure 2-5). The cervical spine contains the top seven vertebrae known as C1 through C7 and is considered the ‘neck’ portion of the spine. There are twelve thoracic vertebrae, T1 to T12, which are the vertebrae that support and are connected to the ribs. Since they are connected to the rib cage they have relatively limited range of motion preventing twisting of the thoracic spine (McKinley et al., 2008). The lumbar spine contains only five vertebrae, L1 through L5, and is often referred to as the lower back region. The sacrum is five vertebrae fused together into one piece. The sacrum is also commonly known as the ‘tailbone’. Each vertebra differs at each spinal level showing distinct

anatomical characteristics and physiological functions. The cervical spine is the focus of this research and will be the only region analyzed in detail.



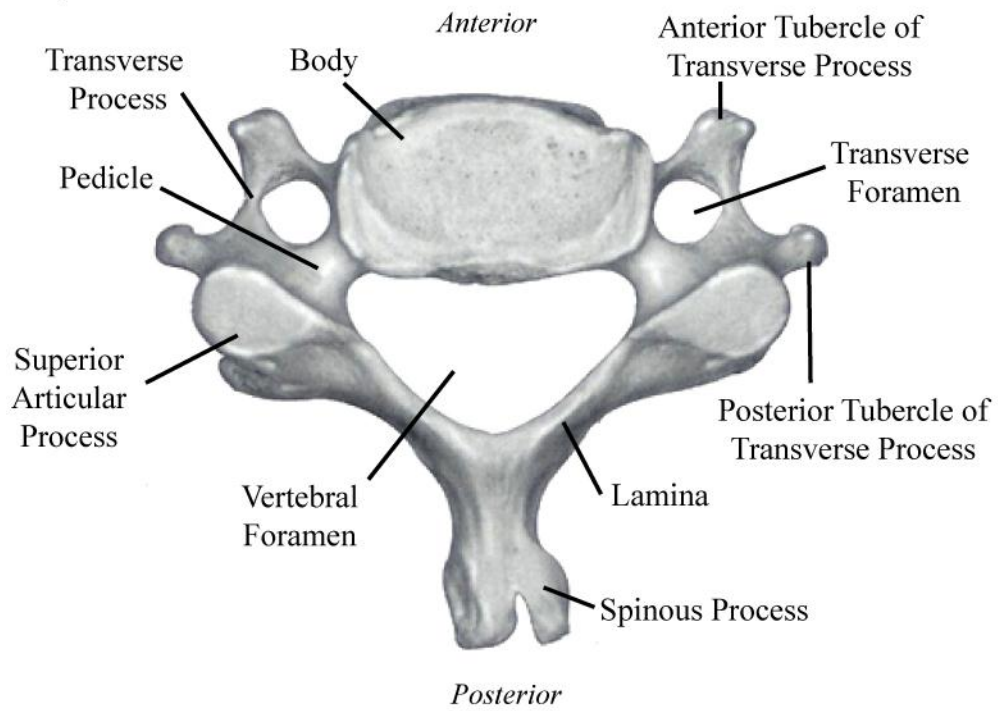
Adapted from www.dorightforyourself.org

Figure 2-5: Labeled Sections of Whole Spine

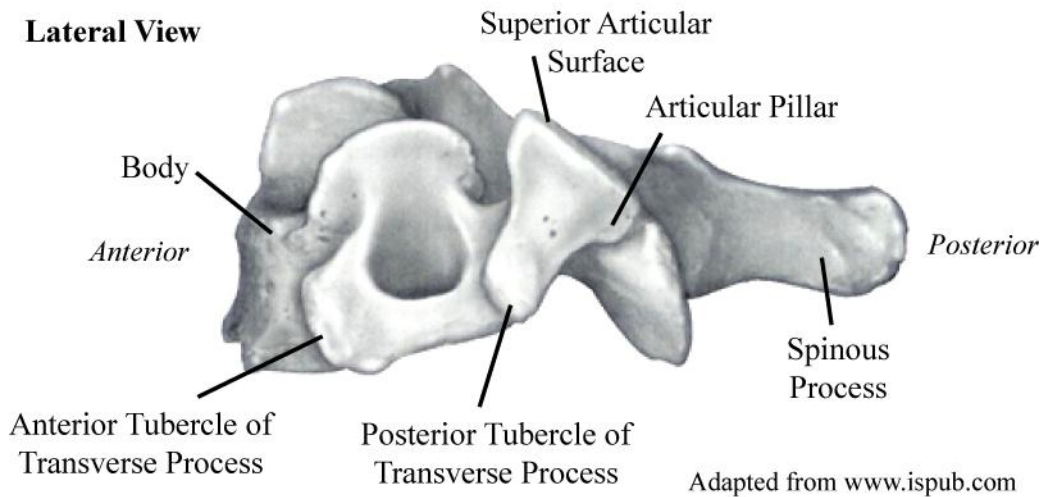
2.2.1 Cervical Vertebrae

A cervical vertebra has very distinct features as seen in Figure 2-6. The main functions of each vertebra are to support the load of the head and restrict movement to protect the spinal cord. The *vertebral body* is the largest bony section. It is comprised of cortical bone on the superficial surface and cancellous bone beneath. The *lamina* and the *spinous process* form the *vertebral arch*, and in conjunction with the posterior surface of the vertebral body, they form the gap known as the *vertebral foramen*. The vertebral foramen of each vertebra aligns to form a canal which protects the spinal cord, known as the *vertebral canal* (Moore et al., 1999). Since the spinal cord is very delicate this canal must keep its shape and integrity to prevent spinal cord damage.

Superior View



Lateral View

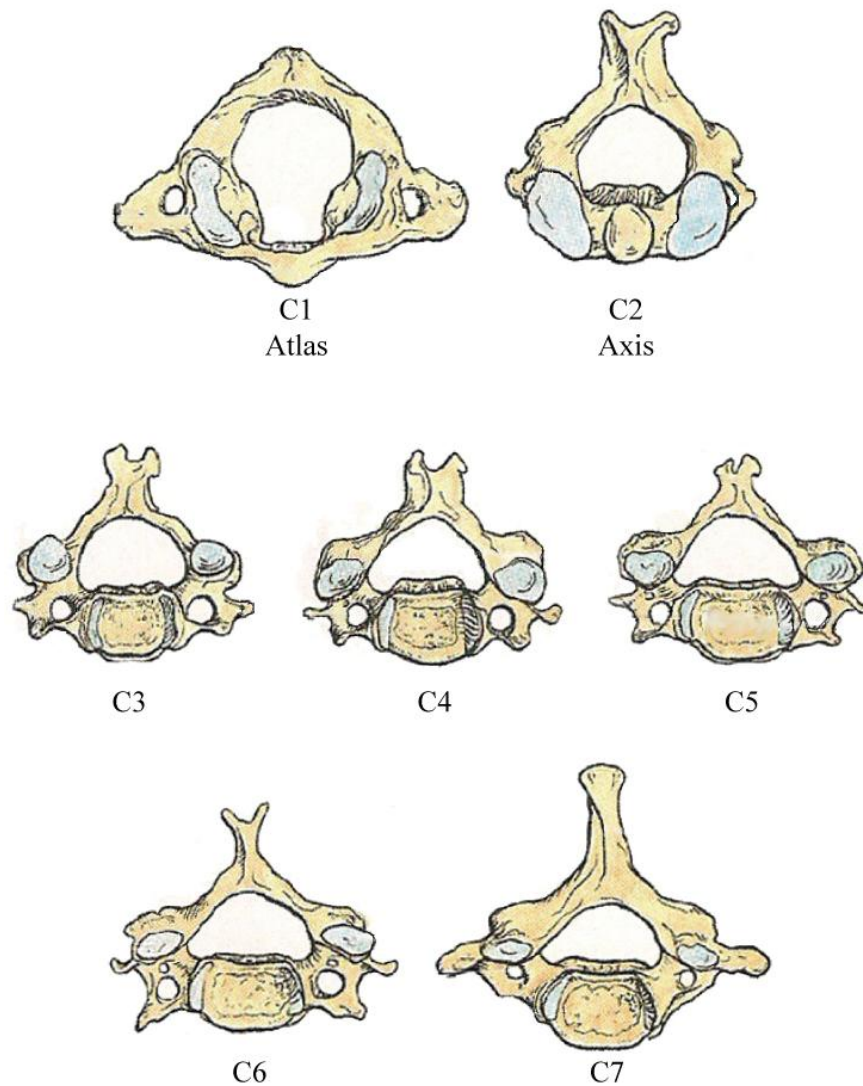


Adapted from www.ispub.com

Figure 2-6: Typical Cervical Vertebra

A 'process' is a bony protrusion from the vertebrae. The various processes are attachment points for ligaments to restrict motion, or for muscles and tendons to initiate motion. The spinous process is the most posterior process and helps to restrict excessive torsion and flexion of the spinal column. The superior and inferior articular processes are the connection points of the facet joints. The transverse process is made up of an anterior and posterior tubercle, and small round nodules. Aside from the vertebral, the other foramina are the transverse, located laterally from the vertebral body. The transverse foramina are unique to the cervical spine. Their function is to allow the vertebral arteries and veins to pass.

The cervical spine has seven vertebrae, C1 through to C7. C1 and C2 are the most unique and are also known as the atlas and axis respectively. C3 through C7 are very similar and only show subtle changes with each level as seen in Figure 2-7.



Adapted from Agur and Dalley (2005)

Figure 2-7: Superior View of Cervical Spine Vertebrae

The transverse foramen, where the vertebral arteries and veins pass, are only present in the cervical vertebrae, and are occasionally absent in C7. The anterior tubercles of the transverse process on C6 are known as the carotid tubercles, because the carotid arteries run along the anterior surface of the bone and can be pressed against the bone to control bleeding if lacerated.

2.2.2 C1 Vertebra (Atlas)

The most superior vertebra, C1, is also known as the atlas. It was named after the mythological Greek figure Atlas, who supported the earth on his shoulders (Moore et al., 1999). The C1 atlas similarly supports the weight of the head. The atlas is a ring shaped bone, and is the widest of the cervical vertebrae (Figure 2-8). It has two kidney shaped, concave superior articular surfaces that support the occipital condyles of the skull; two large protuberances at the sides of the foramen magnum at the base of the skull. The weight of the skull is transmitted through these articular surfaces. Since the surfaces are concave, and support the convex occipital condyles, they allow the head to nod up and down in extension and flexion. The atlas does not have a spinous process, but instead has anterior and posterior arches. The right superior surface of the posterior arch contains a groove for the vertebral artery. The interior surface of the anterior arch contains a facet in which the dens (odontoid process) of C2 rests against.

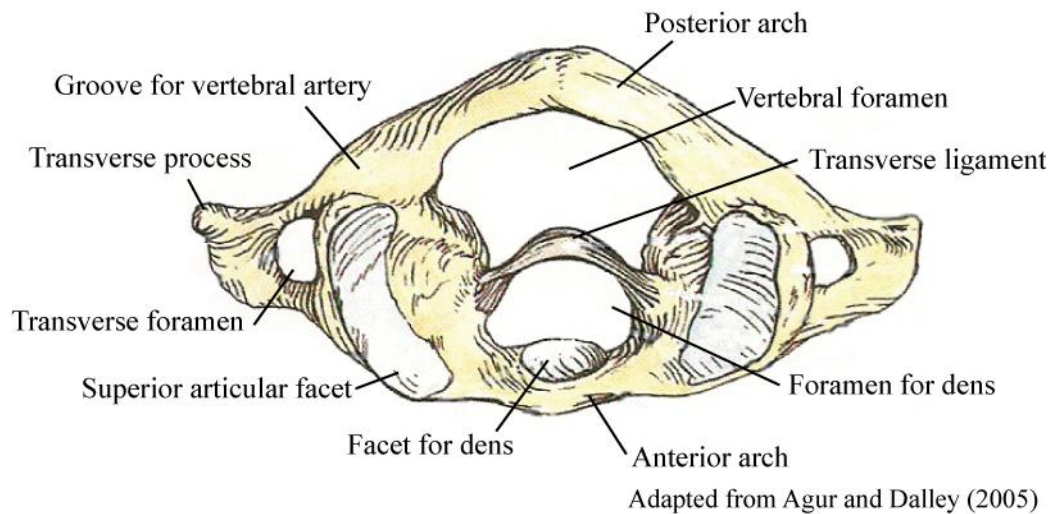
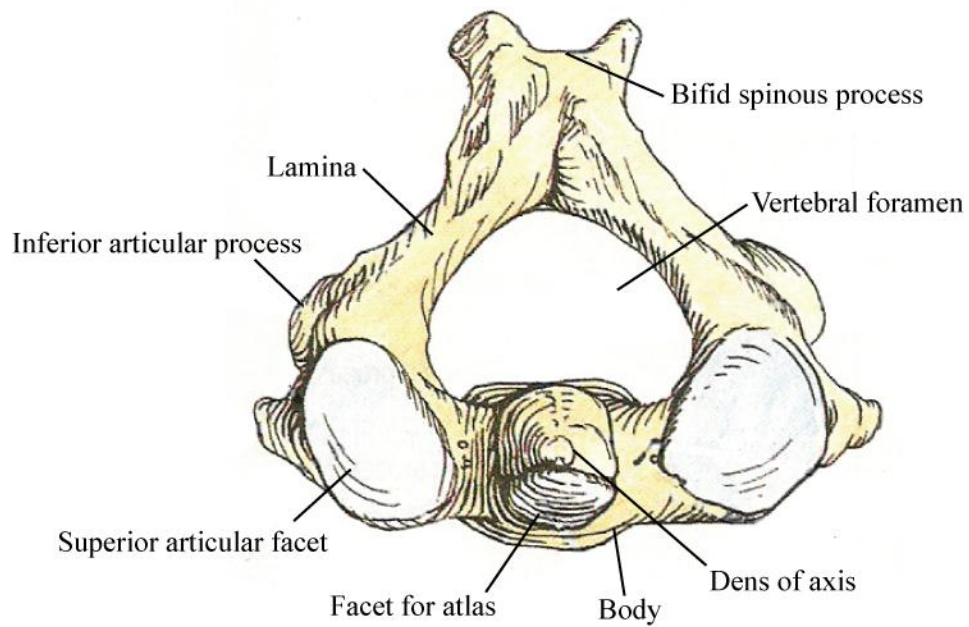


Figure 2-8: C1 (Atlas) superior view

2.2.3 C2 Vertebra (Axis)

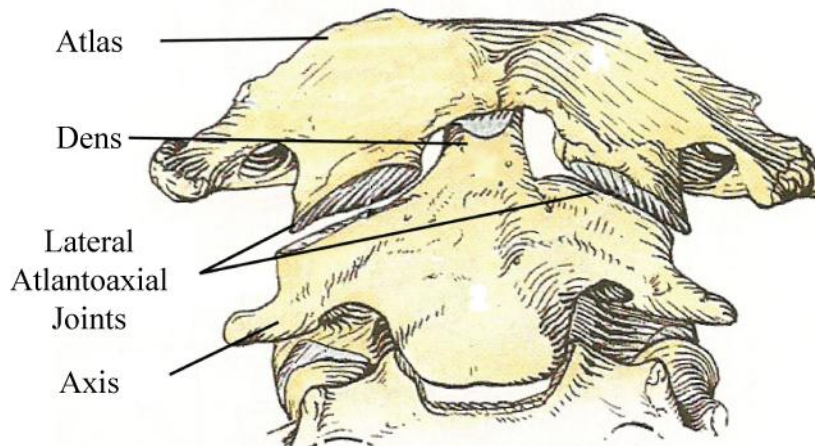
The second vertebra in the cervical spine, C2 is also known as the axis. It is called the axis because it allows rotation of the head, as C1 which carries the skull, rotates on C2. Like the atlas, the axis has two superior articular facets on which the axis rotates (Figure 2-9), where it is connected to C1 by the lateral atlantoaxial joints. The most unique feature of the C2 vertebra is the dens, or odontoid process, which is a blunt and bony protrusion that extends superiorly from the vertebral body into the foramen of the atlas. The dens provides a pivot for which the atlas rotates about. The dens is held in place by the transverse ligament as seen in Figure 2-8, which prevents displacement in the transverse plane.



Adapted from Agur and Dalley (2005)

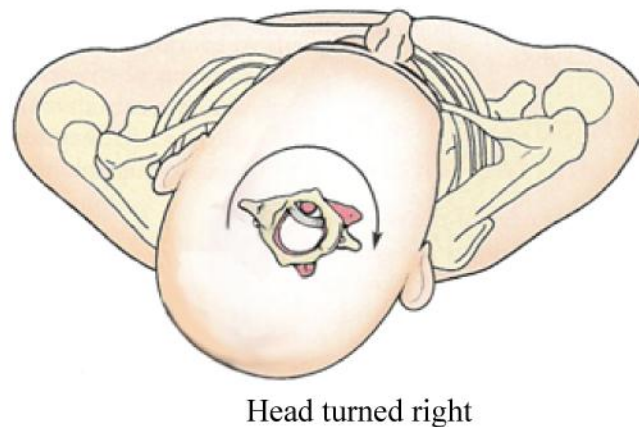
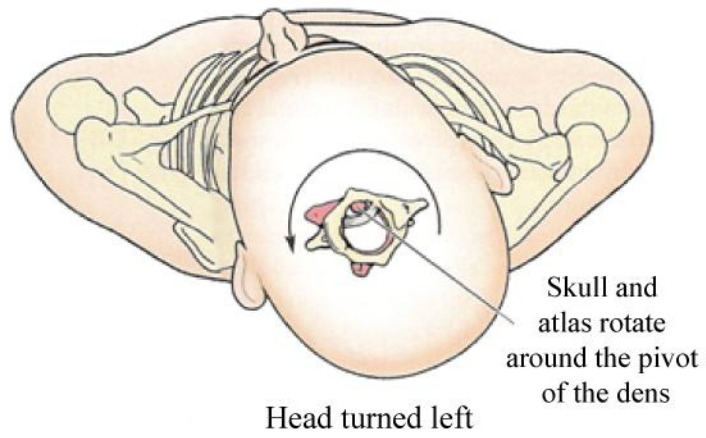
Figure 2-9: C2 (Axis)

The atlas and axis are connected as seen in Figure 2-10. The atlas can rotate on top of the axis by sliding at the lateral atlantoaxial joints. The dens extends superiorly into the foramen of the atlas to act as a pivot point, which the whole head rotates about (Figure 2-11). The axis stays in the same relative position to the other vertebrae, as the atlas rotates inferior to it. It can also easily be seen that the dens is held against the facet of C1 by the transverse ligament.



Adapted from Agur and Dalley (2005)

Figure 2-10: Anterior view of atlas, axis connection



Adapted from Agur and Dalley (2005)

Figure 2-11: Atlas rotating about the axis

2.3 Facet Joints

Facet joints, also known as zygapophysial joints, are pairs of joints, located posterior laterally to the vertebral bodies as seen in Figure 2-12. The joints are present symmetrically on the left and right of the vertebral body. Each vertebra has four facet joints connected to it: two superior and two inferior, which are located two each on the left and right. The facets are oriented at approximately 45 degrees from the transverse plane in the cervical spine, but the orientation differs along the length of the spinal column. The facet joints have a smaller angle from the transverse plane in the cervical spine compared to the thoracic and lumbar spine.

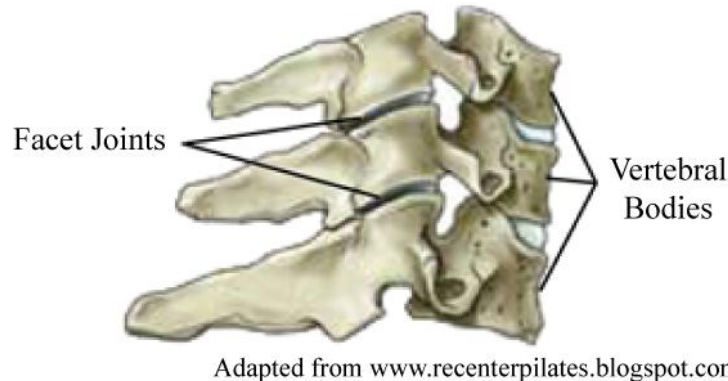
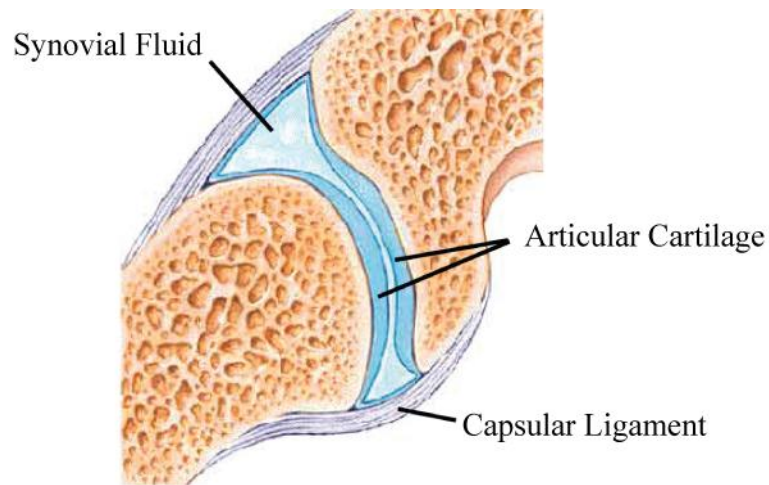


Figure 2-12: Facet joints as seen from right medial view of cervical spine section

Facet joint shape and orientation help to determine the patterns of movement which the spine can undergo (White et al., 1990). They prevent the spine from moving in excessive flexion, extension or rotation. Facet joints are synovial joints; joints that allow movement between two bones, sliding in this case. Synovial joints contain two articulating surfaces covered in articular cartilage to allow for contact and movement (Figure 2-13). The joints are surrounded by capsular ligament, which holds the surfaces together under tension. The capsular ligament also acts to contain synovial fluid within the capsule to act as lubrication. When the vertebral segments move in extension or rotation, the articular cartilage makes contact, and the surfaces glide over each other, gently limiting motion.

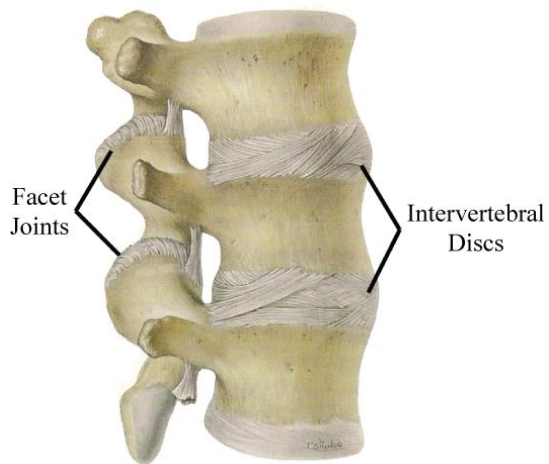


Adapted from www.umm.edu/spinecenter/education/

Figure 2-13: Facet joint cross section view

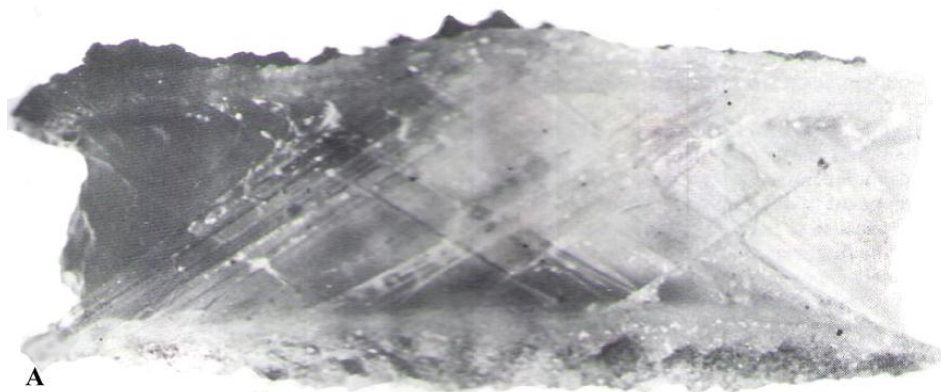
2.4 Intervertebral Disc

The intervertebral discs are located between the vertebral bodies along the spinal column, as seen in Figure 2-14. The discs are responsible for supporting the compressive loading on the spine (White et al., 1990). The disc is made up of three parts: nucleus pulposus, annulus fibrosis, and the cartilaginous endplates. The nucleus pulposus is the fluid-like substance in the centre of the disc, and the annulus fibrosis is made up of layers of fibrous collagen bands and fibrocartilage that surround the nucleus and connect the cartilaginous endplates and adjacent vertebral bodies (Figure 2-15B). The nucleus is comprised of mostly water, where the water content is highest at birth and slowly degenerates with age (Moore et al., 1999). The fibers of the annulus are oriented in the same direction within one layer of a band, at approximately a 30° angle from the transverse plane (Figure 2-15C), but from the opposite direction of the endplate in the adjacent bands (a -30° angle, or 120° from each other).

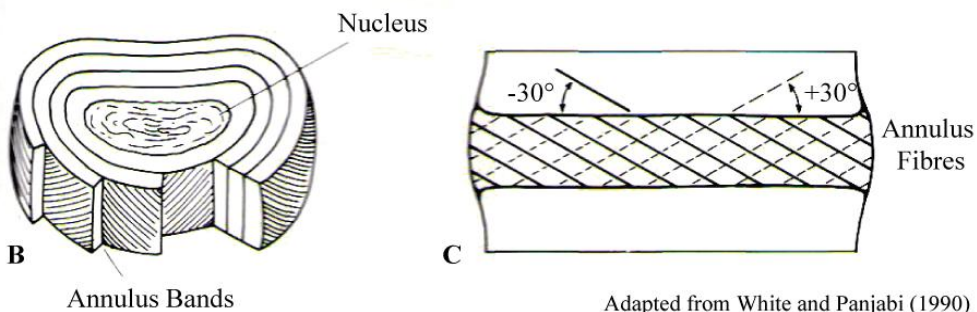


Adapted from Moore and Dalley (1999)

Figure 2-14: Intervertebral discs from lateral view of spinal column



A



B

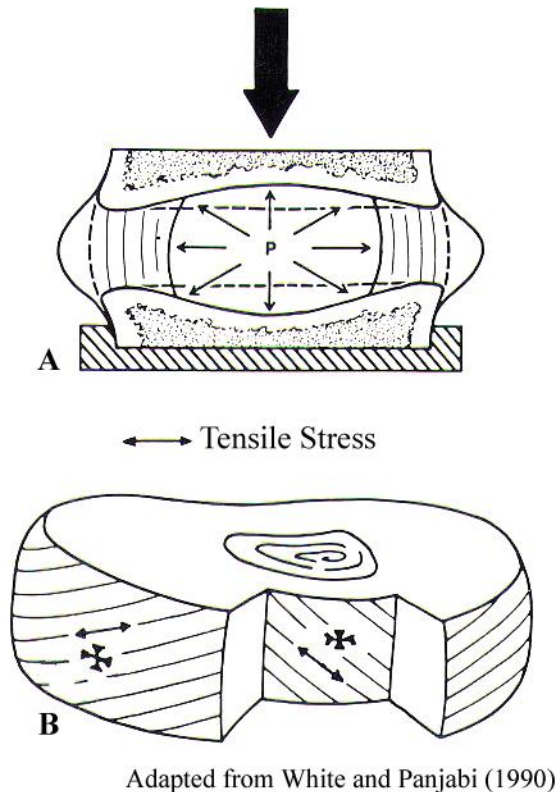
C

Adapted from White and Panjabi (1990)

Figure 2-15: Intervertebral disc

Photograph of disc fibers (A), nucleus surrounded by annulus bands (B), fiber orientation at $\pm 30^\circ$ from the endplates (C)

When a compressive load is applied to the spine, the disc is responsible for transferring the load between adjacent vertebrae (White et al., 1990). When the load is applied, the nucleus becomes pressurized and causes the endplates to deform and the annulus to bulge outwards (Figure 2-16A), putting the fibers under tension (Figure 2-16B).



Adapted from White and Panjabi (1990)

Figure 2-16: Compressive loading on intervertebral disc

Pressure increasing in nucleus under loading (A), fibers under tensile stress due to pressurization of the nucleus (B)

When the disc undergoes bending, it experiences both tension and compression as seen in Figure 2-17. In this case only the side under compression experiences a bulge in the disc. Studies have shown when a vertebral segment is subjected to a concurrent compressive and lateral bending loads; the disc experiences the largest bulge in the posterolateral direction (White et al., 1990). Since the

vertebral canal is posterior to the disc, the spinal cord is in very close proximity to a bulging disc. It has been hypothesized that a simultaneous bending and compressive load on the spine could cause a bulge that would result in low back pain due to the contact of the disc against the nerve roots of the spinal cord during motion (Breig, 1978). The disc has also been shown to bulge more when it has degenerated over time, losing hydration and strength properties (Reuber et al., 1982).

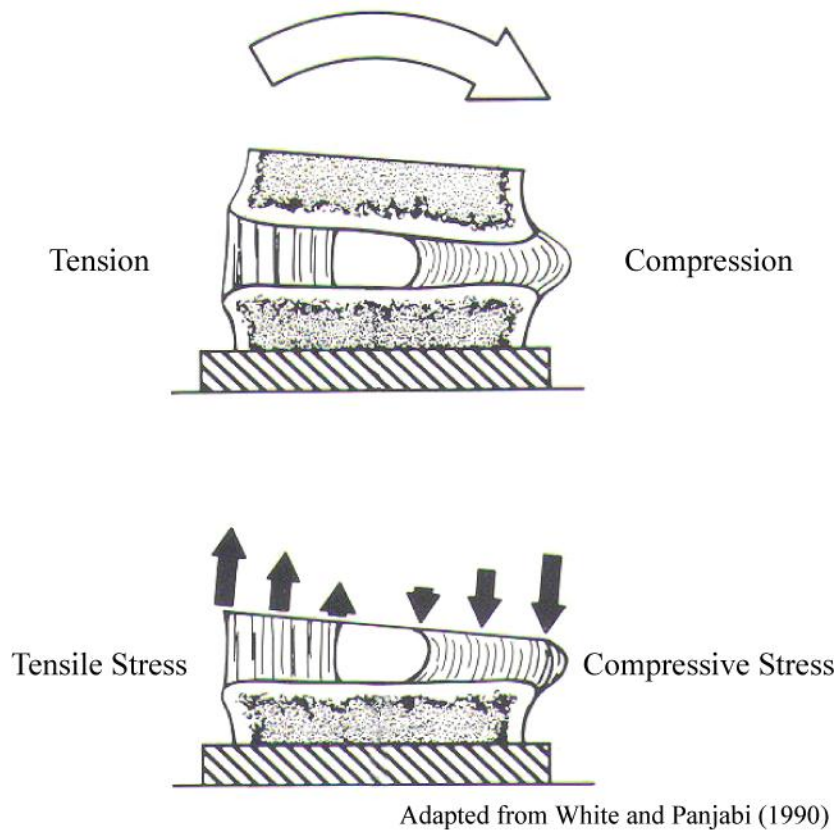


Figure 2-17: Bending load on intervertebral disc

The spaces between the vertebral bodies from C3 to C6 have a unique feature called uncovertebral joints, or Luschka's joints (Hayashi et al., 1985). They exist between the bony lips that project from the superior vertebral body inferiorly, toward the bony lips, also known as uncinete processes, that project superior from the inferior vertebral body (Moore et al., 1999). The lips are on the

posterolateral edge of the vertebral endplate. They are structures with capsules filled with fluid and are covered in cartilage. The main role of these joints is to regulate the movement of a spinal level in extension and lateral bending, in addition to limiting torsion (Kotani et al., 1998).

2.5 Cervical Spine Ligaments

Ligaments are fibrous bands that carry a tensile load in the direction of fiber orientation (White et al., 1990). When an external force is exerted on the spine, ligaments provide tensile resistance to balance the forces. Ligaments are primarily comprised of collagen, water, elastin and proteoglycans (Oza et al., 2006).

The ligaments have four major functions (White et al., 1990), two for motion and stability and two functions for protection. The first function is to allow proper motion of the vertebrae using minimal amounts of energy from the surrounding muscles. Secondly, along with the muscles, the ligaments provide stability for the spine. Third, the ligaments must protect the spinal cord by restricting motion and preventing the disc from protruding into the intervertebral foramen (Moore et al., 1999). Lastly, they must protect the spinal cord in traumatic circumstances. When large loads are applied at high rates the ligaments must restrict motion as well as absorb the large amounts of energy applied to the system (White et al., 1990).

There are two distinctly different regions of the cervical spine, both with different ligaments contributing to the specific function of the neck. The vertebrae from C3 to C7 have the same general shape, and have the same ligaments superior and inferior at each level. They are present between C2-C3, through C7-T1, and also continue down the thoracic and lumbar spine. These ligaments will be referred to as the 'primary cervical spine ligaments' as they are present at several spinal levels. The uppermost region of the cervical spine is referred to as the craniovertebral junction, where the skull connects to the spine (Moore et al., 1999). The ligaments at the craniovertebral junction are different from those found in the rest of the spine, and are known as the craniovertebral ligaments. The craniovertebral ligaments are connected to the occipital bone of the skull, C1 (atlas), and C2 (axis).

2.5.1 Primary Cervical Spine Ligaments

The five primary ligaments of the cervical spine are: the anterior longitudinal ligament, posterior longitudinal ligament, ligamentum flavum, interspinous ligament, and the capsular ligaments, as seen in Figure 2-18 and Figure 2-19.

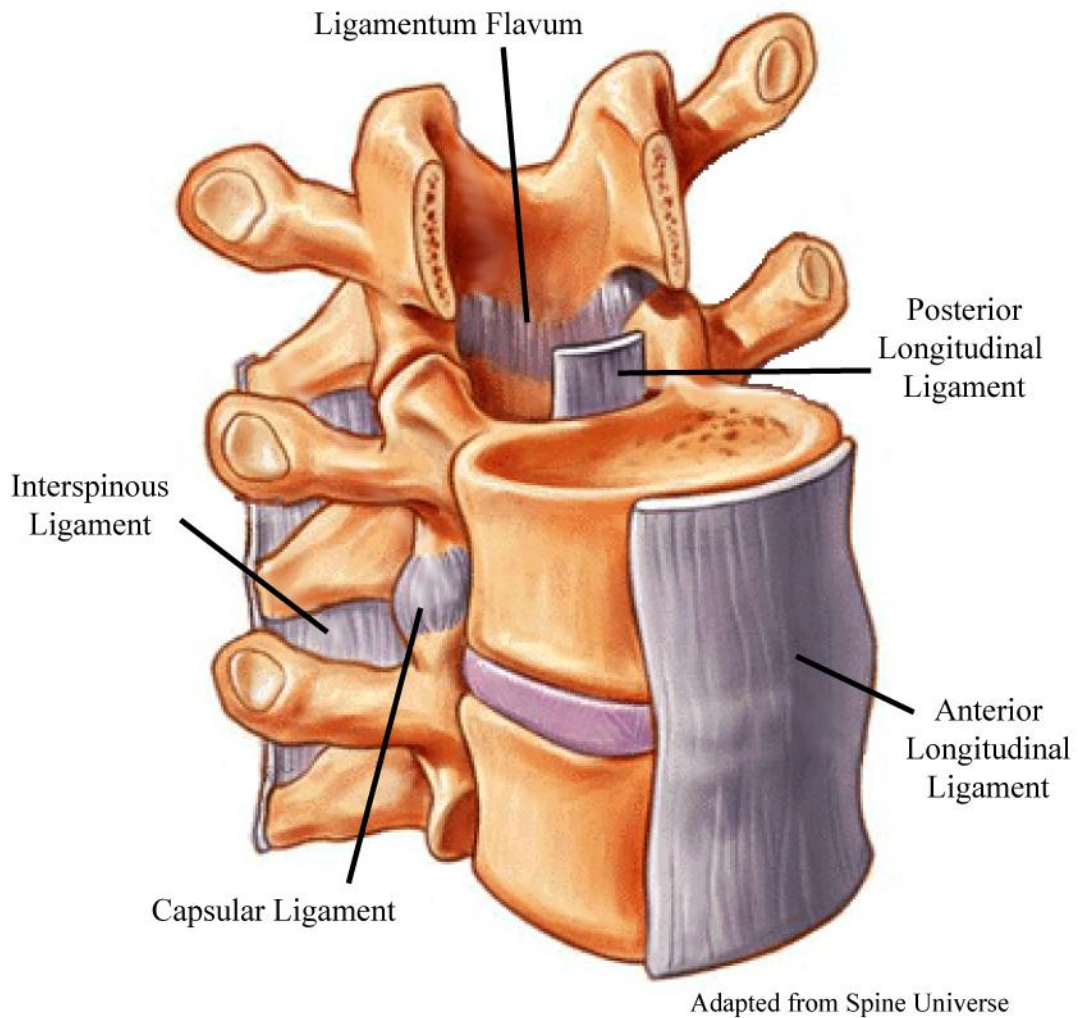


Figure 2-18: Primary cervical spine ligaments

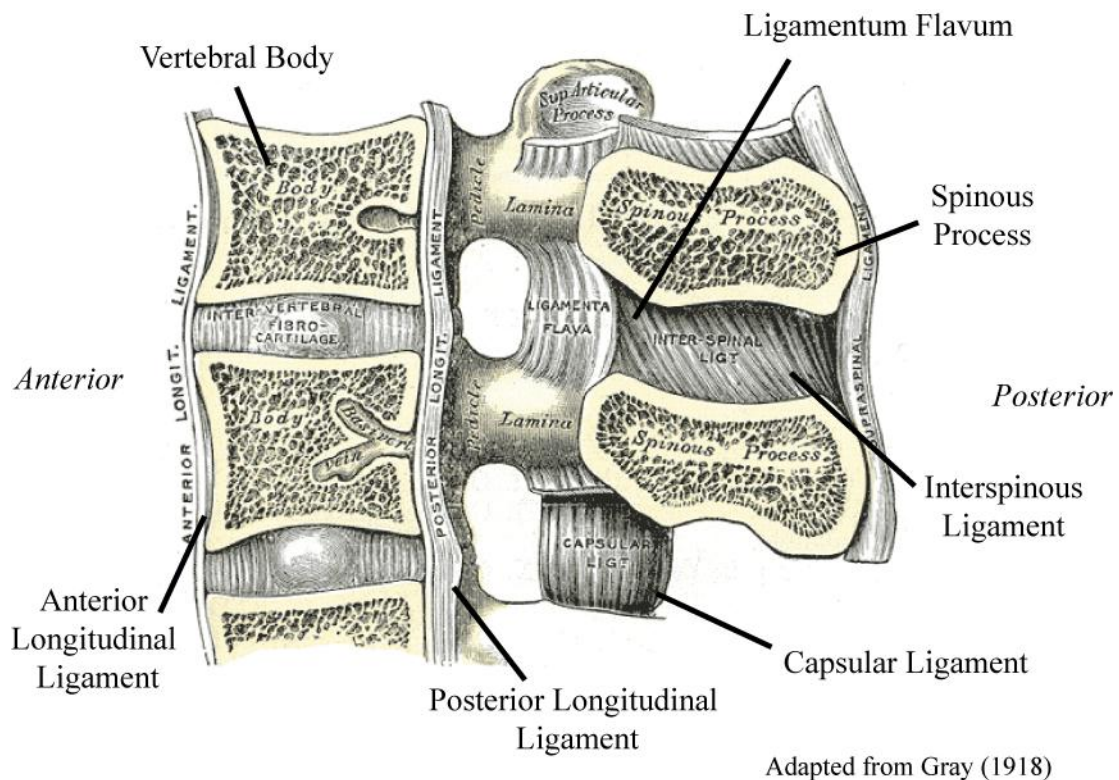


Figure 2-19: Primary cervical spine ligaments (cross section sagittal view)

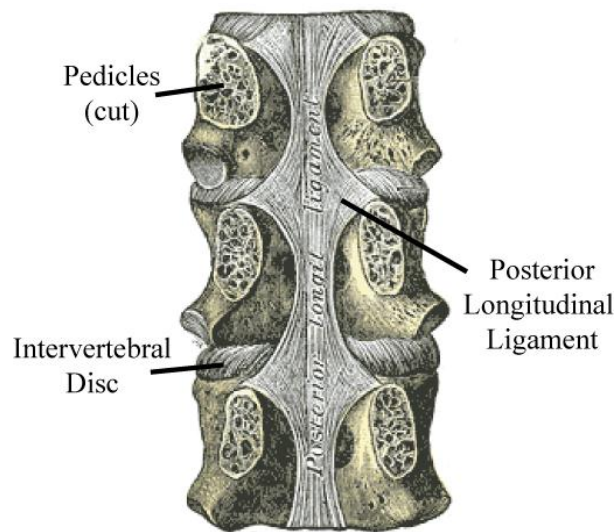
2.5.1.1 Anterior Longitudinal Ligament

The anterior longitudinal ligament (ALL) is a long and broad band of longitudinal fibers that runs from the atlas and occipital bone of the skull to the sacrum. It is continuous with the craniovertebral ligament, the anterior atlantoaxial ligament which runs from the atlas to the base of the skull (Gray, 1918). The ALL runs along the anterior surface of the vertebral bodies and intervertebral discs (Moore et al., 1999). The ALL is firmly affixed to the intervertebral discs and the edges of each vertebral body near the endplates, compared to the middle region of the vertebral bodies where the ligament is more loosely attached (Gray, 1918). There is often a gap between the ligament and the middle of the vertebral body which allows for the passage of blood vessels to the bone. The ALL is made up of many different layers of fibers of different lengths, but are closely interwoven with each other, running longitudinally along the spine (Gray, 1918). The deepest level of fibers are the

shortest, and only run from one vertebrae to the next, while the intermediate level will cross over two or three vertebral bodies and discs. The most superficial layers of the fibers are the longest and can span up to five vertebrae (Gray, 1918). The function of the ALL is to provide stability for the intervertebral joints and prevent hyperextension of the vertebral column (Moore et al., 1999).

2.5.1.2 Posterior Longitudinal Ligament

The posterior longitudinal ligament (PLL) is similar to the ALL as it runs the entire length of the spine, only it begins at C2 and extends along the posterior of the vertebral bodies, inside the vertebral canal, to the sacrum. At C2, the PLL is continuous with the craniovertebral ligament, the tectorial membrane (Gray, 1918). The PLL is much narrower than the ALL (Moore et al., 1999); however it is widest across the intervertebral discs where it is most firmly attached as seen in Figure 2-20. Like the ALL, there is often a gap between the PLL and the center of the vertebral body, to allow for the passage of veins. Also like the ALL there are different layers and lengths of collagen fibers running in the longitudinal direction, where lengths range from adjacent vertebrae (deeper layers) up to four vertebrae (superficial layers). Both the ALL and PLL are thickest at the thoracic region, where the vertebrae are connected to the ribcage which protect vital organs. The PLL has a 10:1 collagen to elastin ratio with closely aligned collagen fibers (Nakagawa et al., 1994), the structural component of the ligament.



Adapted from Gray (1918)

Figure 2-20: Posterior view of vertebral bodies and posterior longitudinal ligament

The posterior longitudinal ligament helps to prevent hyperflexion of the vertebral column. Since it covers the disc, and lies between the disc and the spinal cord, the PLL also serves to prevent herniation; where a large compression or bending force is applied to the spine and the intervertebral disc bulges posteriorly due to the increased pressure in the nucleus pulposus, and risks making contact with and injuring the spinal cord.

2.5.1.3 Ligamentum Flavum

The ligamentum flavum (LF) are very elastic ligaments that join laminae of adjacent vertebral arches, and are located within the vertebral canal, posterior to the spinal cord. The LF has the highest elastin-collagen ratio of the spinal ligaments (Yong-Hing et al., 1976; Viejo-Fuertes et al., 1998). It has been shown to be comprised of 50% to 80% elastin fibres, with a 2:1 elastin to collagen ratio, with collagen fibers exhibiting no favored orientation (Nachemson et al., 1968), compared to the other primary ligaments which only contain 5% to 30% elastin fibres (Pintar, 1986). The LF run vertically between laminae, binding the two arches forming the posterior wall of the vertebral canal (Moore et al., 1999). They exist between vertebrae from C2 to the sacrum, and have been referred to as the most elastic tissue in the human body (White et al., 1990).

The ligamentum flavum prevent separation of the laminae which stops sudden flexion of the spinal column, preventing hyperflexion and injury to the intervertebral discs (Troyer et al., 2011). The high elastic content preserves the normal curvature in the spine as well as helps to return the vertebrae to normal position after movement (Moore et al., 1999).

2.5.1.4 Capsular Ligament

The capsular ligaments (CL), surround the facet joints, as mentioned previously, and are attached to the articular processes of adjacent vertebrae. The capsular ligaments fully enclose the joint in order to keep the synovial fluid contained, but are thin and lax (especially in the cervical spine where they are also longer than in other spinal regions) in order to allow the joint to move. The fibers are orientated perpendicular to the plane in which the facet joints slide (White et al., 1990).

2.5.1.5 Interspinous Ligament

The interspinous ligament (ISL) connects adjacent spinous processes, where the ligament runs from the root to the tip of each process (Gray, 1918; Moore et al., 1999). It is very thin and membranous, and generally weak, especially in the cervical spine region (Gray, 1918). The anterior edge of the ISL is in contact with the LF, and the posterior edge is in contact with the supraspinous ligament or the nuchal ligament.

2.5.1.6 Remaining Spinal Ligaments

There are other spinal ligaments that will not be investigated in detail as they are insignificant in the cervical spine, or do not have bony attachment points on adjacent vertebrae, and therefore unable to be tested for mechanical properties using the technique implemented in this study.

The supraspinous ligament (SL) connects the tips of spinous processes, and is a strong cord that runs along the posterior of the spine, continuous with the ISL between processes (Gray, 1918). This ligament is underdeveloped in the cervical spine but is present from C7 to the sacrum (Moore et al., 1999).

The nuchal ligament (NL) is continuous with the SL into the cervical region connecting with the external occipital protuberance of the skull (Gray, 1918), and is made of thick fibroelastic tissue (Moore et al., 1999) and mainly functions to divide the left and right soft tissues of the neck, and does not contribute to kinematic response. Since C3 to C5 have such short spinous processes, the NL must connect to muscle instead of bone (Moore et al., 1999). Therefore it is difficult to test the mechanical properties as there are no adjacent vertebral bony attachment points. The SL and NL can be seen clearly in Figure 2-21.

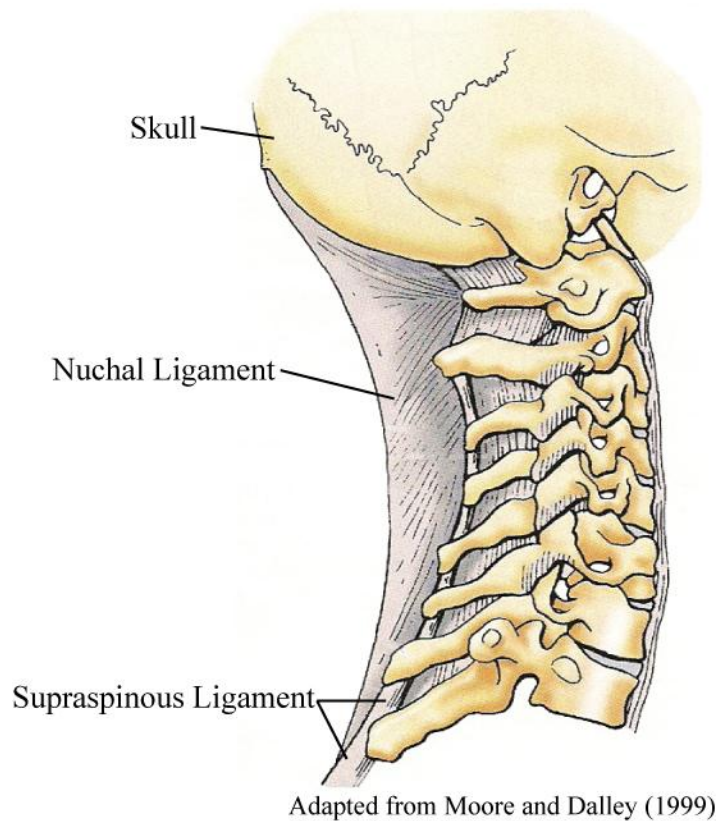


Figure 2-21: Nuchal and supraspinous ligaments, sagittal view

The intertransverse ligaments (ITL) are ligaments that connect adjacent transverse processes throughout the spine. They are insignificant in the cervical spine as they are very small, and indistinguishable from surrounding tissue as they only consist of a few irregular, scattered fibers (Gray, 1918).

2.5.2 Craniovertebral Ligaments

The craniovertebral junction is one of the most complex set of articulations in the human skeleton (Puttlitz, 1999). Therefore the ligaments in this region are also very intricate, mostly due to the movement functions of the neck. Not only must the head be able to rotate, flex and extend with a relatively large degree of motion, but it must also protect the spinal cord. This leads to an increased number of ligaments to limit motion and protect the spinal cord. There are no intervertebral discs in the craniovertebral joint to allow for the greater range of motion (Moore et al., 1999).

The craniovertebral ligaments are divided into two groups, ligaments connecting the occipital bone of the skull to the atlas; the atlanto-occipital joints, and the ligaments connecting the atlas and axis; the atlantoaxial joints. The most significant of these ligaments are the cruciate, alars, anterior and posterior atlanto-occipital and atlantoaxial membranes, tectorial membrane, apical and accessory ligaments. These ligaments can be seen in Figure 2-22 and Figure 2-23.

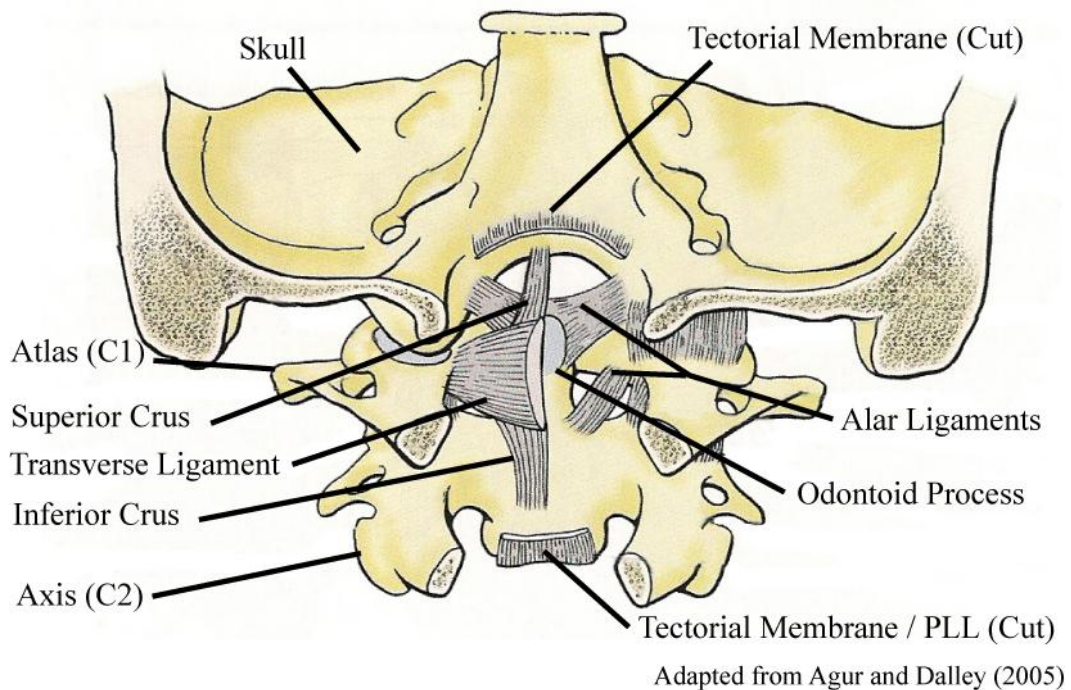
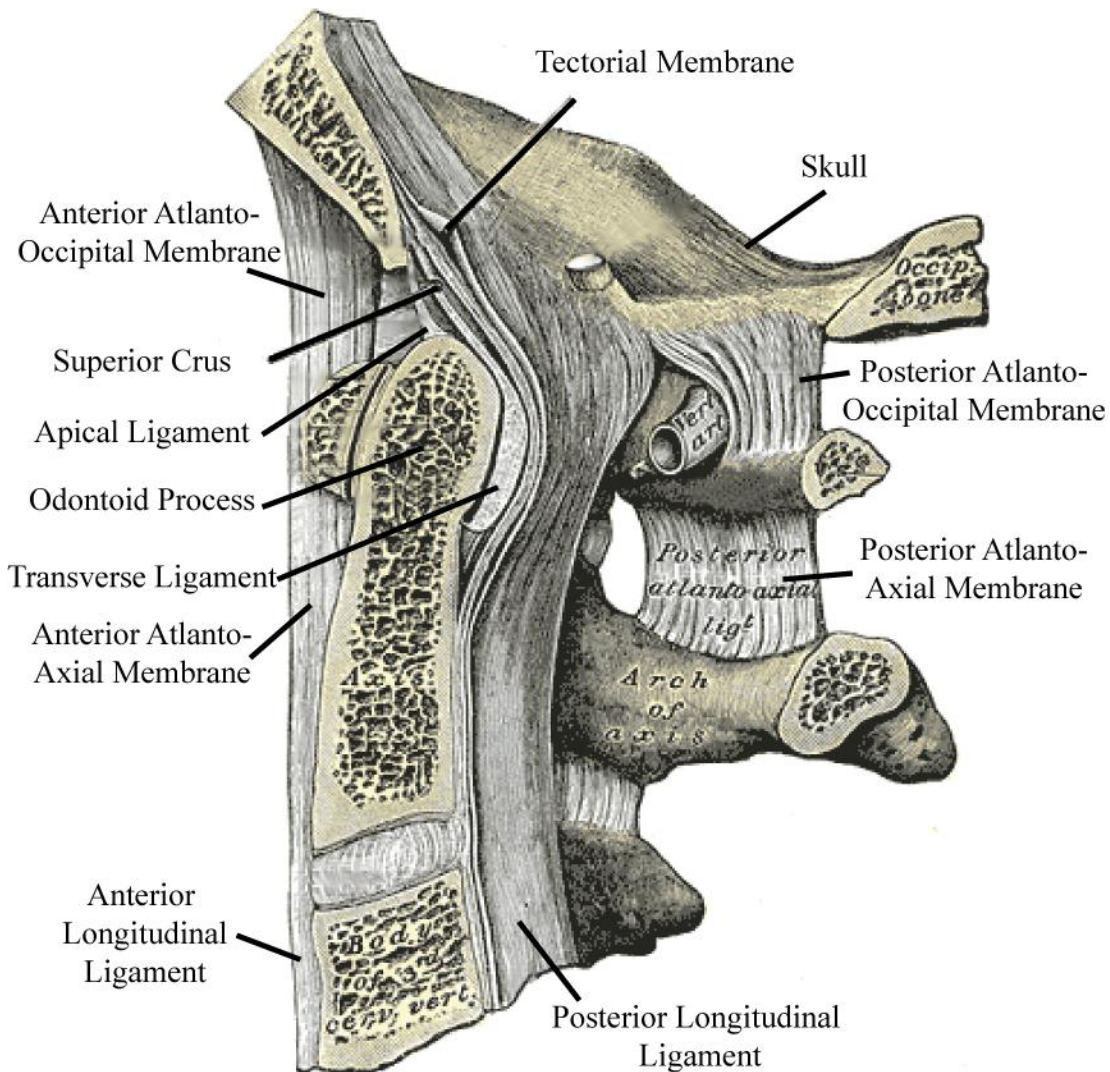


Figure 2-22: Craniovertebral ligaments, sectioned view from posterior



Adapted from Gray (1918)

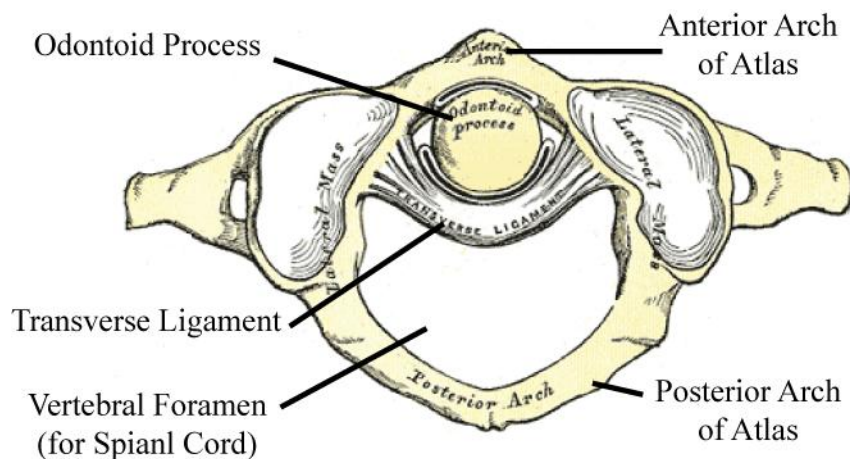
Figure 2-23: Craniovertebral ligaments, sectioned sagittal view

2.5.2.1 Cruciate Ligaments

There are three cruciate ligaments: the atlantal transverse, and the superior (upper) and inferior (lower) longitudinal bands (also known as crus or crux). The name ‘cruciate’ comes from the fact that the ligaments form a cross (Moore et al., 1999), as seen in Figure 2-22. The superior and inferior

longitudinal bands cross to the posterior of the transverse ligament, running vertically, forming a cross. The superior band runs from the transverse ligament to the occipital bone, while the inferior band runs down to the vertebral body of C2, the axis (Moore et al., 1999).

The transverse ligament connects to the medial tubercles of the atlas and runs posterior to the odontoid process as seen in Figure 2-24, but anterior of the tectorial membrane. The transverse ligament fits into a slight groove on the odontoid process and holds it in place against the anterior arch of the atlas, and restricts motion of the atlas; limiting motion to rotation about the axis, and prevents translation in the transverse plane (Moore et al., 1999). The remaining space in the vertebral foramen is for the spinal cord.



Adapted from Gray (1918)

Figure 2-24: Transverse ligament attached to atlas, superior view

2.5.2.2 Alar Ligaments

The alar ligaments are cord-like ligaments that attach to the medial edges of the occipital bone and connect to the lateral sides of the odontoid process (Moore et al., 1999). There are also alar ligaments that attach the odontoid process to the anterior arch of the atlas. They are fibers that connect the dens to the skull and the dens to the atlas. The ligaments are short, and round; about 5 mm in diameter. The function of the alar ligaments is to prevent over rotation of the head, and are commonly referred to as ‘check ligaments’.

2.5.2.3 Apical Ligament

The apical ligament, also known as the ligament of apex dentis, or apical odontoid ligament, extends from the superior tip of the odontoid process to the anterior edge of the foramen magnum between the alar ligaments (Gray, 1918). It is closely intertwined with the deep layers of the anterior atlanto-occipital membrane and superior longitudinal cruciate ligament (Gray, 1918). There is controversy as to whether or not the apical ligament is functionally important (Puttlitz, 1999).

2.5.2.4 Anterior and Posterior Atlanto-Occipital and Atlanto-Axial Membranes

The anterior atlanto-occipital and atlanto-axial membranes (AAOM and AAAM respectively) are a continuation of the anterior longitudinal ligament. They are both strong and wide membranes comprised of dense fibers with a rounded cord along the midline to add strength (Moore et al., 1999). The anterior atlanto-occipital membrane runs from the anterior inferior surface of the occipital bone to the anterior superior surface of the anterior arch of the atlas, while the atlantoaxial membrane runs from the inferior anterior arch of C1 to the superior body of the axis (Gray, 1918). The atlanto-occipital membrane is continuous with the articular capsules, which surround the condyles of the occipital bone. Like the capsular ligaments, they are very thin and loose, so the joint can flex and extend easily (Gray, 1918). The capsules are lined by synovial membrane and filled with synovial fluid to provide sufficient lubrication (Gray, 1918).

The posterior atlanto-occipital and atlantoaxial membranes (PAOM and PAAM respectively) are also both wide membranes but are relatively weak compared to the anterior counterparts (Moore et al., 1999). The posterior atlanto-occipital membrane runs from the posterior inferior surface of the occipital bone to the posterior superior surface of the posterior arch of the atlas, while the atlantoaxial membrane runs from the inferior posterior arch of C1 to the superior lamina of the axis (Gray, 1918). There are also openings towards the lateral sides of the atlanto-occipital membrane to allow a passageway for vertebral arteries. The function of these ligaments is to restrict excessive general motion of the craniovertebral joints (Moore et al., 1999).

2.5.2.5 Tectorial Membrane

The tectorial membrane (TM) is a continuation of the posterior longitudinal ligament. It runs from the body of C2 through the foramen magnum and attaches to the central base of the cranial cavity (Puttlitz, 1999). The tectorial membrane covers the cruciate and alar ligaments. The function of the TM is to limit extreme flexion (Puttlitz, 1999).

Chapter 3

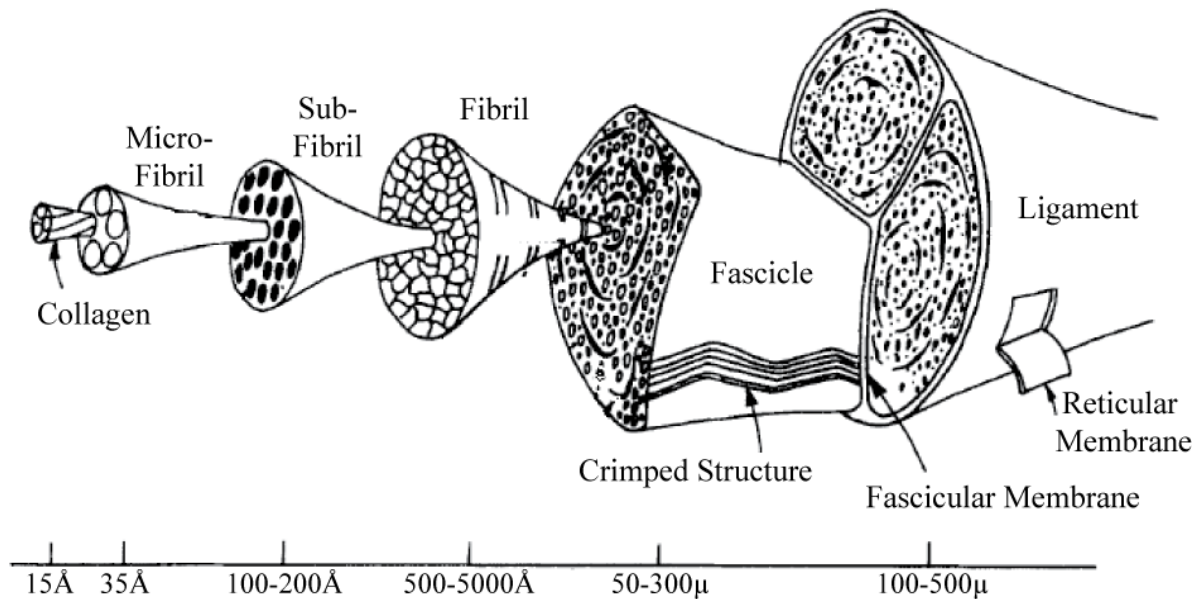
Tissue Mechanics

In a biological system, atoms and molecules are grouped into cells, tissues, organs, and finally make up an individual organism. When investigating motion at an atomic level, quantum, relativistic and statistical mechanics must be used, however, Newton's laws of motion are sufficient when investigating movement at the tissue and organ level (Fung, 1993).

There are two types of tissues in the human body: hard and soft tissue. Bone is considered hard tissue while muscles and ligaments are considered soft tissues, for example. Hard tissues form the structural foundation of the body, the skeleton, to which soft tissues connect. The soft tissues allow for every type of movement within the body, from moving limbs to circulating blood and breathing air.

The basic structural building block for all biological tissues in animals is collagen (Fung, 1993). It is the main connective tissue protein and the most abundant, giving tissues mechanical strength and integrity, and making up 25% to 35% of the body's overall protein content (Di LulloDagger et al., 2002). Y.C. Fung made the analogy that the importance of the role of collagen to humans, is equivalent to role of steel to human civilization (Fung, 1993). Like steel, there are many different kinds of collagen structures, based on how the strands of collagen are wound together. Collagen is defined as a protein made up of different compositions of amino acids, and there are 12 different types of collagen structures that have been identified.

Many collagen molecules form together in a string into what is known as a fibril, and bundles of fibrils group together to form fibers (Fung, 1993). Depending on the tissue, collagen fibers align differently. For example, collagen in the skin aligns differently than collagen in a tendon or ligament. In structures that functionally support a tensile load (such as tendons and ligaments), the collagen fibers are arranged in a parallel manner into primary bundles called fascicles (Figure 3-1). The fascicles are then grouped and enclosed in a reticular membrane to form a tendon or ligament (Kastelic et al., 1978; Fung, 1993).



Adapted from Kastelic et al. (1978)

Figure 3-1: Ligament hierarchy structure

Within a tissue, collagen fibers are mixed with cells and intercellular substance. The intercellular substance is comprised of elastin, reticulin and a hydrophilic gel called ground substance (Fung, 1993). The denser the tissue is, the less ground substance it contains. The composition as well as the hydration of collagen plays a large role in the mechanical properties of the tissue.

When a ligament is in a relaxed state, the collagen bundles are organized in a crimped arrangement (Figure 3-1) and accompanied by elastic fibres (Chazal et al., 1985). When the ligament is loaded, the collagen bundles stretch and lose the crimped pattern. The elastic substance helps to return collagen fibers to the crimped pattern after loading. When a ligament begins to fail, gaps can be seen between the retracted bundles of collagen fibres (Chazal et al., 1985).

Ligament properties are closely related to the number and quality of collagen bonds present. These properties strengthen to about age 20, where material properties plateau before the collagen content begins to decrease with age, resulting in a decline in material properties such as strength, stiffness and the ability to withstand deformation (Cowin et al., 2007).

3.1.1 Mechanical Properties

Intuitively, a larger ligament often is able to withstand a larger load than a smaller ligament, so force relative to size is important. *Stress* is the non-dimensionalized measure of force and is defined as force per unit cross-sectional area ratio, where the force acts perpendicular to the plane in which area is measured. Often the area changes as the structure is loaded. It is called *engineering stress* when only the initial area is used, and *true stress* when instantaneous areas during loading are used. The symbol σ is used to denote normal stress.

$$\sigma = F/A$$

Similarly, deformation of a solid can be described using *strain*, where the deformation normalized by length dimension is removed. Strain is the dimensionless ratio of change in length over initial length. L_0 is used to denote initial length, L for strained length, and ε for strain.

$$\varepsilon = \frac{L - L_0}{L_0} = \frac{\Delta L}{L_0}$$

Strain rate is the rate of change in strain with respect to time. It is useful in making comparisons when two solids have different initial lengths, thus can be compared when they are deformed at the same strain rate, despite a difference in elongation rate (velocity).

$$\dot{\varepsilon} = \frac{d\varepsilon}{dt} = \frac{d}{dt} \left(\frac{L - L_0}{L_0} \right) = \frac{1}{L_0} \frac{dL}{dt} = \frac{v}{L_0} = \frac{\text{velocity}}{\text{initial length}}$$

In a Newtonian fluid, the relation between shear stress and strain rate is linear (and passes through zero), so with increasing strain rate, the shear stress also increases. The constant of proportionality is known as the coefficient of viscosity.

A constitutive equation is an equation that describes a physical property of a material. Thus, it must be independent of frames of reference, and dimensionalized components of physical quantities (Fung, 1993). There are many simple constitutive equations that exist for many materials, such as Hooke's law that relates stress and strain based on a constant material property, known as Young's modulus

(Hooke's Law: $\sigma = E\varepsilon$, where E denotes Young's modulus). Constitutive equations can be used to represent more complex behaviour, like that of biological tissue.

Many biological tissues are known to exhibit time dependent material properties (Burstein et al., 1968), having characteristics of both a viscous fluid and an elastic solid when undergoing deformation. Materials with these properties, including soft tissues are known as *viscoelastic* materials.

Stress relaxation, creep, and hysteresis are several characteristics of viscoelasticity. Stress relaxation occurs when a body is deformed, causing a stress and a strain, and as the strain is held constant, the stress will decrease over time. Creep is similar except a constant load is applied, where the stress remains constant, and the strain increases over time. Hysteresis is when the loading phase is different from the unloading phase curve of a stress-strain relationship graph. Stress-strain curves can be seen for these characteristics in Figure 3-2 and Figure 3-3.

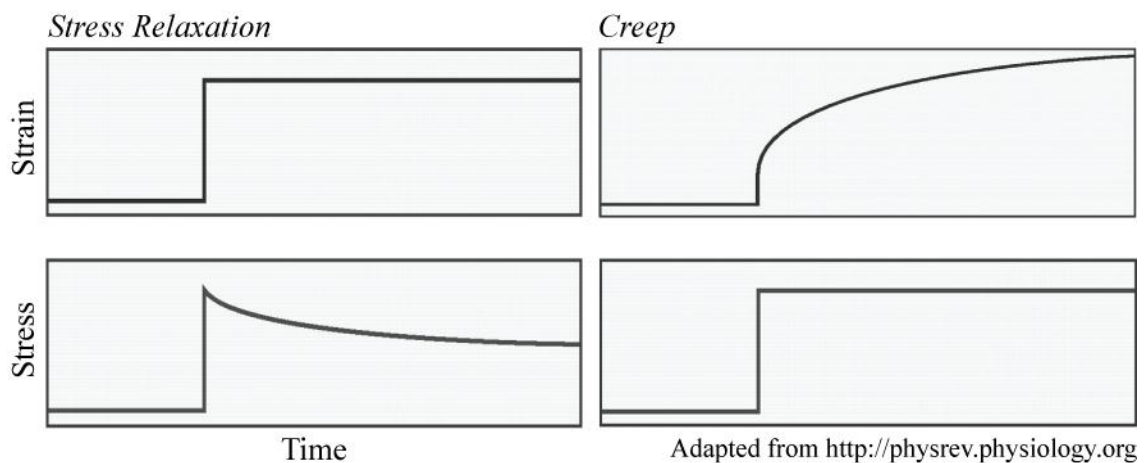


Figure 3-2: Stress/strain vs. time curves for stress relaxation and creep

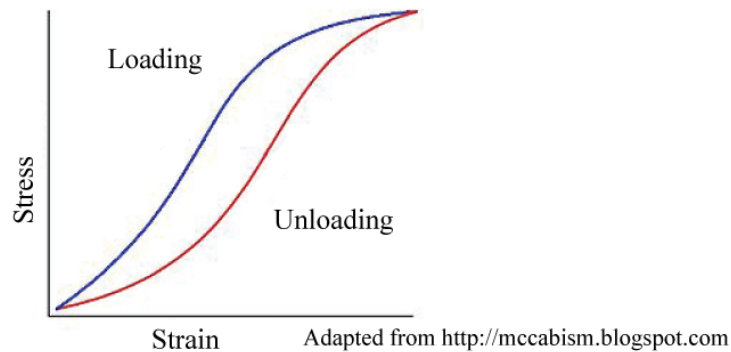


Figure 3-3: Hysteresis nonlinear loading response

If a tissue is tested repeatedly, the load deformation curves will be different. The curves will appear to shift to the right with each repeated test, as seen in Figure 3-4. The relaxation curves are seen to shift upward with repeated tests (Figure 3-4). As repeated tests continue, the difference between curves decreases, until it eventually vanishes (Fung, 1993). When no difference is present between successive tests, the specimen is said to be ‘preconditioned’. This occurs in biological tissues because the internal structure changes based on the loading it undergoes, as collagen fibers align to support the load. When post-mortem tissues are used for mechanical testing, preconditioning is important to return the properties to those of physiological conditions.

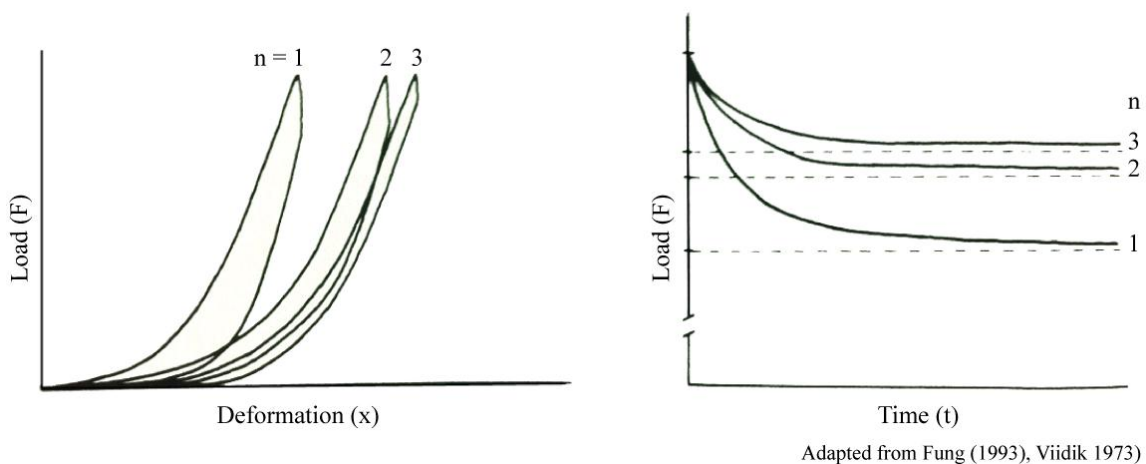


Figure 3-4: Preconditioning of an ACL (Fung, 1993; Viidik, 1973)

Mechanical models are used to represent viscoelastic behaviour, and are composed of a combination of spring and dashpot elements. Linear springs produce an instant deflection proportional to a load, and dashpots produce a velocity proportional to a load (or a load proportional to a velocity). Spring elements have a spring constant k , and dashpots have a viscosity coefficient μ . Three common models are shown in Figure 3-5: Maxwell body, Voigt body, and Kelvin body (standard linear solid). More elements can be added to represent more complex systems. If the system undergoes permanent deformation, a more complex model with extra elements must be used.

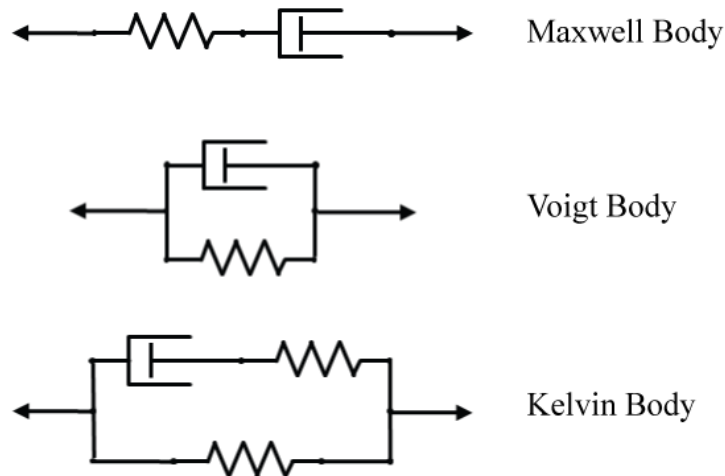


Figure 3-5: Mechanical models used to represent viscoelastic behaviour

Since the response force of a viscoelastic material is proportional to the velocity of an applied load, if the applied load velocity increases, the response force will increase also, demonstrating a stiffening effect (Figure 3-6). The deformation rate is often measured in strain rate, especially when making comparisons to eliminate the length dimensions and compare strictly material properties. In order to find differences between viscoelastic materials, they must be compared at equivalent strain rates. Additionally, when using a mechanical model to represent a viscoelastic material, it must demonstrate the same time sensitivity effects.

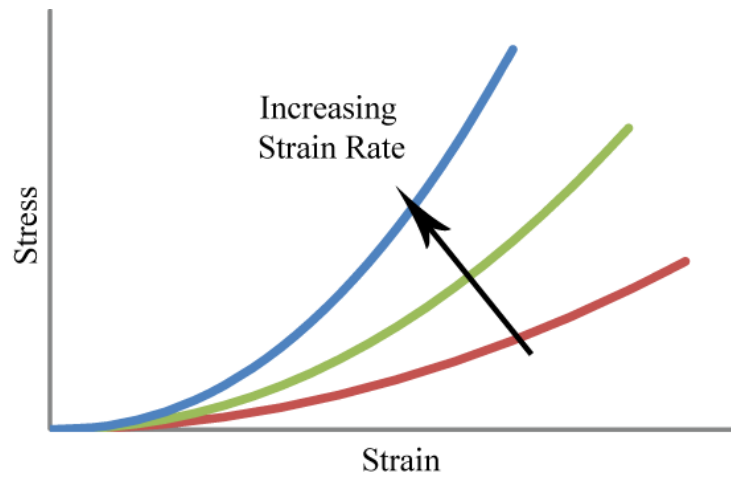
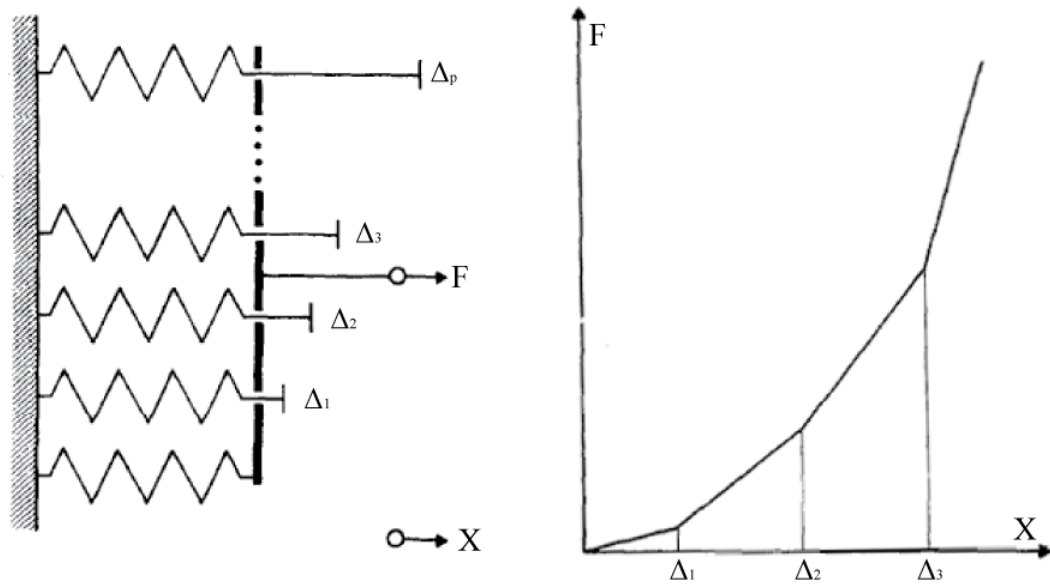


Figure 3-6: Stiffening behaviour of viscoelastic material under increasing strain rates

3.1.2 Ligament Mechanical Properties

These principles of mechanical properties can be applied when analyzing ligament behaviour. When a ligament is loaded, crimped bundles of collagen incrementally become engaged and tightened as the ligament lengthens; resulting in the initial non-linear behavior (Woo et al., 1993), known as the toe region. This is analogous to a mechanical model in which spring elements are incrementally engaged as the ligament is loaded, resulting in incremental increases in stiffness as each spring element is added (Figure 3-7).



Adapted from Frisen, et al. (1969)

Figure 3-7: Loading of a ligament mechanically modeled by incremental loading of spring elements

The complete mechanical model for ligament behaviour is shown in Figure 3-8, as developed by Viidik et al. (1968). As mentioned previously, the spring elements produce a deflection proportional to a load, and the dashpot elements represent the viscoelastic effect. The Coulomb element (black box element) is a stiff frictional body on a rough surface, to represent plastic deformation and the effect of multiple loading cycles. The Coulomb elements on the left model the preconditioning effect as identical successive tests produce different results, but slowly converge until the differences vanish after preconditioning.

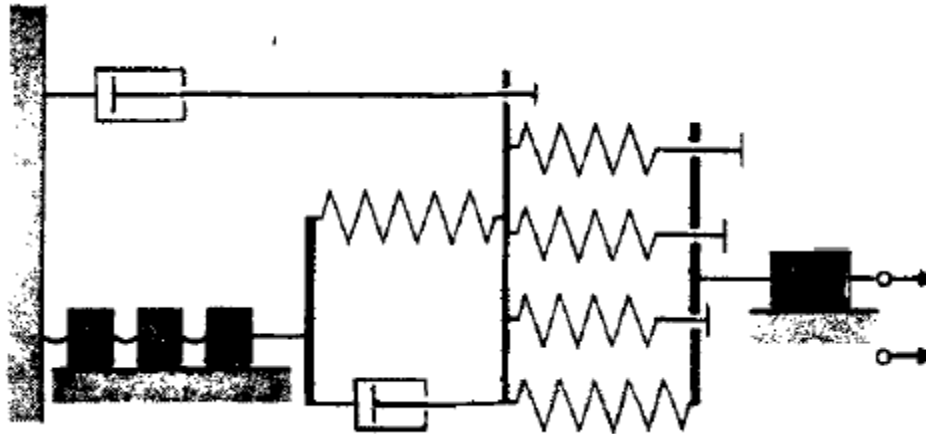


Figure 3-8: Complete mechanical model for ligament behaviour (Viidik, 1973)

When ligaments are cyclically loaded and unloaded, viscoelastic properties are demonstrated by hysteresis (Chazal et al., 1985). When a typical ligament is loaded under tension to failure, the force-elongation curve exhibits a sigmoidal shape up to the ultimate load and the curve has four distinct regions: toe region, linear phase, traumatic phase, and post traumatic phase, as seen in Figure 3-9. The toe region (AB), or ambient phase (Yoganandan et al., 2001), is the initial loading region and has a very low stiffness, where stiffness is the ratio of force over elongation (or slope of the curve). As elongation increases, the ligament fibres begin to straighten and align to support greater load (Figure 3-10), increasing stiffness, thus shape of the curve is concave up at the toe region. Within the spine, the toe region of the ligaments provides spinal movement with minimal muscular energy used, and the small forces induced from large strains in this region decrease the possibility of injury (Panjabi et al., 1981). At point B, the end of the toe region, all of the ligament fibres are fully extended as they all support loads, resulting in almost constant stiffness with increasing load and elongation. This region is known as the linear phase (BC), and demonstrates the greatest stiffness of the loading curve. The toe region and linear phase are often referred to as the physiologic phase (AC; Yoganandan et al., 2001), where the ligament can function normally without damage, or loss of structural integrity. When loaded beyond the physiologic phase, the third region of the curve is the traumatic phase (CD), and is concave downwards, as stiffness decreases with increased force and elongation. During this phase, micro-level failures begin to occur, in the form of fibre tears (Yoganandan et al., 1988).

Loading continues in this phase until failure (point D) is reached, where structural integrity is lost. This point of failure is the ultimate load the ligament can sustain, where stiffness has a value of zero, and also denotes the failure elongation. The final region, the post-traumatic phase (DE), is when the curve drops off as the ligament loses the capability to support load.

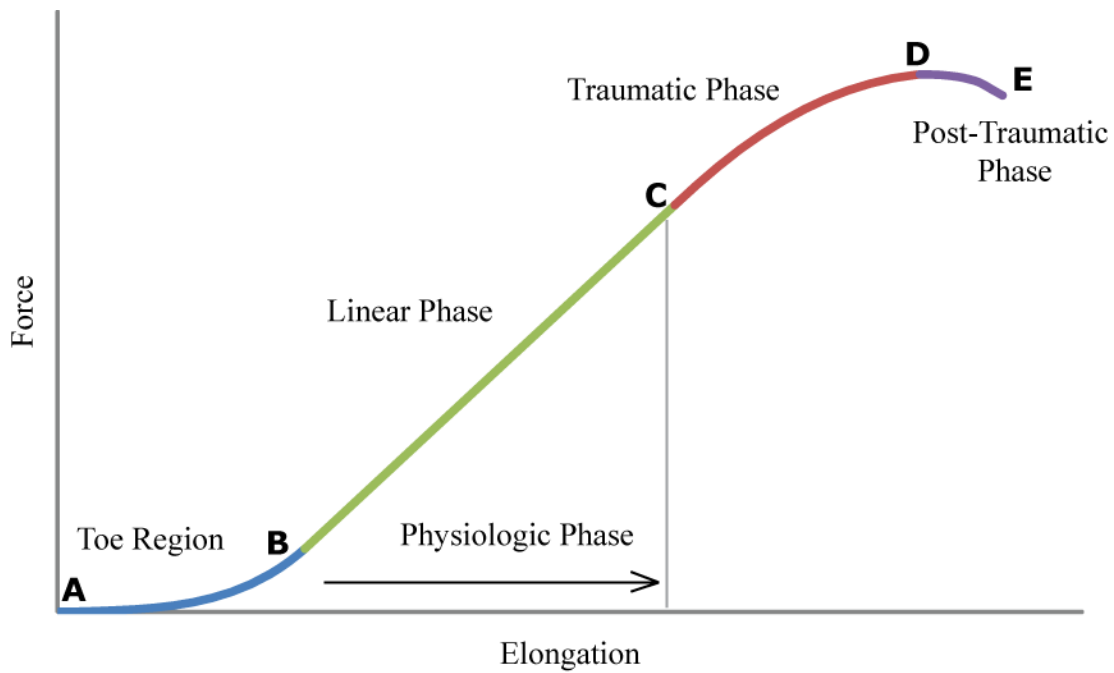
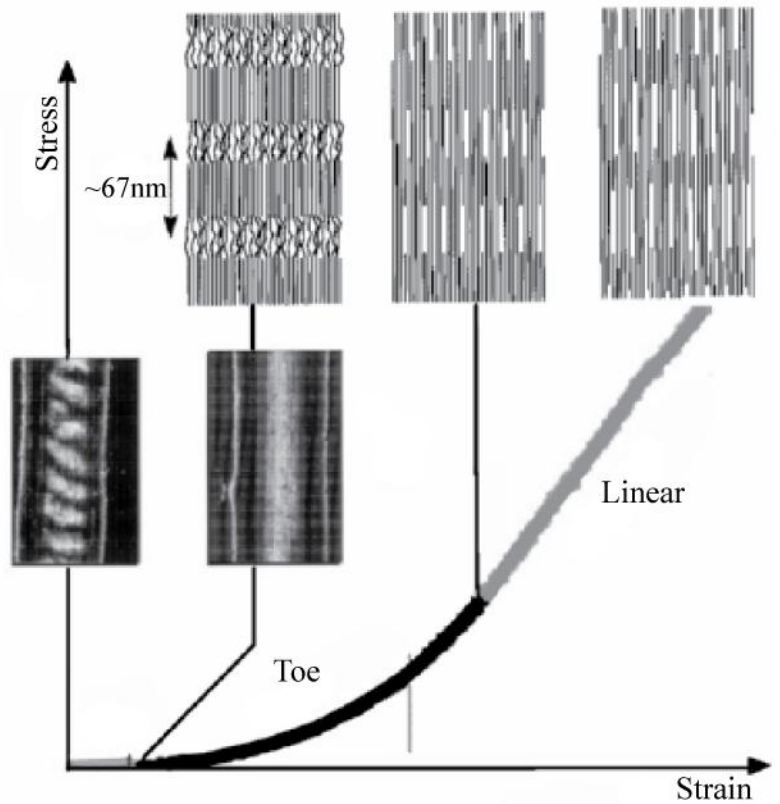


Figure 3-9: Ligament force-elongation curve loading regions



Adapted from Cowin, et al. (2007)

Figure 3-10: Collagen fibres straightening as ligament is loaded

Chapter 4

Literature Review: Mechanical Properties of Cervical Spine Ligaments

Several studies have been performed to determine the mechanical properties of the ligaments of the cervical spine. When the first ligament tests were being conducted, any information found was useful, so no standardized framework for testing was developed. This led to inconsistencies between studies causing inherent difficulties when trying to compare and combine results. The previous testing endeavors were grouped and reviewed in five categories: general methodology, quasi-static studies, high rate studies, craniovertebral ligament studies, limitations of previous studies, and relevant information from segment and whole spine studies.

4.1 General Methodology

Ten previous studies have been conducted on cervical spine ligament material properties to failure under tensile loads; four at quasi-static strain rates (Myklebust et al., 1988; Pintar, 1986; Chazal et al., 1985; Przybylski et al., 1996; Yoganandan et al., 1998; Yoganandan et al., 2000), three at high strain rates (Ivancic et al., 2007; Bass et al., 2007; Shim et al., 2005), one at both quasi-static and high rates (Yoganandan et al., 1989) and two conducted solely on craniovertebral ligaments (Panjabi et al., 1998; Dvorak et al., 1988). It should be noted that in two cases, results were published from the same study in different articles; Yoganandan et al. (1998, 2000) published two articles, and Myklebust et al. (1988) published results from Pintar's PhD thesis (1986). Average cadaver ages used in the studies had a wide range from the youngest of 49 (37 to 53) years old (only craniovertebral ligaments were tested; Panjabi et al., 1998), to the oldest of 81 (71 to 92) years old (Ivancic et al., 2007).

Most ligament dimensions were measured from the ends of the ligament at the bony attachment points, and are consistent among the studies for CL, LF and ISL. The ALL and PLL are continuous ligaments that run the entire length of the spine, attaching to the vertebral bodies on the anterior and posterior sides respectively. This leads to inconsistencies of the measured lengths of these ligaments.

Some studies define the ligament length as the distance between the distal endplate of the superior vertebral body to the caudal endplate of the inferior vertebral body, essentially the thickness of the intervertebral disc (Chazal et al., 1985; Bass et al., 2007; Shim et al., 2005). Other studies defined the ALL and PLL lengths as the mid-height of the superior vertebral body to the mid-height of the inferior vertebral body (Yoganandan et al., 1998; Yoganandan et al., 2000; Pintar, 1986). This is to account for the portions of the ligament that overlies the vertebral body and still contribute to the response. This is to account for the portions of the ligament that overlies the vertebral body and still contribute to the response. When ligaments are modeled as continuous structures along the vertebral column, data from endplate to endplate defined ligaments would insufficiently represent the ligament overlying the vertebral body (Yoganandan et al., 2001). The remaining studies do not report ligament dimensions as results are only reported as force-elongation data, so initial lengths are not needed (Myklebust et al., 1988; Yoganandan et al., 1989; Ivancic et al., 2007).

All ligaments were tested *in situ* as the ligament attachment points to the bone were kept intact. There were two methods used for ligament isolation among the studies. The first was to transect all soft tissues (ligaments and intervertebral disc) of adjacent vertebral bodies except the ligament to be tested (Myklebust et al., 1988; Pintar et al., 1998; Yoganandan et al., 1998; Yoganandan et al., 2000; Yoganandan et al., 1989), so the entire vertebral bodies could be gripped and pulled in tension. The second technique involved sectioning the spine into functional spinal units (FSUs) first; two vertebral bodies with all adjoining soft tissues. The FSUs were then dissected into respective bone-ligament-bone complexes and isolate the ligaments individually by transecting any remaining soft tissues (Ivancic et al., 2007; Bass et al., 2007; Shim et al., 2005). One study (Chazal et al., 1985) did not report isolation technique. Motivation behind the two approaches is not disclosed, although there are apparent advantages and disadvantages to both. Transecting all of the soft tissues from the vertebral bodies to isolate a ligament reduces the risk of the desired ligament being damaged in preparation and structural integrity of the bone remains intact, however this method limits the experiment to a very small sample size since so many adjacent ligaments are sacrificed. Isolating all the ligaments into bone-ligament-bone complexes from an FSU allows all the ligaments from a spinal level to be tested, and yields a greater sample size, however extra care must be taken to isolate the specimens as there is a greater risk of damage to the ligaments, and gripping the bone is more difficult and specialized for

each ligament. Additionally, the first method leaves both capsular ligaments attached and tested simultaneously. This must be taken into account when comparing to data from when they were isolated and tested individually.

Only one study reported the attempt to mimic *in vivo* conditions by testing the ligaments as close to body temperature 37°C and >90% humidity levels as possible (Bass et al., 2007). The remaining studies did not specify test conditions. Very few publications specify performing preconditioning cycles (Chazal et al., 1985; Przybylski et al., 1996; Yoganandan et al., 2000; Bass et al., 2007), while the rest did not mention any preconditioning attempts.

4.2 Quasi-Static Studies

Chazal et al. (1985) was the first known study to publish data on cervical spine ligament properties, and did so for the whole spine. Although forty-three total ligament tests were performed, only four were cervical spine ligaments; one ALL, and three PLL from four different spines, average 55 (50 to 60) years old. The cervical region data was very limited, however, this was the first study to develop a testing protocol that other studies would follow. Ligament lengths were measured before testing with a micrometer, defining the length as the distance between nearest bony attachment points. The cross sectional areas were measured using a palpator device, every 2 mm along the length of the ligament, with the smallest cross sectional area used to calculate stress. Specimens were gripped by clamps designed for each bone, so as not to interfere with the ligament. Tests were performed at *in vivo* hydration conditions in a custom apparatus at 1 mm/min. Force-deflection curves exhibited a typical sigmoidal shape over the loading region, and force, elongation, stress, and strain were measured at toe region, end of linear region (traumatic region onset) and peak force (failure). The results were in agreement with previous lumbar spinal ligament tests, and also found age effects, as ligament failure stress decreased with increasing age, and ligament failure mode of disinsertion from the bone became more prevalent with increased age. No spinal level effects were found. Differences were found between ligaments, but were based primarily on lumbar and thoracic ligaments (Table 4-2).

Chazal et al. (1985) also performed a histological study in addition to ligament tensile tests. Ligaments were examined under a microscope at relaxed, loaded before failure, and post failure states. The cripped pattern was observed in relaxed ligaments, which straightened under loading, and demonstrated breakages post failure.

Myklebust et al. (1988) and Pintar (1986) performed a more comprehensive study using 41 male cadavers, mean age 67 (34 to 83), with a minimum of three test specimens for each of the five primary ligaments at each spinal level. Ligaments were tested *in situ* as all soft tissues aside from the ligament under study were transected, and the capsular ligaments were tested together as a pair. An electrohydraulic testing apparatus was used and the specimens were fixed into the frame by the vertebral bodies and loaded in tension at 10 mm/s. Force-deformation curves displayed a typical sigmoidal shape during loading, and failure force and deflections were reported by Myklebust et al., however Pintar also reported stiffness. It is important to note that the stiffness value reported was the ratio of failure force to failure elongation, and not the slope of the linear portion of the loading region of the curve. These values were in agreement with previous literature, including Chazal et al. (1985). Results were tabulated and organized by spinal level. Spinal level trends were apparent for the ALL, having highest strength at the upper cervical levels, the LF was weakest at the mid-cervical levels, and the CL had highest failure force values at the cervical-thoracic junction. The ISL was the weakest of all ligaments. Strength and stiffness were observed to decrease with age, and failure elongation increased with distance from the vertebral center of rotation. There was a trend for ligaments being stronger on the convex side of the spinal curvature; the anterior of the cervical spine. The explanation of why this trend was observed was not investigated. Results can be seen in Table 4-2.

Pintar (1986) also performed a histological study where collagen fibres were stained red and elastin fibres were stained black, to determine the composition of each ligament. The ALL, PLL, CF, and ISL were comprised of 5% to 30% elastin fibres, while the LF consisted of 50% to 60% elastin fibres. It was also found that one LF sample from the upper cervical spine had very few elastin fibres, suggesting that composition not only varies between ligaments but also between spinal level, which might lead to different mechanical properties at different spinal levels. Recommendations were made

to further investigate the composition of ligaments by spinal level to gain a better understanding of spinal level effects. The ALL and PLL had very similar fibre densities, as well as similar strength properties, while the ISL had a lower fibre density than all other ligaments, possibly explaining why it was consistently weaker than the other ligaments.

Przybylski et al (1996) performed detailed quasi-static testing on ALL and PLL specimens using 20 cadavers with mean age 80 (58-95) years old. Tests were performed at 0.33 mm/s, after preconditioning the ligaments and results were reported based on spinal level. ALL and PLL were shown to possess similar properties except PLL stiffness was greater at all levels, and very few significant level differences were found. Although not significant, the PLL displayed trends of being stiffest at the middle spinal levels. The study recommended testing of younger specimens for future improvements.

Yoganandan et al. (1998; 2000) conducted a study in which cervical spine ligament geometries were measured as well as mechanical properties. Using cryomicrotomy imaging techniques, the lengths and cross sectional areas were measured for the five primary ligaments, from eight cadavers, mean age 63 (42 to 88). The process involved freezing the spine in proper anatomical alignment, then taking images as cross sections were cut in the sagittal plane at 20 to 40 μm increments. The ligament lengths were defined as seen in Figure 4-1. Lengths were defined as mid-height to mid-height of the inferior and superior vertebral bodies for ALL and PLL, the LF and ISL were defined as the distance between bony attachment points, and the CL were defined as the vertical distance between the anterior tip of the superior facet to the posterior tip of the inferior facet. The results provided accurate ratios of ligament lengths to cross sectional areas. Cross sectional areas were taken at the midpoint of each ligament. Lengths and areas were averaged for mid (C2-C5) and lower (C5-T1) cervical spine regions, and all ligaments at the lower region had a larger cross sectional area than the mid region.

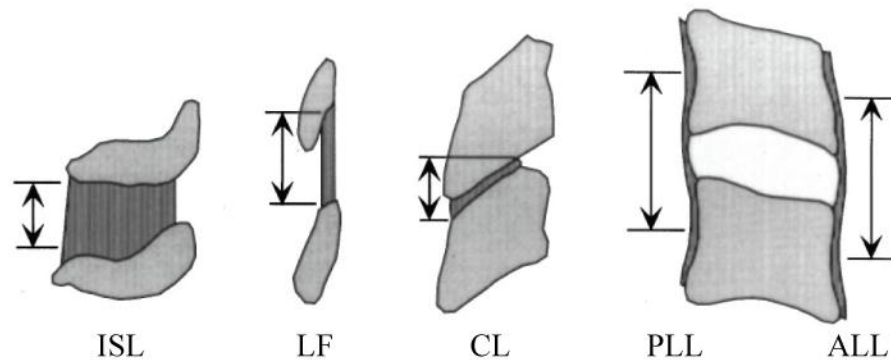


Figure 4-1: Ligament length definitions (Yoganandan et al., 2000)

The second part of the study was to test cervical spine ligaments from 25 more spines; mean age 68 (range not reported) for mechanical properties, yielding 107 specimens suitable for testing. The breakdown of the quantity of the ligaments tested from each spinal level can be seen in Table 4-1. Ligaments were tested *in situ* as all soft tissues aside from the ligament under investigation were transected, and the capsular ligaments were tested together as a pair. Vertebral bodies adjacent to the ligament were secured using Steinmann pins, and specimens were preconditioned prior to tensile tests which were performed at 10 mm/s using an electrohydraulic piston apparatus. Results for stiffness (defined as the slope of the least squares fit to the most linear region), failure energy (total area under force-deflection curve), stress (ratio of failure force to original cross sectional area), and strain (ratio of failure elongation to initial length) were reported. Statistical analysis was performed to compare the mechanical properties. ALL failure stress was higher for C2-C3, C6-C7, and C7-T1 than C3-C4 and C4-C5. PLL failure stress was highest at C5-C6. CL had higher failure stress levels at C3-C4 than C4-C5, and C5-C6. LF had higher stiffness at C7-T1 than C2-C3, and ISL had higher failure stress at C2-C3 compared to all other levels. This is the only previous study to evaluate spinal level differences. Results were categorized and presented by mid (C2-C5) and lower (C5-T1) cervical spine regions based on clinical convention, although smaller groupings were attempted, without any statistical significance for choosing a particular grouping method. ALL and PLL were found to be the stiffest and failed at the highest stress levels, while CL, LF, and ISL had higher failure strains. Results can be seen in Table 4-2.

Table 4-1: Sample size matrix (Yoganandan et al., 1998)

Level	ALL	PLL	CL	LF	ISL
C3-C3	5	3	3	4	3
C3-C4	3	4	4	4	3
C4-C5	4	4	3	5	3
C5-C6	3	3	3	4	3
C6-C7	3	4	4	3	2
C7-T1	5	3	5	4	3
Total	23	21	22	24	17

Table 4-2: Combined results for previous quasi-static ligament tests

	Failure Force (N)			Failure Elongation (mm)		Stiffness (N/mm)			
	<i>Chazal</i>	<i>Myklebust</i>	<i>Przybylski</i>	<i>Chazal</i>	<i>Myklebust</i>	<i>Chazal</i>	<i>Przybylski</i>	<i>Yoganandan</i>	<i>Pintar</i>
ALL	140	111 (56)	97 (59)	2.4	7.6 (3.9)	71.4	48 (27)	17.0 (3.4)	17.9 (9.1)
PLL	185	83 (55)	109 (59)	2.43	6.1 (5.4)	104.3	68 (43)	24.0 (7.2)	21.3 (14.0)
CL	-	215 (102)	-	-	8.7 (5.4)	-	-	35.0 (6.1)	31.9 (17.5)
LF	-	115 (50)	-	-	8.0 (4.7)	-	-	23.0 (7.0)	16.1 (13.8)
ISL	-	34 (20)	-	-	7.3 (5.2)	-	-	7.1 (1.6)	7.0 (3.4)

Average (SD) values

	Failure Stress (MPa)		Failure Strain		
	<i>Chazal</i>	<i>Yoganandan</i>	<i>Chazal</i>	<i>Przybylski</i>	<i>Yoganandan</i>
ALL	11	10.2 (1.8)	0.4	0.39 (0.14)	0.33 (0.06)
PLL	19	9.5 (3.4)	0.5	0.39 (0.13)	0.26 (0.09)
CL	-	6.5 (1.5)	-	-	1.32 (0.29)
LF	-	2.6 (0.8)	-	-	0.83 (0.13)
ISL	-	2.9 (0.8)	-	-	0.65 (0.14)

Average (SD) values

4.3 High Deformation Rate Studies

Yoganandan et al.(1989) conducted the first tensile tests of cervical spine ligaments tested at high rates. Only the ALL and LF were tested for a total of 54 ligaments, from cadavers with average age 70 (46 to 88) years. Ligaments were tested in situ, by securing the vertebral bodies using Steinmann pins and transecting all soft tissues except the desired ligament. Tests were performed using a custom electrohydraulic test fixture at four elongation rates of 8.89, 25, 250, and 2500 mm/s. Although only two ligaments were tested, the main objective of the study was to quantify rate effects on spinal ligament properties. Elongation rates were not constant but differed up 9.5% for the 2500 mm/s test and 4% for the other tests. A slight gap in the apparatus housing was incorporated to allow the fixture to reach elongation rates before engaging the ligaments. Results showed a significant rate effect of increased failure force, increased strain energy, and increased stiffness with increased loading rate. Failure force increased nonlinearly, and stiffness increased linearly with the logarithm of the loading rate, as seen in Figure 4-2. There was no effect on failure elongation. Reported shortcomings of the study were the absence of data for other cervical spine ligaments, change in strain rate amongst tests of constant elongation rates, and the older age of cadavers used. Results from the 2500 mm/s study can be seen in Table 4-3.

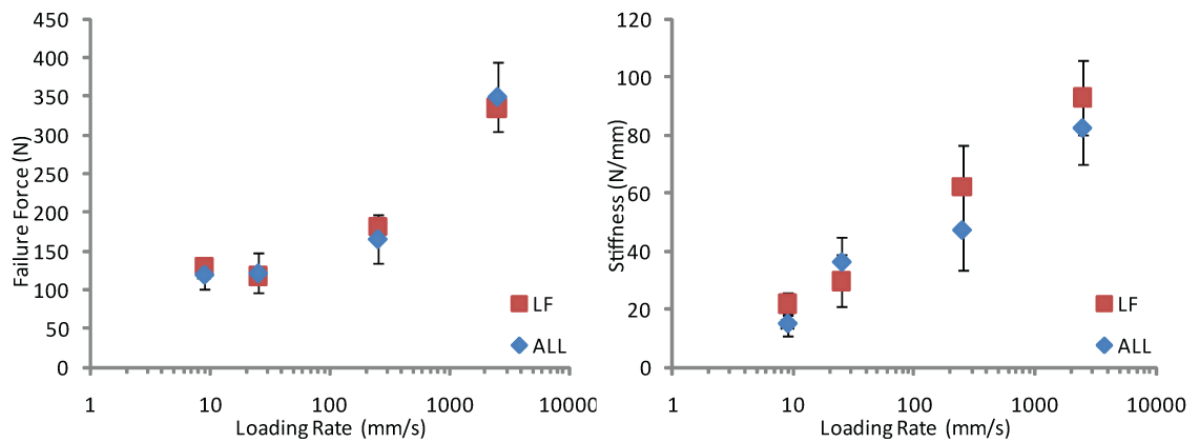


Figure 4-2: Rate effects on failure force and stiffness for ALL and LF (Yoganandan et al., 1989)

Shim et al. (2006) tested the five primary ligaments using a modified tensile split Hopkinson bar with magnesium input/output bars and semiconductor strain gages (Figure 4-3). The modifications to traditional split Hopkinson bar techniques were sufficient in overcoming difficulties in testing biological soft tissues. The modifications allowed transmitted waves of small amplitude to be captured, full capture of the initial toe region by implementing an initial slack to the ligaments, and lastly being able to generate an adequately long incident wave to stretch ligaments to failure. Three spines were tested, ages 40, 65 and 69, for a total of 62 ligament specimens, and were loaded at rates of 10 to 12 m/s. This corresponded to strain rates ranging from 1300 s^{-1} to 3000 s^{-1} . The curves demonstrated the expected sigmoidal shape during loading, and the metrics measured were elastic modulus, ultimate strain and stress, and strain energy to failure. The high deformation rate dynamic properties were compared to static properties from a previous study with strain rates of 0.005 s^{-1} , and significant rate sensitivity was observed. Increased loading rate was shown to shorten the toe region, increase stress and reduce failure elongation. Results can be seen in Table 4-4.

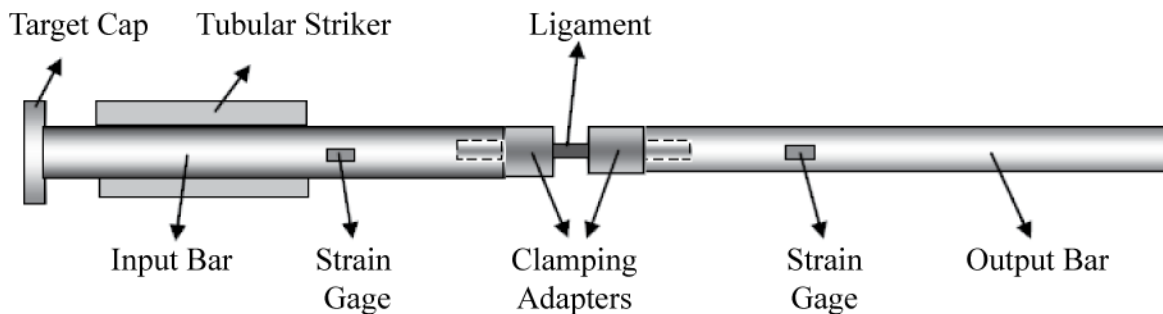


Figure 4-3: Split Hopkinson bar fixture used for high rate testing (Shim et al., 2005)

Bass et al. (2007) tested the ALL, PLL and LF at high elongation rates representative of traumatic events. Eleven cadavers were used, average age 60 (52 to 68) years, for a total of 89 ligament tests. Spines were sectioned into C3-C4, C5-C6, and C7-T1 functional spinal units, and ligaments were isolated into bone-ligament-bone complexes, and potted with a casting resin into aluminum cups, to be loaded in the same orientation as under physiologic loading conditions. Tests were conducted using a servo-hydraulic mechanical test apparatus in an environmental chamber to mimic an *in vivo* environment, as the same authors conducted a prior study on porcine spine ligaments demonstrating

temperature dependent effects (Bass et al., 2007). Ligaments were preconditioned to 10% strain using a sinusoidal input for 20 cycles at 2 Hz prior to testing. Successive tests were then performed to increasing strain levels of 25%, 50%, 75%, 100%, and 300%. The failure test was considered the test with the highest peak force, as when subsequent tests reached lower peak forces evidence was shown that failure was sustained on the previous test. The average deformation rate used was 627 ± 203 mm/s, corresponding to strain rates between 70-150 s^{-1} . Failure force, stress, and strain were reported, where stress was calculated by finding ligament cross sectional areas using length to area ratios from a previous geometric study (Yoganandan et al., 2000). True stress values were calculated assuming the ligaments were incompressible; ligament volume remains constant, where initial area, initial length, and failure length are known:

$$Area_{initial} \times Length_{initial} = Area_{failure} \times Length_{failure}$$

Statistical analysis was performed to identify any differences within three factors: ligament, gender and spinal level. No significant differences were found for failure strain, or failure mode. There were also no significant differences for failure force or stress for gender and spinal level effects. The LF was found to have significant failure force and stress differences from the ALL and PLL (but no difference found between ALL and PLL). Significant rate effects were found when comparing to a previous quasi-static study (Yoganandan et al., 2000). Results can be seen in Table 4-3 and Table 4-4.

Ivancic et al. (2007) performed high deformation rate tests on the five primary ligaments as well as the middle-third disc; the portion of intervertebral disc and vertebral body portions remaining after ALL and PLL bone-ligament-bone complexes have been transected. Six cadavers were used, average age 81 (71 to 92) years, yielding 97 total ligament specimens. Spines were dissected into functional spinal units of either C3-C4, C5-C6, and C7-T1, or C2-C3, C4-C5, and C6-C7, and each FSU was sectioned to isolate the ligaments, before securing the bony ends with bonding resin into grip mounts. ALL and PLL ligaments were secured with a plastic plate and screws at the vertebral body to increase the connection strength of the ligament to the vertebral bone. Ligaments were preloaded to a tensile load of 5 N (defined as zero elongation) and tested using a pneumatic cylinder at an average rate of

723 mm/s (standard deviation: 106). Peak force, elongation and energy-absorbed values were reported, as well as stiffness at 25%, 50%, and 75% of peak force. This study observed rate effects for increased strain rate leading to higher failure force, smaller failure elongation, increased stiffness, and absorbing less energy compared to previous studies at quasi-static rates. Results can be seen in Table 4-3. This group also performed the identical study on ligaments procured from spines previously used for whole-spine whiplash trauma experiments (Tominaga et al., 2006). The ligaments which had sustained whiplash trauma were reported to have a significantly lower failure force.

The study also calculated average physiological elongations using a mathematical finite element model, and compared the tensile test results to the numerical physiological ranges. Some LF and ISL specimens failed within the physiological region, leading investigators to conclude these ligaments play a very minor role in spine stability. Similar stability results have been shown in a previous study in which a physiological load was applied to an FSU, and range of motion was measured as ligaments were slowly transected (Panjabi et al., 1975).

Studies followed different testing protocols which are summarized including the average age of specimens in Table 4-5.

Table 4-3: Combined results from high rate ligament tests (force, elongation, stiffness)

Ligament	Failure Force (N)			Failure Elongation (mm)		Stiffness (N/mm)	
	Yoganandan	<i>Bass</i>	<i>Ivancic</i>	Yoganandan	<i>Ivancic</i>	Yoganandan	<i>Ivancic</i>
ALL	350(45)	400 (239)	138 (112)	6.3 (0.6)	4.0 (1.0)	83 (7)	50 (53)
PLL	-	435 (289)	164 (80)	-	4.2 (1.5)	-	72 (50)
CL	-	-	220 (84)	-	4.9 (1.4)	-	69 (34)
LF	335 (28)	231 (119)	244 (143)	7.9 (0.7)	4.2 (1.5)	93 (13)	118 (83)
ISL	-	-	86 (68)	-	5.9 (2.9)	-	22 (13)

Average (SD) values

Table 4-4: Combined results from high rate ligament tests (stress, strain, and modulus)

Ligament	Failure Stress (MPa)		Failure Strain		Modulus (MPa)
	<i>Shim</i>	<i>Bass</i>	<i>Shim</i>	<i>Bass</i>	<i>Shim</i>
ALL	22.0 (5.7)	33 (20)	0.22 (0.06)	1.33 (0.73)	187 (83)
PLL	23.0 (12.9)	33 (25)	0.32 (0.12)	1.26 (0.78)	189 (164)
CL	7.2 (3.3)	-	0.39 (0.14)	-	27 (14)
LF	8.1 (2.5)	5.3 (2.8)	0.41 (0.23)	1.58 (1.56)	37 (15)
ISL	1.9 (1.4)	-	0.28 (0.09)	-	10 (5)

Average (SD) values

Table 4-5: Average age and testing conditions of previous studies

Previous Study	Age	<i>in vivo</i> Conditions	Preconditioning	Grip Method
Chazal et al (1985)	55 (50-60)			
Myklebust et al (1988)	67 (34-83)			Pins
Yoganandan et al (1998)	68			Pins
Yoganandan et al (1989)	70 (46-88)		Yes	Pins
Shim et al (2005)	58 (40-69)			Resin
Ivancic et al (2007)	81 (71-92)			Resin
Bass et al (2007)	60 (52-68)	Yes	Yes	Resin
Przybylski et al (1996)	80 (58-95)		Yes	Resin

4.4 Craniovertebral Ligament Studies

Many craniovertebral ligaments were tested by Myklebust et al. (1988) and Pintar (1986) when the quasi-static study was performed on all spinal ligaments. The ligaments investigated were the anterior and posterior atlanto-occipital membranes, the anterior and posterior atlanto-axial membranes (referred to in the study as ALL and LF respectively, at the C1-C2 spinal level), tectorial membrane, joint capsules (Occiput-C1, C1-C2), apical ligament, alar ligaments, and vertical cruciate ligament.

The only ligament of note that was not tested was the transverse ligament, perhaps due to only being attached to the atlas; the testing method used did required two vertebrae to grip. A minimum of three of each ligament was tested at a rate of 10 mm/s, using the same aforementioned techniques. The main difference between the force-deflection curves was the craniovertebral ligaments typically had a longer toe region than the ligaments from the rest of the spine, which was thought to be due to the increased range of motion of the craniovertebral joint. The results can be seen in Table 4-6.

Table 4-6: Craniovertebral ligament property summary (Myklebust et al., 1988; Pintar, 1986)

Ligament	Spinal Level	Failure Force (N)	Failure Elongation (mm)	Stiffness (N/mm)
AAOM	OC-C1	232 (23)	18.9 (2.7)	16.9 (3.2)
PAOM	OC-C1	83 (17)	18.1 (2.7)	5.7 (0.4)
AAAM	C1-C2	263 (152)	11.8 (7.0)	24.0 (11.7)
PAAM	C1-C2	111 (85)	9.6 (4.3)	11.6 (11)
TM	OC-C2	76 (44)	11.9 (2.5)	7.1 (2.3)
CL	OC-C1	320 (129)	9.9 (8.4)	32.6 (28.0)
	C1-C2	314 (143)	9.3 (4.5)	32.3 (23.5)
Apical	OC-C2	214 (115)	8.0 (5.3)	28.6 (29.0)
Alars	OC-C2	357 (220)	14.1 (7.2)	21.2 (15.7)
Cruciate	OC-C2	436 (69)	12.5 (4.9)	19.0 (0.2)

Average (SD) values

Dvorak et al. (1988) performed tensile tests on the alar and transverse ligaments. Seven cadavers were used, average age 76 (45 to 90) years old. The initial dimensions were recorded for left and right alar ligaments, and the transverse ligament. Strength values were reported, as ligaments were tested to failure at a rate of 1 mm/s, using a hydraulic Instron testing machine. No difference was found between left and right alar ligaments, and the average failure force was 213.7 (68.7) N. The average failure force for the transverse ligament was 354 (168) N.

Shim et al. (2006) also performed quasi-static and high rate tensile tests on two craniovertebral ligaments using the split Hopkinson bar. Two alar ligaments and three transverse ligaments were tested. Since alar ligaments contain a left and right portion, one was tested at the slow rate (0.005 s^{-1}) while the other from the same spine was tested at a high rate (approximately 1700 s^{-1}). Since only one transverse ligament was available from each spine, each specimen was tested at the quasi-static rate (to 10% strain) where no failure occurred, then tested to failure high rate (approximately 570 s^{-1}). The results showed significant rate effects consistent with the primary ligaments; force and stiffness increased, and elongation decreased with rate. Results can be seen in Table 4-7 comparing results from quasi-static and high rate tests.

Table 4-7: Alar, transverse ligament properties at quasi-static and high rates (Shim et al., 2005)

		Elastic Modulus (MPa)	Failure Stress (MPa)	Failure Strain (%)
Alar	Quasi	11.7 (5.1)	4.3 (1.3)	71.7 (4.6)
	High	46.6 (14.0)	10.9 (1.3)	34.4 (6.6)
TL	Quasi	42.6 (5.5)	7.7 (1.1)	25.4 (0.6)
	High	294.2 (14.0)	15.2 (3.4)	6.7 (1.6)

Average (SD) values

Panjabi et al, (1998) performed tensile tests at slow and fast extension rates to determine the mechanical properties of the alar and transverse ligaments. Eleven cadavers were used, mean age 49 (37 to 53) years old to test a total of 19 alar and 11 transverse ligaments. Specimens were constantly hydrated with physiologic saline solution (0.9% NaCl) during dissection and preparation. Ligaments were isolated into bone-ligament-bone complexes and potted into using a quick setting polyester resin after bones had been secured by drilling holes and inserting pins. A custom pneumatic testing apparatus was used, with a gap to allow the piston to reach a constant rate before engaging the ligament. Ligaments were initially tested at a slow rate of 0.1 mm/s to an estimated sub-injury load of 70 N (Alar), and 140 N (TL), as a previous study (Dvorak et al., 1988) had documented these ligaments to fail at average load of 200 N and 350 N respectively. Force-deformation curves were fit

to a second order polynomial, and any ligaments thought to have sustained damage, by a sudden drop in force greater than 2 N, were not used for high rate testing. Five alar and four TL were deemed suitable for fast testing at average speeds of 920 mm/s. Significant rate effects were found for both ligaments with increased failure force and stiffness, and decreased failure elongation with increased rate. Results can be seen in Table 4-8, where high rate data is compared to the data from the Shim et al. (2005) study. Results are comparable for failure force, but stiffness values are significantly higher for the Panjabi et al. (1998) study, despite the elongation rate being significantly lower; 920 mm/s compared to approximately 12,000 mm/s.

Table 4-8: Alar and transverse ligament property comparison (Panjabi et al., 1998; Shim et al., 2005)

			Stiffness (N/mm)	Failure Force (N)	Failure Strain (%)
Alar	<i>Panjabi</i>	Quasi	80.1 (9.4)	-	-
		High	2316 (888)	367 (83)	3.1 (1.3)
	<i>Shim</i>	High	244.9 (98.4)	398 (69)	34.4 (6.6)
TL	<i>Panjabi</i>	Quasi	141.3 (21.3)	-	-
		High	1472 (691)	436 (55)	2.3 (0.9)
	<i>Shim</i>	High	260 (68)	269 (24)	6.7 (1.6)

Average (SD) values

4.5 Limitations of Previous Isolated Ligament Studies

From the tables above (Table 4-2 and Table 4-3) of the combined data from previous studies it can be seen there is a lack of consistency as to which and how parameters were measured and reported. This makes it inherently difficult to make comparisons. The tests are also not performed at constant strain rates. Some tests used constant elongation rates which do not correspond to constant strain rates due to different ligament lengths. In addition, age effects and testing conditions are significant areas where improvement is necessary.

4.5.1 Age Limitations

All prior studies of the primary cervical spine ligaments have data gathered from older post mortem human subjects, the youngest average age was 58 (50 to 60) years old (Chazal et al., 1985). As mentioned previously, ligament properties strengthen to about age 20, followed by a decrease in strength and stiffness (Cowin et al., 2007). It has also been shown in prior studies that mechanical properties of the cervical spine decrease with increasing age of specimens (Neumann et al., 1992; Neumann et al., 1994; Tkaczuk, 1968; Nachemson et al., 1968).

No previous studies have directly investigated the age effect on cervical spine ligaments; however these effects have been explored in lumbar ligament studies. One lumbar spine ligament study of the ALL and PLL associated decreases in failure force, stress, and elongations with increased age (Tkaczuk, 1968). Age effects have also been observed in the LF at the lumbar level (Nachemson et al., 1968), as failure stress and modulus of elasticity was found to decrease by a factor of four between the ages of 20 to 80.

A study by Iida et al (2002) tested the effects of aging and spinal degeneration on lumbar ISL and SSL properties. Failure force and elastic stiffness were measured and were both found to decrease with age, however no correlation was found with disc degeneration and ligament properties. Both tensile strength and elastic modulus values were shown to decrease by about 50% from age 40 to age 80.

Significant discrepancies between previous studies comparing lumbar ALL failure forces have been attributed to age differences (Neumann et al., 1992). Neumann et al. (1992) reported average failure forces of 1060 (304) N (specimens aged 21 to 43), Chazal et al. (1985) reported forces of 511 (47) N (ages 63 to 80), and Pintar et al. (1986) reported forces 444 (267) N (mean age 67). Forces were shown to decrease by over 50% with an average age increase of 35 years. Chazal et al. (1985) and Pintar et al. (1986) also reported properties for cervical spine ligaments in the same studies using older cadavers.

Increased cadaver age, and decreased vertebral mineral content were shown to have a strong effect on isolated lumbar ALL specimens (Neumann et al., 1994) particularly at slow elongation rates, as the strength decreased by a factor of 2 (29 to 13 MPa) over the age range of 21 to 79 years old, and stiffness differed by as much as 5 times across regions (increased stiffness at mid substance, and decreased stiffness at insertion point) of the ligament compared to younger specimens. Increased bone mineral content was also shown to increase failure elongation (Neumann et al., 1994).

4.5.2 Testing Conditions Limitations

Most previous studies do not test specimens under *in vivo* conditions. Many studies kept the ligaments hydrated with a saline solution, but only one study (Bass et al., 2007) also tested the ligaments at body temperature of approximately 37.8° C. A study in 2007, published after most ligament test studies, showed that the ALL ligament in porcine specimens exhibited strong temperature dependence (Bass et al., 2007), and due to the similarity between porcine and human ligaments, temperature must be taken into account especially for dynamic responses. The porcine ligaments were shown to have a 70% increase in failure force and a 57% increase in stiffness (Figure 2-1) when specimens were dynamically tested at room temperature (21.1°C) compared to body temperature (37.8°C), thus data from previous studies may be represented as stiffer than under normal physiological conditions. Only the ALL, PLL and LF have been tested at *in vivo* conditions, while there have been no previous tests on the CL, ISL or craniovertebral ligaments at representative temperature and humidity environments.

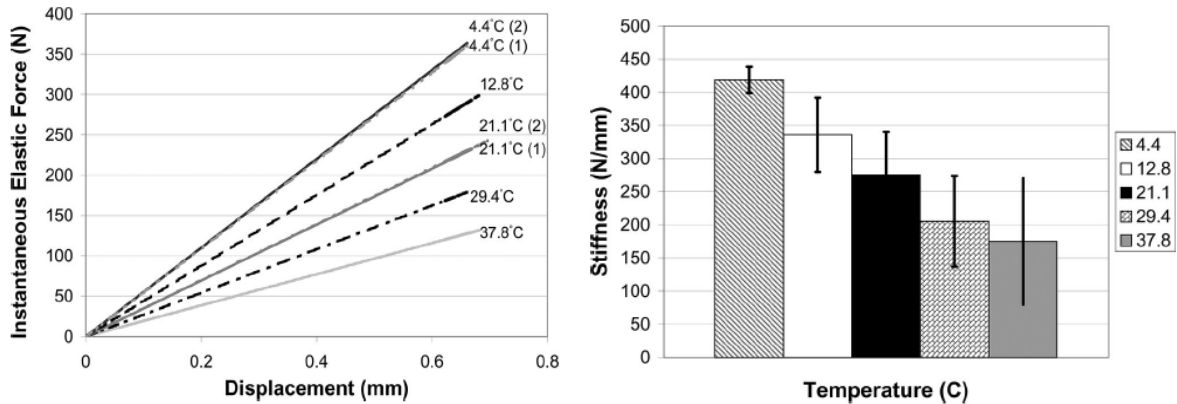


Figure 4-4: Temperature-dependent viscoelasticity of porcine spinal ligaments (Bass et al., 2007)

Preconditioning of the ligaments was not always performed prior to ligament testing in previous studies. Preconditioning of the ligaments is important as it returns the structural collagen fibers to proper physiological conditions by removing any crimping in the ligaments as a result of being stored in a frozen and fixed position (Hashemi et al., 2005), and results in a response that is repeatable and more representative of normal physiological response (Van Ee et al., 2000).

The method of gripping the ligament specimens is also inconsistent among previous studies, as several studies use Steinmann pins to secure the vertebral bodies, while other studies use a resin potting method. The use of pins to secure vertebral structures in ALL lumbar testing has been shown to account for up to 40% of the specimen strain when comparing values between crosshead deformations and image captured marker strains on the ligament surface, due to localized strains at the pin insertion sites (Neumann et al., 1992).

4.5.3 Uninvestigated Effects

The post failure response has never been reported, which is shown to affect the kinematic response of cervical spine finite element models (DeWit et al., 2010). Previous studies that show force-deformation curves usually only display the curve to the point of failure, or shortly afterwards to demonstrate the drop in force. If the ligaments do not instantaneously fail at this point, however still

support a load, albeit a lesser load, it will still contribute to the response. In a finite element model, if the ligament fails instantaneously, the entire load must be immediately shared between other components. By reporting the post-failure region, ligament properties in finite element models can be modified to represent the failure mode, and improve kinematic spine response.

A comprehensive investigation of gender and spinal level effects at strain rates applicable to automotive crash scenarios has also not been explored in enough detail. One study testing ligaments at high rates compared gender and spinal level and found no significant effects (Bass et al., 2007), as sample size was relatively small. A quasi-static study by Yoganandan et al.(1998) evaluated the effect of spinal level for the six different levels but results were inconsistent. When the spinal levels were divided into six levels, each level had only two to six samples. With the high level of scatter in biological testing and so few samples, any outliers would have a dramatic effect on the statistical analysis.

Mechanical properties are very limited for the craniovertebral ligaments. Only one study performed tests on all the ligaments spanning multiple vertebrae at quasi-static rates (Pintar, 1986; Myklebust et al., 1988). Two studies performed both quasi-static and high rate tests on the alar and transverse ligaments, and produced very similar results for failure force; however there was a large discrepancy between stiffness values between the two studies. Since most craniovertebral ligaments are singular in each spine, and due to the complexity of the craniovertebral joint, it is impossible to isolate and test all ligaments from one spine; any additional data from these ligaments proves to be valuable.

The lack of consistency between studies leads to great difficulties when trying to combine and compare ligament properties. Each study is unique in how the ligaments are defined and prepared, the age of specimens used, the environmental conditions, preconditioning and elongation rates the tests are conducted at, as well the metrics which are measured from produced force-deflection curves. A more consistent protocol is required, in which all variables remain relatively constant to reduce the effects of external factors (age, preparation techniques, test conditions, etc), and isolate the effects of factors hypothesized to influence neck response (elongation rate, gender, spinal level).

4.6 Relevant Findings from Segment and Whole-Spine Studies

There have been several studies performed on cervical spine segments and whole-spine specimens under various loading mechanisms. These studies are primarily useful for quantifying injury, correlating injury to loading mechanisms, and providing useful validation cases for numerical studies. Although ligament properties are usually not investigated in detail, some findings from the studies may be directly related to ligament mechanical properties and provide justification for ligament property investigations.

Ligaments have been shown to be loaded in tension from compressive loading to the head, in whole-spine testing, due to flexion/extension of the neck, depending on the orientation of the spine prior to impact. Damage to the PLL and ALL were shown to occur in flexion and extension respectively, due to an axial impact to the crown of the skull of cadaver subjects at speeds from 2.5 m/s to 8 m/s (Pintar et al., 1995). Variation in responses was thought to be attributed to age and gender effects.

A study has shown that increase in age results in a decrease in failure force of whole cervical spines under compressive loading (Pintar et al., 1998). An interaction was also found between loading rate and age, where rate effects decrease with an increase in age. Since most failures occurred in the bone, the interaction may be attributed to the degradation of bone with age, as the alteration of bone marrow content may affect viscosity (Pintar et al., 1998). This may also affect ligament properties, as ALL and PLL properties have been shown to correlate with bone mineral content in the vertebrae (Neumann et al., 1994).

4.6.1 Level Effects

The mid-cervical spine (C2-C5) was shown to be significantly stiffer than the lower region (C5-T1) in compression and in extension tests performed on respective segments of four adjacent vertebrae (Shea et al., 1991). Failure occurred in the soft tissues prior to bone fractures in all specimens. This may suggest spinal level differences in the soft tissue properties.

Range of motion in flexion and extension was found to be significantly greater in the C5-C6 ($22.8 \pm 2.3^\circ$) compared to the C7-T1 ($13.8 \pm 2.8^\circ$), and C7-T1 was shown to be significantly stronger in flexion than C3-C4, in cervical spine segment tests (Nightingale et al., 2002). Another study found

different ranges of motion in whole cervical spine specimen impact testing, where the middle regions (C4-C5, C5-C6) had larger ranges of motion, although not significantly different (Ito et al., 2004). These findings also suggest possible level effects.

4.6.2 Gender Effects

Gender differences have been found in a study investigating the range of motion of the head and neck among young and healthy volunteers (aged 19 to 25), where female subjects had a larger range of motion in flexion and extension, lateral bending, and rotation (Ferrario et al., 2002). Range of motion studies performed on cervical spine segments also reported a significant difference between genders, where the female range of motion was greater at all levels (Stemper et al., 2003).

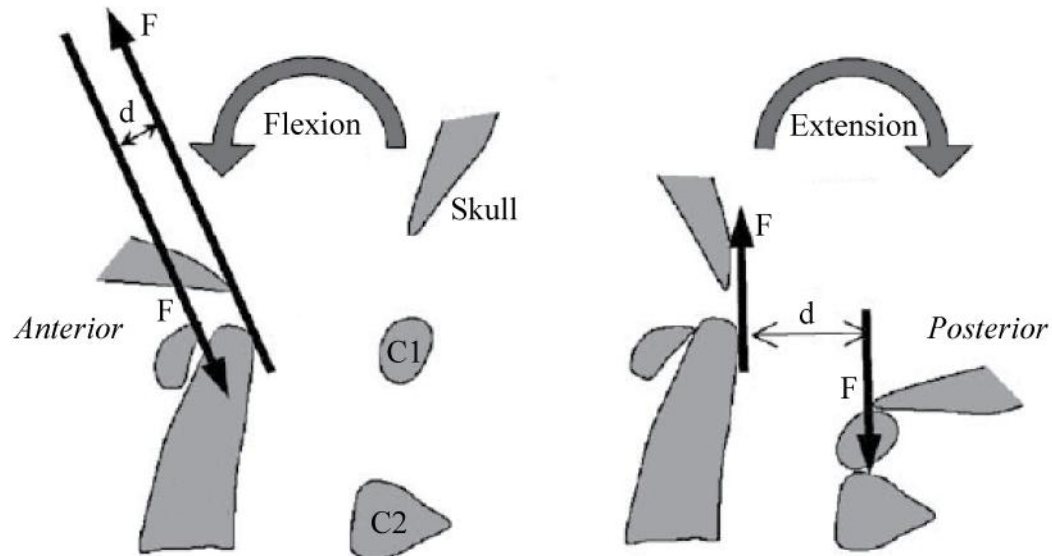
In a cervical spine segment study testing specimens to failure in flexion, male specimens were found to be significantly stiffer and stronger than female specimens (Nightingale et al., 2007), as male subjects failed under greater moment in flexion, and had a larger range of motion in both flexion and extension than female ligaments. Gender differences may likely be attributed to differences in size, as the larger male specimens could support a larger load (Nightingale et al., 2007).

The study by Pintar et al (1998), where significant age effects were found in compressive loading of whole cervical spines, also found gender effects. The study found significant gender effects where female specimens failed at 75% the failure force of male specimens. Since most samples were from the 50 to 95 year old range, this could be a result of osteoporosis in elderly female subjects, so the study recommended that gender comparisons be made amongst younger populations.

4.6.3 Craniovertebral Segment Studies

The mechanical properties of the ligaments that connect the dens to the skull are important, as these ligaments are thought to play a significant role in tensile loading of the dens, resulting in fracture (Nightingale et al., 2002; Nightingale et al., 2007). Under flexion, the compression force of the skull and the anterior arch of the C1, and the tensile force of the ligaments on the dens create a couple moment (Figure 4-5). In extension, the posterior elements are under compression, holding C2 in place, while the skull moves upwards, creating increased tension in the ligaments and force on the dens. For a specified moment, the shorter moment arm in flexion (d , as seen in Figure 4-5), requires a

greater reaction force generated by the ligaments in tension from the dens. The greater force results in increased risk of fracture in flexion compared to extension, and are consistent with lower moment tolerances in flexion compared to extension found in the study (Nightingale et al., 2002). These findings stress the importance of accurate craniovertebral ligament properties for mathematical modeling.



Adapted from Nightingale, et al. (2002)

Figure 4-5: Couple moment in craniovertebral joint causing fracture due to increased tension on dens

Under lateral bending, both the Skull-C1, and C1-C2 segments contribute the equivalent amount to the range of motion (Goel et al., 1988). There was also no difference found in range of motion between left and right lateral bending of the Skull-C2 complex (Goel et al., 1988), suggesting that ligament properties are symmetrical between left and right portions. The study also recommends testing on younger specimens.

Failure mode was seen to transition from bone fracture (dens) to mid-substance ligamentous failure (alar), as Skull-C2 segments were tested in axial rotation at increasing strain rates (Chang et al., 1992). This suggests the strain rate effect on increasing stiffness reduces the failure elongation of the

alars, causing injury at smaller deformations. The effect of increasing strain rate on stiffness was shown to have an upper bound, as there were no significant effects on stiffness, or failure torque between 100°/sec and 400°/sec loading rate (Chang et al., 1992).

Chapter 5

Methods

5.1 Cadaver Morphology

The research methods employed in this study were approved by the Office of Research Ethics at the University of Waterloo. Cadaver age was limited to younger than 50 years old as the prevalence of osteoporosis has been shown to dramatically increase over the age of 50, especially in females (Kanis et al., 1994; Vernon-Roberts et al., 1973), and it has been shown that spinal ligament properties are closely related to vertebral bone mineral density (Pintar et al., 1998; Neumann et al., 1994). An upper limit of 50 years old also ensured that a sufficient quantity of spine samples was available, as younger spines were inherently more difficult to acquire.

A total of 17 cadaver cervical spines (8 male and 9 female) were tested with an average age of 44 (27 to 50) years old, height 167 (145 to 184) cm, and body mass 67.1 (36.8 to 159.1) kg. For each spine used, medical history was reviewed to ensure no spinal disease or previous injuries had occurred. Full cadaver spine statistics can be seen in Table 5-1. Cervical spines (Skull-T2) were acquired from Sciencecare Inc. (Phoenix, AZ) and National Disease Research Interchange (NDRI, Philadelphia, PA) and were kept frozen until thawed for preparation and testing. It has been shown that freezing ligaments has little or no effect on the viscoelastic or structural properties (Woo et al., 1986), furthermore, refreezing of ligament specimens has also been shown to have little or no effect on the mechanical properties (Moon et al., 2006). Spine *E* consisted of C2-T1 (only primary ligaments), and Spine *Q* consisted of only C1-C2 (only craniovertebral ligaments). As mentioned previously, primary *ligaments* are defined as the ligaments existing between C2-T1.

Table 5-1: Cadaver spine statistics

Spine ID	Age	Gender	Height (cm)	Weight (kg)	Supplier	Cause of Death
A	46	M	177.8	65.9	Science Care	Pancreatic cancer
B	46	M	180.3	63.6	Science Care	Malignancy of sinus
C	36	M	175.3	60.9	Science Care	Liver disease
D	27	M	152.4	68.2	Science Care	Sepsis
E	48	F	162.6	48.6	NDRI	Sepsis
F	47	F	162.6	45.0	Science Care	Melanoma
G	49	F	165.1	59.1	Science Care	Breast cancer
H	48	F	170.2	159.1	Science Care	Pulmonary fibrosis
I	48	M	182.9	56.4	Science Care	Myotonic muscular dystrophy
J	44	M	154.9	63.6	Science Care	Compression asphyxia
K	47	F	162.6	77.3	Science Care	(Pending toxicology)
L	47	F	162.6	40.9	Science Care	Respiratory failure
M	43	M	170.2	63.6	Science Care	Cancer of liver
N	45	F	147.3	72.7	Science Care	Cancer
O	50	F	152.4	36.8	Science Care	Cervical cancer
P	40	M	185.4	93.2	Science Care	(Pending toxicology)
Q	29	F	167.6	65.9	NDRI	Glioblastoma

5.2 Ligament Isolation and Preparation

Spines were thawed for isolation, and soft tissues were transected from between adjacent vertebral bodies (at every second intervertebral junction) to section the spine into functional spinal units (FSUs), each consisting of two vertebrae with connecting soft tissues (Figure 5-1). Each spine yielded three FSUs depending on how they were sectioned; C2-C3, C4-C5, and C6-C7, or C3-C4, C5-C6, and C7-T1 (Figure 5-2). The remaining craniovertebral segment from each spine could

produce ligaments from either Skull-C1, or Skull-C2. Thus, two spines were required to produce ligaments from every spinal level.

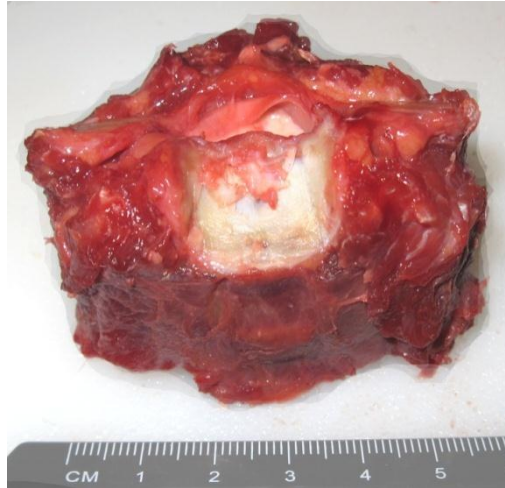
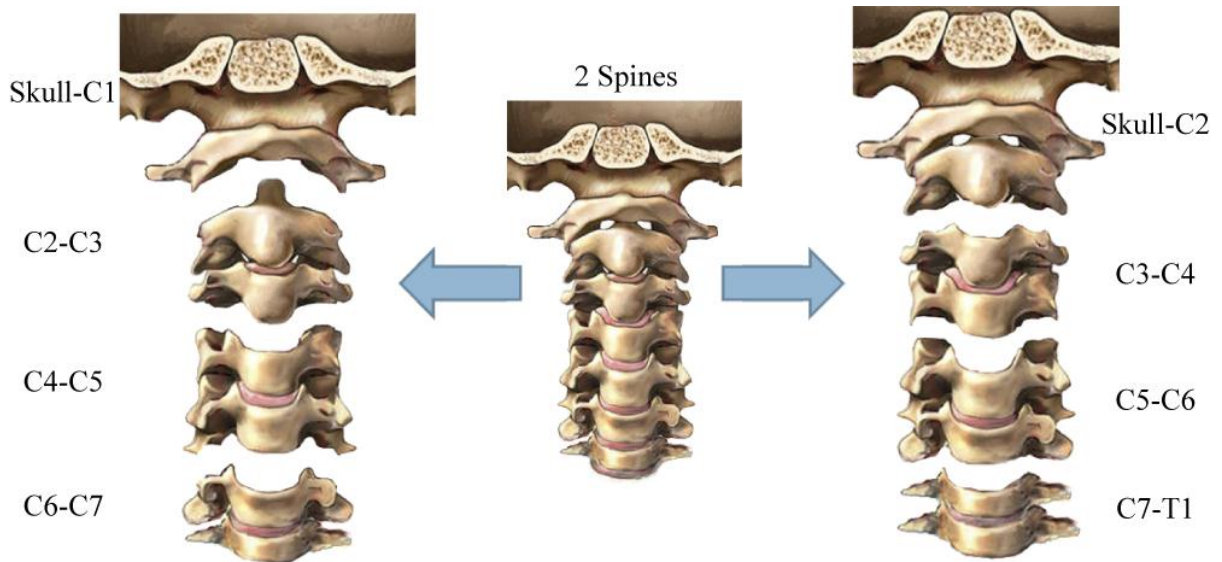


Figure 5-1: Functional spinal unit without soft tissues removed

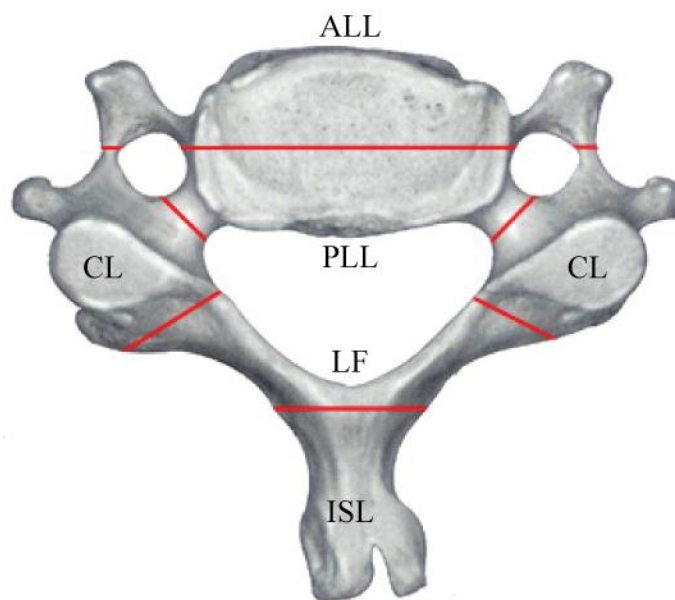


Adapted from www.hon.nucleusinc.com

Figure 5-2: Cervical spine sectioned into FSU's two different methods

5.2.1 Primary Cervical Spine Ligament Isolation

Non-ligamentous soft tissue, such as muscle, fascia, blood vessels, and nerve roots were carefully removed from the FSU segments to expose as much bone and ligament as possible. FSUs were then cut perpendicular to the transverse plane using a band saw, at the same location on the bone at both the superior and inferior vertebrae (Figure 5-3) to isolate specimens into bone-ligament-bone complexes. The primary ligaments to be tested were the anterior longitudinal ligament (ALL), posterior longitudinal ligament (PLL), capsular ligaments (CL), ligamentum flavum (LF), and interspinous ligament (ISL).



Adapted from www.ispub.com

Figure 5-3: FSU cuts to isolate ligaments

Initially, the spinous process was cut as close to the vertebral foramen as possible (Figure 5-3), with close attention not to damage the ligamentum flavum, in order to isolate the interspinous ligament. The lamina was then cut on each side of the LF adjacent to the facet joints, without damaging the capsular ligaments in order to isolate the LF. The transverse processes and pedicles of each spinal unit were then cut to isolate the CL's and vertebral bodies, which were still connected by the intervertebral disc and ligaments. The vertebral bodies were then cut along the coronal plane to

divide the segment into the anterior longitudinal ligament and posterior longitudinal ligament. Soft tissues were carefully transected from each specimen to leave only the ligament under study, as identified by the fibrous appearance; except for the LF, which had a characteristic yellow colour. To isolate the ALL and PLL, the intervertebral disc was removed from the centre of the vertebral bodies until the vertical ligament fibres could be distinguished from the removed oblique annulus fibres. This procedure produced six bone-ligament-bone complexes from each FSU, to be tested *in situ*, as ligaments were not removed from bony insertions (Figure 5-4). Each FSU contained two capsular ligaments which were tested separately. This method procures more samples than leaving the vertebrae intact and transecting all other ligaments, except for the desired ligament.

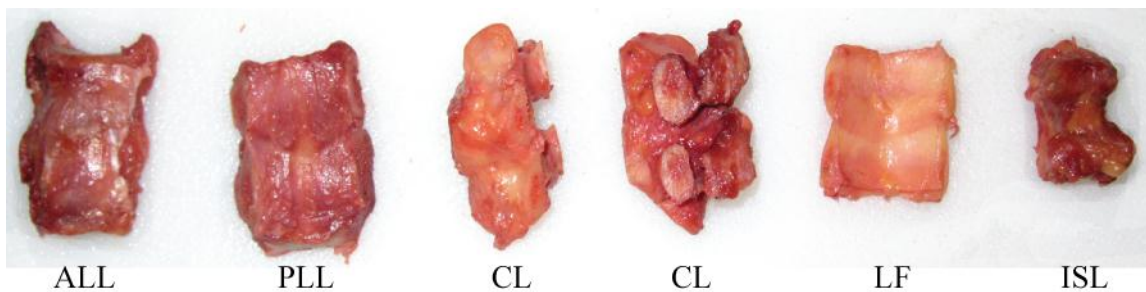


Figure 5-4: Isolated cervical spine bone-ligament-bone complexes

Of a possible 288 tentatively available ligaments, 277 were successfully isolated; a 96% success rate. Eleven ligaments were either damaged prior to shipment, or damaged in the isolation process. A minimum of 4 ligaments were procured for each spinal level, but on average 8 ligaments were isolated from each level; not including the CL which averaged 15 per level, due to 2 ligaments available at each level. The ligament quantity by spinal level matrix is seen in Table 5-2.

Table 5-2: Isolated ligaments by spinal level matrix

	ALL	PLL	CL	LF	ISL
C2-C3	6	6	11	6	6
C3-C4	9	10	20	8	10
C4-C5	6	6	11	4	6
C5-C6	10	10	20	9	10
C6-C7	6	6	10	6	6
C7-T1	10	10	20	9	10
Total	47	48	92	42	48

Ligament lengths were defined as the distance between bony attachment points along the direction of physiological loading and fibre orientation, and measured using digital calipers. Average ligament lengths by spinal level can be seen in Table 5-3. The ALL and PLL length measurements were defined as the distance between endplates of the respective vertebral bodies. This technique was used to correspond with how the ligament lengths were represented in the finite element model used to determine appropriate strain rates (Fice et al., 2009). Measurements were also taken from centre to centre of adjacent vertebral bodies for the ALL and PLL in order to calculate ligament areas according to the length-area ratio method presented by Yoganandan et al. (2000).

Table 5-3: Ligament length measurements (mm) by spinal level

	ALL	PLL	CL	LF	ISL
C2-C3	4.5 (0.3)	4.2 (0.8)	3.8 (1.2)	7.3 (0.9)	10.7 (1.6)
C3-C4	4.3 (1.5)	4.3 (1.1)	3.9 (0.6)	7.4 (1.1)	8.9 (1.7)
C4-C5	5.2 (1.2)	4.3 (0.8)	4.5 (1.1)	8.3 (1.1)	9.7 (1.1)
C5-C6	4.2 (1.4)	3.8 (0.9)	4.4 (1.1)	8.4 (1.1)	10.3 (1.6)
C6-C7	4.1 (0.7)	4.5 (0.4)	3.7 (0.3)	9.7 (2.1)	11.7 (2.5)
C7-T1	3.5 (0.8)	3.5 (0.8)	4.1 (0.8)	9.6 (1.0)	12.54 (2.28)
Average	4.2 (1.2)	4.0 (0.9)	4.1 (0.9)	8.5 (1.5)	10.63 (2.20)

Average (SD) values

5.2.2 Craniovertebral Ligament Isolation

Ligaments were isolated into the tectorial membrane/vertical cruciate/apical/alar ligament complex (TM complex, tested together for modeling purposes), transverse ligament (TL), anterior atlanto-occipital membrane (AAOM), posterior atlanto-occipital membrane (PAOM), anterior atlanto-axial membrane (AAAM), and posterior atlanto-axial membrane (PAAM). Each spine yielded only two ligaments: TM complex and TL, or AAOM and PAOM, or AAAM or PAAM.

The tectorial membrane covers the dens and transverse ligament and runs from C2 through the foramen magnum attaching to the central base of the cranial cavity, as the TL connects the lateral aspects of the C1 and passes beneath the TM and over the odontoid. To isolate the TM complex and TL, the posterior vertebral arch was cut from the C1, all bone was cut from the C2 except the vertebral body and the odontoid process, and the posterior section of the occiput was removed, as seen in Figure 5-5B. A notch was cut into the anterior arch of the C1, to initiate a stress point for fracture. The C1 was then snapped into two pieces, held together by the TL, as seen in Figure 5-5A. The TL was free to slide between the TM and the odontoid process, but could not be removed without damage to the TM complex. The TM complex was then tested, with the TL in place. The soft tissues were then transected from the Skull-C2 segment, isolating the TL for testing. The length of the TM

complex was defined as the distance from the base of the skull to the most superior connection point on the C2, the width was defined as the smallest width along the TM and the cross sectional area was measured after the tensile test. The length of the TL was easily measured as the distance between bony connection points when the ligament was fully elongated under slight tension, and the width and thickness were easily measured using digital calipers and very straight forward.

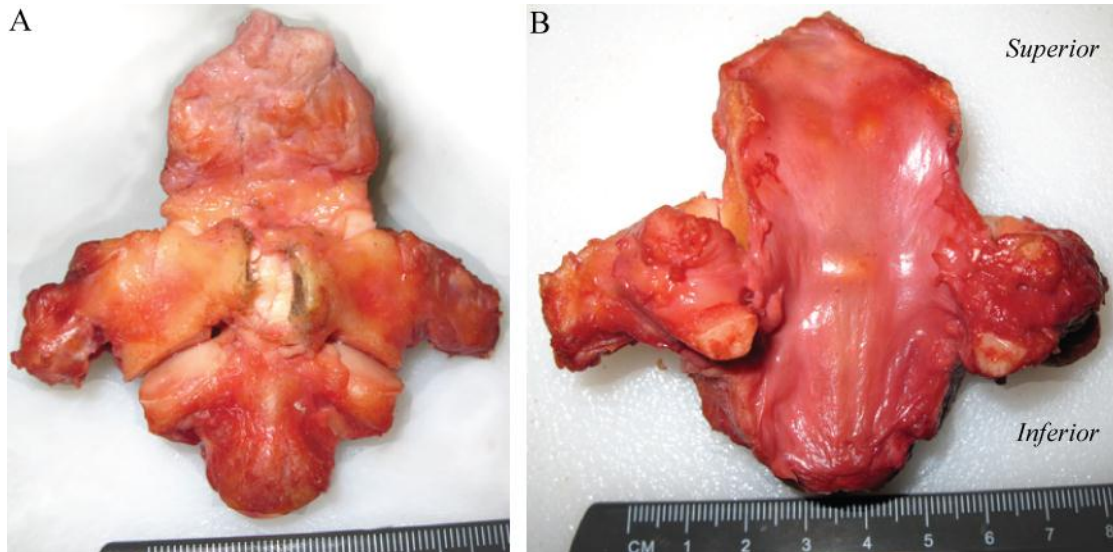


Figure 5-5: Skull-C2 segment with TM complex isolated. A - Anterior view, with fractured C1. B- Posterior view of TM

The AAOM and PAOM are the only two ligaments present on a Skull-C1 segment. The ligaments were too wide to fit inside the test fixture grips, so they were carefully separated into left and right portions along the direction of the fibres, with care to not damage any ligament fibers. The length of each portion was defined as the average of the medial and lateral lengths, the thickness was defined as the average of the medial and lateral thickness, and the shortest width was used to calculate area.

The AAAM and PAAM connect the C1 and C2 and are extensions of the ALL and LF, respectively. Only one specimen of each was tested due to limited spine availability. Lengths were calculated as the average of the middle and lateral lengths, width was defined as the narrowest point, and thickness was measured after testing to calculate areas.

The quantity of each craniovertebral ligament procured, average (SD) length and area measurements are shown in Table 5-4.

Table 5-4: Craniovertebral ligament quantity and dimensions

	Quantity	Length (mm)	Area (mm ²)
TM Complex	8	18.92 (3.88)	33.02 (5.46)
TL	6	20.79 (3.48)	18.89 (3.05)
AAOM	14	12.51 (2.16)	87.03 (28.38)
PAOM	14	13.92 (3.28)	48.84 (10.85)
AAAM	1	12.47	50.34
PAAM	1	15.72	21.55

5.2.3 Ligament Preparation for Testing

The bone ends of the ligament specimens were secured using wires, aluminum strips, copper rods and wood screws to prevent slipping and ensure a secure grip (Figure 5-6). Specimens were held into place within 1 3/4" diameter by 1" deep polyethylene cups, and potted using a fast casting resin (Fast Cast, Goldenwest MFG, Grass Valley, CA). After the resin cured, the other ends of the specimens were potted. The casting resin was used to firmly hold the bone ends and the interior of the cups were scored to increase friction and prevent any slipping of the hardened resin within the cup. Care was taken to ensure the ligaments did not get coated in resin that could otherwise interfere with measuring ligament properties. The specimens were potted with the ligament fibers aligned with the elongation axis of the test apparatus, such that the ligaments were tested at the same orientation as experienced under physiological loading conditions (Figure 5-7). Craniovertebral ligaments were prepared in a similar manner, with bone ends trimmed to fit into the cups.

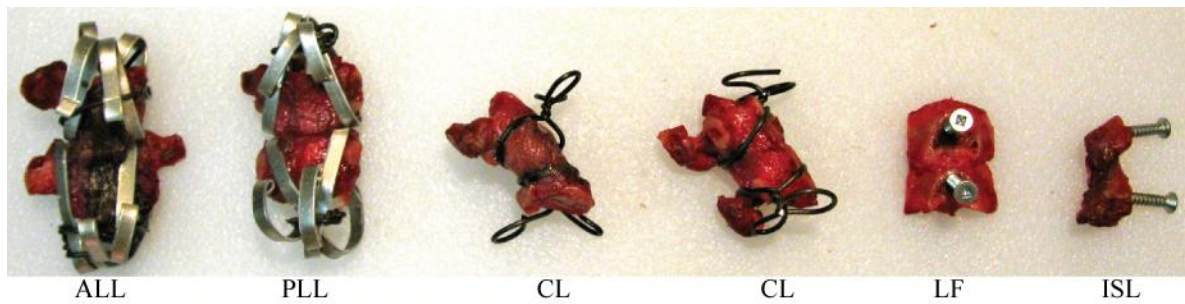


Figure 5-6: Ligaments secured with hardware before potting

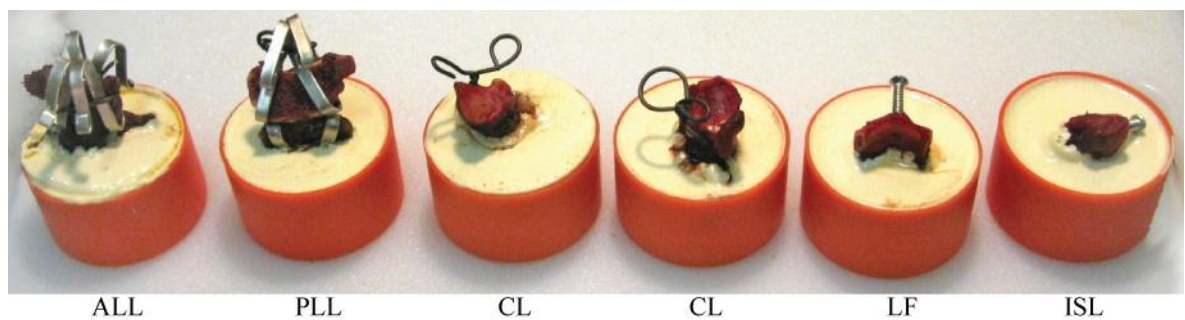


Figure 5-7: Ligament specimens half potted

The stiffness of the resin potting method was measured by potting a 3/8" steel bolt, and testing in tension. The stiffness of the fixture was found to be approximately 4000 N/mm (Figure 5-8). This corresponded to a worst case scenario of less than 6% strain of the primary ligaments (PLL), and a maximum of less than 10% strain of the craniovertebral ligaments (TM complex). This method was deemed sufficient compared to using Steinmann pins to secure vertebral bodies which has been shown to account for up to 40% of the ligament strain (Neumann et al., 1992).

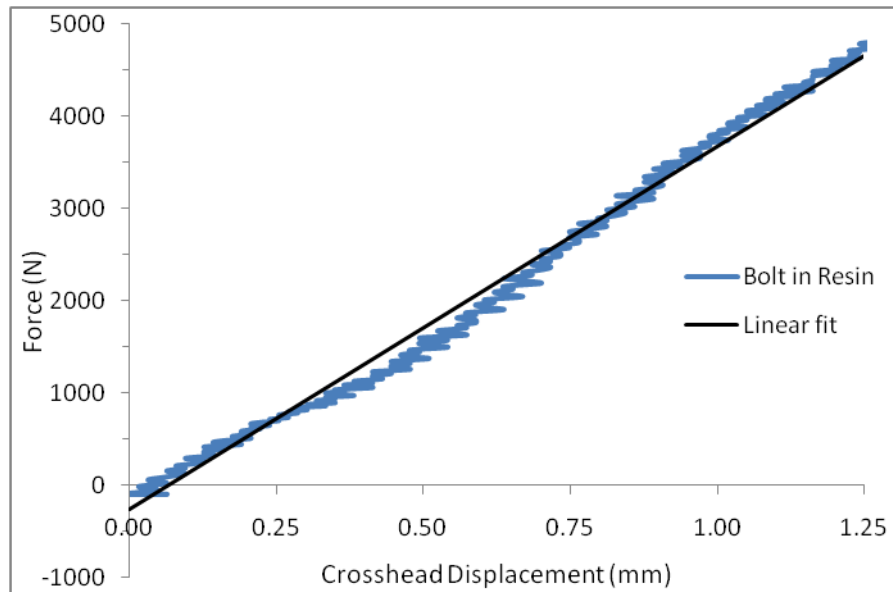


Figure 5-8: Stiffness of 3/8" steel bolt using resin and cup potting method

5.3 Testing Methods

Due to the importance of testing the ligaments at body temperature (Bass et al., 2007), the cooling rate of the ligaments needed to be investigated to determine if an environmental chamber was required, or if the ligaments could be heated prior to loading into the fixtures and testing. After the ligaments had been potted and ready for testing, they were heated in a saline solution warm water bath until they reached approximately 41°C. Ligaments were heated higher than body temperature, with care not to overheat and damage specimens, to determine the amount of time required to cool to body temperature (37.8°C). A thermocouple was placed inside the soft tissue surrounding the ligament, and the ligament was allowed to cool in a room of ambient temperature 23.3°C, and temperature was recorded at 30 second intervals. The ligaments cooled to below body temperature in less than 90 seconds as seen in Figure 5-9. It was determined that an environmental chamber was required.

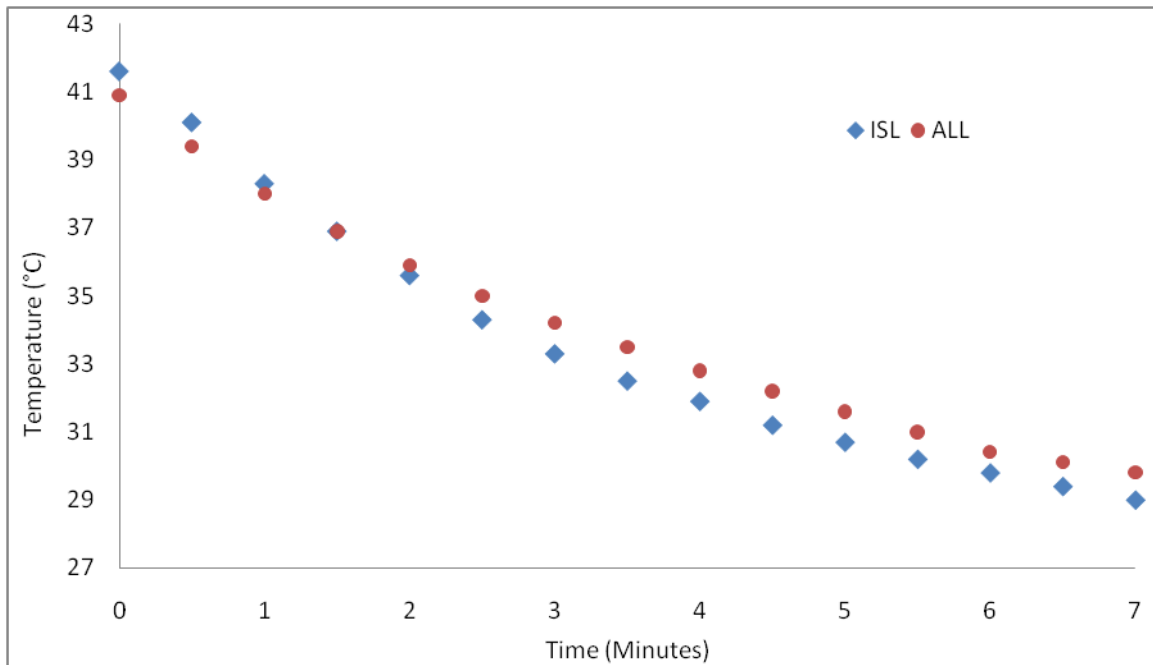


Figure 5-9: Ligament cooling time of ALL and ISL in 23.3°C ambient room temperature

Environmental chambers were constructed for each testing apparatus using Lexan (polycarbonate polymer) in order to view the specimen during testing, and prevent convective heat loss and drying of the ligaments. Heating coils were mounted inside the chamber to keep the specimen at body temperature, but mounted at a safe distance as to not damage the ligaments.

Ligaments were tested in tension at quasi-static (0.5 s^{-1}), medium (20 s^{-1}) and high ($150\text{-}250 \text{ s}^{-1}$) strain rates. The range of strain rates used in this study were identified based on the ligament response of a previously validated finite element cervical spine model (Fice, 2010; Fice et al., 2009) for a 22g frontal crash scenario. It was found for the 22 g loading case that the CL and ISL experienced higher strain rates as they are located further from the segment centres of rotation than the ALL, PLL and LF, which are located closer to the centres of rotation, located approximately in the centre of the inferior vertebral body (Bogduk et al., 2000). Consequently the CL and ISL were tested at 250 s^{-1} and the ALL, PLL and LF at 150 s^{-1} . All fast rate craniovertebral ligaments were tested at 150 s^{-1} .

Tests were performed at different elongation rates, based on initial ligament lengths to achieve constant desired strain rates across all samples. Quasi-static elongation rates ranged from 1 mm/s (PLL) to 8 mm/s (ISL), medium rates ranged from 60 mm/s (CL) to 331 mm/s (ISL), and high rates ranged from 465 mm/s (ALL, PLL) to 3,540 mm/s (ISL). All ligaments were preconditioned at a frequency of approximately 1 Hz, for 20 cycles to 10% strain (Figure 5-10), prior to being tested to failure, as consistent with previous studies (Bass et al., 2007).

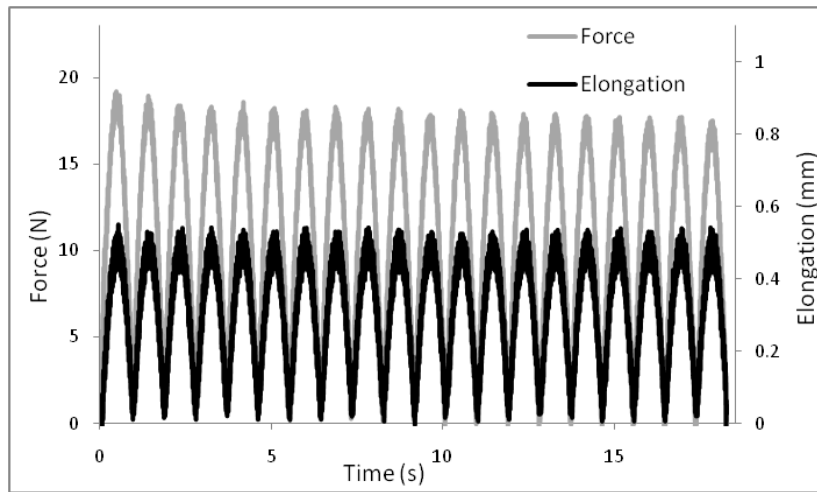


Figure 5-10: Force-time and elongation-time preconditioning loading cycles for typical ALL

The quasi-static tests were performed within an environmental chamber using a hydraulic tensile testing fixture (Figure 5-11). Specimens were loaded into the fixture at zero force preload and no slack in the ligaments, and cups were held into place with custom grips with machined grooves on the cup contacting surface to securely hold the specimen cups in place. Clamps were placed around the grips and tightly fastened to secure the testing specimen (Figure 5-12). Ligaments were continuously sprayed with saline solution to stay hydrated, and a thermocouple was placed in contact with the ligament to measure temperature, accurate within 0.1°C. A heating coil within the environmental chamber would gradually heat the ligament and surrounding air, and preconditioning and tensile testing to failure would begin when the temperature of the ligament reached approximately body temperature; 37.8°C ± 1°C. Force-elongation data were measured at a frequency of 500 Hz, and used

a 2225 N (500 lb) strain gauge load cell (Omegadyne Inc. Model LC412-500) to measure force and an LVDT to measure the specimen elongation.

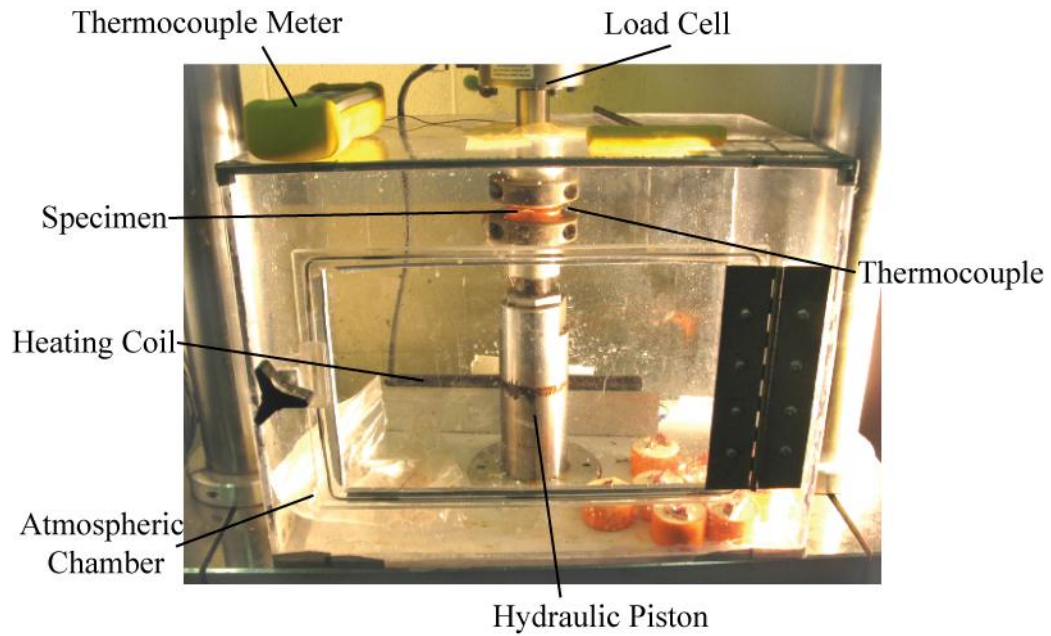


Figure 5-11: Quasi-static tensile fixture

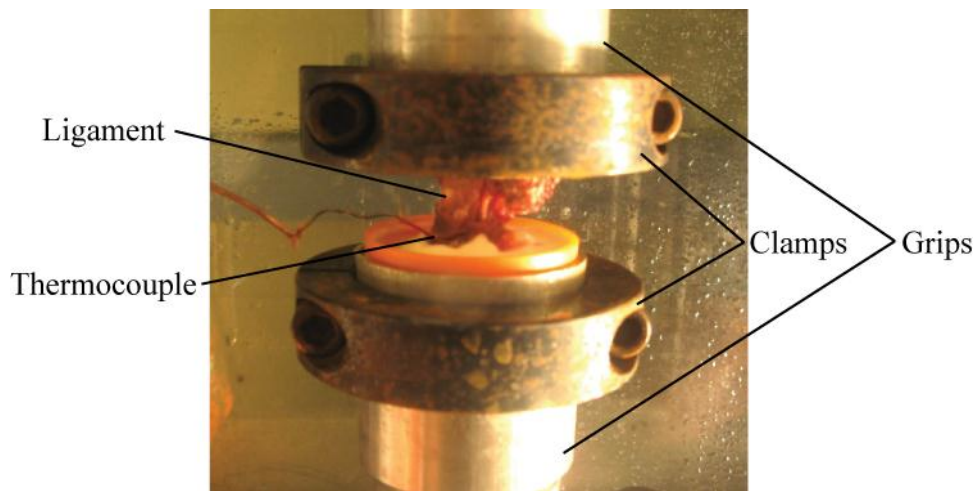


Figure 5-12: Quasi-static fixture: zoomed view of specimen

The medium and high elongation rate tests were performed on a custom designed electromagnetic tensile testing fixture powered by linear shaft motors (Nippon Pulse, Model S250Q) which allowed ligaments to be tested in tension at deformation velocities up to 4 m/s at constant strain rates (Figure 5-13). The apparatus was designed and constructed by Jeff Moulton, at the University of Waterloo. The electromagnetic fixture was equipped with a coupling mechanism to allow the fixture crosshead to reach the desired velocity prior to engaging the ligament. Ligament specimens were loaded into the fixture, using the same grip and clamp devices as the quasi-static fixture. The environmental chamber was located within the fixture to minimize the volume of the chamber, and the specimen was pulled out of the environmental chamber after testing. Loading and failure of the ligaments occurred within the chamber so specimens were tested at *in vivo* conditions. Ligaments were continuously hydrated using saline solution, and preconditioning was initiated when ligaments reached body temperature. Motion restrictors (modified vise-grips) were used to lock the coupling mechanism in place for preconditioning, and then removed before testing (Figure 5-14). Results were plotted as force displacement curves, and force-elongation data were measured at a frequency of 25,000 Hz. The electromagnetic test fixture used a quartz 10 kN force transducer (Kistler 9321B) and charge amplifier (Kistler Type 5010B) to measure force and a linear encoder (RSF Elektronik MS 40) with 10 micron resolution to measure specimen elongation. The test frames were verified at a series of medium strain rates to ensure that both apparatus produced repeatable and consistent results.

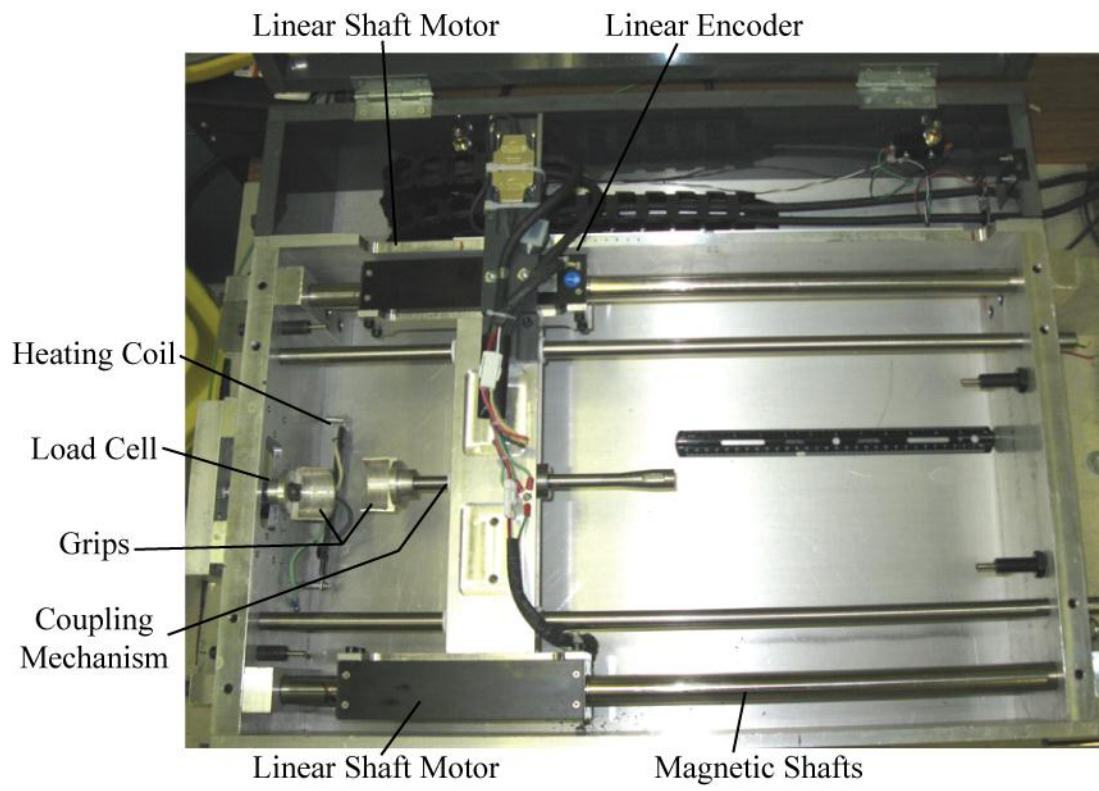


Figure 5-13: High-speed electromagnetic fixture

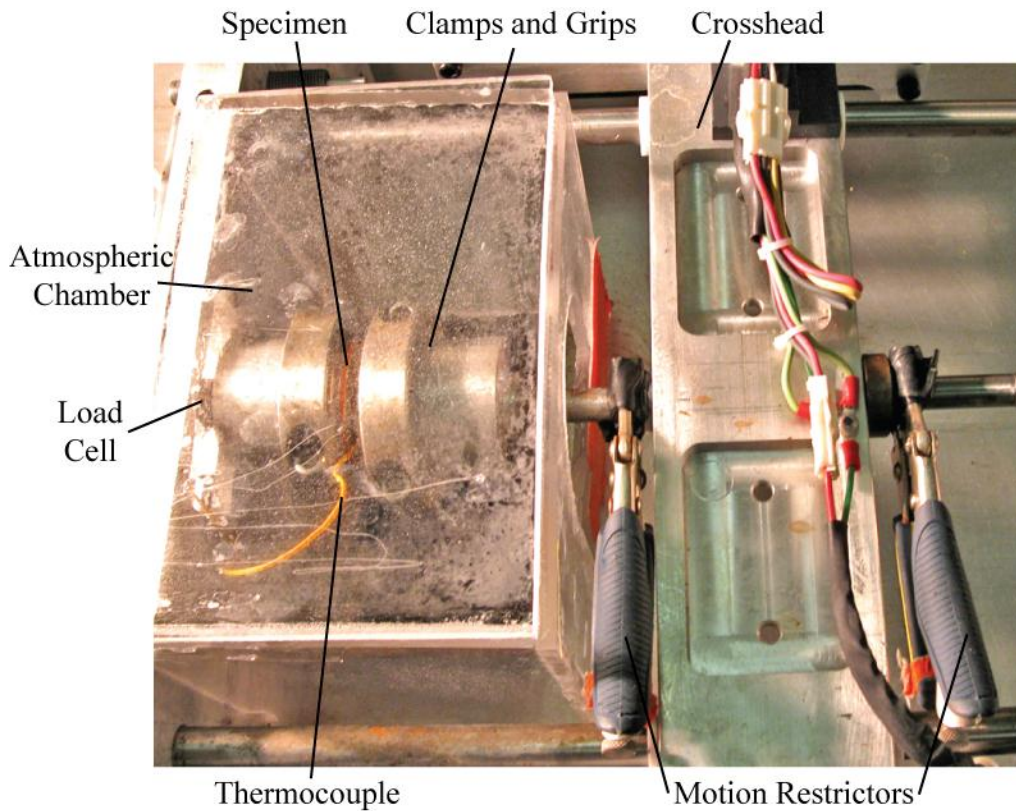


Figure 5-14: High-speed fixture: zoomed view of specimen in environmental chamber

5.4 Data Processing

Results were plotted as force displacement curves. Force-elongation data were measured at a frequency of 500 HZ for quasi-static testing and 25,000 Hz for medium and high rate testing. Slight vibrations in the hydraulic testing frame resulting in noise in the quasi-static data. The noise was present in both axes (x: displacement, and y: force), so the data could not be filtered. High order polynomials (4th, 5th, and 6th) were fit to the loading region of the curve (Figure 5-15), and used to replace the loading portion of the raw data, with care taken to not eliminate any characteristics in the curve.

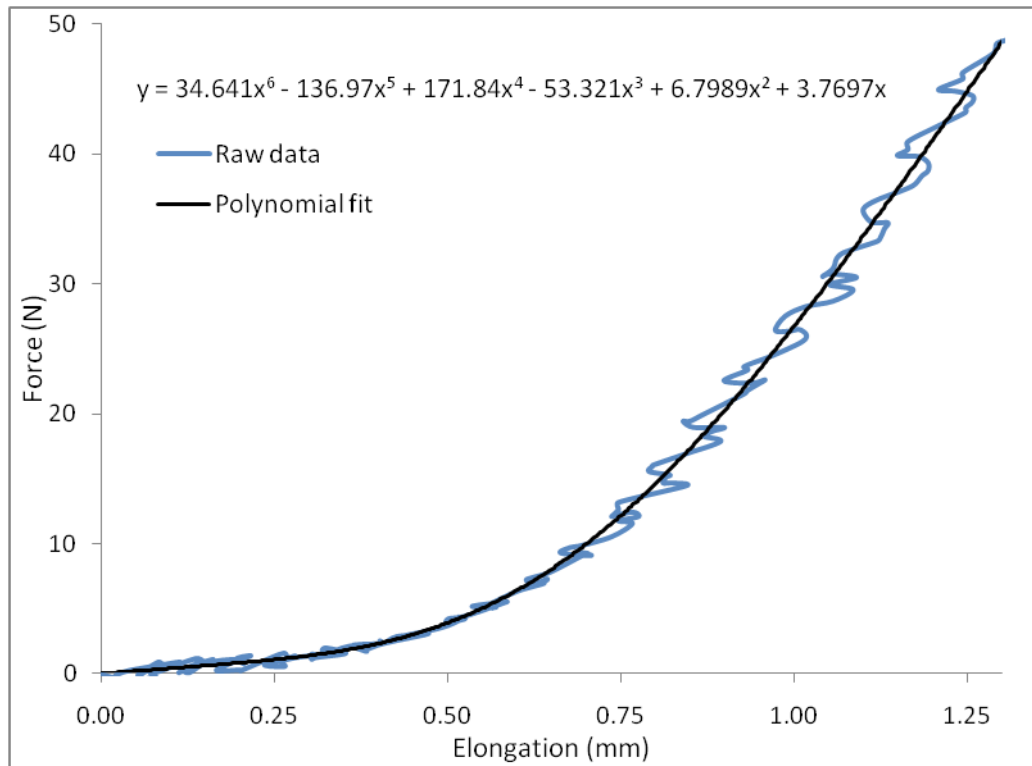


Figure 5-15: Polynomial fit to loading region raw quasi-static data to eliminate noise (ALL)

Since the electromagnetic fixture utilized a coupling crosshead mechanism to allow the crosshead to reach desired velocity before engaging the ligament, the point when the ligament was first engaged, to be defined as ‘zero elongation’ was unknown. The tapered head of the coupling rod eliminated any impact forces, so the transition to loading was smooth. The force profile of the curve before engaging the ligament was non-zero, due to friction in the coupling mechanism. The zero elongation point was determined by tracing the loading curve backwards until adjacent points had a slope of zero (Figure 5-16), which was then defined as the engagement point of the ligament. The curve was scaled by this force value (force to zero), in order to have a zero force, zero elongation starting point. Average force to zero values can be seen in Table 5-5. Force to zero values were on average ~2% of the failure force values for the high rate tests, and 3.66% of the failure force value for the medium tests. The largest ratio of force to zero to failure force was 9.2% for medium rate ISL tests, due to several ligaments failing below 50 N.

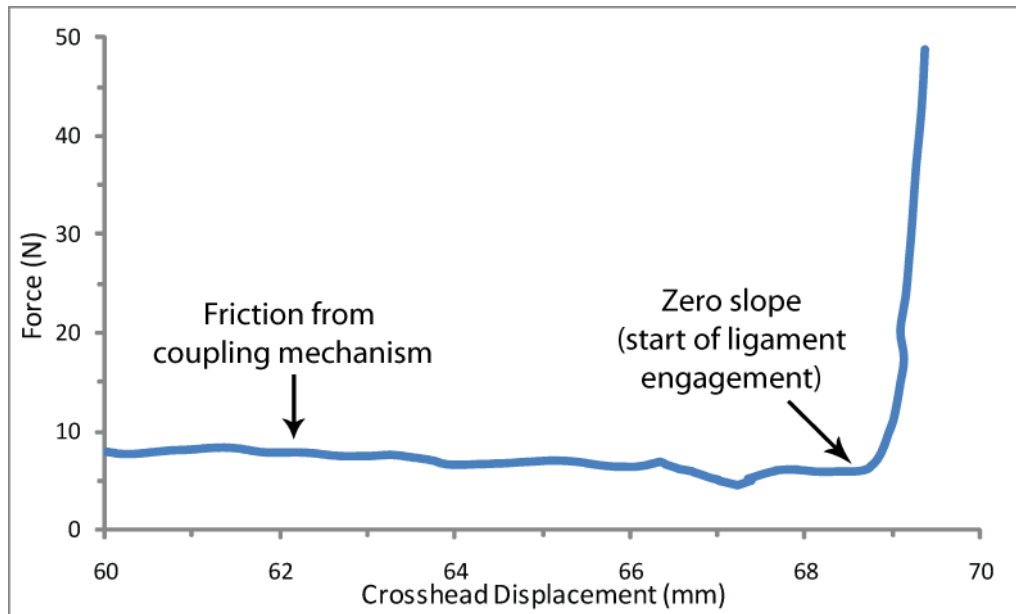


Figure 5-16: Start of ligament engagement at zero slope (PLL shown)

Table 5-5: Average force difference to zero for ligament curves

		ALL	PLL	CL	LF	ISL
High	Force to zero (N)	8.5 (5.7)	10.0 (8.7)	5.3 (3.9)	5.7 (3.8)	2.5 (5.8)
	Failure force (N)	450 (132)	437 (135)	286 (73)	258 (99)	98 (66)
	Ratio (%)	2.1 (1.6)	2.2 (2.0)	1.9 (1.5)	2.6 (2.1)	2.7 (5.7)
Medium	Force to zero (N)	6.4 (5.3)	7.6 (3.9)	6.2 (4.1)	7.5 (3.9)	5.2 (2.4)
	Failure force (N)	384 (166)	497 (167)	270 (91)	328 (121)	93 (69)
	Ratio (%)	2.0 (1.9)	2.0 (1.9)	2.4 (1.6)	2.7 (1.8)	9.2 (6.5)

Average (SD) values

Values of distinctive points were measured and recorded from the curves including failure force, failure elongation, stiffness and toe region, as seen in Figure 5-17. The failure force and failure elongation were defined as the maximum force the ligament reached during loading, and the elongation at which the failure force was reached. Stiffness was identified by fitting and optimizing a

least squares fit line to the linear portion of the curve. The toe region elongation was defined at the transition point of a bilinear curve fit of the loading region; toe region and linear region (Chandrashekar et al., 2008) as shown in Figure 5-18, where the maximum value in the loading region corresponds to the maximum point present on linear region after the least squares line was optimized. The bilinear fit method applied two linear lines to the loading region, constrained to begin at zero force and zero elongation, with the slopes of both lines and the transition point adjusted using a Microsoft Excel solver function to minimize the sum of squares of the force differences between the raw data curve and fit lines. These properties are structural, where ligament dimensions contribute to the response, as larger ligaments could potentially support greater loads. Failure stress, failure strain, modulus, and toe strain were then calculated based on the initial ligament lengths and areas, where areas were calculated using length to area ratios from a geometric study performed by Yoganandan et. al (2000). These values are material properties since dimensions were taken into account. By analyzing the data using both methods, it could be determined if differences were due to varying structural or material properties. Eight metrics in total were measured from each ligament curve and compiled for analysis: failure force, failure elongation, stiffness, toe region, failure stress, failure strain, modulus, toe region strain. Each ligament was analyzed for gender, spinal level, and strain rate effects.

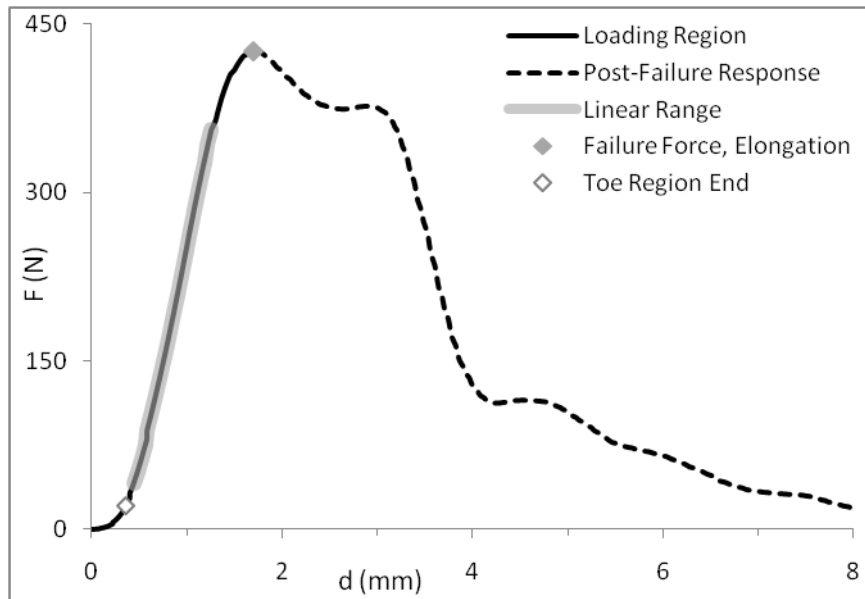


Figure 5-17: Typical ligament response with distinctive points shown (PLL)

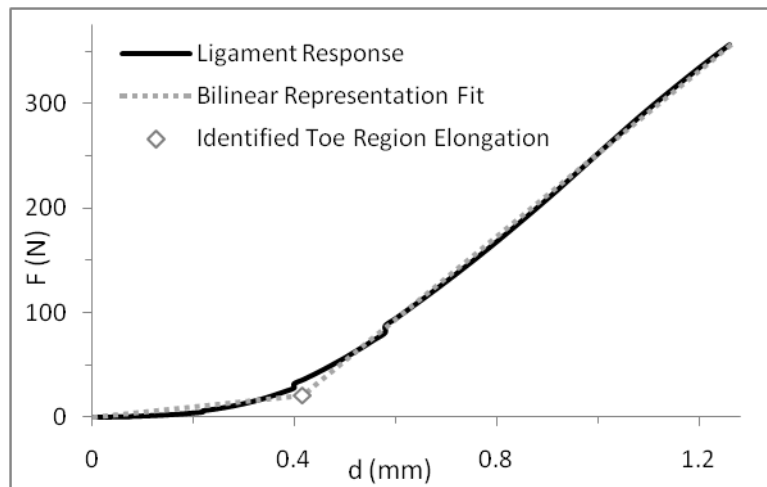


Figure 5-18: Bilinear fit to loading region to define toe region (PLL)

5.5 Statistical Analysis

Statistical analysis was performed on the results from the 3x3x2 factorial experiment using a nested design multi-factor Analysis of Variance (ANOVA) with unbalanced replicates. Main and interaction

effects of the experiment factors (strain rate, spinal level, and gender) were analyzed simultaneously for each ligament. Effects that were established to be statistically significantly different ($\alpha = 0.05$) were further analyzed using Tukey post-hoc to determine which levels of a factor differed from one another. Analysis was performed using SAS version 9.2 software.

5.5.1 Statistical Background

The three factors involved in the experimental ligament testing were gender, spinal level and strain rate. Gender has two levels; male and female, and spinal level and strain rate both have three levels; upper, middle, lower and quasi-static, medium, and high respectively. The spinal levels were divided as upper (C2-C3 and C3-C4), middle (C4-C5 and C5-C6), and lower (C6-C7 and C7-T1). A preliminary investigation of the results at individual spinal levels was undertaken to ensure no trends were present within groups, and would be masked by this grouping. Ligaments could not be compared on a level by level basis due to limited sample size. The dependent variables that were measured and used in order to determine effects were *failure force*, *failure elongation*, *stiffness*, *toe region*, *failure stress*, *failure strain*, *modulus*, and *toe region strain*.

The experiment was considered a 3x3x2 factorial design, with unbalanced replicates, and required a nested design multi-factor Analysis of Variance (ANOVA) in order to determine significant effects. A 3x3x2 factorial experiment has three different factors, with three, three and two levels respectively within each factor. Due to inherent difficulties in biological testing, it is difficult to have equal replicates for each test, so they are deemed ‘unbalanced replicates’. An unbalanced replicate implies that all specific testing circumstances may have a different number of repeated trials. Different numbers of repeated trials are due to loss of ligaments during isolation, etc.

A nested design is used because effects that are restricted to a single level of a factor are said to be nested within that factor (Winer, 1962). In this case, spinal levels are nested within each spine as seen in Figure 5-19. Although the effects of each spine are not being considered, they must not be excluded from the analysis. Two test cases with the same level of each factor (gender, rate, spinal level), may be different simply because they are from different spines. This grouping helps to

discriminate unique effects limited to a certain spine, which otherwise may be interpreted as effects caused by other factors.

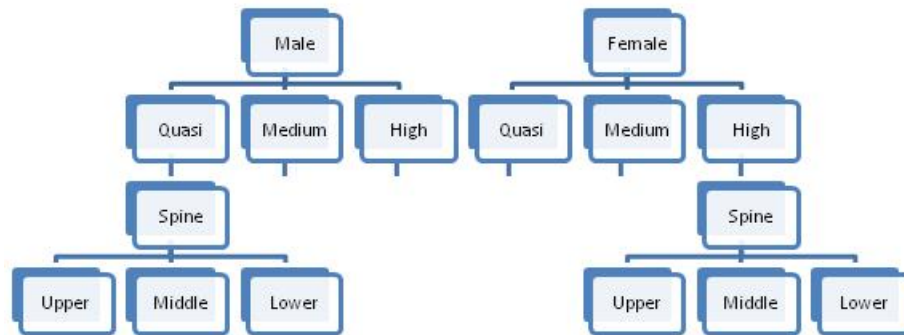


Figure 5-19: Hierarchical nested design of the experiment

A repeated measures ANOVA test is suitable because the purpose is to test for significant differences between means (StatSoft, Inc., 2010) of different effects, and repeated measures allows for testing within a spine and between spines. This is done by comparing the means. ANOVA is more statistically powerful than a simple *t*-test, because each factor can be tested while controlling other factors (StatSoft, Inc., 2010). Therefore, fewer observations (data points) are required to find a significant effect. ANOVA also tests interaction effects, to determine if different factors play a role when applied together, for example, strain rate might affect upper spinal ligaments differently than lower spinal level ligaments.

ANOVA compares the means and variances within groups to those between groups. For example, it compares the mean and variance of the quasi-static tests, to the mean and variance of all three rates combined. The main principles involved are the *Sums of Squares*, and *Degrees of Freedom*. Sums of Squares estimates the variance of a sample, and is computed by taking the sum of all the squared differences from the mean.

$$SS = \sum_{i=1}^n (y_i - \bar{y})^2$$

Where y_i is a random variable, and \bar{y} is the mean, for a particular sample size of n elements.

The Degrees of Freedom (DoF) are the total number of measurements being used, less the number of groups the measurements are subdivided into. So if an estimation is being made using 20 measurements from three spinal level groups, the degrees of freedom are: $20 - 3 = 17$. However if an estimate is being made using 10 measurements from only the lower spinal level, the degrees of freedom are: $10 - 1 = 9$.

The next meaningful representation is the *Mean Square*. The mean square of an estimate is simply the average of the sums of squares, and is computed by dividing the sums of squares by the degrees of freedom. The mean square becomes useful when making comparisons.

$$MS = SS/df$$

For almost any given experiment there will be a certain effect due to error. In other words, under identical conditions, measurements will differ, without explanation. This is especially true for biological testing. It is important when making comparisons between means, that these errors do not influence the conclusions. The variance associated with these errors is known as the *Mean Square Error*. It is calculated from the average of the sums of squares, of each group. Each group (with all factors constant, for example: ALL, male, upper spinal level, high rate) will have a respective variance that is only due to experimental error, as there are no effects from gender, spinal level or rate changing within the group. The *MSE* is the average error of all specific testing cases, and represents the error within the experiment.

These are the tools ANOVA uses to compare means and determine significant effects. If there is no difference between means of two separate groups, the mean square error of the combined groups should be the same as the mean square error – the only variance in both cases is due to the experimental error. For example, if there is no difference between male and female ligaments, the sums of squares of both genders combined should be the same as the mean square error of just the male group, as all variance is due to experimental error. However, if there is a difference, the sums of squares that is calculated from the combined groups will result in a large variance. This variance

when compared to the variance due to experimental error will be very different; therefore there may be a difference between groups.

Given experimental testing with small sample sizes, and a relatively high variance (especially biological testing) there is a possibility that the result is due to chance, and not actually representative of the true population. Thus conclusions must be made with a certain *confidence* or *reliability*, and this is done using *F-Value*. It compares the ratio of different means to the likelihood of that ratio actually being equal to 1 (no difference). The F-value is based on the degrees of freedom of the two estimates being compared and the confidence level the ratio of the means is not equal to 1. The confidence level, determines the level of significance of the comparison, where $\alpha = 0.05$ means there is a 95% probability the two samples are different. ANOVA uses the ratio of the mean square to the mean square error, and calculates an F-Value to determine the confidence level α , of a significant effect. In this study, effects with confidence level greater than 95% ($\alpha < 0.05$) were deemed significant.

$$MS/MSE > F \text{ value}_{\alpha=0.05}$$

Since declaring significant effects is based on probabilities of samples, it is possible that an error may occur outside of the probability range. A type I error (false positive) is when an effect is determined to be significant, when in reality it is not. A type II error (false negative) is when an effect is not found to be significant, when in reality it is significant.

If a significant effect is found within a 3 level factor using ANOVA, it does not distinguish which factors are different from each other. A post-hoc analysis (or *a posteriori* test) is used to make multiple comparisons and determine which effects are different. Different post-hoc tests are more conservative than others in terms of making a type I error. Tukey's HSD (hsd- honestly significant difference) test is a relatively conservative approach especially when sample sizes differ, it is applicable to a wide variety of situations, and is relatively simple to use. The test compares the means of every factor to the means of the other factors, simultaneously using pair wise comparisons. It is more conservative than Bonferroni post hoc tests which have been used in previous related

studies (Ivancic et al., 2007; Bass et al., 2007). Tukey is generally regarded as the preferred post-hoc test (Winer, 1962), so it was chosen for this experiment.

An example of the ANOVA procedure for testing the effects of gender, loading rate, and spinal level on stiffness can be seen in Table 5-6. The error terms between factors, and within a factor are represented by Spine(Gender*Rate) and Spine*Level(Gender*Rate), and the MS term is the MSE term used to calculate the F-value. The statistical analysis software calculated the confidence level for each calculated F-value.

Table 5-6: Example procedure of ANOVA for effects on stiffness of ALL

ANOVA – ALL (stiffness)					
<i>Source</i>	<i>SS</i>	<i>DoF</i>	<i>MS</i>	<i>F-value</i>	<i>α</i>
Gender	16966	1	16966	3.50	0.086
Rate	62498	2	31249	6.44	0.013
Gender*Rate	1772	2	886	0.18	0.835
Spine(Gender*Rate)	58211	12	4851		
Level	2707	2	1354	0.72	0.505
Gender*Level	339	2	170	0.09	0.914
Rate*Level	20146	4	5037	2.69	0.079
Gender*Rate*Level	22674	4	5669	3.02	0.058
Spine*Level(Gender*Rate)	24384	13	1876		
Total	209697	42	4993		

Chapter 6

Results of Younger Ligament Testing

Two hundred sixty-two total primary cervical spine ligaments were successfully tested as summarized in Table 6-1. Ligaments were tested with approximate even distribution between gender, rate, and spinal level. An emphasis was placed on testing ligaments at rates that were representative of automotive crash events.

Table 6-1: Quantity of ligaments tested by type, gender, rate and spinal level

Ligament	Quantity	Gender		Rate			Spinal Level		
		<i>Male</i>	<i>Female</i>	<i>Quasi-static</i>	<i>Medium</i>	<i>High</i>	<i>Upper</i>	<i>Middle</i>	<i>Lower</i>
ALL	43	21	22	16	12	15	13	14	16
PLL	48	24	24	16	13	19	16	16	16
CL	86	41	45	25	25	36	31	28	27
LF	42	21	21	14	13	15	14	13	15
ISL	43	21	22	14	12	17	13	14	16
Total	262	128	134	85	75	102	87	85	90

The values obtained from the ligament curves can be found in Appendix A, and force-elongation curves can be found in Appendix B. For the following results, significant effects ($p < 0.05$) were reported in **bold**. Within significant effects, levels of a factor which differ from one another, as determined by Tukey post-hoc analysis, were distinguished by different asterisk (*+) notation, and levels with no significant difference share asterisk notation. Significant effects are outlined in the text, where the significantly different factor is compared to the average of the two factors that were not shown to be significantly different from each other. Trends were shown in colour, even if effect is not significant, in order to easily identify consistent trends which were present in different ligaments. No interaction effects were found between rate, spinal level, and gender effects.

6.1 Loading Rate Effects

Loading rate was found to be the most significant effect in this study. Example raw-data curves are shown for rate effects on CL, for middle level female ligaments (Figure 6-1), illustrating the most characteristic shape effects. Importantly, post-ultimate load response has never been reported prior to this study, and was of interest as the ligaments often fail in a stepwise manner. The most consistent rate effects were for stiffness and modulus; both increased with increased deformation rate, and the trends were significant for most ligaments. Failure force and stress showed increasing trends with higher strain rate, although not always statistically significant. There was also a trend for strain at ultimate load (defined as ‘failure strain’) to decrease with increasing rate for most ligaments, but this was not as consistent when considering failure elongation.

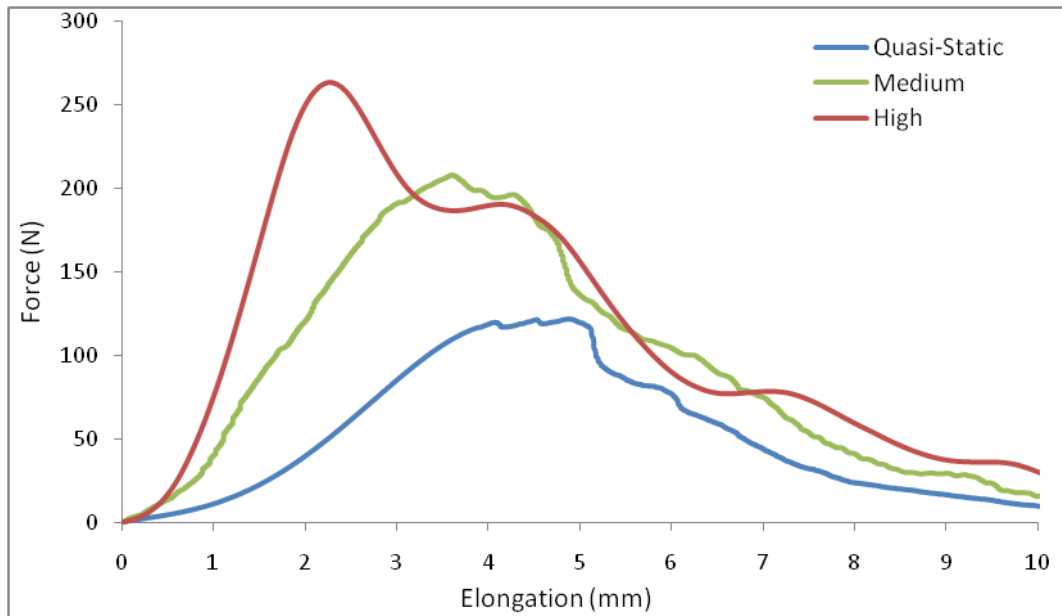


Figure 6-1: Rate effect shown by example curves for CL (female, middle level). The most characteristic shape curve from each rate was chosen, to illustrate rate effects.

For the ALL, stiffness was higher ($p = 0.013$, note: confidence levels represent significant difference within a factor) for the high rate value, with a 60% increase compared to medium and quasi-static rates. Similar results were found for the modulus ($p < 0.01$) with the high rate value being 80%

higher than both the medium and quasi-static values. Also for the ALL, the high rate failure stress was 44% higher ($p = 0.032$) than the value for quasi-static. The PLL demonstrated significant rate effects for stiffness and modulus, where the high rate stiffness value increased by 68% ($p = 0.049$) compared to quasi-static, and the modulus for high rate was 129% higher ($p = 0.011$) compared to the quasi-static value. Failure force for CL was 30% lower ($p = 0.027$) for quasi-static compared to both medium and high rate values. Failure stress was also significant ($p < 0.01$) with quasi-static failing at a 42% lower value than both medium and high rates. LF had no significant rate effects, but did exhibit the same trends for stiffness and modulus as the other ligaments. ISL failed at 44% longer elongation ($p = 0.027$) at quasi-static rates compared to medium and high rates. It also failed at 53% longer strain ($p < 0.01$) at quasi-static compared to medium and high rates. Also for ISL, medium and high rates were 173% stiffer ($p = 0.021$) than quasi-static.

Detailed average values for loading rate effects can be seen in Table 6-2. Stiffness showed the most consistent rate effect among the ligaments so results are shown graphically for the strain rate effect on stiffness on a logarithmic scale for the primary ligaments in Figure 6-2. Graphs show the mean values, standard deviations, and range of values for each rate.

Table 6-2: Loading rate effects for cervical spine ligaments

Ligament	Rate	Failure Force (N)	Failure Elongation (mm)	Stiffness (N/mm)	Toe Region (mm)	Failure Stress (MPa)	Failure Strain	Modulus (MPa)	Toe Region Strain
ALL	Q	342 (149)	3.97 (1.05)	139 (58)	1.28 (0.48)	31.9 (13.2)*	1.15 (0.49)	50 (22)	0.39 (0.25)
	M	384 (166)	3.89 (1.49)	164 (57)	1.04 (0.72)	35.8 (14.9)*+	0.93 (0.41)	68 (33)	0.24 (0.14)
	H	450 (132)	3.79 (0.98)	242 (65)*	0.72 (0.31)	45.6 (11.9)+	0.90 (0.31)	106 (25)*	0.16 (0.07)
	<i>p</i>	<i>0.12</i>	<i>0.96</i>	<i>0.01</i>	<i>0.08</i>	<i>0.03</i>	<i>0.58</i>	<i><0.01</i>	<i>0.11</i>
PLL	Q	341 (104)	2.68 (1.06)	215 (68)*	0.69 (0.42)	29.3 (12.1)	0.76 (0.31)	63 (22)*	0.20 (0.13)
	M	497 (167)	2.87 (0.89)	288 (90)*+	0.47 (0.34)	43.8 (19.3)	0.73 (0.21)	98 (40)*+	0.12 (0.08)
	H	437 (135)	2.78 (0.70)	362 (151)+	0.70 (0.32)	39.4 (15.2)	0.65 (0.20)	142 (69)+	0.17 (0.10)
	<i>p</i>	<i>0.23</i>	<i>0.98</i>	<i>0.04</i>	<i>0.51</i>	<i>0.25</i>	<i>0.68</i>	<i>0.01</i>	<i>0.59</i>
CL	Q	195 (62)*	4.37 (1.42)	85 (41)*	0.88 (0.50)	3.5 (1.2)*	0.97 (0.32)	6.9 (3.2)*	0.2 (0.12)
	M	270 (91)	4.18 (1.89)	122 (43)	0.51 (0.46)	6.0 (2.2)	1.12 (0.51)	10.1 (3.4)	0.14 (0.13)
	H	286 (73)	4.33 (1.78)	142 (40)	0.68 (0.21)	6.1 (1.7)	1.11 (0.46)	11.8 (3.6)	0.17 (0.05)
	<i>p</i>	<i>0.03</i>	<i>0.77</i>	<i>0.04</i>	<i>0.05</i>	<i><0.01</i>	<i>0.23</i>	<i>0.01</i>	<i>0.30</i>
LF	Q	243 (118)	5.61 (1.38)	118 (70)	3.08 (1.58)	5.6 (2.4)	0.62 (0.12)	24.6 (15.1)	0.33 (0.16)
	M	328 (121)	4.92 (1.53)	141 (65)	2.04 (1.13)	8.0 (3.1)	0.58 (0.13)	28.6 (13.3)	0.23 (0.12)
	H	258 (99)	4.18 (1.50)	144 (70)	1.73 (1.28)	6.5 (2.4)	0.52 (0.16)	29.5 (15.5)	0.22 (0.13)
	<i>p</i>	<i>0.10</i>	<i>0.10</i>	<i>0.76</i>	<i>0.13</i>	<i>0.11</i>	<i>0.07</i>	<i>0.79</i>	<i>0.16</i>
ISL	Q	56 (37)	6.72 (1.91)*	13 (8)*	1.89 (1.20)*	4.5 (2.9)	0.65 (0.17)*	13.7 (10)	0.18 (0.13)*
	M	93 (69)	4.70 (1.50)	36 (25)	0.72 (0.67)+	7.5 (6.5)	0.40 (0.12)	33.2 (25.7)	0.06 (0.05)+
	H	98 (66)	4.64 (1.25)	35 (17)	1.20 (0.54)*+	8.3 (6.2)	0.45 (0.12)	29.9 (15)	0.12 (0.06)*+
	<i>p</i>	<i>0.07</i>	<i>0.03</i>	<i>0.02</i>	<i>0.03</i>	<i>0.15</i>	<i><0.01</i>	<i>0.06</i>	<i>0.02</i>

Average (SD) values with **asterisk**** are statistically significant $p < 0.05$

Colour shading shows trends

p-value shown

Increasing with rate

Decreasing with rate

Medium is lowest

Medium is highest

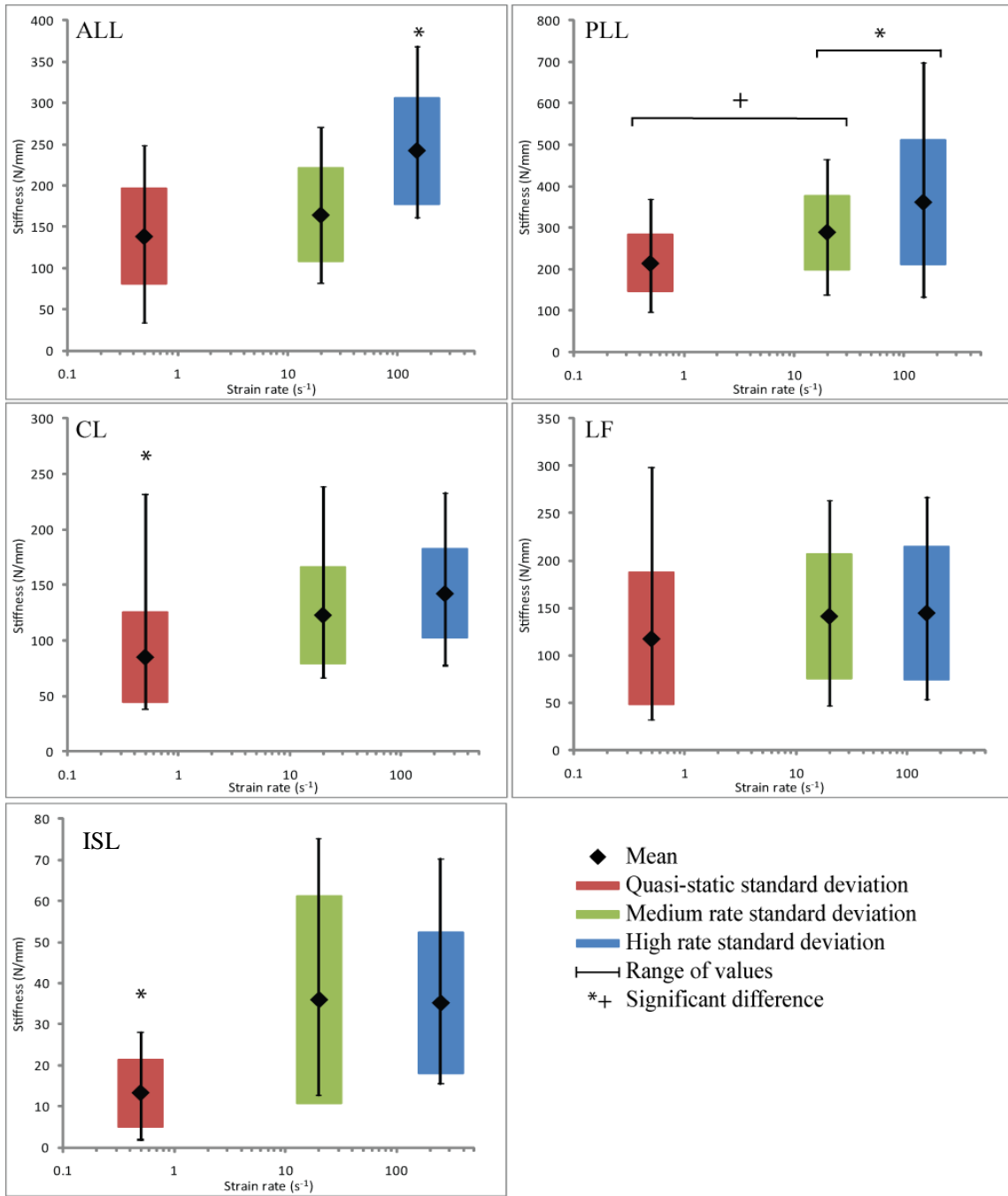


Figure 6-2: Strain rate effect on stiffness for primary ligaments

6.2 Spinal Level Effects

Spinal level effects were investigated by comparing results at three different levels defined as upper (C2-C4), middle (C4-C6) and lower (C6-T1), after a preliminary investigation ensured no trends would be masked within the level groups. Results were qualitatively evaluated, as sample sizes were often too small to perform a statistical analysis, to ensure there were no consistent trends within proposed level groupings. Although the LF did not demonstrate any significant rate effects, it had several significant level effects. There were consistent trends for several ligaments having different values in the middle level compared to the upper and lower levels of the spine.

The ALL failed at a 33% lower ($p < 0.01$) strain at the middle level compared to the lower level. The PLL failed at a 33% lower ($p < 0.01$) stress at the lower level than both the middle and upper levels. The CL had a 23% shorter ($p < 0.01$) failure elongation at the upper level compared to both the middle and lower levels. The middle level of the CL also had a 21% lower ($p = 0.03$) stiffness, a 22% lower ($p = 0.04$) failure stress, and a 29% lower ($p < 0.01$) modulus than the middle level. The lower level of the LF failed at a 61% higher ($p < 0.01$) force than both the upper and middle levels, and 43% higher ($p = 0.02$) stress than both the upper and middle levels. The failure elongation was 58% higher ($p < 0.01$) at the lower level than the upper level. The modulus of the LF was 64% higher ($p = 0.04$) at the lower level than both the upper and middle levels. The LF was one of the only ligaments to have toe region effects. Toe region elongation was 89% longer ($p < 0.01$) at the lower level compared to both the upper and middle, and toe region strain was 63% longer ($p < 0.01$) at the lower level compared to both the upper and the middle levels. The failure elongation for the ISL was 35% longer ($p = 0.033$) for the lower level than the upper level. The ISL also had toe region elongation effects, as the lower level was 80% longer ($p = 0.02$) than both the upper and middle levels.

Detailed average values for spinal level effects can be seen in Table 6-3.

Table 6-3: Spinal level effects for cervical spine ligaments

Ligament	Level	Failure Force (N)	Failure Elongation (mm)	Stiffness (N/mm)	Toe Region (mm)	Failure Stress (MPa)	Failure Strain	Modulus (MPa)	Toe Region Strain
ALL	Up	454 (159)	3.85 (1.05)	199 (69)	1.00 (0.40)	43.2 (14.4)	0.98 (0.44)*+	81 (34)	0.27 (0.18)
	Mid	329 (152)	3.36 (1.14)	168 (68)	0.90 (0.48)	32.1 (11.7)	0.79 (0.33)+	79 (38)	0.23 (0.19)
	Low	396 (133)	4.31 (1.06)	180 (85)	1.14 (0.71)	38.4 (15.1)	1.21 (0.39)*	66 (35)	0.31 (0.21)
	<i>p</i>	0.3	0.11	0.51	0.59	0.42	<0.01	0.14	0.19
PLL	Up	414 (153)	3.01 (0.92)	253 (116)	0.72 (0.28)	39.9 (13.8)	0.72 (0.22)	102 (49)	0.18 (0.09)
	Mid	474 (158)	2.73 (0.80)	328 (142)	0.52 (0.39)	44.0 (20.2)	0.78 (0.23)	122 (75)	0.14 (0.11)
	Low	374 (117)	2.57 (0.89)	297 (120)	0.67 (0.41)	27.8 (9.2)*	0.69 (0.30)	87 (50)	0.18 (0.12)
	<i>p</i>	0.06	0.24	0.11	0.09	<0.01	0.95	0.09	0.24
CL	Up	251 (84)	3.63 (1.18)*	129 (45)*	0.68 (0.40)	5.9 (2.1)*	0.95 (0.27)	11.5 (4.0)*	0.18 (0.10)
	Mid	247 (85)	4.50 (1.50)	102 (42)+	0.73 (0.41)	4.6 (2.0)+	1.03 (0.36)	8.2 (3.2)+	0.17 (0.10)
	Low	267 (87)	4.86 (2.14)	128 (52)*+	0.66 (0.42)	5.4 (2.0)*+	1.26 (0.60)	9.8 (4.0)*+	0.17 (0.10)
	<i>p</i>	0.52	<0.01	0.03	0.77	0.04	0.06	<0.01	0.8
LF	Up	234 (80)	3.84 (1.36)*	130 (62)	1.58 (1.15)	5.9 (2.1)	0.51 (0.15)	23.9 (11.3)	0.21 (0.14)
	Mid	216 (106)	4.74 (1.22)*+	99 (59)	1.86 (1.45)	5.7 (2.9)	0.57 (0.12)	21.0 (12.9)	0.22 (0.15)
	Low	363 (103)*	5.99 (1.30)+	169 (67)	3.29 (1.15)*	8.3 (2.5)*	0.62 (0.14)	36.7 (14.6)*	0.35 (0.10)*
	<i>p</i>	<0.01	<0.01	0.1	<0.01	0.02	0.22	0.04	<0.01
ISL	Up	76 (62)	4.61 (1.26)*	31 (22)	1.07 (0.62)	8.1 (6.6)	0.49 (0.13)	31.6 (23.1)	0.12 (0.07)
	Mid	66 (43)	5.04 (1.60)*+	27 (21)	0.94 (0.55)	5.8 (4.6)	0.48 (0.15)	23.7 (19.9)	0.09 (0.06)
	Low	104 (70)	6.18 (2.09)+	27 (19)	1.79 (1.26)*	6.8 (5.5)	0.53 (0.22)	22.2 (14.1)	0.16 (0.14)
	<i>p</i>	0.13	0.03	0.79	0.02	0.69	0.86	0.22	0.25
Average (SD) values with asterisk*+ are statistically significant $p < 0.05$								Increasing upper-lower	
Colour shading shows trends								Decreasing upper-lower	
<i>p</i> -value shown								Middle is lowest	
								Middle is highest	

6.3 Gender Effects

Only two ligaments had significant gender effects; the ALL and CL. For the ALL, male ligaments had a 33% higher ($p = 0.038$) modulus than female, and for CL, the male ligaments failed at a 22% higher ($p = 0.046$) force than female. There were some consistent trends in the results. Male values were higher for every ligament for failure force, and all ligaments except PLL for failure stress. Male ligaments appear to fail at a higher elongation for most ligaments, however not at a higher strain, thus this was likely due to longer initial length.

Detailed average values for gender effects can be seen in Table 6-4.

Table 6-4: Gender effects for cervical spine ligaments

Ligament	Gender	Failure Force (N)	Failure Elongation (mm)	Stiffness (N/mm)	Toe Region (mm)	Failure Stress (MPa)	Failure Strain	Modulus (MPa)	Toe Region Strain
ALL	Male	449 (155)	3.88 (1.14)	206 (74)	0.90 (0.40)	41.6 (15.4)	0.87 (0.30)	85 (36)*	0.20 (0.10)
	Female	337 (131)	3.85 (1.15)	159 (69)	1.13 (0.66)	35.1 (12.8)	1.12 (0.48)	64 (33)	0.34 (0.24)
	<i>p</i>	<i>0.06</i>	<i>0.81</i>	<i>0.09</i>	<i>0.09</i>	<i>0.3</i>	<i>0.15</i>	<i>0.04</i>	<i>0.07</i>
PLL	Male	436 (155)	2.93 (0.99)	287 (114)	0.69 (0.41)	36.4 (16.4)	0.68 (0.23)	101 (44)	0.16 (0.10)
	Female	406 (139)	2.61 (0.71)	299 (142)	0.58 (0.31)	38.1 (16.6)	0.74 (0.26)	107 (73)	0.17 (0.11)
	<i>p</i>	<i>0.73</i>	<i>0.48</i>	<i>0.85</i>	<i>0.38</i>	<i>0.52</i>	<i>0.51</i>	<i>0.64</i>	<i>0.99</i>
CL	Male	281 (86)*	4.67 (1.99)	120 (42)	0.67 (0.41)	5.6 (2.3)	1.11 (0.53)	10.0 (3.6)	0.17 (0.10)
	Female	230 (77)	3.97 (1.32)	120 (53)	0.72 (0.40)	5.1 (1.8)	1.04 (0.34)	9.8 (4.3)	0.17 (0.10)
	<i>p</i>	<i>0.05</i>	<i>0.2</i>	<i>0.86</i>	<i>0.13</i>	<i>0.38</i>	<i>0.75</i>	<i>0.89</i>	<i>0.38</i>
LF	Male	289 (108)	5.05 (1.6)	147 (68)	2.45 (1.47)	6.9 (2.6)	0.57 (0.12)	30.1 (14.8)	0.27 (0.14)
	Female	260 (125)	4.72 (1.53)	122 (67)	2.11 (1.42)	6.4 (3.0)	0.56 (0.16)	25.1 (14.2)	0.26 (0.15)
	<i>p</i>	<i>0.38</i>	<i>0.34</i>	<i>0.38</i>	<i>0.45</i>	<i>0.53</i>	<i>0.49</i>	<i>0.38</i>	<i>0.73</i>
ISL	Male	86 (56)	5.23 (1.64)	29.3 (22.6)	1.31 (0.76)	7.0 (5.1)	0.47 (0.11)	27.4 (20.7)	0.12 (0.07)
	Female	80 (66)	5.43 (1.99)	27.2 (18.4)	1.28 (1.13)	6.7 (6.1)	0.53 (0.22)	23.8 (17.6)	0.13 (0.12)
	<i>p</i>	<i>0.47</i>	<i>0.83</i>	<i>0.51</i>	<i>0.69</i>	<i>0.67</i>	<i>0.27</i>	<i>0.48</i>	<i>0.9</i>
Average (SD) values with asterisk*+ are statistically significant $p < 0.05$								<i>Male higher</i>	
Colour shading shows trends								<i>Female higher</i>	
<i>p-value shown</i>									

6.4 Craniovertebral Ligament Results

Forty-four total craniovertebral specimens were tested successfully, with an approximately even gender distribution within each ligament as summarized in Table 6-5. Ligament curves demonstrated the expected sigmoidal shape. Only one ligament was tested for both the AAAM and the PAAM, due to availability of spines. Significant effects ($p < 0.05$) are identified using **bold** type font. Only the TM complex (tectorial membrane, vertical cruciate, apical, and alar ligaments) exhibited significant rate effects, and there were no consistent trends among the other ligaments. Gender effects were also inconsistent, with only a significant gender effect for failure force of TL, and modulus of PAOM. Detailed values for craniovertebral ligaments are found in Appendix A, and raw data ligament curves can be found in Appendix B.

Table 6-5: Quantity of craniovertebral ligaments tested by type, gender and rate

Ligament	Quantity	Gender		Rate	
		<i>Male</i>	<i>Female</i>	<i>Quasi-static</i>	<i>High</i>
TM Complex	8	4	4	3	5
TL	6	3	3	2	4
AAOM	14	5	9	6	8
PAOM	14	4	10	6	8
AAAM	1	-	1	1	-
PAAM	1	-	1	1	-
Total	44	16	28	19	25

Significant Effects

Since only one sample of the AAAM and the PAAM were tested, no gender or rate effects could be analyzed. Mechanical properties from the quasi-static tensile tests can be seen in Table 6-6.

The TM complex was the only ligament exhibiting consistent rate effects, as it demonstrated a decrease in failure elongation ($p < 0.01$) with increasing strain rate, from 8.55 mm (2.57) at quasi-static to 4.71 mm (0.96) at high rate, a decrease in failure strain ($p = 0.04$) with increasing rate, from 0.43 (0.10) at quasi-static to 0.27 (0.04) at high rate, and an increase in stiffness ($p = 0.03$) with

increasing rate from 219 N/mm (51) at quasi-static to 590 N/mm (183) at high rate. There was a significant gender effect ($p = 0.04$) for the failure force of the TL, as female ligaments failed at a higher force than male ligaments at 528 N (84) and 392 N (52) respectively. The PAOM had significant gender effects ($p = 0.02$) and rate effects ($p = 0.046$), as the male ligaments had a higher modulus 1.63 MPa (0.93) than female ligaments of 1.02 MPa (0.35), and modulus increased with strain rate from 1.12 MPa (0.40) at quasi-static to 1.5 MPa (0.96) at high rate.

Detailed average values for rate and gender effects can be seen in Table 6-7 and Table 6-8 respectively.

Table 6-6: Tensile properties of AAAM and PAAM

Ligament	Failure Force (N)	Failure Elongation (mm)	Stiffness (N/mm)	Toe Region (mm)	Failure Stress (MPa)	Failure Strain	Modulus (MPa)	Toe Region Strain
AAAM	1068	6.59	221	0.95	21.2	0.53	4.4	0.08
PAAM	87	7.77	43	1.35	4.5	0.49	2.0	0.09

Table 6-7: Loading rate effects for craniovertebral ligaments

Ligament	Rate (s ⁻¹)	Failure Force (N)	Failure Elongation (mm)	Stiffness (N/mm)	Toe Region (mm)	Failure Stress (MPa)	Failure Strain	Modulus (MPa)	Toe Region Strain
TM Complex	Quasi (0.5)	1006 (416)	8.55 (2.57)	219 (51)	1.31 (0.38)	33 (12)	0.43 (0.10)	7.4 (2.5)	0.07 (0.01)
	High (150)	1582 (370)	4.71 (0.96)	590 (183)	1.25 (0.39)	46 (11)	0.27 (0.04)	17.3 (5.5)	0.07 (0.02)
	<i>p</i>	<i>0.08</i>	<0.01	0.03	<i>0.62</i>	<i>0.12</i>	0.04	<i>0.07</i>	<i>0.62</i>
TL	Quasi (0.5)	534 (116)	4.75 (0.31)	196 (22)	1.97 (0.07)	29 (11)	0.25 (0.08)	10.6 (3.0)	0.10 (0.03)
	High (150)	423 (76)	5.45 (0.36)	178 (42)	2.45 (0.30)	23 (6)	0.26 (0.03)	9.7 (2.9)	0.12 (0.02)
	<i>p</i>	<i>0.07</i>	<i>0.19</i>	<i>0.36</i>	<i>0.14</i>	<i>0.19</i>	<i>0.82</i>	<i>0.63</i>	<i>0.55</i>
AAOM	Quasi (0.5)	516 (192)	6.00 (1.32)	140 (45)	1.81 (1.06)	6.6 (2.3)	0.46 (0.10)	1.8 (0.4)	0.14 (0.07)
	High (150)	509 (108)	6.02 (1.74)	167 (64)	1.38 (0.73)	5.9 (1.4)	0.49 (0.16)	1.9 (0.7)	0.11 (0.04)
	<i>p</i>	<i>0.98</i>	<i>0.59</i>	<i>0.67</i>	<i>0.87</i>	<i>0.54</i>	<i>0.59</i>	<i>0.98</i>	<i>0.72</i>
PAOM	Quasi (0.5)	198 (80)	6.99 (2.30)	59 (28)	1.21 (0.71)	3.8 (1.0)	0.52 (0.13)	1.1 (0.4)	0.11 (0.06)
	High (150)	162 (52)	6.02 (4.18)	74 (54)	1.22 (0.54)	3.6 (1.3)	0.39 (0.20)	1.6 (1.0)	0.08 (0.05)
	<i>p</i>	<i>0.72</i>	<i>0.56</i>	<i>0.41</i>	<i>0.57</i>	<i>0.93</i>	<i>0.16</i>	0.05	<i>0.26</i>

Average (SD) values, with **significant** effects and *p-values* shown

Table 6-8: Gender effects for craniovertebral ligaments

Ligament	Rate	Failure Force (N)	Failure Elongation (mm)	Stiffness (N/mm)	Toe Region (mm)	Failure Stress (MPa)	Failure Strain	Modulus (MPa)	Toe Region Strain
TM Complex	Male	1357 (669)	6.73 (3.09)	438 (207)	1.41 (0.43)	42 (18)	0.32 (0.12)	13.7 (5.6)	0.07 (0.01)
	Female	1375 (241)	5.57 (2.08)	464 (298)	1.14 (0.24)	40 (32)	0.34 (0.10)	13.4 (8.6)	0.07 (0.02)
	<i>p</i>	0.43	0.02	0.38	0.29	0.6	0.57	0.59	0.73
TL	Male	392 (52)	5.09 (0.63)	156 (22)	2.14 (0.24)	20 (3)	0.22 (0.03)	7.9 (1.5)	0.09 (0.02)
	Female	528 (84)	5.35 (0.37)	212 (16)	2.44 (0.41)	30 (6)	0.29 (0.03)	12.1 (1.3)	0.13 (0.01)
	<i>p</i>	0.04	0.51	0.07	0.29	0.06	0.08	0.11	0.17
AAOM	Male	486 (149)	6.49 (1.50)	140 (49)	1.52 (1.07)	6.6 (1.7)	0.53 (0.16)	1.9 (0.5)	0.12 (0.07)
	Female	547 (140)	5.37 (1.39)	176 (64)	1.63 (0.62)	5.6 (1.9)	0.40 (0.06)	1.8 (0.7)	0.12 (0.03)
	<i>p</i>	0.18	0.48	0.59	0.74	0.44	0.15	0.71	0.89
PAOM	Male	187 (105)	5.2 (1.5)	82 (46)	1.1 (0.62)	3.75 (1.3)	0.42 (0.1)	1.6 (0.8)	0.09 (0.06)
	Female	149 (43)	7.9 (4.7)	48 (21)	1.6 (0.54)	3.3 (0.9)	0.5 (0.2)	1.0 (0.3)	0.1 (0.05)
	<i>p</i>	0.54	0.16	0.12	0.21	0.64	0.33	0.02	0.42

Average (SD) values, with **significant** effects and *p-values* shown

Chapter 7

Discussion of Ligament Testing

The aim of this study was to provide a more complete set of data for cervical spine ligament mechanical properties, for a younger population, loaded at rates representative of automotive accidents. The relatively large sample size used in this study also allowed for a more comprehensive analysis of gender and spinal level effects to be performed. In general, the current study reported higher values of failure force and stiffness and lower values of failure elongation compared to previous studies at comparable rates.

High degree of scatter is present in all biological testing, due to variations within spines and between spines, so there is always a risk of trends or effects being masked by the scatter. These effects are impossible to eliminate, as there will always be differences between individuals. However, the challenges that scatter present can be overcome with larger sample sizes. This study evaluated the largest quantity of primary cervical spine ligaments known to date (262 specimens), compared to the sample size from the largest previous study of 107 ligaments (Yoganandan et al., 1998; Yoganandan et al., 2000).

Although previous studies have used the same ligament length to area ratio technique for determining ligament cross sectional areas (Yoganandan et al., 1998; Yoganandan et al., 2000; Bass et al., 2007), it must be noted that the values for failure stress, failure strain, modulus, and toe region strain are only approximations, as the areas were calculated based on average ligament length to area ratios from a previous cryometric geometry study (Yoganandan et al., 1998; Yoganandan et al., 2000). This technique involved sacrificing the ligament to accurately measure the cross sectional area, consequently it was not able to be used in this study to determine the specific ligament areas. There was no practical method for measuring the areas directly due to the complex shape of the ligaments and impeding bony attachment points. Furthermore, as the ligament was loaded, the cross sectional area will change, and there was no feasible method to measure instantaneous cross sectional area as the specimen is tested, due to the environmental chamber. One study which did not test the ligaments to failure measured cross sectional areas following testing (Troyer et al., 2011). This method was not

appropriate for failure tests, since spinal ligaments have been shown to have large variations in strain across the width and length of the specimen, resulting in failure occurring at numerous locations, thus making it impossible to acquire a full mid-substance sample in the transverse plane (Neumann et al., 1992). Optical methods can be used, but were not available at the time of testing and can be difficult to employ with an environmental chamber.

Most ligaments failed by transection, but a small number of ALL and PLL failed by avulsion fracture (ligament remained intact, but bone fractured near connection point), and insertion site failure (ligament failed at connection point to bone). All failure modes were included in the analysis, as there was no notable difference in terms of the general response. The failure mode was not found to be influenced by strain rate, spinal level or gender, which was in agreement with findings reported by Bass et al.(2007).

It was noted that the LF displayed a substantially longer toe region and a more gradual increase in stiffness, especially compared to the longitudinal ligaments which had a more abrupt increase in stiffness at the toe region. The rapid increase from toe region to linear phase in the longitudinal ligaments compared to the ligamentum flavum is due to the close alignment of collagen fibrils (Kirby et al., 1989). Initially the fibril orientation of the PLL is distributed about 78° ($\pm 38^\circ$ from the physiological loading direction), but reduces to 24° ($\pm 12^\circ$) when subjected to a strain of 0.3 where alignment progresses no further as the fibrils are elongated and demonstrate a constant stiffness. The LF fibrils however are initially oriented at 135° ($\pm 67.5^\circ$ from loading direction), and reduce to 78° ($\pm 39^\circ$) at a strain of 0.3 and continue to narrow under further loading, as stiffness gradually increases. The high elastin content and broad orientation of the collagen fibrils of the LF are responsible for the more gradual increase in stiffness and longer toe region.

This is the first study to report the post-failure response of the ligaments, which has been shown to have a significant effect on neck response in mathematical models (DeWit et al., 2010). The ligaments do not abruptly fail, but tend to exhibit a more gradual stepwise failure response, still supporting a reduced load after the ultimate load. It has been well documented that when ligaments are loaded, the nonlinear response is analogous to the incremental loading of spring elements, as collagen bundles are engaged (Frisen et al., 1969; Woo et al., 1993). The progressive stepwise failure

of the ligaments suggests that failure occurs in a similar way; bundles of collagen fail incrementally (Neumann et al., 1992) when each bundle reaches respective failure elongation resulting in the typical stepwise failure response shape.

7.1 Rate Effects

The results demonstrated the anticipated rate effects particularly for stiffness and failure force, both increasing with increased rate, at a significant level for most of the ligaments. Although trends were present, the LF was the only ligament to not show significant rate effects. The viscoelastic properties of the ligaments are mainly attributed to the collagen content of the ligament (Lucas et al., 2009; Kirby et al., 1989; Fung, 1993), therefore the rate effects on the properties of the ligamentum flavum are expected to be less significant (Bass et al., 2007), due to the higher elastin-collagen ratio (Nachemson et al., 1968; Kirby et al., 1989).

7.2 Spinal Level and Gender Effects

The large number of specimens used in the study allowed the ligaments to be grouped into three spinal levels; upper (C2-C4), middle (C4-C6), and lower (C6-T1). This has not been possible in past studies due to limited sample sizes, so only clinical groupings of middle (C2-C5) and lower (C5-T1) had been used (Yoganandan et al., 1998). A preliminary analysis was performed on the data for the six spinal levels to ensure that no trends were present within the proposed groupings. Level effects were often not significant, except for the LF which demonstrated several level effects; however there were apparent trends among the other ligaments. The middle segments (C4-C6) often had the lowest stiffness and modulus and lowest failure force and stress (ALL, CL, LF, ISL). This is of interest because numerous studies have reported these segments as having the largest range of motion in flexion and extension (Van Mameren et al., 1990; Lind et al., 1989; Dvorak et al., 1988; Ito et al., 2004) and axial rotation (Penning et al., 1987). One study found range of motion in flexion/extension to be significantly greater in the C5-C6 ($22.8 \pm 2.3^\circ$) compared to the C7-T1 (13.8 ± 2.8 ; Nightingale et al., 2002). These similarities between the results of the current study and previous segment tests suggest ligament properties may differ between spinal levels, thus may play a role in the larger range

of motion. Conversely, the PLL had the highest stiffness in the middle region, consistent with a previous study (Przybylski et al., 1996). Since the PLL is the closest ligament to the center of rotation of the vertebral bodies, it plays a limited role in restricting range of motion of the spine.

Failure elongation was shown to be significantly lower at the upper levels compared to the lower levels for CL, LF, and ISL. Since these trends were not present for failure strain it was established the differences were due to ligament lengths being longer at the lower level.

The current study found gender trends consistent with previous studies. Several previous studies have found gender effects for soft tissue cervical spine tests. Female cervical spines failed at 75% the compressive force as male spines (Pintar et al., 1998), male segments were significantly stronger and stiffer than female segments in flexion (Nightingale et al., 2007), and female range of motion has been reported to be larger, both in volunteer tests (Ferrario et al., 2002), and segment tests (Stemper et al., 2003). The current study found significant differences for ALL modulus, and CL failure force, where male values were significantly higher. Although these were the only significant effects, there were consistent trends for failure of male ligaments occurring at a higher force and stress for all ligaments, with stiffness and modulus higher for ALL, LF and ISL among male specimens, which would account for the increased stiffness and strength and flexion, and decreased range of motion. The trends were less pronounced for the stress, strain and modulus values, which suggests differences could be due to structural differences where length and cross sectional area contribute to the higher strengths and longer failure elongations among the male specimens.

7.3 Comparison with Previous Studies

The results of the present study were found to exhibit similar trends to previous studies as summarized in Table 7-1. Generally, the results of the present study demonstrated higher failure force, stress, stiffness, and reduced elongation and strain at failure than previous studies. While there may be some differences due to differences in strain rates and testing conditions, the differences observed in the current study are thought to primarily be attributed to the younger age of the specimens. The current study used specimens with an average age of 44 (27 to 50) years old, while previous tests had average ages above 55 years old (Chazal et al., 1985) up to 81 years old (Ivancic et al., 2007). Significant discrepancies between previous studies in the literature comparing lumbar ligament failure forces have been attributed to age differences (Neumann et al., 1992). Neumann et al. (1992) reported average failure forces of 1060 (304) N (specimens aged 21-43), Chazal et al. (1985) reported forces of 511 (47) N (ages 63-80), and Myklebust et al. (1986) reported forces 444 (267) N (mean age 67). Forces decreased by over 50% with an average age increase of 35 years.

Values for failure force and stiffness are shown for ALL and PLL at quasi-static rates based on the mean age of specimens for each respective study (Figure 7-1). Results from the current study are compared to values reported in previous studies (Chazal et al., 1985; Myklebust et al., 1986; Przybylski et al., 1996; Yoganandan et al., 1998). A trend is present for failure force and stiffness for both ALL and PLL to decrease with increasing age.

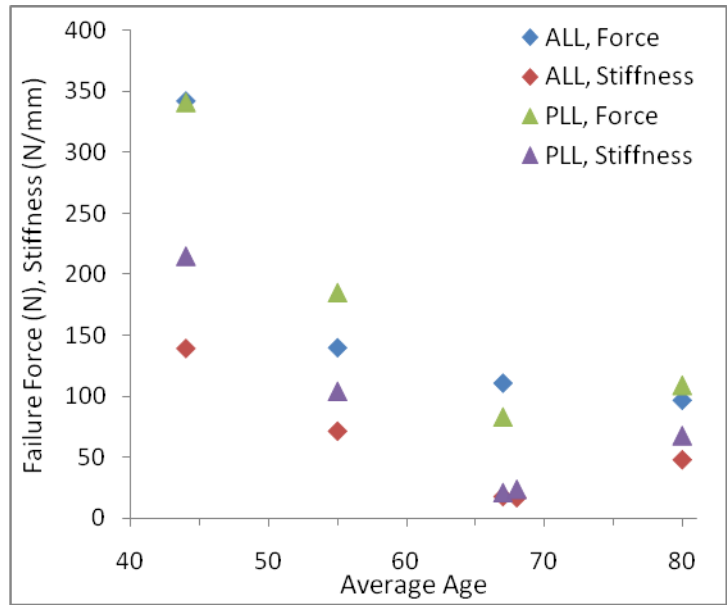


Figure 7-1: Age compared to failure force and stiffness of current and previous cervical spine ALL and PLL studies

Table 7-1: Comparison of data from current study to literature, grouped by comparable elongation rates

Ligament	Failure Force (N)			Failure Elongation (mm)			Stiffness (N/mm)			
	<i>Myklebust et al</i>	<i>Current Study</i>	Ratio	<i>Myklebust et al</i>	<i>Current Study</i>	Ratio	<i>Yoganandan et al</i>	<i>Current Study</i>	Ratio	
Quasi-static										
ALL	111 (56)	342 (149)	3.1	7.6 (3.9)	4.0 (1.1)	0.5	17 (3.4)	139 (58)	8.2	
PLL	83 (55)	341 (104)	4.1	6.1 (5.4)	2.7 (1.1)	0.4	24 (7.2)	215 (68)	9.0	
CL	215 (102)*	195 (62)	0.9	8.7 (5.4)*	4.4 (1.4)	0.5	35 (6.1)*	85 (41)	2.4	
LF	115 (50)	243 (118)	2.1	8.0 (4.7)	5.6 (1.4)	0.7	23 (7.0)	118 (70)	5.1	
ISL	34 (20)	56 (37)	1.6	7.3 (5.2)	6.7 (1.9)	0.9	7.1 (1.6)	13 (8)	1.8	
High										
	<i>Bass et al</i>	<i>Ivancic et al</i>	<i>Current Study</i>	Ratio	<i>Ivancic et al</i>	<i>Current Study</i>	Ratio	<i>Ivancic et al</i>	<i>Current Study</i>	Ratio
ALL	400 (239)	138 (112)	450 (132)	1.7	4.0 (1.0)	3.8 (1.0)	0.9	50 (53)	242 (65)	4.8
PLL	435 (290)	164 (80)	437 (135)	1.5	4.2 (1.5)	2.8 (0.7)	0.7	72 (50)	362 (151)	5.0
CL	-	220 (84)	286 (73)	1.3	4.9 (1.4)	4.3 (1.8)	0.9	69 (34)	142 (40)	2.1
LF	231 (119)	244 (143)	258 (99)	1.1	4.2 (1.5)	4.2 (1.5)	1.0	118 (83)	144 (70)	1.2
ISL	-	86 (68)	98 (66)	1.1	5.9 (2.9)	4.6 (1.3)	0.8	22 (13)	35 (17)	1.6

Ratio is the average the present study to the average of all previous studies

*CL were tested as a pair

The standard deviations of the properties with respect to the percentage of the mean values were lower than the previous reported standard deviations, and graphically, at similar high strain rates, the ligament curves from the current study (750-2500 mm/s) appear to have less scatter than a previous study (620-830 mm/s) (Figure 7-2) (Ivancic et al., 2007). The ligaments also noticeably fail at higher forces, especially for the ALL and PLL, for the current study, which was expected due to the age difference between means (37 years). The more apparent difference in the ALL and PLL could be related to the bone content. One study of lumbar ligaments has shown the high dependence of the longitudinal ligament structural properties on the vertebral mineral content, which decreases with age (Neumann et al., 1994).

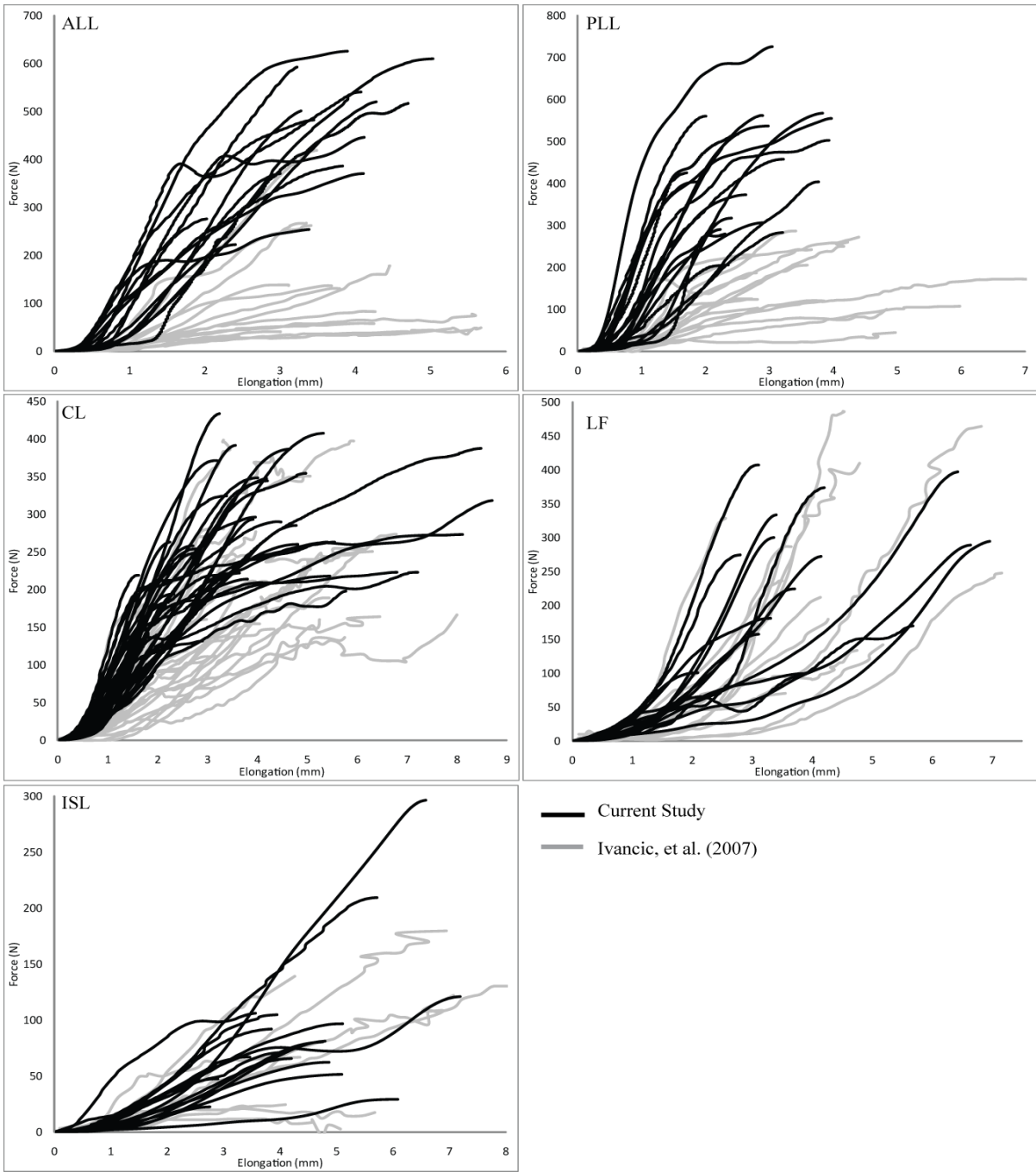


Figure 7-2: Graphical comparison of ligament force-deflection curves between current study (750-2500 mm/s) results at high strain rate and Ivancic et al. (2007) (620-830 mm/s)

Every effort was made to simulate *in vivo* testing conditions in the current study, where testing conditions were often found to be inconsistent between previous studies. Only one study reported the attempt to mimic *in vivo* conditions by testing the ligaments as close to body temperature 37°C and hydration levels as possible (Bass et al., 2007). In a recent study, Bass et al.(2007) showed that the ALL ligament in porcine subjects exhibited strong temperature dependence, and due to the similarity between porcine and human ligaments, temperature must be taken into account especially for dynamic responses (Bass et al., 2007). Porcine ligament specimens tested at room temperature (21.1°C) showed a 50% higher failure force than those tested at body temperature (37.8°C), so data from previous studies may provide higher stiffness than that expected under normal physiological conditions, so differences due to age may be even more prominent.

Preconditioning of ligaments prior to testing was important as it returns the structural collagen fibers to physiological conditions by removing any crimping in the ligaments as a result of being stored in a frozen and fixed position (Hashemi et al., 2005), and demonstrates a response more representative of normal physiological conditions (Van Ee et al., 2000). Only four previous studies performed preconditioning cycles (Chazal et al., 1985; Przybylski et al., 1996; Yoganandan et al., 2000; Bass et al., 2007), which could also contribute to the differences observed between the current study and existing data.

7.4 Confounding Differences when Comparing with Previous Studies

Since there are inconsistencies between previous studies and the current study, experimental factors were expected to affect the results differently. For example, confounding factors would be: younger specimens were expected to increase failure force, while using an environmental chamber to keep ligaments warm and moist was expected to reduce failure force. A matrix was developed to illustrate how the differences in experimental procedure could contribute to differences between results of past studies compared to the current study (Table 7-2), at similar strain rates. An upward arrow (↑) means results would be expected to be higher in the current study due to an effect, while a downward arrow (↓) means results would be expected to be lower. Younger ligaments have increased failure force and the ability to withstand deformation (increased elongation) (Neumann et al., 1994; Cowin et al.,

2007), in vivo test conditions lower the failure force (Bass et al., 2007), preconditioned specimens have increased failure elongation (Fung, 1993), and securely potting the bone ends of the specimens decreases the failure elongation compared to using pins inserted into the vertebral bodies (Neumann et al., 1992).

Table 7-2: Anticipated effects of experimental factors on results from current study contributing to a difference between previous studies

Loading Rate	Previous Study	Failure Force		Failure Elongation		
		Age	<i>in vivo</i> Conditions	Age	Precondition	Grip Method
Quasi-Static	Chazal et al (1985)	↑	↓	↑	↑	-
	Myklebust et al (1988)	↑	↓	↑	↑	↓
	Yoganandan et al (1998)	↑	↓	↑	↑	↓
Quasi/High	Yoganandan et al (1989)	↑	↓	↑	-	↓
High	Ivancic et al (2007)	↑	↓	↑	↑	-
	Bass et al (2007)	↑	-	↑	-	-

7.5 Discussion of Craniovertebral Ligament Study

The goal of this aspect of the study was to provide a more detailed data set for the mechanical properties of the craniovertebral ligaments, for a younger population at strain rates relevant to automotive crash scenarios, as these properties have been highlighted as areas for improvement in previous finite element model studies (Panzer, 2006). Statistical analysis was performed to investigate what effect increasing deformation rate had, if any, and additionally to determine if there was a significant difference in mechanical properties between male and female ligaments. There was no difference in failure mode, as all ligaments failed by transection. As with all biological testing, a large amount of scatter was present in the data, primarily attributed to morphological and physiological variations between spines. Since there was only one of each ligament available from each spine, it was difficult to procure enough spines for large sample sizes for each ligament.

Importantly, this study presents the most detailed data available to date, which is essential for the development and validation of detailed numerical models.

The results from the current study were comparable to other studies at quasi-static rates (Table 7-3, Figure 7-3, and Figure 7-4), and high rates (Table 7-4). At quasi-static rates, the current study demonstrated higher failure force and stiffness values, and lower failure elongation values than previously reported data. This was expected as the primary difference between the studies was an average age difference of 24 years. The mean age of the specimens from the previous study was 67 years old (Pintar, 1986), compared to 43 years old in the current study. As outlined previously, the literature has shown that cervical spine ligament properties deteriorate with increasing age. The previous study also did not perform preconditioning cycles on the ligaments which may also contribute to the difference. The AAOM and PAOM values from left and right halves are compared to results from full ligaments, and are considerably stronger and stiffer than previously reported. The anterior atlanto-axial, and atlanto-occipital membranes were substantially stronger than the posterior membranes, as expected (Moore et al., 1999).

Table 7-3: Comparison of data from current study to literature, at quasi-static rates

Quasi-Static Ligament	Failure Force (N)		Failure Elongation (mm)		Stiffness (N/mm)	
	<i>Pintar et al.</i>	<i>Current Study</i>	<i>Pintar et al.</i>	<i>Current Study</i>	<i>Pintar et al.</i>	<i>Current Study</i>
TM complex	1083 (261)	1006 (416)	8.0 (5.3)	8.5 (2.6)	76 (33)	219 (51)
AAOM*	232 (23)	512 (143)	18.9 (2.7)	6.0 (1.5)	16.9 (3.2)	155 (57)
PAOM*	83 (17)	177 (65)	18.1 (2.7)	6.4 (3.4)	5.7 (0.4)	68 (44)
AAAM	263 (152)	1068	11.8 (7.0)	6.6	24 (11.7)	224
PAAM	111 (85)	87	9.6 (4.3)	4.4	11.6 (11)	43

Average (SD) values reported

*Note: tested as halves for current study, complete ligaments for previous study

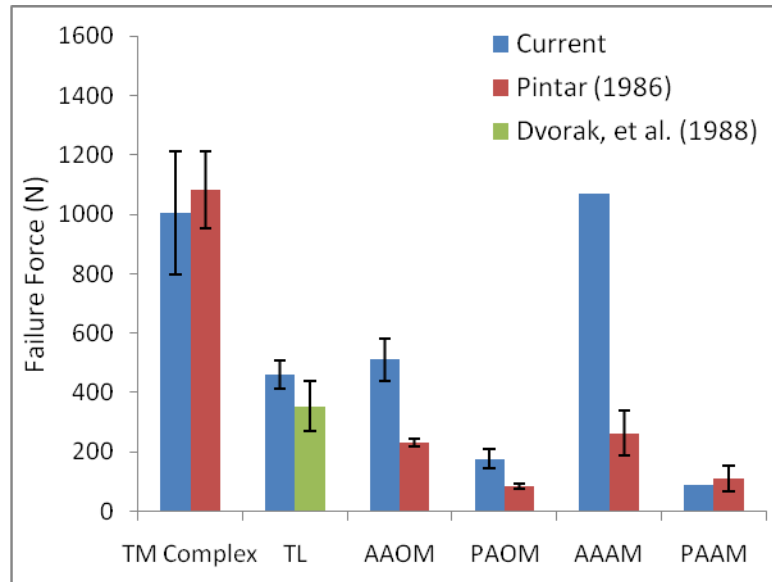


Figure 7-3: Comparison of failure force data between studies at quasi-static rates

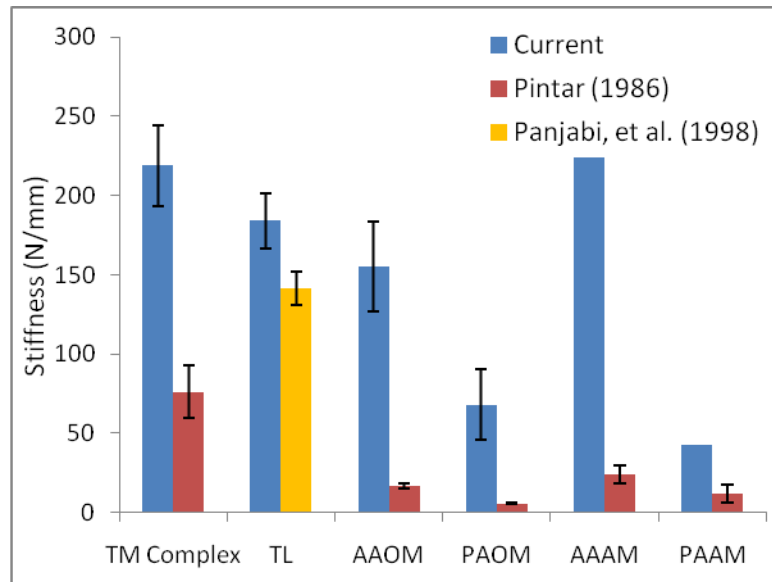


Figure 7-4: Comparison of stiffness data between studies at quasi-static rates

It is difficult to make comparisons at higher deformation rates due to the lack of data in the literature, and inconsistent testing procedures between studies. Although all were classified as high rate tests,

there were differences in the deformation velocity. The current study involved high rate tests from 1.5 to 3.5 m/s (depending on initial ligament length, all high rate tests were performed at 150 s⁻¹). Panjabi et al. (1998) performed all tests at 0.92 m/s (51-79 s⁻¹) using a pneumatic test fixture, and Shim et al. (2005) performed tests at speeds between 10 and 12 m/s (570-1700 s⁻¹) using a split tensile Hopkinson bar system. Despite the differences in elongation rates, the results for failure force, failure elongation and stiffness are comparable to the results by Shim et al. (Table 3). Failure force values were comparable between all three studies, however Panjabi et al. (1998) reported unusually low values for failure elongation (less than 0.5 mm), and since stiffness is correlated to elongation, stiffness values were unusually high (Figure 7-5). The values from the Panjabi et al. (1998) appear unusually high when plotted on a log scale graph of strain rate, as the high rate stiffness value for the alar is higher than the stiffness value of the TM complex from the current study, which includes several ligaments including the alar, and is from specimens of younger mean age. The TL stiffness value from the high rate Panjabi et al. (1998) study also seems unusually high compared to the values from the current study and from Shim et al. (2005). Panjabi et al. (1998) did not perform preconditioning cycles on the ligaments, which may contribute to shorter failure elongation (Fung, 1993).

Table 7-4: Comparison of data from current study to literature, at high rates

High Rate	Failure Force			Failure Elongation (mm)			Stiffness (N/mm)		
Ligament	<i>Panjabi et al.</i>	<i>Shim et al.</i>	<i>Current Study</i>	<i>Panjabi et al.</i>	<i>Shim et al.</i>	<i>Current Study</i>	<i>Panjabi et al.</i>	<i>Shim et al.</i>	<i>Current Study</i>
Alar/TM Complex	367 (83)	398 (69)	1582 (371)	0.35 (0.15)	2.4 (0.03)	4.71 (0.96)	2316 (888)	245 (98)	590 (183)
TL	436 (55)	269 (24)	460 (97)	0.42 (0.17)	1.41 (0.41)	5.22 (0.48)	1472 (691)	260 (68)	184 (35)

Average (SD) values reported

Strain rates(s⁻¹) for Alar/TL: Panjabi (79/51), Shim (1700/570), current study (150/150)

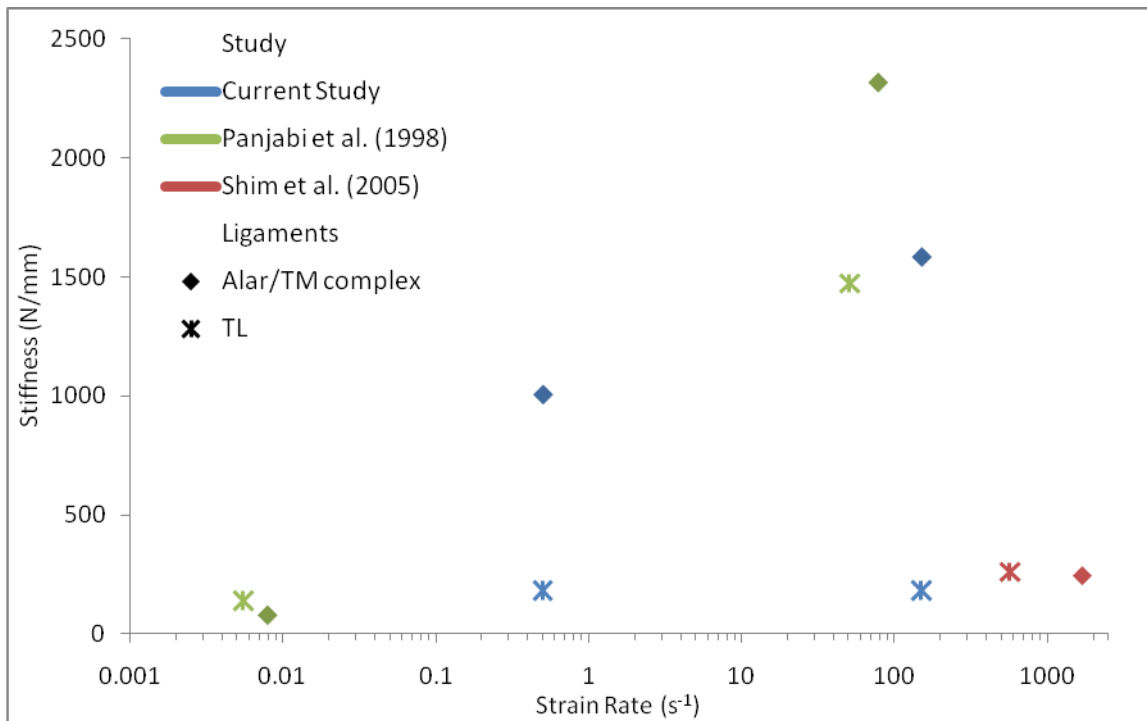


Figure 7-5: Stiffness comparison between studies on logarithmic rate scale

Statistically significant gender effects were observed, but were not consistent among the ligaments. The large amount of scatter in the data makes it difficult to identify statistical significance within strain rate and gender effects with small sample sizes. As mentioned, since each craniovertebral ligament is only present once in each spine, it is difficult to acquire a large amount of test specimens.

The AAAM and PAAM only had one specimen each due to limited spine samples. The data from these ligaments is useful in establishing a frame of reference for these ligaments as they were tested at *in vivo* conditions and procured from a young female spine (29 years old).

The post-ultimate load response region was shown for the first time for craniovertebral ligaments, and ligaments appeared to fail in a characteristic stepwise manner; likely due to the subsequent failure of bundles of collagen fibres. This was particularly apparent for the TM complex, which also consisted of several ligaments, which may have failed incrementally resulting in the stepwise failure. The TL

however, typically failed in a more abrupt fashion. This is possibly due to the presence of cartilage in the tissue (Milz et al., 2001) as it acts as an articular facet of the dens, and contains very few elastic fibres (Saldinger et al., 1990), resulting in a more abrupt failure mode. These shape characteristics of the curves are important for finite element modeling purposes, as the post ultimate load region has been shown to have a significant effect on the response of the neck (DeWit et al., 2010).

Chapter 8

Development of Average Curves

The intended purpose of the data obtained from the ligament tests was to support the development of finite element models of the cervical spine. A common approach used to model ligaments is implementing beam elements with mechanical properties in the form of force-displacement curves (Fice et al., 2009). Statistically significant trends were found in the results, which were used to develop mechanically meaningful average curves. Unique curves were developed for each ligament, at each strain rate, for each respective gender and spinal level, based on the level of significance of each effect. Each unique curve could then be built into the model depending on gender and spinal level.

Average curves cannot be created by simply averaging the force and elongation points, as each curve has a different response during loading. Two previous studies have developed average curves, by first normalizing the raw data curves, followed by averaging the non-dimensionalized values at each elongation point (Pintar et al., 1992; Yoganandan et al., 1998; Yoganandan et al., 2000). The average curves were then scaled to the average failure force and elongation values. The normalization and averaging processes removed the non-linear features of the curves, so the average curve did not display the characteristic sigmoidal loading shape, particularly the toe region characteristics. This is an issue when used in a model, as the shape of the curve directly determines the ligament behavior. The toe region is important because it is representative of the physiological range of motion; without a toe region, models would initially behave unrepresentatively stiff.

Average curves were developed in the current study by using the average values of distinct points and curve traits (toe region, failure force and elongation, stiffness), and fitting polynomial and linear curves to the points to form the sigmoidal shape. This method generated curves with the average measured metrics from the raw data curves, while maintaining the characteristic shape.

8.1 Average Curves for Rate Effects

Rate effects were deemed most important as they were often the most significant effects, and have been consistently demonstrated by previous studies. Curves were initially developed for quasi-static, medium, and high strain rates based on average values (Table 6-2). All significant effects were incorporated into the curves, and trends were also represented. Rate effects are expected to be proportional with strain rate, so effects observed at the medium rate should lie within the range of the quasi-static and high strain rates. There were limited scenarios where this was not the case, where values did not increase or decrease with rate, but alternatively results from the medium strain rate tests were the highest or lowest. The unusual trends were assumed to be due to biological variance in the specimens and thus not represented accordingly in the average curves. For these cases the medium rate value was averaged with the closer bound with no statistical difference (of quasi-static or high rate) in order to represent the corrected trend.

For example, the medium rate toe region for the ISL was shown to be significantly different than the quasi-static value, but not different from the high rate value. Therefore the medium and high rate values were averaged together, as shown in Table 8-1.

Table 8-1: Correction method for medium rate values outside quasi-static high rate bounds, shown for ISL (Toe Region)

Strain Rate	Toe Region (mm)	Corrected Toe Region (mm)
Quasi-Static	1.89	1.89
Medium	0.72	0.96
High	1.2	0.96

The initial points used to develop the curves included the starting point (zero force, zero elongation), the toe region (force and elongation), end of the linear region (force), and failure point (failure force, failure elongation). The force was measured for each raw ligament curve at the toe region elongation (as determined by the bilinear fit method). Only the elongation values as reported in the results

section had rate effects; no trends were observed for the force values at the end of the toe region, so values were averaged for all three rates for all ligaments (Table 8-2). Stiffness trends were most significant for rate effects, so the loading curves were extended linearly from the toe region according to the stiffness values. The loading portions were extended linearly until the onset of the traumatic phase, where stiffness begins to decrease. This threshold was set by a force, as determined by the ratio of the force at the end of the linear region to the failure force, from the raw data curves (Table 8-2). No rate effect trends were observed in the ratios, so values were averaged; the force however was still dependent on the average failure force for each rate. Finally the failure point was plotted from average failure elongation and average failure force for each rate.

Table 8-2: Average values for toe region force and traumatic force ratio

Ligament	Toe Region Force (N)	Traumatic Force Ratio
ALL	40	0.75
PLL	40	0.72
CL	23	0.64
LF	41	0.83
ISL	10	0.71

The characteristic points used to develop the average rate curves can be seen in Figure 8-1. All curves start at zero force, zero elongation (B). The loading region extends linearly from the end of the toe region (C) to the force of the onset of the traumatic region (D), and maximum force is reached at the failure point (E). Additional points were added to ensure the curve shape is representative when polynomial curves were fit to the points. Points A, and F were added for the slope of the curves to be zero at zero elongation and failure, respectively. Intermediate points were added between B and C, and D and E so the fitted polynomials would have smooth transitions between characteristic points.

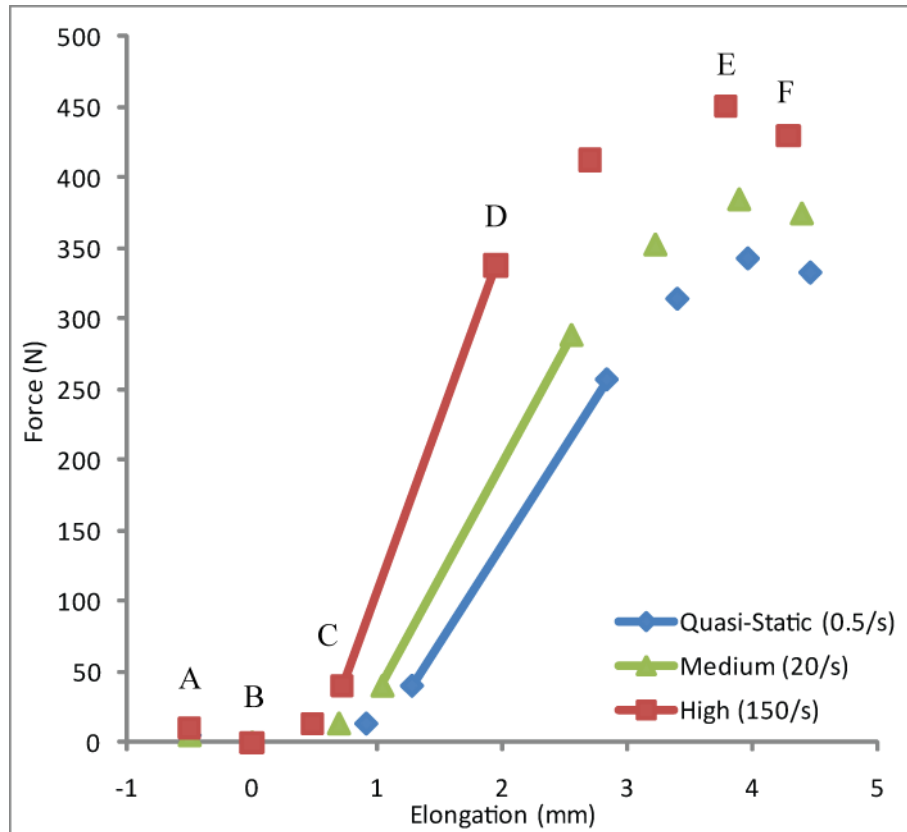


Figure 8-1: Characteristic points used to develop average rate curves (ALL shown)

Two different polynomial curves were fit to the points: one for the toe region and one for the traumatic region. The toe region polynomial forcing conditions were zero slope at zero elongation, and no slope discontinuities at the transition point to the linear region, while the forcing conditions for the traumatic region polynomial were no slope discontinuities at the transition point from the linear region and slope equal to zero at failure. Finite element software requires no discontinuities in slope throughout the function to ensure model stability. The maximum change in slope between points for all ligament curves was 50%, and curves were tested using finite element software to ensure curves were sufficiently smooth and no instabilities occurred. The polynomial equations were used to determine incremental points for the curves in the respected regions. The traumatic region polynomial curve was designed to slightly underestimate force as it approached the failure point, to ensure the maximum force of the curve never exceeded the failure force value from the results. This

produced a slight discontinuity at failure, but is negligible in model response. Finite element codes such as LS-DYNA, have no requirement for number of points in a material property curve, only that all transitions between regions are smooth. Each average curve contained 27 points: 4 points for the characteristic points from average values (initial point, end of toe region, end of linear region, and failure), 12 points for the toe region, and 11 points for the traumatic region. Average rate effect curves for ALL is shown in Figure 8-2, and PLL, CL, LF and ISL are shown in Figure 8-3. Values are shown in Table 8-3.

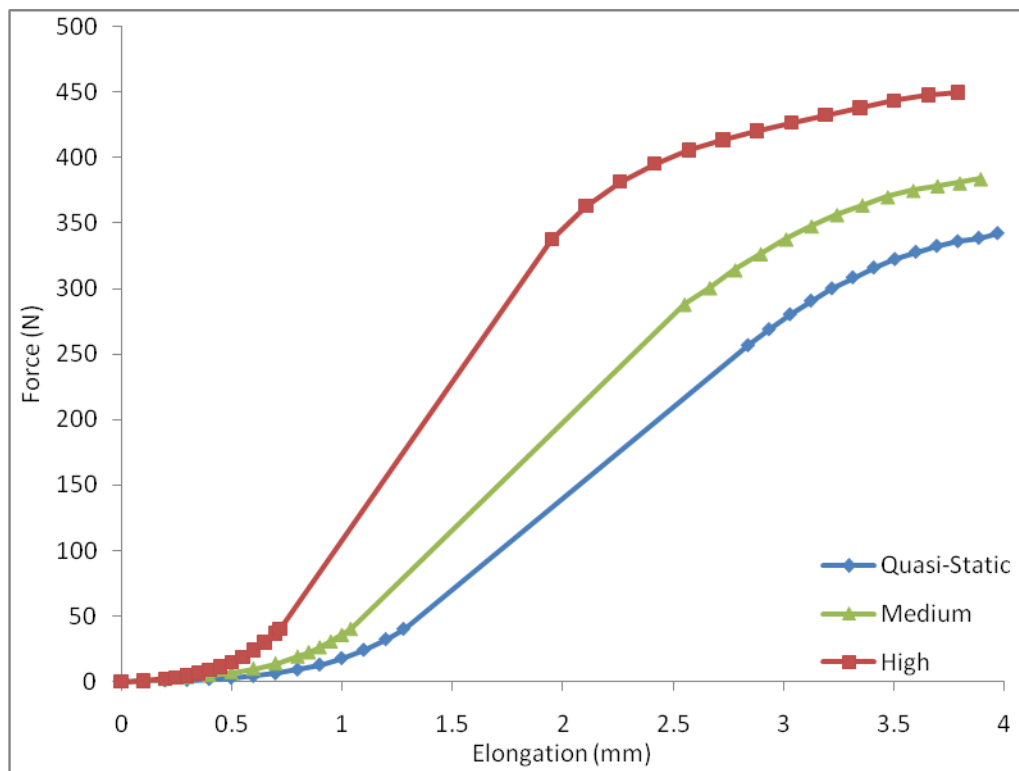


Figure 8-2: Average rate effect curves for ALL

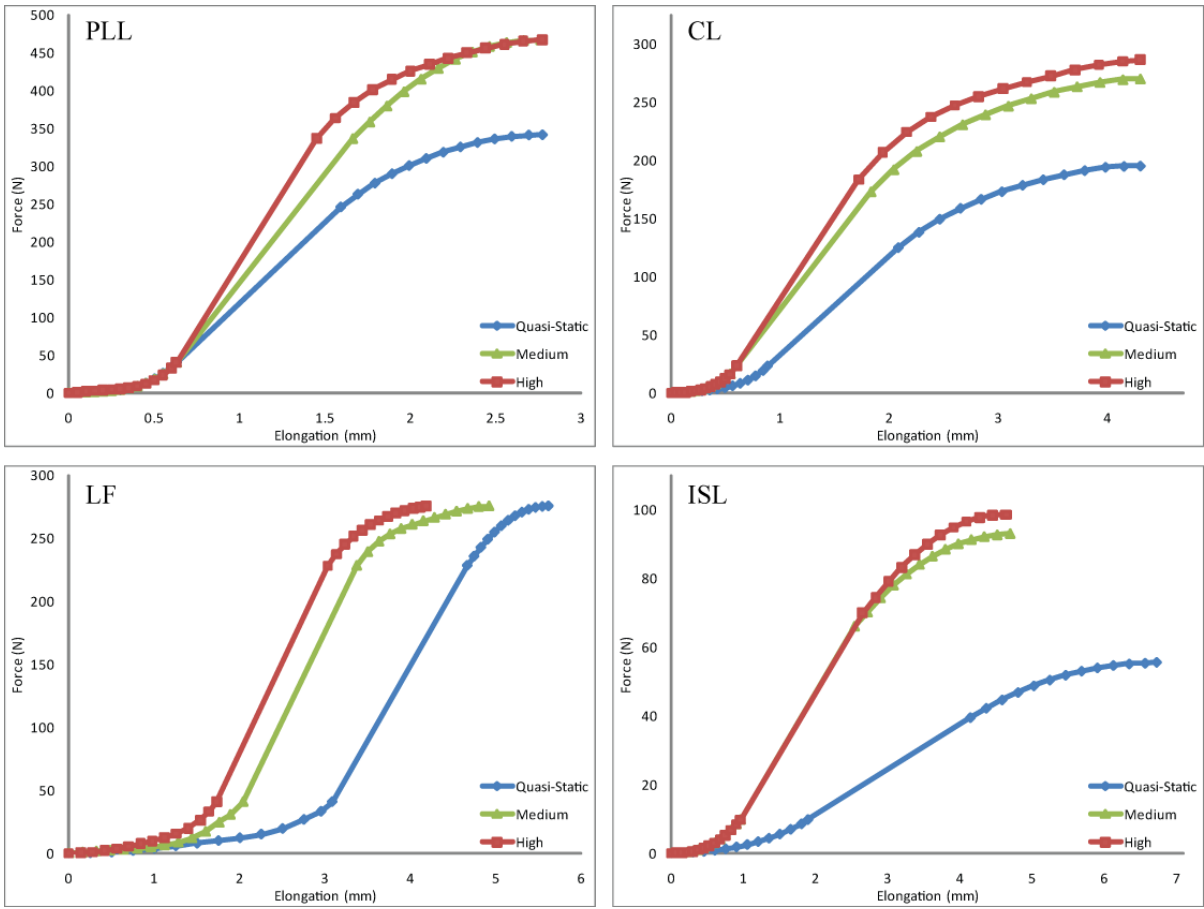


Figure 8-3: Average rate effect curves for PLL, CL, LF, and ISL

Table 8-3: Average curve values for rate effects

Quasi-Static		ALL				Quasi-Static		PLL				Quasi-Static		CL			
<i>d</i>	<i>f</i>	Medium		High		<i>d</i>	<i>f</i>	Medium		High		<i>d</i>	<i>f</i>	Medium		High	
<i>d</i>	<i>f</i>	<i>d</i>	<i>f</i>	<i>d</i>	<i>f</i>	<i>d</i>	<i>f</i>	<i>d</i>	<i>f</i>	<i>d</i>	<i>f</i>	<i>d</i>	<i>f</i>	<i>d</i>	<i>f</i>	<i>d</i>	<i>f</i>
0.00	0.00	0.00	0.00	0.00	0.00	0.00	0.00	0.00	0.00	0.00	0.00	0.00	0.00	0.00	0.00	0.00	0.00
0.10	0.23	0.10	0.89	0.10	0.65	0.05	0.69	0.05	0.33	0.05	0.78	0.07	0.27	0.05	0.04	0.05	0.04
0.20	0.56	0.20	1.94	0.20	2.08	0.10	1.09	0.10	0.67	0.10	1.74	0.14	0.60	0.09	0.21	0.09	0.13
0.30	1.02	0.30	3.19	0.25	3.17	0.15	1.34	0.15	1.08	0.15	2.72	0.21	1.01	0.14	0.51	0.14	0.50
0.40	1.69	0.40	4.79	0.30	4.58	0.20	1.65	0.20	1.66	0.20	3.65	0.28	1.52	0.18	0.99	0.18	1.04
0.50	2.69	0.50	6.89	0.35	6.37	0.25	2.25	0.25	2.54	0.25	4.57	0.35	2.19	0.23	1.67	0.23	1.75
0.60	4.12	0.60	9.74	0.40	8.60	0.30	3.41	0.30	3.86	0.30	5.60	0.42	3.07	0.27	2.60	0.27	2.66
0.70	6.15	0.70	13.63	0.45	11.38	0.35	5.39	0.35	5.80	0.35	6.95	0.49	4.26	0.32	3.82	0.32	3.79
0.80	8.95	0.80	18.93	0.50	14.77	0.40	8.44	0.40	8.59	0.40	8.94	0.56	5.86	0.36	5.38	0.36	5.23
0.90	12.71	0.85	22.24	0.55	18.90	0.45	12.75	0.45	12.47	0.45	11.96	0.63	7.98	0.41	7.33	0.41	7.05
1.00	17.65	0.90	26.05	0.60	23.87	0.50	18.47	0.50	17.72	0.50	16.52	0.70	10.76	0.45	9.74	0.45	9.34
1.10	24.03	0.95	30.44	0.65	29.81	0.55	25.65	0.55	24.63	0.55	23.19	0.77	14.37	0.50	12.67	0.50	12.24
1.20	32.11	1.00	35.47	0.70	36.84	0.60	34.24	0.60	33.54	0.60	32.66	0.84	18.97	0.54	16.18	0.54	15.89
1.28	40.00	1.04	40.00	0.72	40.00	0.63	40.00	0.63	40.00	0.63	40.00	0.88	23.00	0.60	23.00	0.60	23.00
2.84	256.50	2.55	288.00	1.95	337.50	1.59	245.50	1.66	336.00	1.45	336.00	2.08	124.80	1.83	172.80	1.72	183.04
2.94	268.70	2.67	300.60	2.11	363.07	1.69	262.47	1.76	357.97	1.56	362.90	2.27	138.02	2.04	191.91	1.94	206.37
3.03	280.06	2.78	314.30	2.26	381.75	1.79	277.00	1.86	379.13	1.67	384.21	2.46	149.26	2.25	207.58	2.16	224.01
3.13	290.45	2.90	326.74	2.42	395.40	1.89	289.50	1.96	398.00	1.78	400.97	2.65	158.63	2.46	220.22	2.38	237.04
3.22	299.87	3.01	337.93	2.57	405.60	1.99	300.32	2.06	414.58	1.89	414.32	2.84	166.41	2.67	230.56	2.60	246.86
3.32	308.30	3.13	347.87	2.73	413.60	2.09	309.72	2.16	428.87	2.00	425.19	3.03	172.92	2.88	239.20	2.82	254.60
3.41	315.76	3.24	356.56	2.88	420.37	2.19	317.88	2.26	440.87	2.11	434.30	3.22	178.45	3.09	246.59	3.04	261.09
3.51	322.25	3.36	363.99	3.04	426.56	2.29	324.90	2.36	450.57	2.22	442.18	3.41	183.26	3.30	253.00	3.26	266.91
3.60	327.75	3.47	370.17	3.19	432.51	2.39	330.80	2.46	457.99	2.33	449.15	3.60	187.48	3.51	258.57	3.48	272.33
3.70	332.29	3.59	375.10	3.35	438.26	2.49	335.52	2.56	463.11	2.44	455.31	3.79	191.11	3.72	263.29	3.70	277.36
3.79	335.84	3.70	378.64	3.50	443.52	2.59	338.92	2.66	465.94	2.55	460.58	3.98	193.92	3.93	266.99	3.92	281.73
3.89	338.42	3.80	380.87	3.66	447.71	2.69	340.79	2.76	466.49	2.66	464.65	4.15	194.68	4.14	269.35	4.14	284.88
3.97	342.00	3.89	384.00	3.79	450.00	2.77	341.00	2.77	467.00	2.77	467.00	4.30	195.00	4.30	270.00	4.30	286.00

d: displacement, *f*: force

Table 8-3: Continued

		LF				ISL					
Quasi-Static		Medium		High		Quasi-Static		Medium		High	
<i>d</i>	<i>f</i>	<i>d</i>	<i>f</i>	<i>d</i>	<i>f</i>	<i>d</i>	<i>f</i>	<i>d</i>	<i>f</i>	<i>d</i>	<i>f</i>
0.00	0.00	0.00	0.00	0.00	0.00	0.00	0.00	0.00	0.00	0.00	0.00
0.25	0.06	0.16	0.73	0.14	0.10	0.15	0.09	0.08	0.03	0.08	0.03
0.50	0.70	0.32	1.50	0.28	0.73	0.30	0.24	0.15	0.12	0.15	0.12
0.75	1.94	0.48	2.23	0.42	1.90	0.45	0.47	0.23	0.29	0.23	0.29
1.00	3.66	0.64	2.96	0.56	3.49	0.60	0.79	0.30	0.56	0.30	0.56
1.25	5.65	0.80	3.75	0.70	5.37	0.75	1.22	0.38	0.94	0.38	0.94
1.50	7.73	0.96	4.78	0.84	7.46	0.90	1.78	0.45	1.46	0.45	1.46
1.75	9.82	1.12	6.28	0.98	9.72	1.05	2.47	0.53	2.13	0.53	2.13
2.00	12.09	1.28	8.56	1.12	12.29	1.20	3.31	0.60	2.97	0.60	2.97
2.25	14.98	1.44	12.00	1.26	15.47	1.35	4.32	0.68	4.00	0.68	4.00
2.50	19.36	1.60	17.06	1.40	19.85	1.50	5.52	0.75	5.24	0.75	5.24
2.75	26.57	1.76	24.28	1.54	26.31	1.65	6.91	0.83	6.71	0.83	6.71
2.95	33.00	1.89	30.50	1.64	32.87	1.80	8.50	0.90	8.43	0.90	8.43
3.08	40.70	2.04	40.70	1.73	40.70	1.89	9.75	0.96	9.75	0.96	9.75
4.66	227.84	3.37	227.84	3.03	227.84	4.14	39.48	2.54	65.96	2.65	69.86
4.74	235.11	3.50	238.65	3.13	237.10	4.36	42.22	2.72	70.07	2.83	74.41
4.82	242.17	3.63	246.87	3.23	244.91	4.58	44.64	2.90	74.22	3.01	79.01
4.90	248.55	3.76	252.74	3.33	251.14	4.80	46.80	3.08	77.91	3.19	83.13
4.98	254.24	3.89	257.03	3.43	256.18	5.02	48.73	3.26	81.16	3.37	86.76
5.06	259.24	4.02	260.37	3.53	260.37	5.24	50.41	3.44	83.97	3.55	89.90
5.14	263.55	4.15	263.20	3.63	263.93	5.46	51.84	3.62	86.36	3.73	92.56
5.22	267.16	4.28	265.82	3.73	267.01	5.68	53.03	3.80	88.34	3.91	94.73
5.30	270.08	4.41	268.37	3.83	269.68	5.90	53.98	3.98	89.93	4.09	96.42
5.38	272.28	4.54	270.80	3.93	271.92	6.12	54.68	4.16	91.15	4.27	97.62
5.46	273.76	4.67	272.94	4.03	273.61	6.34	55.13	4.34	92.01	4.45	98.33
5.54	274.51	4.80	274.43	4.11	274.45	6.56	55.34	4.52	92.52	4.63	98.37
5.61	275.00	4.92	275.00	4.18	275.00	6.72	55.60	4.70	92.90	4.64	98.40

d: displacement, f: force

8.2 Incorporating Spinal Level and Gender Effects into Average Curves

The average rate curves combined spinal level and gender effects. The spinal level and gender effects were converted into ratios of the effect of one factor to the average of all factors combined (referred to as ‘ratio to average’ values). For example: the ratio of the value for upper spinal level failure force to the value of the overall failure force average of all levels. The spinal level and gender effects would be applied to the curves so characteristic values measured from the gender and spinal level effect curves would reflect the ratios compared to the average rate curves. The ratio to average values can be seen in Table 8-4 and Table 8-5 for spinal level and gender respectively. Spinal levels were grouped into upper (C2-C4), middle (C4-C6) and lower (C6-T1) regions according to the values and level of significance obtained from the statistical analysis.

Table 8-4: Spinal level effect ratios to average values

Ligament	Level	Failure Force (N)	Failure Elongation (mm)	Stiffness (N/mm)	Toe Region (mm)
ALL	Up	1.158	0.989	1.095	0.98
	Mid	0.839	0.864	0.925	0.882
	Low	1.01	1.123	0.991	1.117
PLL	Up	0.983	1.083	0.866	1.142
	Mid	1.126	0.98	1.123	0.825
	Low	0.888	0.927	1.017	1.06
CL	Up	1	0.844	1.075	0.98
	Mid	0.97	1.047	0.85	1.055
	Low	1.05	1.13	1.067	0.954
LF	Up	0.849	0.785	0.967	0.693
	Mid	0.787	0.969	0.736	0.816
	Low	1.322	1.225	1.257	1.443
ISL	Up	0.91	0.865	1.084	0.829
	Mid	0.798	0.946	0.965	0.729
	Low	1.253	1.159	0.965	1.388

Table 8-5: Gender effect ratios to average values

Ligament	Gender	Failure Force (N)	Failure Elongation (mm)	Stiffness (N/mm)	Toe Region (mm)
ALL	M	1.146	1.01	1.131	0.882
	F	0.861	0.99	0.875	1.108
PLL	M	1.035	1.058	0.98	1.095
	F	0.965	0.942	1.02	0.92
CL	M	1.104	1.086	0.998	1.04
	F	0.905	0.923	1.001	0.968
LF	M	1.051	1.033	1.091	1.075
	F	0.949	0.965	0.909	0.925
ISL	M	1.037	0.981	1.039	1.055
	F	0.964	1.019	0.963	0.992

To incorporate the spinal level and gender effects, the points from the average curve (developed for each rate) were scaled for each effect, so the values from the scaled curve reflected the ratios to the average values. Since scaling a curve to adjust one value was confounded to affect other values (increasing force would also increase stiffness), the scaling factors were weighted based on the significance (p-value) of the effect. The scaling factors were also not necessarily uniformly applied to the average curve; forces were scaled uniformly, but displacement values were scaled by different numbers for the values of the toe region, and the values of the traumatic region. This also minimized the confounding effect. Table 8-6 shows an example of how the scaling factors were applied to the average curves. For example, to apply the effects for upper spinal level, the elongation values would be multiplied by the scaling factors *a*, *b*, and *c*; *a* for the toe region, and *b* for the traumatic region, and the force values would be multiplied by *c*.

Table 8-6: Average curve scaling factors for effects

Region	Average Curve		Spinal Level								
	d	f	Upper		Middle		Lower		Gender		
	d	f	d	f	d	f	d	f	Male	Female	
Toe Region	0	0	a	c	d	f	h	j	k	m	n
	.	.									
	1.28	40									
Traumatic Region	2.84	256.5	b	e	i	o	p	q	r	s	t
	.	.									
	3.97	342									

After the scaling factors had been applied, ratios could be calculated using the values of the characteristic points from the scaled curves to the values from the average rate curves (curve ratios). These ratios needed to match the effect-average ratios (results ratios) from the results (The average rate curves combined spinal level and gender effects. The spinal level and gender effects were converted into ratios of the effect of one factor to the average of all factors combined (referred to as 'ratio to average' values). For example: the ratio of the value for upper spinal level failure force to the value of the overall failure force average of all levels. The spinal level and gender effects would be applied to the curves so characteristic values measured from the gender and spinal level effect curves would reflect the ratios compared to the average rate curves. The ratio to average values can be seen in Table 8-4 and Table 8-5 for spinal level and gender respectively. Spinal levels were grouped into upper (C2-C4), middle (C4-C6) and lower (C6-T1) regions according to the values and level of significance obtained from the statistical analysis.

Table 8-4 Since some factors were confounding, and it was impossible to make all ratios match, the significance level of each factor was used to weight the effects. The difference was calculated between the result ratios, and the curve ratios, and multiplied by the significance level. This term was referred to as the error term.

$$\text{Error Term} = |\text{Results Ratio} - \text{Curve Ratio}| \times (100 \times (1 - p_{\text{value}}))$$

There was an error term for each of the four characteristic point values, for each spinal level (4x3) and each gender (4x2), for a total of 20 error terms (12+8). The scaling factors were obtained by using a solver function to minimize the sum of the error terms by adjusting the scaling factors. Therefore terms with the lowest p-values, had the highest weighting, and contributed the most to the sum of the error terms, so the scaling factors were adjusted to best represent the most significant effects. The scaling factors are shown in Table 8-7.

Table 8-7: Spinal level and gender effect scaling factors for average curves

Ligament	Spinal Level						Gender			
	Upper		Middle		Lower		Male		Female	
	<i>d</i>	<i>f</i>	<i>d</i>	<i>f</i>	<i>d</i>	<i>f</i>	<i>d</i>	<i>f</i>	<i>d</i>	<i>f</i>
ALL	0.96	1.15	0.86	0.83	1.15	1.03	0.88	1.15	1.11	0.86
	1.00		0.87		1.11		0.95		1.04	
PLL	1.13	0.97	0.83	1.14	1.06	0.88	1.09	1.03	0.92	0.97
	1.11		0.95		0.94		1.06		0.94	
CL	0.83	0.96	0.99	0.95	1.16	1.11	1.04	1.10	0.97	0.90
	0.86		1.06		1.10		1.09		0.92	
LF	0.70	0.86	0.84	0.80	1.41	1.31	1.07	1.05	0.92	0.95
	0.77		0.94		1.28		1.04		0.97	
ISL	0.83	0.91	0.74	0.81	1.38	1.24	1.05	1.03	0.99	0.97
	0.86		0.93		1.19		1.02		1.00	

Note: for each ligament, upper elongation scaling factors are applied to toe region values, lower factors are applied to traumatic region

The resulting curves with one scaling factor applied to each (either spinal level or gender) compared to the initial average quasi-static curve for the ALL can be seen in Figure 8-4. For modeling purposes both a spinal level and gender scaling factor would be applied by multiplying the scaling factors together for each region of the curve (Figure 8-5). Since no spinal level and gender interaction effects were found, scaling factors are independent of each other.

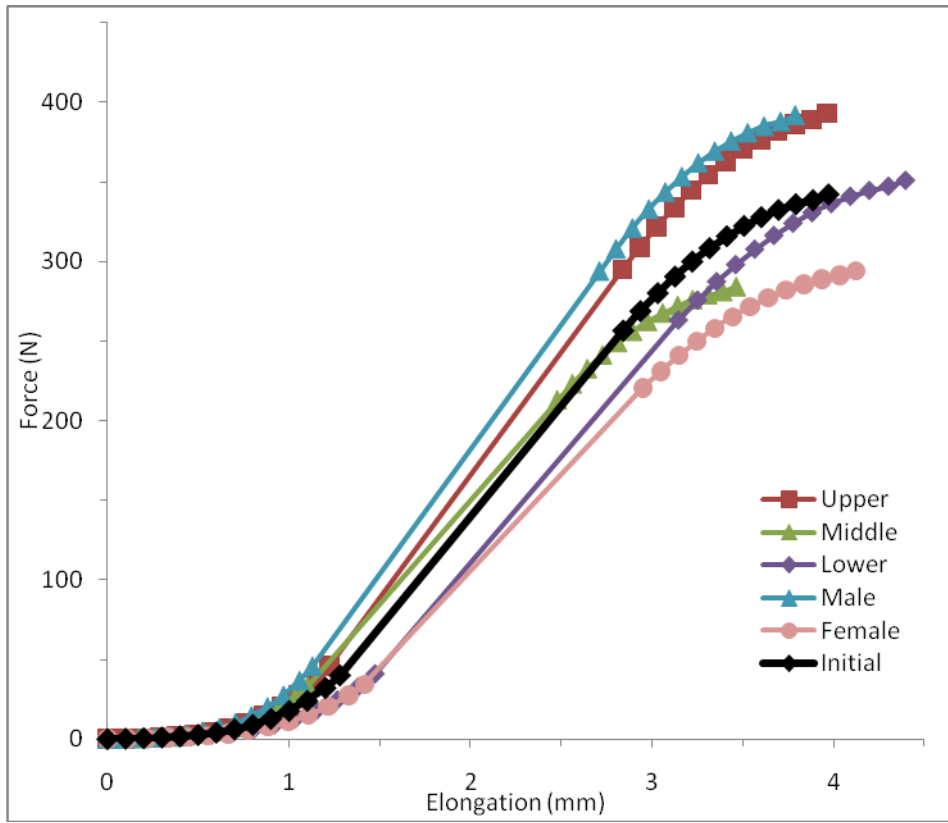


Figure 8-4: Average quasi static ALL curve with spinal level and gender scaled curves

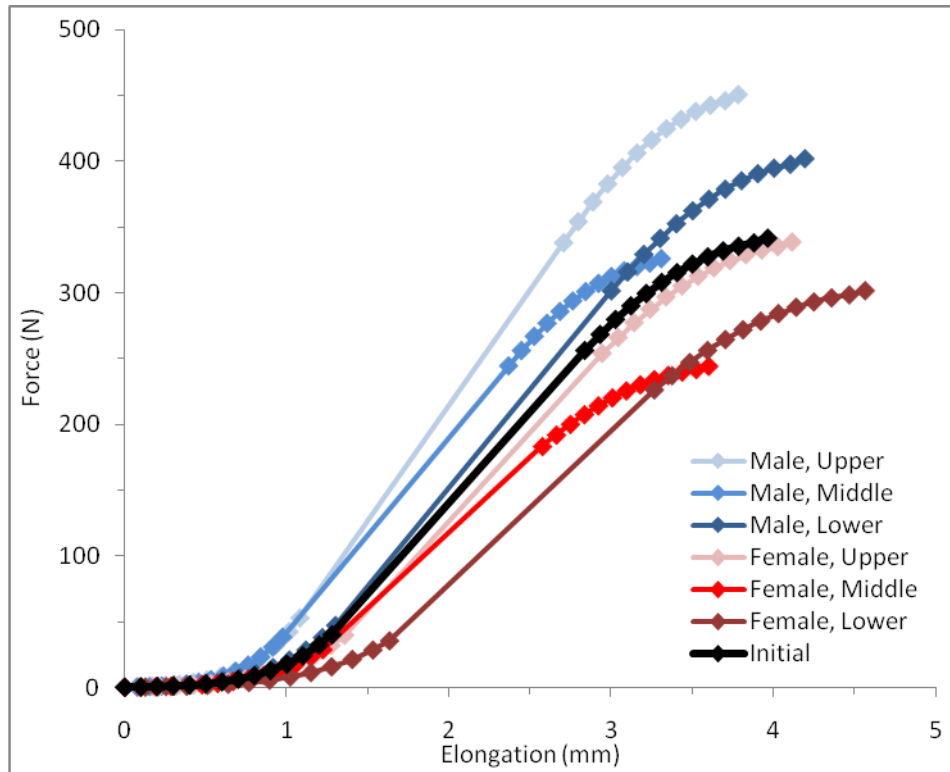


Figure 8-5: Combined gender and spinal level average curves for quasi-static ALL

8.3 Addition of Post-Failure Response Region to Average Curves

As there were no obvious differences in post-failure response for the curves based on strain rate, spinal level, or gender effects, only one post-failure response was used for each ligament for all average curve circumstances. To determine the most representative curve for each ligament, the quasi-static strain rate curves were normalized so each curve reached failure at a value of 1 for force and elongation. The median curve was then selected as the curve that most demonstrated the characteristic failure shape, and fell closest to the middle of the outermost extreme curves. Although this method is subjective, it was deemed acceptable as the curve only needed to provide a guideline to be used to characterize the failure response in the model. The normalized curve was reduced to 20 points for simplicity, ensuring the curve shape was still maintained. Post-failure response curves were added to the average curves, and multiplied by the failure force and elongation of the curve it

was added to. Normalized post-failure region curves are shown in Figure 8-6 and values are shown in Table 8-8.

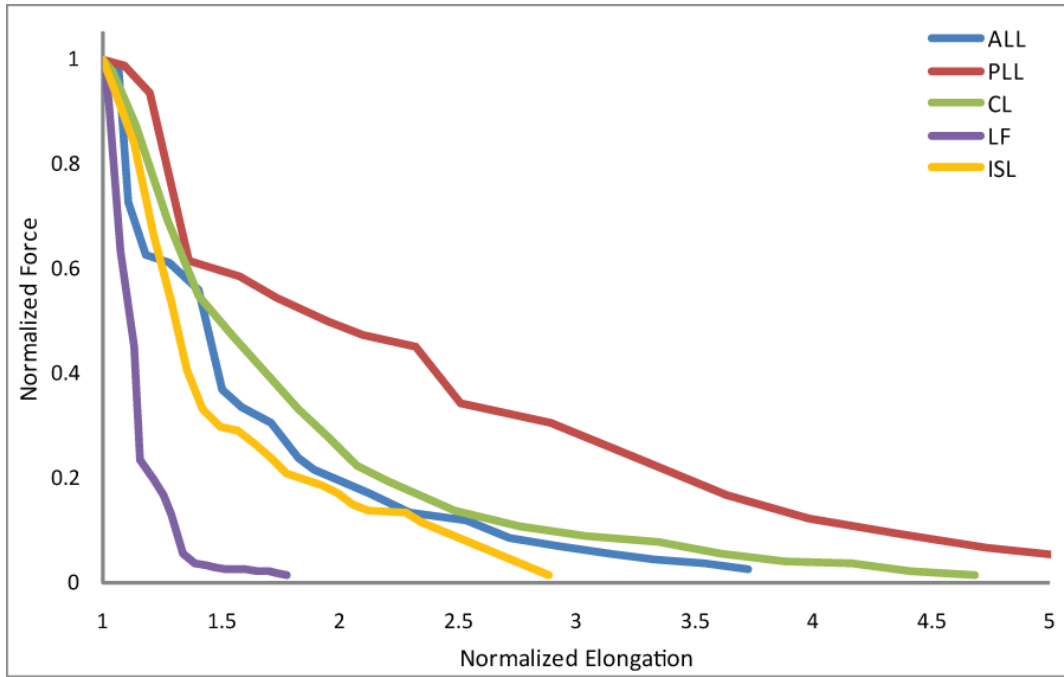


Figure 8-6: Post-failure normalized curve response for primary ligaments

Table 8-8: Post-failure normalized values for primary ligaments

ALL		PLL		CL		LF		ISL	
<i>d</i>	<i>f</i>	<i>d</i>	<i>f</i>	<i>d</i>	<i>f</i>	<i>d</i>	<i>f</i>	<i>d</i>	<i>f</i>
1.00	1.00	1.00	1.00	1.00	1.00	1.00	1.00	1.00	1.00
1.06	0.98	1.09	0.99	1.04	0.98	1.01	0.97	1.04	0.95
1.11	0.73	1.20	0.93	1.14	0.87	1.03	0.92	1.06	0.92
1.19	0.63	1.37	0.61	1.27	0.69	1.07	0.63	1.14	0.84
1.28	0.61	1.58	0.58	1.41	0.55	1.13	0.45	1.21	0.66
1.41	0.56	1.73	0.55	1.55	0.47	1.16	0.23	1.29	0.54
1.50	0.37	1.95	0.50	1.68	0.40	1.22	0.20	1.36	0.41
1.59	0.33	2.10	0.47	1.82	0.33	1.26	0.17	1.42	0.33
1.72	0.31	2.32	0.45	1.96	0.28	1.29	0.13	1.49	0.30
1.83	0.24	2.51	0.34	2.08	0.22	1.34	0.06	1.57	0.29
1.90	0.22	2.89	0.31	2.21	0.19	1.39	0.04	1.64	0.26
2.12	0.17	3.26	0.24	2.49	0.14	1.44	0.03	1.71	0.24
2.30	0.14	3.63	0.17	2.76	0.11	1.47	0.03	1.77	0.21
2.54	0.12	3.99	0.12	3.04	0.09	1.52	0.03	1.93	0.19
2.72	0.09	4.37	0.09	3.35	0.08	1.56	0.02	1.99	0.17
2.92	0.07	4.74	0.07	3.61	0.06	1.60	0.02	2.06	0.15
3.14	0.06	5.13	0.05	3.88	0.04	1.65	0.02	2.13	0.14
3.33	0.05	5.53	0.03	4.16	0.04	1.70	0.02	2.28	0.13
3.55	0.04	5.89	0.03	4.42	0.02	1.73	0.02	2.35	0.11
3.73	0.03	6.51	0.01	4.69	0.01	1.78	0.01	2.89	0.02

d: displacement, *f*: force

8.4 Validation of Average Curve Development

To ensure validity of the average curves, values were crosschecked back with values from the raw data curves. The value obtained from a particular case (ligament, rate, spinal level, gender) from the average curves, was compared to the average value obtained from the same test circumstance. Sample sizes usually ranged between 1-4 samples for each particular case for each ligament, with the exception of CL (2-6 samples, due to two ligaments per FSU). The value measured from the average curve was checked to see if it fell within 1 or 2 standard deviations of the average results from the raw data for failure force, failure elongation, stiffness, and toe region (Table 8-9). No standard

deviation exists for instances with only one sample, so the average standard deviation of the other circumstances for that ligament was used. In total, 80% of the values fell within one standard deviation, and 89% of the values fell within two standard deviations. One contributor to the error was when a particular instance only had two samples, and the values were similar. This resulted in a very small standard deviation in which it was rare the average curve value would fall within. When these cases (SD less than 20% the value of the average SD), were replaced with the average standard deviation, the total increased to 85% within one SD and 94% within 2 SD. The quantity within standard deviations is much higher for the CL, illustrating the importance of increased sample size.

Table 8-9: Quantity of specific instance values to fall within standard deviations of raw data results

	1 SD	2 SD
ALL	75%	88%
PLL	82%	88%
CL	90%	97%
LF	82%	93%
ISL	71%	82%
Total	80%	89%

8.5 Craniovertebral Average Curves

The same process was used to develop the average curves for the craniovertebral ligaments. Since there were so few significant effects however, only two different curves for rate effects were developed for the TM complex; only one average curve was developed for the other ligaments as seen in Figure 8-7, and values for the average curves are shown in Table 8-10. Normalized post-failure response region curves are shown in Figure 8-8 and values are shown in Table 8-11. Average curves were not developed for the AAAM and the PAAM due to the limited sample size.

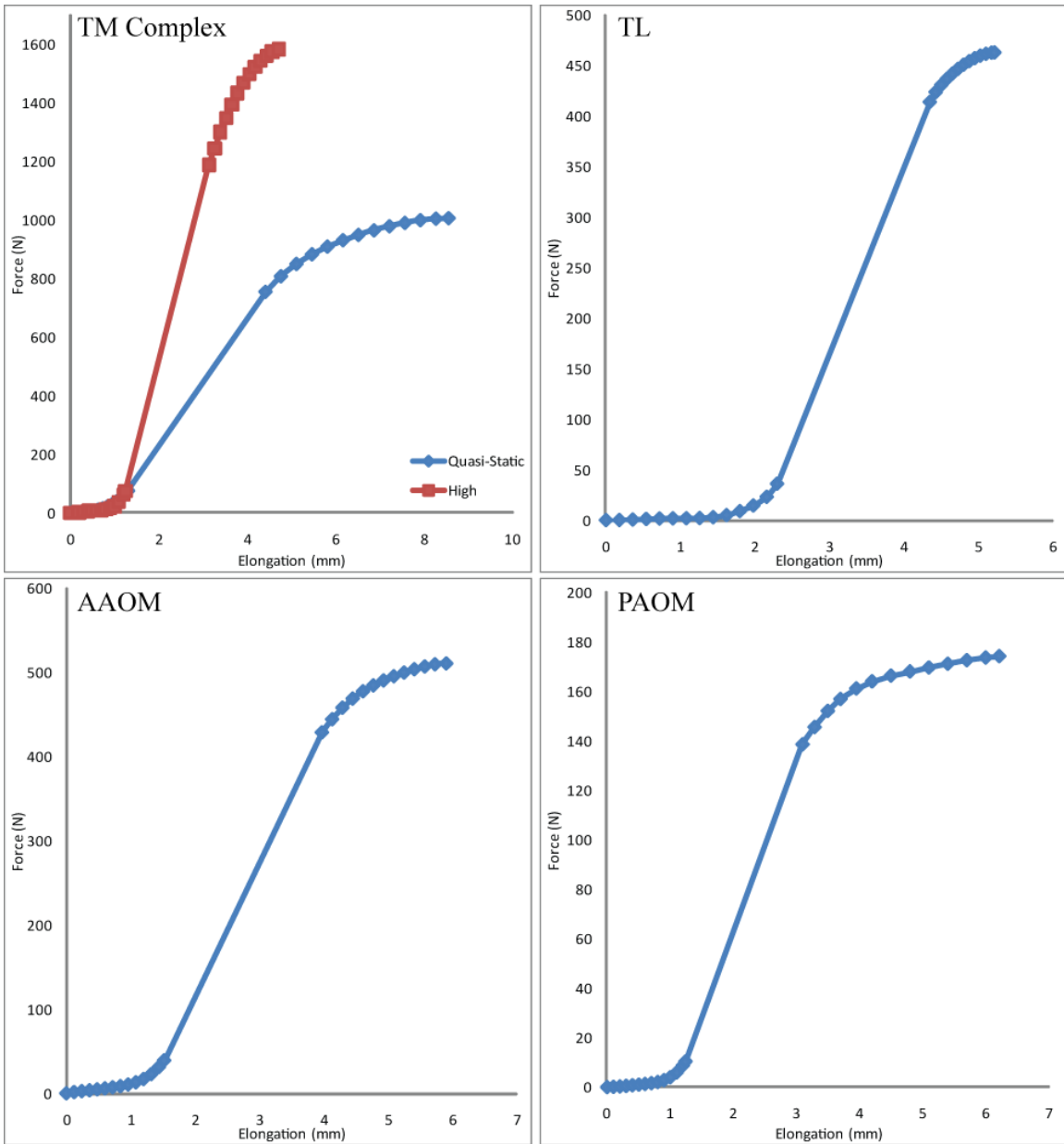


Figure 8-7: Average craniovertebral curves

Table 8-10: Average curve values for craniovertebral ligaments

TM Complex				TL		AAOM		PAOM	
Quasi-Static		High Rate		<i>d</i>	<i>f</i>	<i>d</i>	<i>f</i>	<i>d</i>	<i>f</i>
<i>d</i>	<i>f</i>	<i>d</i>	<i>f</i>						
0.00	0.00	0.00	0.00	0.00	0.00	0.00	0.00	0.00	0.00
0.11	1.56	0.10	0.46	0.18	0.02	0.12	1.40	0.10	0.11
0.21	2.80	0.20	1.21	0.36	0.51	0.24	2.57	0.20	0.28
0.32	3.97	0.30	3.61	0.54	1.08	0.36	3.64	0.30	0.50
0.42	5.38	0.40	5.83	0.72	1.50	0.48	4.70	0.40	0.75
0.53	7.38	0.50	7.41	0.90	1.70	0.60	5.79	0.50	1.00
0.63	10.35	0.60	8.39	1.08	1.79	0.72	7.00	0.60	1.27
0.74	14.64	0.70	9.26	1.26	2.05	0.84	8.45	0.70	1.61
0.84	20.60	0.80	10.97	1.44	2.90	0.96	10.36	0.80	2.08
0.95	28.57	0.90	14.96	1.62	4.94	1.08	13.03	0.90	2.81
1.05	38.80	1.00	23.14	1.80	8.95	1.20	16.95	1.00	4.00
1.16	51.51	1.10	37.86	1.98	14.50	1.32	22.74	1.10	5.90
1.26	66.80	1.20	61.99	2.16	23.00	1.44	31.27	1.20	8.84
1.31	75.00	1.25	75.00	2.30	36.00	1.52	39.00	1.24	10.40
4.41	754.50	3.13	1186.50	4.35	414.00	3.98	429.00	3.10	138.40
4.76	807.63	3.26	1243.30	4.43	423.74	4.14	444.64	3.29	145.37
5.11	849.80	3.39	1298.66	4.51	430.76	4.30	458.38	3.50	151.88
5.46	882.83	3.52	1348.32	4.58	436.85	4.46	469.21	3.70	156.71
5.81	909.16	3.65	1392.65	4.66	442.15	4.62	477.85	3.95	160.97
6.16	930.68	3.78	1431.97	4.73	446.79	4.78	484.87	4.20	163.83
6.51	948.85	3.91	1466.53	4.81	450.85	4.94	490.73	4.50	166.14
6.86	964.57	4.04	1496.55	4.88	454.37	5.10	495.76	4.80	167.85
7.21	978.30	4.17	1522.15	4.96	457.37	5.26	500.18	5.10	169.38
7.56	989.98	4.30	1543.43	5.03	459.82	5.42	504.06	5.40	170.91
7.91	999.06	4.43	1560.42	5.11	461.65	5.58	507.39	5.70	172.37
8.26	1004.50	4.56	1573.08	5.18	462.77	5.74	509.99	6.00	173.44
8.55	1006.00	4.71	1582.00	5.22	463.00	5.91	511.00	6.21	174.00

d: displacement, *f*: force

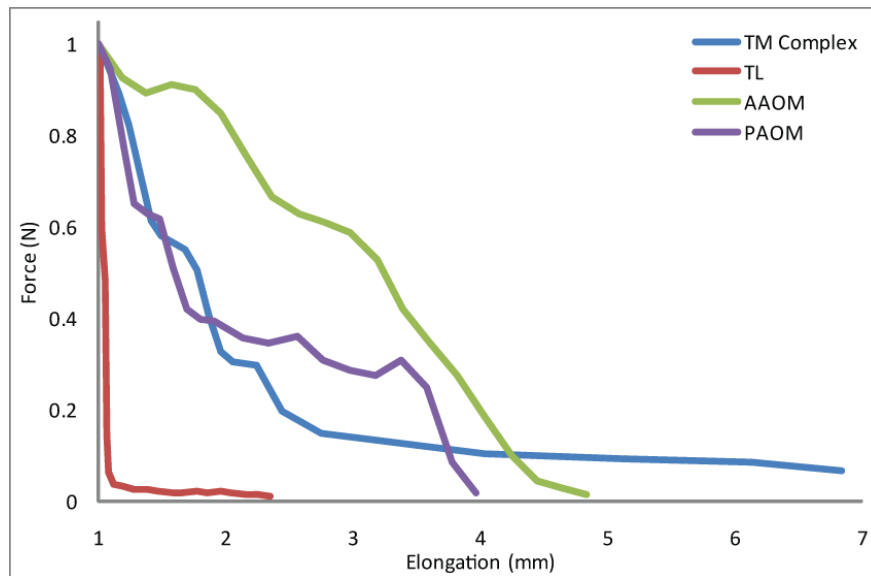


Figure 8-8: Post-failure normalized curve response for primary ligaments

Table 8-11: Post-failure normalized values for craniovertebral ligaments

TM Complex		TL		AAOM		PAOM	
<i>d</i>	<i>f</i>	<i>d</i>	<i>f</i>	<i>d</i>	<i>f</i>	<i>d</i>	<i>f</i>
1.00	1.00	1.00	1.00	1.00	1.00	1.00	1.00
1.08	0.95	1.01	0.98	1.19	0.93	1.10	0.95
1.16	0.89	1.04	0.59	1.38	0.89	1.20	0.77
1.25	0.82	1.06	0.48	1.58	0.91	1.29	0.65
1.33	0.72	1.07	0.14	1.76	0.90	1.39	0.63
1.42	0.61	1.08	0.06	1.96	0.85	1.49	0.62
1.50	0.58	1.12	0.04	2.16	0.76	1.59	0.51
1.59	0.56	1.20	0.03	2.36	0.66	1.70	0.42
1.68	0.55	1.28	0.03	2.57	0.63	1.81	0.40
1.77	0.51	1.39	0.03	2.78	0.61	1.92	0.39
1.87	0.40	1.47	0.02	2.98	0.59	2.13	0.36
1.96	0.33	1.59	0.02	3.19	0.53	2.34	0.35
2.05	0.30	1.66	0.02	3.39	0.42	2.56	0.36
2.25	0.30	1.78	0.02	3.61	0.35	2.77	0.31
2.44	0.20	1.85	0.02	3.82	0.28	2.97	0.29
2.75	0.15	1.97	0.02	4.04	0.18	3.18	0.27
4.04	0.10	2.05	0.02	4.25	0.10	3.38	0.31
5.12	0.09	2.16	0.01	4.44	0.04	3.59	0.25
6.13	0.09	2.25	0.01	4.63	0.03	3.78	0.09
6.83	0.07	2.35	0.01	4.84	0.02	3.97	0.02

d: displacement, f: force

Chapter 9

Conclusions and Recommendations

9.1 Conclusions

The ligaments of the cervical spine provide a significant contribution to the dynamic response of the neck in automotive crash events, where victims are predominantly young males under the age of 40 (Robertson et al., 2002). Damage to these ligaments has been associated with neck strain and whiplash injuries. The mechanical properties of the cervical spine ligaments are needed for a younger population, at relevant strain rates, for the prediction of head/neck kinematic response and the prediction of injury using numerical models. Injury predictors in a model are sensitive to material property changes of the soft tissues, stressing the importance of ligament properties for this application.

Previous studies have been performed but have limitations. All previous studies have been performed using older cadavers, most with average age older than 60 years old, which is not representative of the age of victims most commonly involved in automobile accidents, and ligament mechanical properties have been shown to decrease with age. Spinal level and gender effects have also not been examined in detail. Previous studies were performed without consistent testing conditions, making it difficult to compare results and impractical to combine results, establishing the need for a larger, more comprehensive study. In particular, many studies did not implement preconditioning cycles on the specimens prior to testing or perform the tests under representative temperature and humidity conditions which has been shown to have a significant effect on test results (Bass et al. 2007).

Extensive testing and analyses were undertaken on young cervical spine ligaments averaging 44 (27 to 50) years old, to evaluate the effect of loading rate, spinal level and gender at strain rates applicable to automotive crash scenarios. A limit of 50 years old was placed on cadaver specimens used in the study as osteoporosis has been shown to occur more frequently at the age of 50 (Kanis et al., 1994), and ligament properties have been shown to be correlated with the bone mineral content (Neumann et

al., 1994). An upper limit of 50 years old also ensures a sufficient quantity of spines, as uninjured cervical spines are not readily available under the age of 40.

Spines were dissected in functional spinal units and ligaments were isolated into bone-ligament-bone complexes, as bone ends were secured in polyethylene cups using a casting resin. Tests were performed replicating *in vivo* temperature ($\sim 37^{\circ}\text{C}$) and humidity levels after specimens were appropriately preconditioned for 20 cycles at 10% strain. Ligament specimens were tested at quasi-static (0.5 s^{-1}), medium (20 s^{-1}), and high ($150, 250\text{ s}^{-1}$) strain rates, and analyzed by loading rate, spinal level and gender. Spinal levels were defined as upper (C2-C4), middle (C4-C6) and lower (C6-T1), with groups investigated to ensure no between level effects were masked. The following metrics were examined: failure force, failure elongation, stiffness of the linear loading region, and toe region. In these cases, it was noted that the results could be dependent on structural factors, as ligament size was not considered. To analyze the material properties of the ligaments, the failure stress, failure strain, modulus, and toe region strain were also analyzed. Post-failure response was also reported for all ligaments.

Values reported from the younger specimens of this study were consistently stronger and stiffer than results from previous studies involving older test specimens. The most significant effects were found to be increasing deformation rate with increased stiffness, modulus, failure force, and failure stress. This effect was statistically significant for the anterior longitudinal ligament, posterior longitudinal ligament, capsular ligament and interspinous ligament, and trends were present for the ligamentum flavum. The ligamentum flavum was the only ligament to show consistent and significant spinal level effects, as the lower level failed at a higher failure force, stress, and longer elongation and had a higher modulus compared to the upper and middle spinal levels. Generally, gender effects were not found to be significant; however, male ligaments displayed trends typically failing at a higher force, and stress and often having a higher stiffness and modulus compared to female ligaments. The craniovertebral ligaments did not demonstrate gender effects or expected rate effects, except for the tectorial membrane complex (tectorial membrane, vertical cruciate, apical, alars ligaments) in which failure elongation and strain decreased with increasing strain rate, and stiffness increased with increasing rate. The results obtained provide a more detailed set of mechanical properties of human

craniovertebral ligaments for younger specimens than previously available in the literature, offering a better understanding of the ligament behaviour.

Values of characteristic points were measured from the ligament force-deflection curves and used to develop average curves. Average curves were initially developed for rate effects, which were consistently the most significant effects. Scaling factors were then applied to the curves to represent spinal level and gender effects. Values measured from the average curves were validated against values from the raw data curves to ensure average curves were representative of the results.

The results presented in this study provide a detailed measure of ligament response and failure of a younger population, at strain rates relevant to automotive crash scenarios, and provide a new data set to support the development of detailed finite element models of the cervical spine for the prediction of response and prevention of injury.

9.2 Recommendations

Recommendations for future isolated cervical spine ligament studies include direct measurement of the ligament cross sectional areas while the ligament is loaded. It is difficult to measure cross sectional areas accurately without damaging the ligaments, however optical techniques can be employed to measure area under loading. These methods were not accessible at the time of testing, and are difficult to implement with the use of an environmental chamber. Emphasis was put on force-deflection properties to correspond with ligaments being modeled as beam elements in most finite element models, thus accurate stress-strain curves were not needed. The length to area ratios method was used from previous studies to provide non-dimensionalized properties (failure stress, strain, modulus) in order to make estimated comparisons with dimensionalized properties (length, force, stiffness) to determine if significant effects were due to structural or material properties, however results were not conclusive. In order to make more accurate comparisons, or provide accurate stress-strain curves, ligament areas must be measured during loading to calculate true stress and true strain.

Additional testing of young ligaments of larger sample sizes would be beneficial to further explore spinal level and gender effects, with tests performed under the same testing conditions. One of the

main concerns with previous data was the lack of consistency between studies of the conditions the tests were performed under, and what metrics were reported. This makes comparisons between studies difficult and combination of results between studies impossible. Additional testing performed in the future under identical testing conditions as the current study, due to the importance of simulating *in vivo* conditions, would allow for direct combination of the results, effectively increasing the sample size even further. Although the current study analyzed level effects by grouping ligaments into three levels (upper, middle, lower), and did not find significant trends within groupings, larger sample sizes would also promote further investigation of level effects grouped by individual level.

















Appendix A















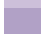

Raw Data Ligament Values

The results from the ligament tests are presented in the following pages. Within this Appendix and Appendix B, all spines are colour coded, with spinal level shown by the shade of colour, with lighter shades representing upper spinal levels and dark shades representing lower spinal levels. Within strain rate groupings, spines have the same colour, i.e. for all high rate ligaments, blue values are from the same spine.

Male		Spinal Level		Female
		Upper (C2-C4)		
		Middle (C4-C6)		
		Lower (C6-T1)		

Spine ID	Age	Gender	Rate	Colour
A	46	M	Quasi-static	
B	46	M	Quasi-static	
C	36	M	High	
D	27	M	High	
E	48	F	Quasi-static	
F	47	F	Quasi-static	
G	49	F	High	
H	48	F	High	
I	48	M	Medium	
J	44	M	Medium	
K	47	F	Medium	
L	47	F	Medium	
M	43	M	All	
N	45	F	High	
O	50	F	Quasi-static	
P	40	M	High	
Q	29	F	Quasi-static	Craniovertebral

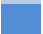





ALL QUASI-STATIC STRAIN RATE											
Spine	Level		Length (mm)	Failure Force (N)	Failure Elongation (mm)	Stiffness (N/mm)	Toe Region (mm)	Failure Stress (MPa)	Failure Strain	Modulus (MPa)	Toe Strain
C080686 Male A	C2-C3		4.63	701.79	5.01	225.43	1.41	62.56	1.08	93.04	0.30
	C4-C5		4.18	321.95	3.06	158.31	0.84	32.21	0.73	66.20	0.20
	C6-C7		3.5	519.04	5.05	171.89	1.06	43.61	1.44	50.55	0.30
C090278 Male B	C3-C4		6.88	261.64	3.74	124.19	0.85	22.16	0.54	72.36	0.12
	C5-C6		7.13	379.88	5.14	119.36	1.12	26.11	0.72	58.50	0.16
	C7-T1		4.81	317.23	4.93	123.75	1.73	25.25	1.02	47.38	0.36
UB08L002 Female E	C3-C4		3.04	320.76	2.75	160.36	1.60	33.77	0.91	51.32	0.53
	C5-C6		4.48	198.52	2.36	92.59	1.75	19.74	0.53	41.25	0.39
	C7-T1		3.07	342.34	3.67	125.14	1.25	26.42	1.20	29.64	0.41
C090033 Female F	C3-C4		3.35	508.90	4.01	218.47	1.24	53.34	1.20	76.71	0.37
	C5-C6		3.62	250.51	3.58	108.73	1.08	27.55	0.99	43.29	0.30
	C7-T1		4.03	448.15	4.93	140.61	0.93	43.34	1.22	54.80	0.23
S090252 Male, M	C7-T1		2.71	378.99	2.49	247.53	0.34	30.78	0.92	54.49	0.13
C100923 Female O	C3-C4		2.04	261.12	4.20	108.05	1.42	34.47	2.06	29.10	0.70
	C5-C6		1.86	132.08	3.00	60.01	1.48	16.02	1.61	13.54	0.80
	C7-T1		2.52	135.88	5.70	32.70	2.47	14.34	2.26	8.70	0.98

PLL QUASI-STATIC STRAIN RATE											
Spine	Level		Length (mm)	Failure Force (N)	Failure Elongation (mm)	Stiffness (N/mm)	Toe Region (mm)	Failure Stress (MPa)	Failure Strain	Modulus (MPa)	Toe Strain
C080686 Male A	C2-C3		5.42	491.05	4.05	170.31	1.31	43.46	0.75	81.69	0.24
	C4-C5		4.18	462.85	4.29	198.05	1.27	46.05	1.03	82.37	0.30
	C6-C7		4.5	334.49	3.22	171.65	1.12	21.33	0.72	49.25	0.25
C090278 Male B	C3-C4		6.47	420.73	4.58	167.10	0.28	35.37	0.71	90.90	0.04
	C5-C6		4.33	502.79	3.24	261.25	0.18	32.22	0.75	72.50	0.04
	C7-T1		3.57	181.49	2.09	145.80	0.85	13.00	0.59	37.28	0.24
UB08L002 Female E	C3-C4		3.04	183.52	3.31	95.91	1.13	19.18	1.09	30.47	0.37
	C5-C6		3.75	232.12	1.81	180.90	0.22	19.60	0.48	57.29	0.06
	C7-T1		4.18	199.27	1.02	262.14	0.39	13.33	0.24	73.31	0.09
C090033 Female F	C3-C4		3.57	380.42	2.48	325.60	0.97	35.82	0.70	109.44	0.27
	C5-C6		2.89	364.13	2.34	195.00	0.21	28.76	0.81	44.50	0.07
	C7-T1		2.1	353.20	3.07	267.33	0.36	27.89	1.46	44.33	0.17
S090252 M	C7-T1 M		3.18	277.25	1.02	368.39	0.18	15.36	0.32	64.90	0.06
C100923 Female O	C3-C4		2.9	406.48	2.03	203.26	0.95	54.68	0.70	79.29	0.33
	C5-C6		1.82	343.16	2.29	215.28	0.76	34.03	1.26	38.85	0.42
	C7-T1		2.99	319.27	2.00	206.68	0.83	28.59	0.67	55.33	0.28


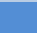









CL QUASI-STATIC STRAIN RATE											
Spine	Level		Length (mm)	Failure Force (N)	Failure Elongation (mm)	Slope (N/mm)	Toe Region (mm)	Failure Stress (MPa)	Failure Strain	Modulus (MPa)	Toe Strain
C080686 Male A	C2-C3		6.29	276.64	6.72	94.67	0.23	3.93	1.07	8.46	0.04
			5.89	177.01	1.87	125.40	0.18	2.68	0.32	11.20	0.03
	C4-C5		6.22	180.33	3.12	83.19	1.02	2.59	0.50	7.43	0.16
C090278 Male B	C3-C4		5.11	147.96	5.36	59.79	0.68	2.59	1.05	5.34	0.13
			4.57	161.81	3.65	61.24	1.58	3.16	0.80	5.47	0.35
	C5-C6		6.77	263.20	5.26	72.20	1.03	2.96	0.78	5.50	0.15
			7.52	327.21	4.35	104.42	0.92	3.31	0.58	7.95	0.12
C7-T1		6.16	234.16	5.96	95.39	1.14	2.90	0.97	7.27	0.19	
UB08L002 Female E	C3-C4		3.17	154.27	3.01	59.91	0.57	4.35	0.95	5.35	0.18
			3.94	181.22	5.93	67.60	0.36	4.11	1.51	6.04	0.09
	C5-C6		5.07	128.28	5.87	38.40	0.62	1.93	1.16	2.92	0.12
	C7-T1		5.03	207.62	4.38	74.59	0.31	3.14	0.87	5.68	0.06
			4.44	196.28	4.31	95.37	1.33	3.37	0.97	7.26	0.30
C090033 Female F	C3-C4		4.07	137.82	4.23	61.16	1.16	3.03	1.04	5.46	0.29
			4.18	216.70	3.65	104.60	1.85	4.63	0.87	9.34	0.44
	C5-C6		4.43	157.33	5.06	47.68	0.97	2.70	1.14	3.63	0.22
			5.51	187.69	4.12	76.43	1.86	2.59	0.75	5.82	0.34
C7-T1		4.37	276.91	7.76	144.40	0.82	4.83	1.78	11.00	0.19	
S090252 Male, M	C7-T1		3.87	354.29	2.99	232.00	1.24	6.97	0.77	17.67	0.32
C100923 Female O	C3-C4		3.12	141.10	3.00	89.25	0.33	4.04	0.96	7.97	0.11
			2.72	187.60	1.98	121.66	0.31	6.16	0.73	10.87	0.11
	C5-C6		3.49	122.58	4.27	44.18	0.86	2.67	1.22	3.36	0.25
			3.35	122.51	4.88	45.88	1.47	2.79	1.46	3.49	0.44
			3.37	166.01	4.47	60.91	0.37	3.75	1.33	4.64	0.11
C7-T1		4.08	163.64	3.14	62.31	0.72	3.05	0.77	4.75	0.18	

LF		QUASI-STATIC STRAIN RATE									
Spine	Level	Length (mm)	Failure Force (N)	Failure Elongation (mm)	Stiffness (N/mm)	Toe Region (mm)	Failure Stress (MPa)	Failure Strain	Modulus (MPa)	Toe Strain	
C080686 Male A	C2-C3	7.01	267.34	3.72	167.81	1.72	7.01	0.53	30.82	0.25	
	C4-C5										
	C6-C7	11	326.18	6.34	173.79	3.71	6.43	0.58	37.67	0.34	
C090278 Male B	C3-C4	9.17	164.59	6.66	57.20	3.70	3.30	0.73	10.51	0.40	
	C5-C6	8.95	214.13	6.53	115.91	4.43	5.19	0.73	25.13	0.49	
	C7-T1	11.29	194.32	7.19	108.60	5.21	3.73	0.64	23.54	0.46	
UB08L002 Female E	C3-C4	9.35	110.77	4.93	31.88	0.57	2.57	0.53	6.91	0.06	
	C5-C6	9.31	275.08	5.06	138.03	2.87	6.41	0.54	29.92	0.31	
	C7-T1										
C090033 Female F	C3-C4	7.41	269.86	6.77	128.05	4.52	6.69	0.91	23.52	0.61	
	C5-C6	9.36	190.85	6.71	94.67	4.63	4.42	0.72	20.52	0.49	
	C7-T1	10.27	198.12	5.81	104.12	4.06	4.18	0.57	22.57	0.40	
S090252 Male, M	C7-T1	9.3	429.35	4.55	298.57	2.96	10.01	0.49	64.72	0.32	
C100923 Female O	C3-C4	5.61	112.73	2.52	36.26	1.05	3.69	0.45	6.66	0.19	
	C5-C6	7.03	125.29	4.87	45.71	0.35	3.86	0.69	9.91	0.05	
	C7-T1	10.57	518.67	6.91	145.38	3.46	10.64	0.65	31.52	0.33	
















ISL		QUASI-STATIC STRAIN RATE									
Spine	Level		Length (mm)	Failure Force (N)	Failure Elongation (mm)	Stiffness (N/mm)	Toe Region (mm)	Failure Stress (MPa)	Failure Strain	Modulus (MPa)	Toe Strain
C080686 Male A	C2-C3		10.04	74.17	4.71	26.07	2.07	7.62	0.47	26.87	0.21
	C4-C5		10.02	41.04	5.61	20.08	1.06	4.22	0.56	20.70	0.11
	C6-C7		9.73	129.44	5.42	51.54	2.87	9.80	0.56	37.95	0.29
C090278 Male B	C3-C4		8.56	46.63	5.28	13.02	1.03	5.62	0.62	13.42	0.12
	C5-C6		12.37	37.80	8.57	8.02	0.66	2.25	0.69	5.91	0.05
	C7-T1		16.03	34.48	8.37	11.08	1.63	1.58	0.52	8.16	0.10
UB08L002 Female E	C3-C4		8	23.55	5.99	9.71	1.17	3.03	0.75	10.01	0.15
	C5-C6										
	C7-T1		12.9	106.41	7.11	24.01	2.67	6.07	0.55	17.68	0.21
C090033 Female F	C3-C4										
	C5-C6		8.57	46.36	6.76	11.04	1.92	3.98	0.79	8.13	0.22
	C7-T1		10.89	49.08	11.54	9.39	3.24	3.32	1.06	6.91	0.30
S090252 Male, M	C7-T1		13.16	52.81	6.67	12.95	2.82	2.96	0.51	9.54	0.21
C100923 Female O	C3-C4		7.99	16.22	4.67	4.31	0.47	2.09	0.58	4.44	0.06
	C5-C6		8.44	9.16	5.17	1.84	0.25	0.80	0.61	1.35	0.03
	C7-T1		8.52	111.58	8.20	28.17	4.62	9.64	0.96	20.74	0.54

ALL MEDIUM STRAIN RATE											
Spine	Level		Length (mm)	Failure Force (N)	Failure Elongation (mm)	Stiffness (N/mm)	Toe Region (mm)	Failure Stress (MPa)	Failure Strain	Modulus (MPa)	Toe Strain
S090450 Male I	C2-C3		4.07	621.16	5.05	195.09	0.84	42.27	1.24	54.03	0.21
	C4-C5		4.49	663.53	4.68	199.39	1.09	60.52	1.04	81.66	0.24
	C6-C7		3.77	231.10	2.69	104.90	0.82	18.68	0.71	31.97	0.22
S090305 Female L	C3-C4		3.67	417.70	5.68	114.70	1.51	39.75	1.55	40.06	0.41
	C5-C6		4.58	195.80	4.87	81.56	1.40	19.66	1.06	37.51	0.31
	C7-T1		3.42	597.10	5.85	175.30	0.88	62.93	1.71	63.19	0.26
S090365 Male J	C2-C3		4.33	218.10	1.78	179.00	0.63	17.74	0.41	63.05	0.14
	C4-C5		5.42	354.91	1.87	269.80	0.24	37.45	0.35	154.32	0.04
	C6-C7		3.92	209.20	3.41	108.10	1.41	23.63	0.87	47.86	0.36
C090115 Female K	C2-C3										
	C4-C5		4.05	343.40	2.67	178.70	0.53	37.33	0.66	78.68	0.13
	C6-C7		5.37	347.32	5.27	133.90	2.86	33.44	0.98	69.22	0.53
S090252 Male, M	C5-C6		4.53	411.09	2.96	230.47	0.25	36.68	0.65	93.16	0.06











CL MEDIUM STRAIN RATE											
Spine	Level		Length (mm)	Failure Force (N)	Failure Elongation (mm)	Slope (N/mm)	Toe Region (mm)	Failure Stress (MPa)	Failure Strain	Modulus (MPa)	Toe Strain
S090450 Male I	C2-C3		3.34	357.57	3.53	149.10	0.46	9.56	1.06	13.32	0.14
			3.81	157.07	4.04	76.46	0.56	3.68	1.06	6.83	0.15
	C4-C5		4.53	307.27	5.56	76.41	0.85	6.06	1.23	6.83	0.19
			3.76	347.94	4.48	102.36	0.04	8.27	1.19	9.14	0.01
			4.15	197.30	3.55	93.19	1.02	3.62	0.86	7.10	0.25
S090305 Female L	C3-C4		3.7	263.17	11.90	114.29	0.95	5.42	3.22	8.70	0.26
			3.02	238.61	3.83	163.40	0.59	7.06	1.27	14.60	0.20
	C5-C6		3.58	158.11	2.92	86.08	0.77	3.95	0.82	7.69	0.22
			4.78	208.09	3.62	74.28	0.70	3.32	0.76	5.66	0.15
			5.24	316.46	5.92	92.78	0.30	4.60	1.13	7.07	0.06
S090365 Male J	C7-T1		4.05	438.95	4.47	171.55	0.16	8.25	1.10	13.07	0.04
			3.52	383.08	2.80	238.54	0.16	8.29	0.80	18.17	0.05
	C2-C3		3.21	216.01	3.05	120.34	1.24	6.01	0.95	10.75	0.39
			3.29	299.38	5.06	147.30	0.14	8.13	1.54	13.16	0.04
			4.44	174.86	2.54	113.80	0.10	3.52	0.57	10.17	0.02
C4-C5		4.16	157.50	2.50	81.08	0.07	3.38	0.60	7.24	0.02	
		3.78	424.57	4.38	191.35	0.15	8.55	1.16	14.57	0.04	
C090115 Female K	C6-C7		3.62	207.35	5.91	103.76	1.86	4.36	1.63	7.90	0.51
			3.42	245.31	2.20	138.02	0.13	6.41	0.64	12.33	0.04
	C2-C3		3.19	161.15	3.74	66.24	0.22	4.51	1.17	5.92	0.07
			3.73	225.53	2.92	113.94	0.48	5.40	0.78	10.18	0.13
			3.78	177.32	3.99	114.95	0.13	3.57	1.06	8.75	0.03
S090252 Male, M	C5-C6		3.3	333.63	4.30	89.75	0.20	7.70	1.30	6.84	0.06
			3.68	336.56	3.47	166.76	1.15	6.97	0.94	12.70	0.31
			3.04	411.83	3.94	175.94	0.41	10.32	1.30	13.40	0.13


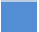


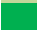














LF		MEDIUM STRAIN RATE									
Spine	Level		Length (mm)	Failure Force (N)	Failure Elongation (mm)	Stiffness (N/mm)	Toe Region (mm)	Failure Stress (MPa)	Failure Strain	Modulus (MPa)	Toe Strain
S090450 Male I	C2-C3		8.08	222.93	3.24	217.30	1.10	5.07	0.40	39.92	0.14
	C4-C5		9.54	266.90	4.84	113.50	2.43	5.14	0.51	20.85	0.25
	C6-C7		13.19	514.56	8.21	263.77	3.08	8.46	0.62	57.18	0.23
S090305 Female L	C3-C4		7.52	225.97	4.65	65.03	1.01	5.52	0.62	11.94	0.13
	C5-C6		7.92	231.83	5.10	69.63	2.95	6.35	0.64	15.09	0.37
	C7-T1		9.22	481.46	5.79	162.77	2.20	11.32	0.63	35.29	0.24
S090365 Male J	C2-C3		6.18	347.64	3.23	130.72	0.38	10.33	0.52	24.01	0.06
	C4-C5		6.84	98.54	2.71	46.20	0.52	3.12	0.40	10.02	0.08
	C6-C7		9.12	328.55	6.13	121.92	4.01	7.81	0.67	26.43	0.44
C090115 Female K	C2-C3		8.09	316.84	3.62	230.70	1.21	7.19	0.45	42.38	0.15
	C4-C5		8.43	331.75	4.92	116.41	2.32	8.53	0.58	25.24	0.28
	C6-C7		7.2	420.56	6.61	153.73	3.33	12.66	0.92	33.33	0.46
S090252 Male, M	C5-C6		7.92	471.48	5.00	142.21	2.00	12.90	0.63	30.83	0.25




















ALL		HIGH STRAIN RATE									
Spine	Level		Length (mm)	Failure Force (N)	Failure Elongation (mm)	Stiffness (N/mm)	Toe Region (mm)	Failure Stress (MPa)	Failure Strain	Modulus (MPa)	Toe Strain
S090017 Male D	C2-C3		4.72	483.01	3.49	279.11	0.40	41.74	0.74	113.85	0.09
	C4-C5		6.33	609.25	4.07	208.17	1.19	46.91	0.80	101.45	0.19
	C6-C7		4.27	582.87	5.85	367.84	0.66	51.13	1.37	137.79	0.15
S091076 Male C	C3-C4		3.43	517.14	4.72	231.22	1.28	62.97	1.38	96.57	0.37
	C5-C6										
	C7-T1										
C090542 Female G	C2-C3		4.44	593.81	3.19	249.52	0.64	48.38	0.72	90.26	0.14
	C4-C5		6.83	221.94	2.45	161.43	0.72	25.26	0.36	125.50	0.10
	C6-C7		3.87	386.08	3.85	180.79	0.35	33.58	0.99	60.85	0.09
C090300 Female H	C3-C4		3.77	276.44	2.00	259.11	0.49	31.20	0.53	110.25	0.13
	C5-C6										
	C7-T1										
S090252 Male, M	C3-C4		4.35	626.12	3.92	351.31	0.59	64.59	0.90	157.64	0.13
C090960 Female N	C3-C4		4.25	371.25	3.03	208.90	0.89	42.49	0.71	101.61	0.21
	C5-C6		3.2	253.48	3.41	224.60	0.32	33.34	1.06	94.52	0.10
	C7-T1		3.1	445.79	4.14	314.53	0.76	56.18	1.34	122.89	0.24
C100697 Male P	C3-C4		5.45	520.71	4.31	167.70	1.01	58.88	0.79	103.34	0.19
	C5-C6		4.64	501.65	3.32	252.66	1.06	47.42	0.72	110.82	0.23
	C7-T1										

PLL HIGH STRAIN RATE											
Spine	Level		Length (mm)	Failure Force (N)	Failure Elongation (mm)	Stiffness (N/mm)	Toe Region (mm)	Failure Stress (MPa)	Failure Strain	Modulus (MPa)	Toe Strain
S090017	C2-C3		3.87	425.94	1.70	425.21	0.40	33.02	0.44	127.57	0.10
Male	C4-C5		5.77	475.94	3.16	276.54	0.54	41.90	0.55	140.48	0.09
D	C6-C7		4.54	306.14	2.34	239.36	0.33	23.03	0.52	81.74	0.07
S091076	C3-C4		4.69	205.20	2.36	146.10	0.63	20.20	0.50	67.45	0.13
Male	C5-C6		4.69	279.66	2.30	547.55	1.43	19.94	0.49	183.08	0.30
C	C7-T1		4.35	516.53	2.50	443.89	0.59	39.70	0.57	148.42	0.14
C090542	C2-C3		3.89	554.96	3.97	490.04	0.48	54.60	1.02	187.56	0.12
Female	C4-C5		4.29	726.24	3.04	696.39	0.37	82.74	0.71	340.35	0.09
G	C6-C7		4.96	503.23	3.93	534.88	0.78	37.94	0.79	200.04	0.16
C090300	C3-C4		5.7	536.90	2.97	360.00	0.73	58.10	0.52	222.04	0.13
Female	C5-C6		3.75	404.05	1.86	378.15	0.31	33.84	0.50	118.76	0.08
H	C7-T1		4.68	560.64	2.01	531.33	0.52	41.68	0.43	184.86	0.11
S090252	C3-C4		4.3	372.84	2.50	312.69	0.63	36.47	0.58	131.53	0.15
Male, M											
C090960	C3-C4		4.25	282.79	3.20	133.25	0.84	34.46	0.75	69.00	0.20
Female	C5-C6		3.2	290.29	2.23	285.24	0.72	33.04	0.70	103.88	0.23
N	C7-T1		3.1	318.18	2.40	309.00	1.19	27.48	0.77	82.73	0.38
C100697	C3-C4		4.75	567.83	3.82	254.00	0.70	55.03	0.80	116.93	0.15
Male	C5-C6		5.28	561.95	2.89	328.25	0.76	46.87	0.55	144.56	0.14
P	C7-T1		3.13	404.18	3.70	186.64	1.37	28.40	1.18	41.05	0.44

CL HIGH STRAIN RATE											
Spine	Level	Length (mm)	Failure Force (N)	Failure Elongation (mm)	Stiffness (N/mm)	Toe Region (mm)	Failure Stress (MPa)	Failure Strain	Modulus (MPa)	Toe Strain	
S090017 Male D	C2-C3	3.25	221.94	3.58	118.60	0.50	6.10	1.10	10.59	0.15	
		3.42	289.97	4.48	167.23	0.51	7.57	1.31	14.94	0.15	
	C4-C5	6.29	284.85	4.78	92.30	0.82	4.05	0.76	8.25	0.13	
		5.72	272.77	7.95	99.45	0.75	4.26	1.39	8.88	0.13	
		C6-C7	3.83	324.94	6.94	94.00	0.63	6.46	1.81	7.16	0.16
3.54	388.04		8.48	77.16	0.41	8.35	2.40	5.88	0.12		
S081076 Male C	C3-C4	4.19	391.79	3.56	162.80	0.75	8.35	0.85	14.54	0.18	
		3.96	281.46	2.74	151.34	0.53	6.35	0.69	13.52	0.13	
	C5-C6	3.73	142.29	2.20	133.34	0.59	2.91	0.59	10.16	0.16	
		C7-T1	4.12	198.11	5.78	77.26	0.60	3.66	1.40	5.88	0.15
C090542 Female G	C2-C3		3.21	248.97	2.71	202.33	0.51	6.93	0.84	18.07	0.16
		2.69	261.18	2.31	144.72	0.67	8.67	0.86	12.93	0.25	
	C4-C5	3.4	222.09	3.65	143.80	0.63	5.84	1.07	12.85	0.19	
		3.73	131.37	2.91	89.66	0.71	3.15	0.78	8.01	0.19	
		C6-C7	4.18	263.27	5.55	141.60	0.49	4.80	1.33	10.78	0.12
3.26	218.41		5.45	135.05	0.39	5.10	1.67	10.29	0.12		

C090300	C3-C4		3.96	293.47	3.92	136.80	1.40	6.62	0.99	12.22	0.35
Female			3.96	354.42	4.97	126.80	0.71	8.00	1.26	11.33	0.18
H	C5-C6		3.9	223.21	6.80	117.15	0.42	4.36	1.74	8.92	0.11
			4.44	324.41	3.38	202.56	0.92	5.56	0.76	15.43	0.21
	C7-T1		3.32	218.82	1.63	232.36	0.49	5.02	0.49	17.70	0.15
			2.7	262.95	5.31	185.09	0.52	7.42	1.97	14.10	0.19
S090252	C3-C4		3.63	222.54	3.72	154.26	0.80	5.48	1.02	13.78	0.22
Male, M			4.13	408.13	5.32	127.03	0.48	8.83	1.29	11.35	0.12
C090960	C3-C4		4.1	274.33	2.71	193.13	0.83	5.98	0.66	17.25	0.20
Female			4.9	263.55	2.25	195.68	0.71	4.80	0.46	17.48	0.14
N	C5-C6		3.6	295.79	3.96	150.70	0.75	6.26	1.10	11.48	0.21
			4.3	348.09	4.01	154.45	0.74	6.17	0.93	11.76	0.17
	C7-T1		3.1	347.69	4.19	156.24	0.93	8.54	1.35	11.90	0.30
			3.4	183.00	2.08	148.14	0.41	4.10	0.61	11.28	0.12
C100697	C3-C4		4.13	433.33	3.25	196.40	0.94	9.37	0.79	17.55	0.23
Male			4.44	371.90	3.19	195.90	0.64	7.48	0.72	17.50	0.14
P	C5-C6		3.96	344.92	4.20	129.40	1.01	6.63	1.06	9.86	0.26
			4.2	318.52	8.70	90.33	0.87	5.78	2.07	6.88	0.21
	C7-T1		4.46	260.51	4.81	89.20	0.97	4.45	1.08	6.79	0.22
			4.93	386.55	4.62	113.06	0.79	5.97	0.94	8.61	0.16

LF HIGH STRAIN RATE											
Spine	Level		Length (mm)	Failure Force (N)	Failure Elongation (mm)	Stiffness (N/mm)	Toe Region (mm)	Failure Stress (MPa)	Failure Strain	Modulus (MPa)	Toe Strain
S090017 Male D	C2-C3		8.1	300.59	3.35	193.55	1.57	6.82	0.41	35.55	0.19
	C4-C5										
	C6-C7		8.58	295.08	6.95	128.10	4.29	7.46	0.81	27.77	0.50
S091076 Male C	C3-C4										
	C5-C6		7.88	169.67	5.68	78.14	0.43	4.67	0.72	16.94	0.05
	C7-T1		8.13	373.77	4.20	266.47	2.46	9.97	0.52	57.77	0.30
C090542 Female G	C2-C3		6.47	101.98	2.10	94.10	0.65	2.90	0.32	17.29	0.10
	C4-C5		8.5	100.30	3.88	53.50	0.94	2.17	0.46	9.83	0.11
	C6-C7		8.84	289.40	6.63	85.49	3.73	7.10	0.75	18.53	0.42
C090300 Female H	C3-C4		8.1	157.72	3.11	107.80	1.64	3.58	0.38	19.80	0.20
	C5-C6		7.42	275.15	2.80	257.28	1.18	8.04	0.38	55.77	0.16
	C7-T1										
S090252 Male, M	C3-C4		8.13	272.21	4.15	95.82	1.37	6.15	0.51	17.60	0.17
C090960 Female N	C3-C4		7.0	333.58	3.40	195.03	1.47	8.75	0.49	35.82	0.21
	C5-C6										
	C7-T1		10.1	400.79	3.11	250.89	1.33	8.60	0.31	54.39	0.13
C100697 Male P	C3-C4		6.32	180.58	3.31	102.30	0.78	5.25	0.52	18.79	0.12
	C5-C6		7.24	224.08	3.70	120.73	1.46	6.71	0.51	26.17	0.20
	C7-T1		8.57	397.48	6.42	137.80	3.86	10.05	0.75	29.87	0.45

ISL HIGH STRAIN RATE											
Spine	Level		Length (mm)	Failure Force (N)	Failure Elongation (mm)	Stiffness (N/mm)	Toe Region (mm)	Failure Stress (MPa)	Failure Strain	Modulus (MPa)	Toe Strain
S090017	C2-C3		10.50	29.50	6.09	15.48	2.07	2.90	0.58	15.96	0.20
Male	C4-C5										
D	C6-C7		11.01	114.93	5.07	27.90	1.57	7.69	0.46	20.54	0.14
S091076	C3-C4		10.78								
Male	C5-C6		10.78	105.93	3.56	68.90	0.29	7.24	0.33	50.74	0.03
C	C7-T1		12.94	108.21	3.84	37.30	0.77	6.16	0.30	27.47	0.06
C090542	C2-C3		9.01	209.29	5.86	59.62	1.40	23.94	0.65	61.46	0.16
Female	C4-C5		9.51	80.74	3.46	32.73	0.89	8.75	0.36	33.74	0.09
G	C6-C7		10.57	121.34	7.19	35.47	0.68	8.45	0.68	26.12	0.06
C090300	C3-C4		10.67	105.06	3.94	50.38	1.12	10.15	0.37	51.93	0.10
Female	C5-C6		9.88	71.27	4.02	34.11	0.49	5.31	0.41	25.12	0.05
H	C7-T1		13.74	66.04	4.19	25.70	1.16	3.54	0.30	18.92	0.08
S090252	C3-C4		7.37	65.20	2.89	26.46	0.81	9.12	0.39	27.28	0.11
Male, M											
C090960	C3-C4		10.50	80.37	4.73	29.13	1.59	7.89	0.45	30.03	0.15
Female	C5-C6		10.00	81.35	4.80	29.72	1.78	5.99	0.48	21.89	0.18
N	C7-T1		9.40	296.50	6.58	70.10	2.29	23.23	0.70	51.62	0.24
C100697	C3-C4		5.84	23.00	2.75	17.53	1.21	4.06	0.47	18.07	0.21
Male	C5-C6		11.22	62.54	4.87	18.75	1.17	4.10	0.43	13.81	0.10
P	C7-T1		14.16	51.71	5.09	17.37	1.19	2.69	0.36	12.79	0.08

TM Complex										
Gender	Rate	Length (mm)	Failure Force (N)	Failure Elongation (mm)	Stiffness (N/mm)	Toe Region (mm)	Failure Stress (MPa)	Failure Strain	Modulus (MPa)	Toe Strain
M	H	16.66	1955.56	5.10	550.30	0.77	57.45	0.31	16.17	0.05
M	Q	23.22	551.39	11.34	162.82	1.72	19.04	0.49	5.62	0.07
M	H	20.28	1856.68	5.78	636.72	1.55	54.22	0.29	18.59	0.08
M	H	23.53	1065.53	4.72	401.53	1.61	38.32	0.20	14.44	0.07
F	H	12.12	1687.93	3.16	878.80	0.91	49.70	0.26	25.88	0.08
F	Q	16.76	1368.21	8.05	231.52	1.22	37.20	0.48	6.30	0.07
F	H	16.22	1344.91	4.79	483.02	1.43	31.50	0.30	11.31	0.09
F	Q	20.08	1099.44	6.26	262.21	0.98	42.85	0.31	10.22	0.05

TL										
Gender	Rate	Length (mm)	Failure Force (N)	Failure Elongation (mm)	Stiffness (N/mm)	Toe Region (mm)	Failure Stress (MPa)	Failure Strain	Modulus (MPa)	Toe Strain
M	Q	23.22	452.77	4.53	180.63	1.92	21.22	0.20	8.46	0.08
M	H	26.00	365.18	5.77	137.04	2.11	16.52	0.22	6.20	0.08
M	H	19.62	359.30	4.98	151.56	2.39	21.38	0.25	9.02	0.12
F	H	20.86	448.05	5.38	196.23	2.83	29.71	0.26	13.01	0.14
F	Q	16.01	616.74	4.97	211.96	2.02	37.08	0.31	12.74	0.13
F	H	19.00	520.37	5.70	228.34	2.47	24.34	0.30	10.68	0.13

Ligament	Gender	Rate	Length (mm)	Failure Force (N)	Failure Elongation (mm)	Stiffness (N/mm)	Toe Region (mm)	Failure Stress (MPa)	Failure Strain	Modulus (MPa)	Toe Strain
AAAM	F	Q	12.47	1068.22	6.59	221.19	0.95	21.21	0.53	4.39	0.08
PAAM	F	Q	15.72	97.33	7.77	42.68	1.35	4.52	0.49	1.98	0.09

AAOM											
Gender	Rate	Length (mm)	Failure Force (N)	Failure Elongation (mm)	Stiffness (N/mm)	Toe Region (mm)	Failure Stress (MPa)	Failure Strain	Modulus (MPa)	Toe Strain	
M	Q	13.08	799.05	6.52	218.14	1.61	8.06	0.50	2.20	0.12	
M	Q	14.20	310.64	5.09	122.22	0.95	3.16	0.36	1.24	0.07	
M	H	11.92	391.91	7.01	90.69	1.05	7.38	0.59	1.71	0.09	
M	H	10.52	426.12	8.82	100.31	0.92	7.37	0.84	1.73	0.09	
M	Q	12.19	583.68	8.05	108.34	2.78	8.36	0.66	1.55	0.23	
M	Q	15.76	474.36	6.63	121.35	3.44	6.57	0.42	1.68	0.22	
M	H	10.80	485.08	4.32	209.69	0.24	6.49	0.40	2.81	0.02	
M	H	10.69	419.02	5.49	148.78	1.16	5.64	0.51	2.00	0.11	
F	H	11.91	632.60	4.23	249.82	1.41	7.11	0.35	2.81	0.12	
F	H	12.59	443.42	5.56	140.27	1.72	4.46	0.44	1.41	0.14	
F	H	15.15	627.53	4.72	257.87	1.91	4.62	0.31	1.90	0.13	
F	H	16.71	647.86	8.02	138.93	2.67	4.12	0.48	0.88	0.16	
F	Q	11.50	306.30	4.44	101.37	1.03	4.60	0.39	1.52	0.09	
F	Q	12.00	622.58	5.28	168.44	1.03	8.87	0.44	2.40	0.09	

PAOM										
Gender	Rate	Length (mm)	Failure Force (N)	Failure Elongation (mm)	Stiffness (N/mm)	Toe Region (mm)	Failure Stress (MPa)	Failure Strain	Modulus (MPa)	Toe Strain
M	Q	11.13	259.33	6.37	64.60	1.36	4.11	0.57	1.02	0.12
M	Q	11.25	312.07	6.18	101.68	1.23	4.87	0.55	1.59	0.11
M	H	11.765	224.59	6.58	50.54	0.78	6.17	0.56	1.39	0.07
M	H	11.385	167.19	4.04	90.86	1.89	4.50	0.35	2.44	0.17
M	H	15.925	119.54	3.46	51.33	0.97	2.31	0.22	0.99	0.06
M	H	14.155	243.19	3.49	200.32	0.49	4.34	0.25	3.57	0.03
M	Q	14.835	100.25	7.77	36.91	0.41	2.43	0.52	0.89	0.03
M	Q	15.67	162.54	4.97	64.16	0.47	2.88	0.32	1.14	0.03
F	H	14.475	168.60	4.70	71.70	2.02	3.03	0.32	1.29	0.14
F	H	13.975	156.71	4.86	56.96	1.54	2.33	0.35	0.85	0.11
F	H	21.265	108.72	4.98	33.25	1	3.18	0.23	0.97	0.05
F	H	19.845	104.71	16.07	35.15	1.03	2.85	0.81	0.96	0.05
F	Q	15	136.54	11.27	20.92	2.35	3.45	0.75	0.53	0.16
F	Q	12.5	219.29	5.42	67.56	1.42	4.94	0.43	1.52	0.11

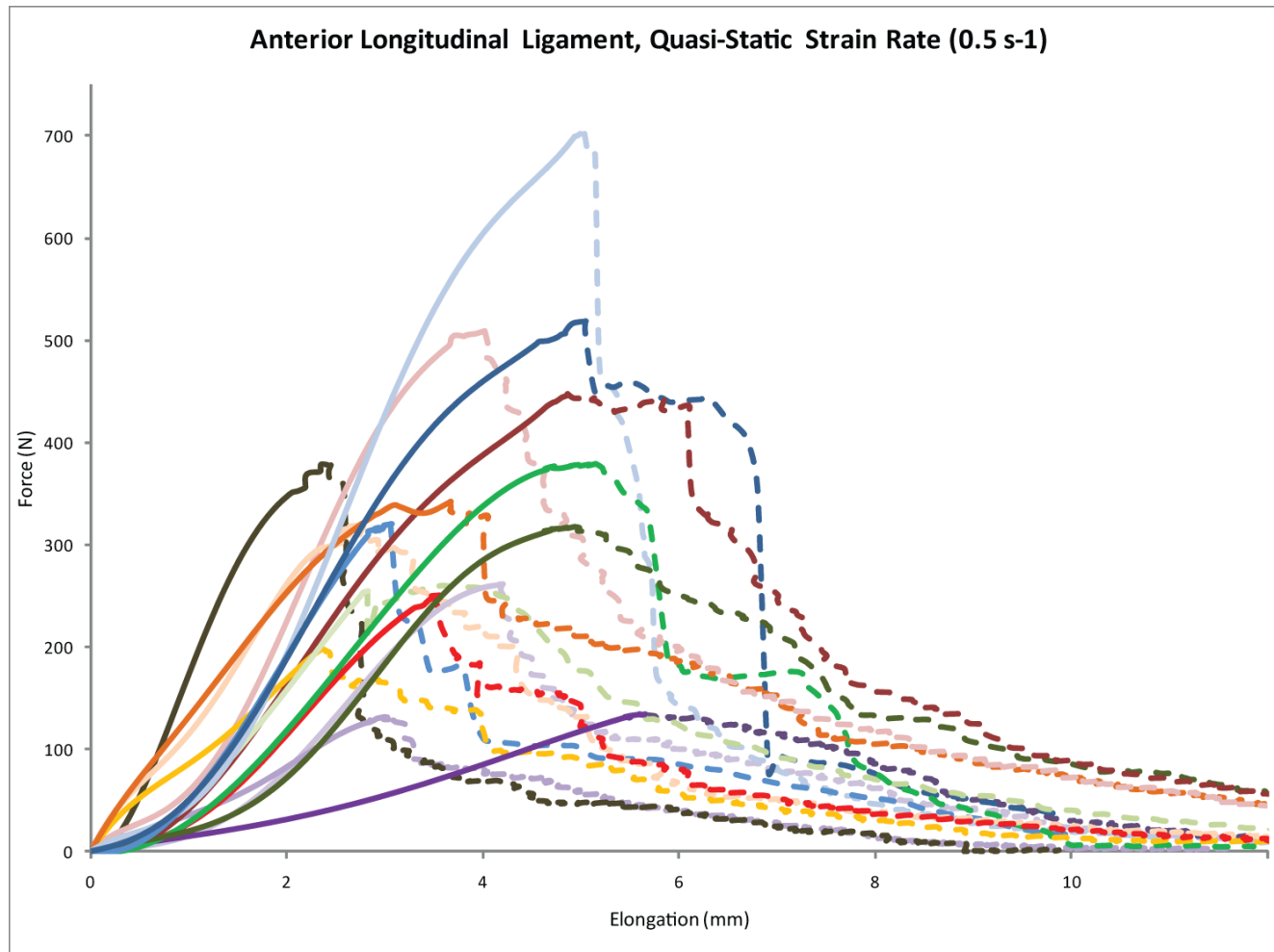
Appendix B

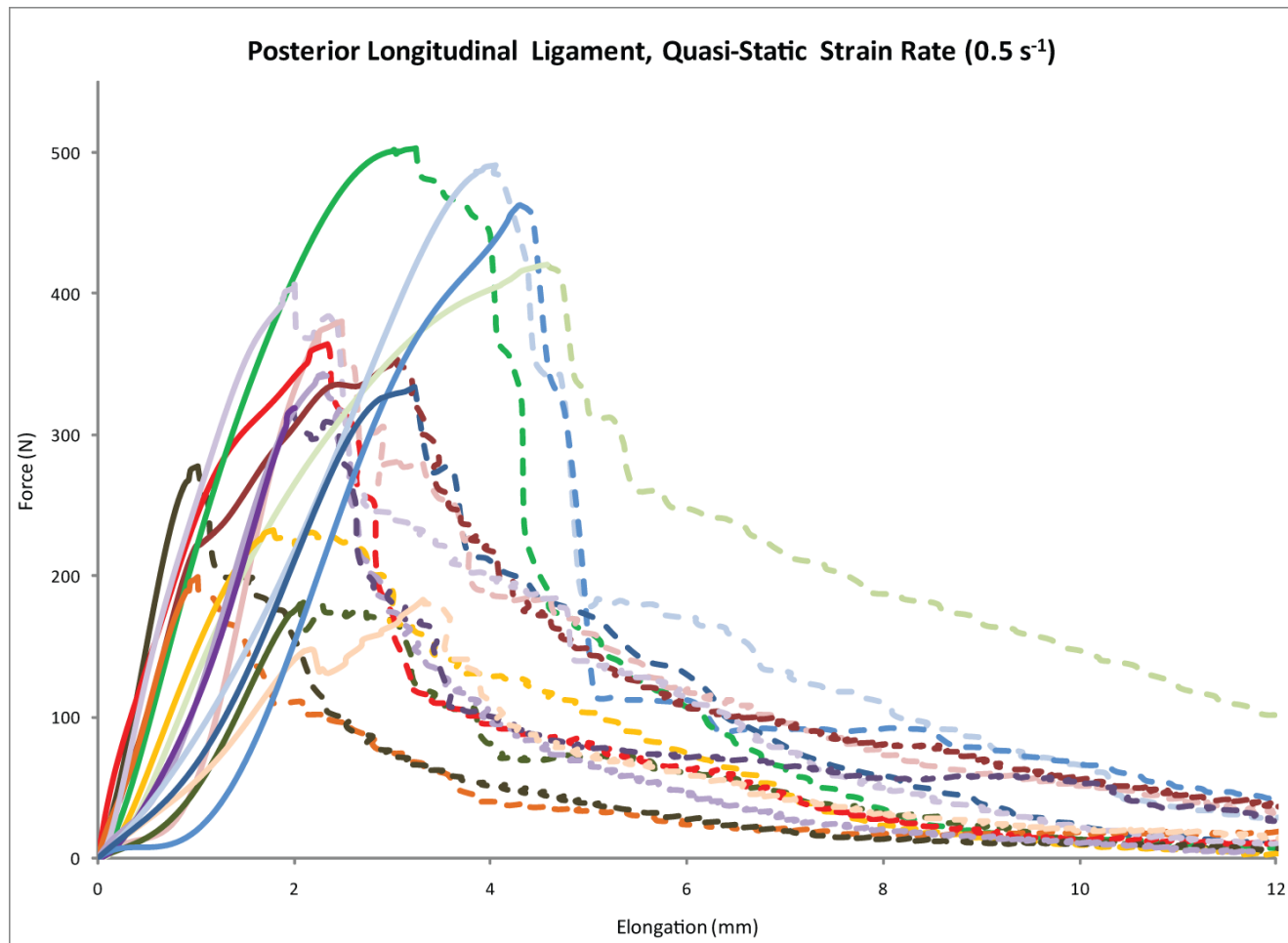
Ligament Curves

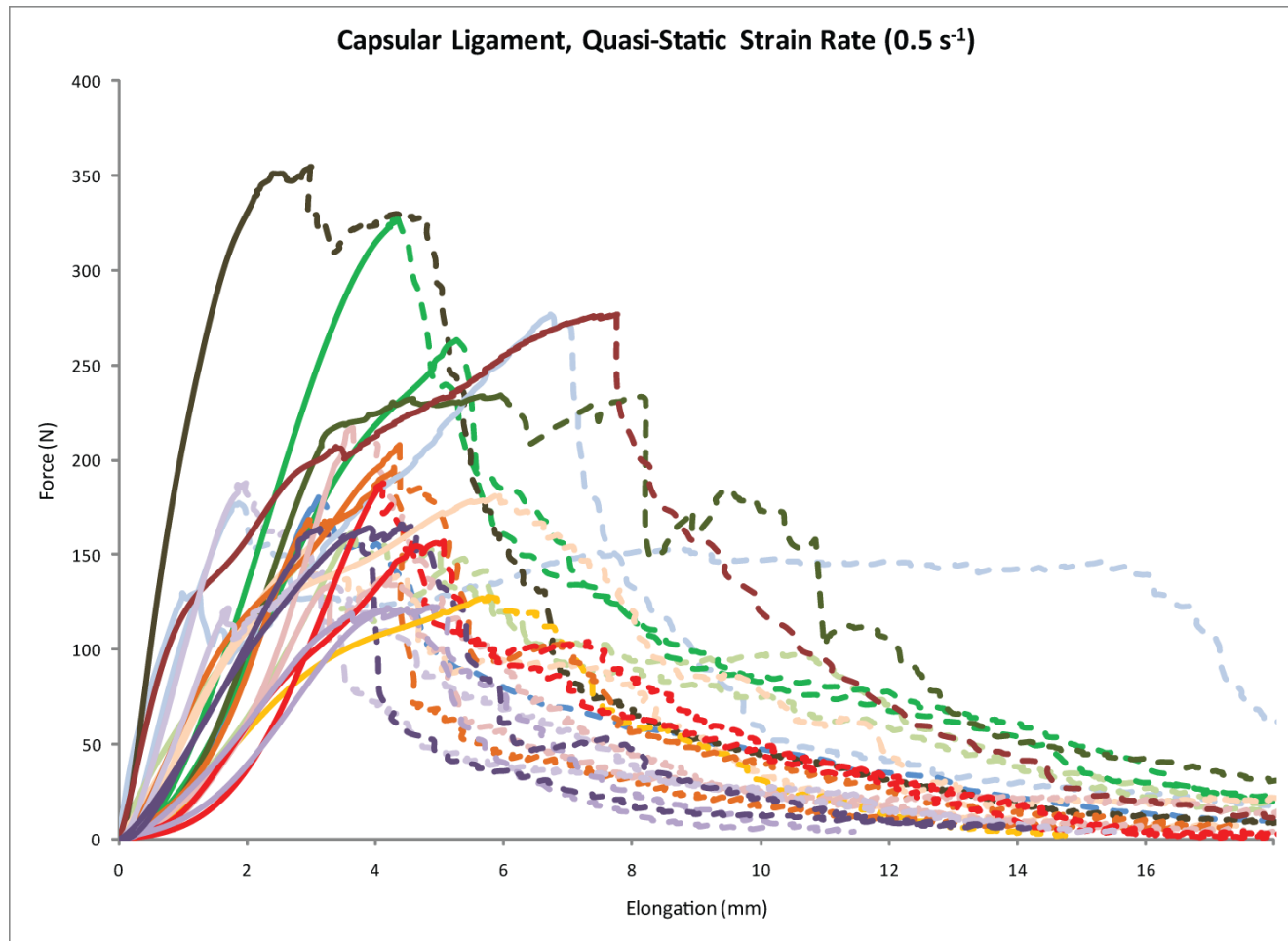
The ligament curves are presented in the following pages. All curves are colour coded. Curve colours match ligament values as reported in Appendix A. Each spine is colour coded, with spinal level shown by the shade of colour, with lighter shades representing upper spinal levels and dark shades representing lower spinal levels. Within strain rate groupings, spines have the same colour, i.e. all blue curves in high rate graphs are from the same spine. Dashed lines represent post failure region. Craniovertebral ligaments are coloured by rate and gender (legend on graph)

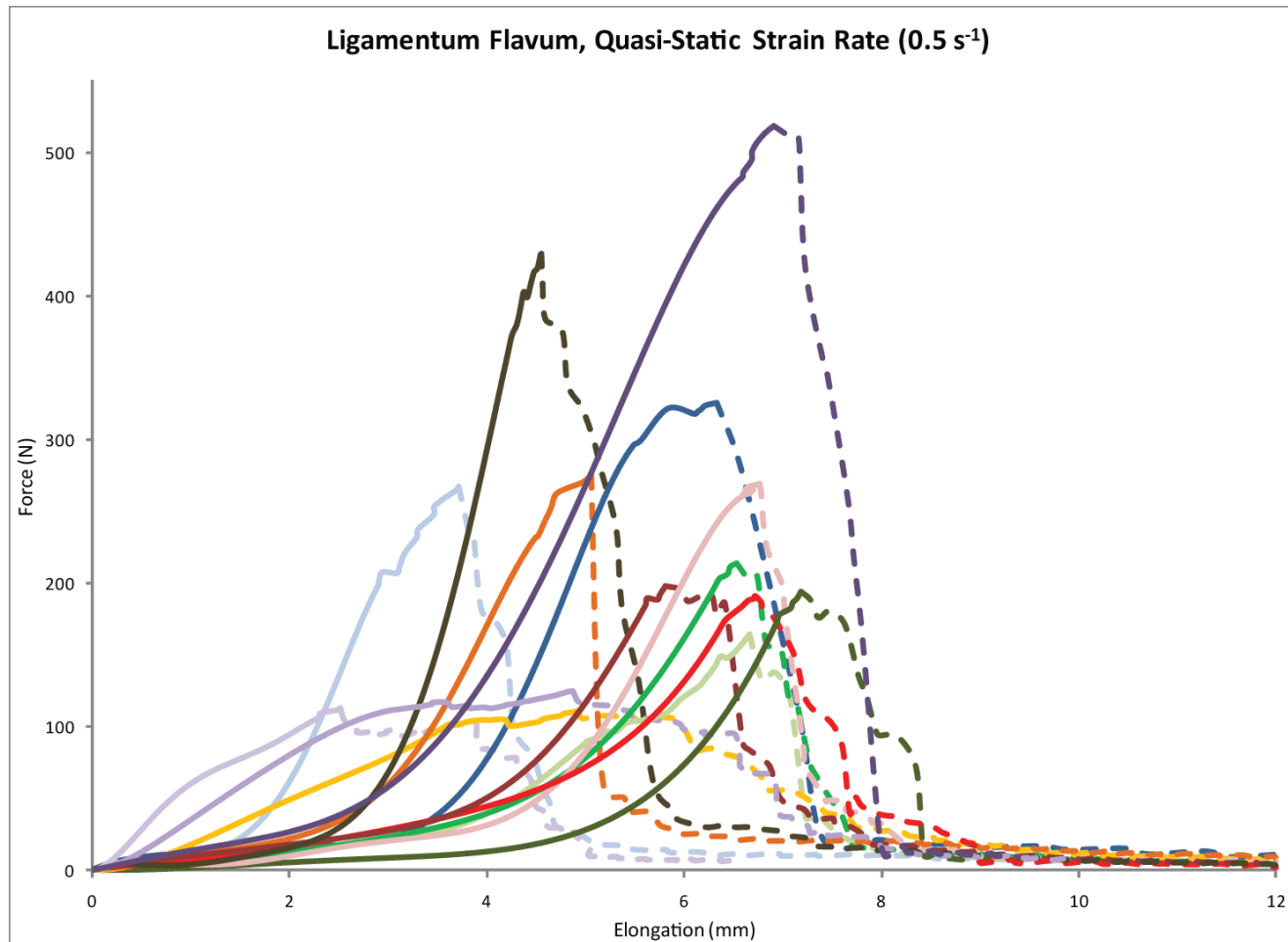
Male			Spinal Level	Female		
			Upper (C2-C4)			
			Middle (C4-C6)			
			Lower (C6-T1)			

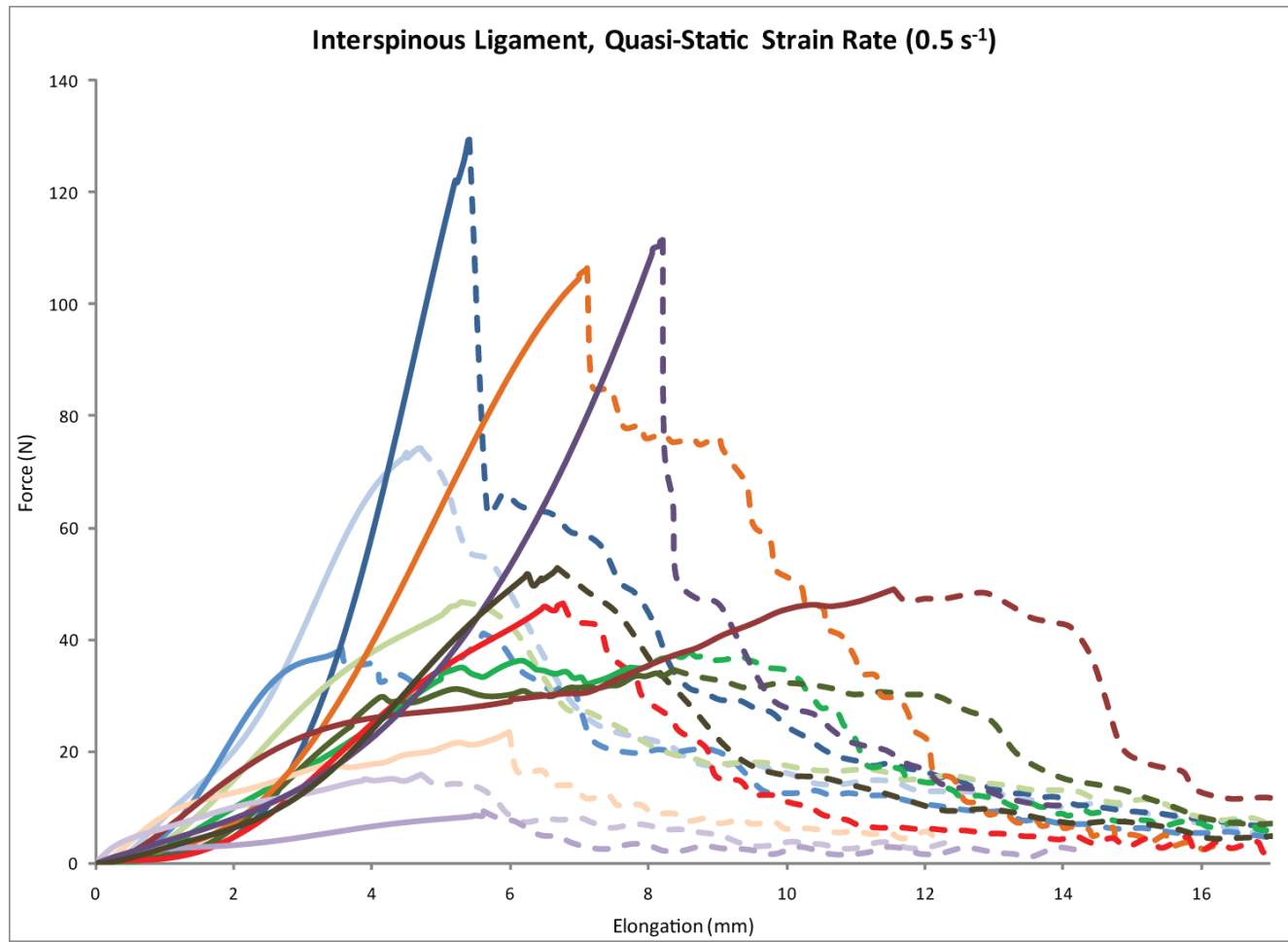
Spine ID	Age	Gender	Rate	Colour
A	46	M	Quasi-static	
B	46	M	Quasi-static	
C	36	M	High	
D	27	M	High	
E	48	F	Quasi-static	
F	47	F	Quasi-static	
G	49	F	High	
H	48	F	High	
I	48	M	Medium	
J	44	M	Medium	
K	47	F	Medium	
L	47	F	Medium	
M	43	M	All	
N	45	F	High	
O	50	F	Quasi-static	
P	40	M	High	
Q	29	F	Quasi-static	Craniovertebral

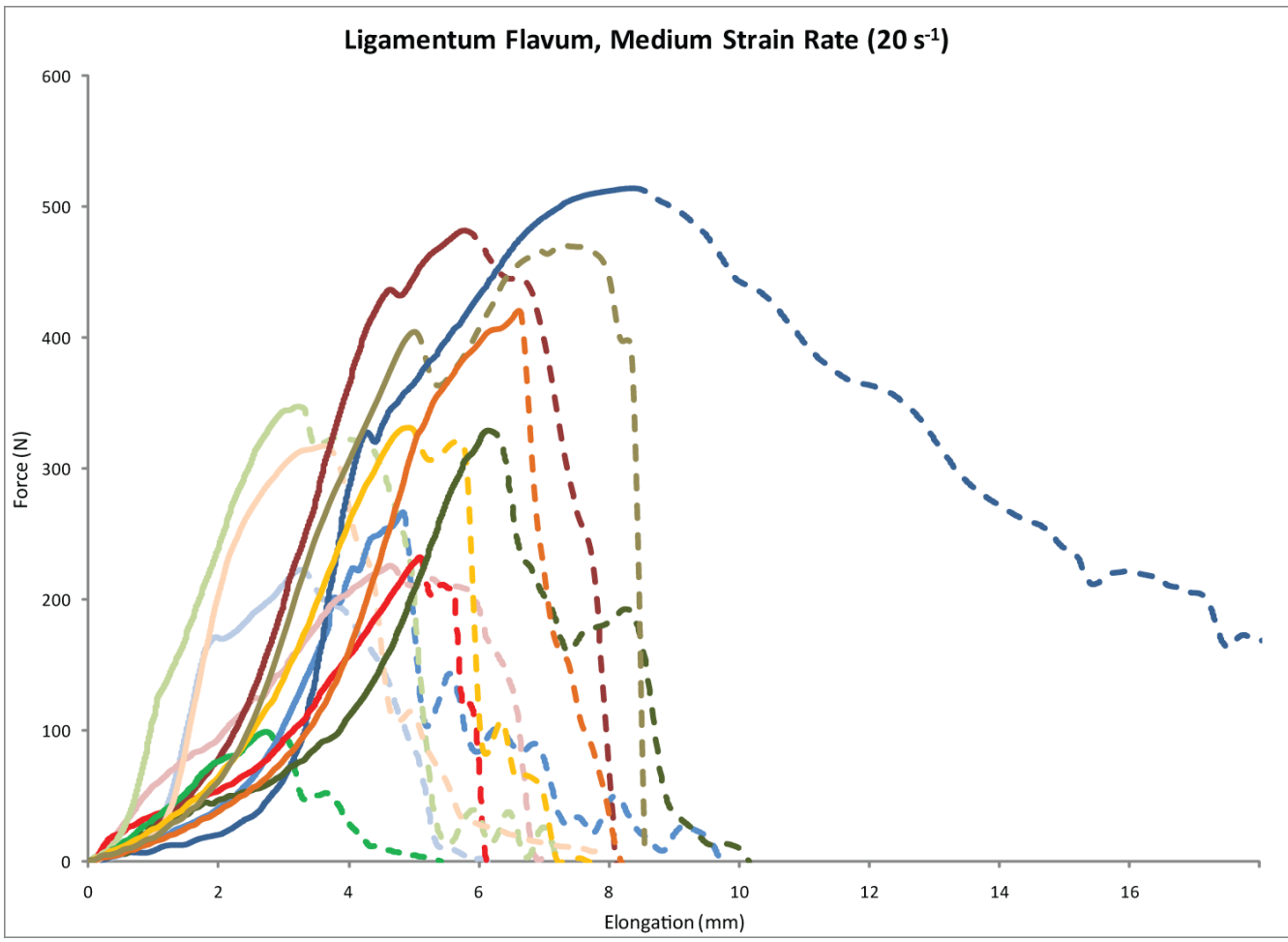


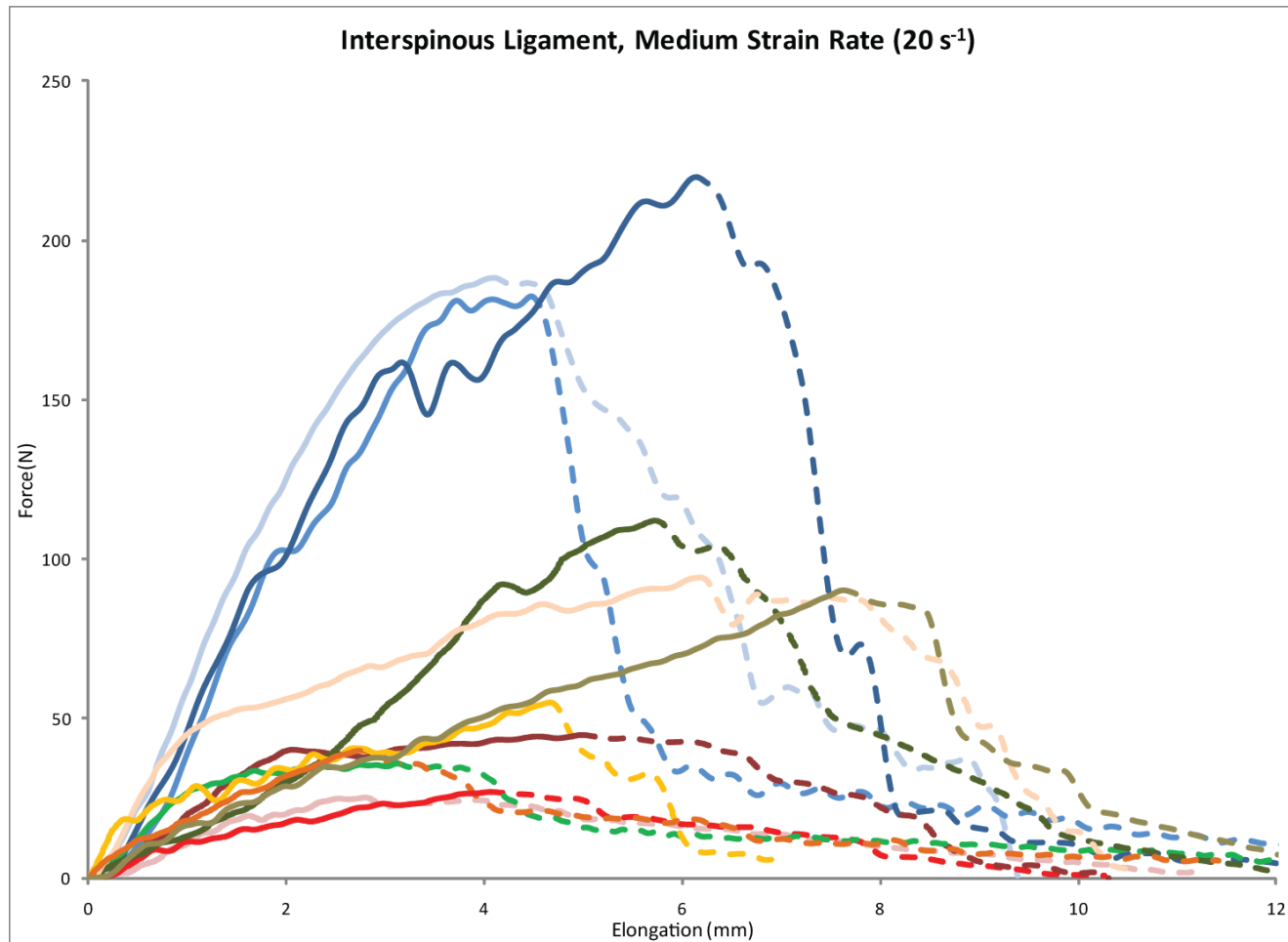


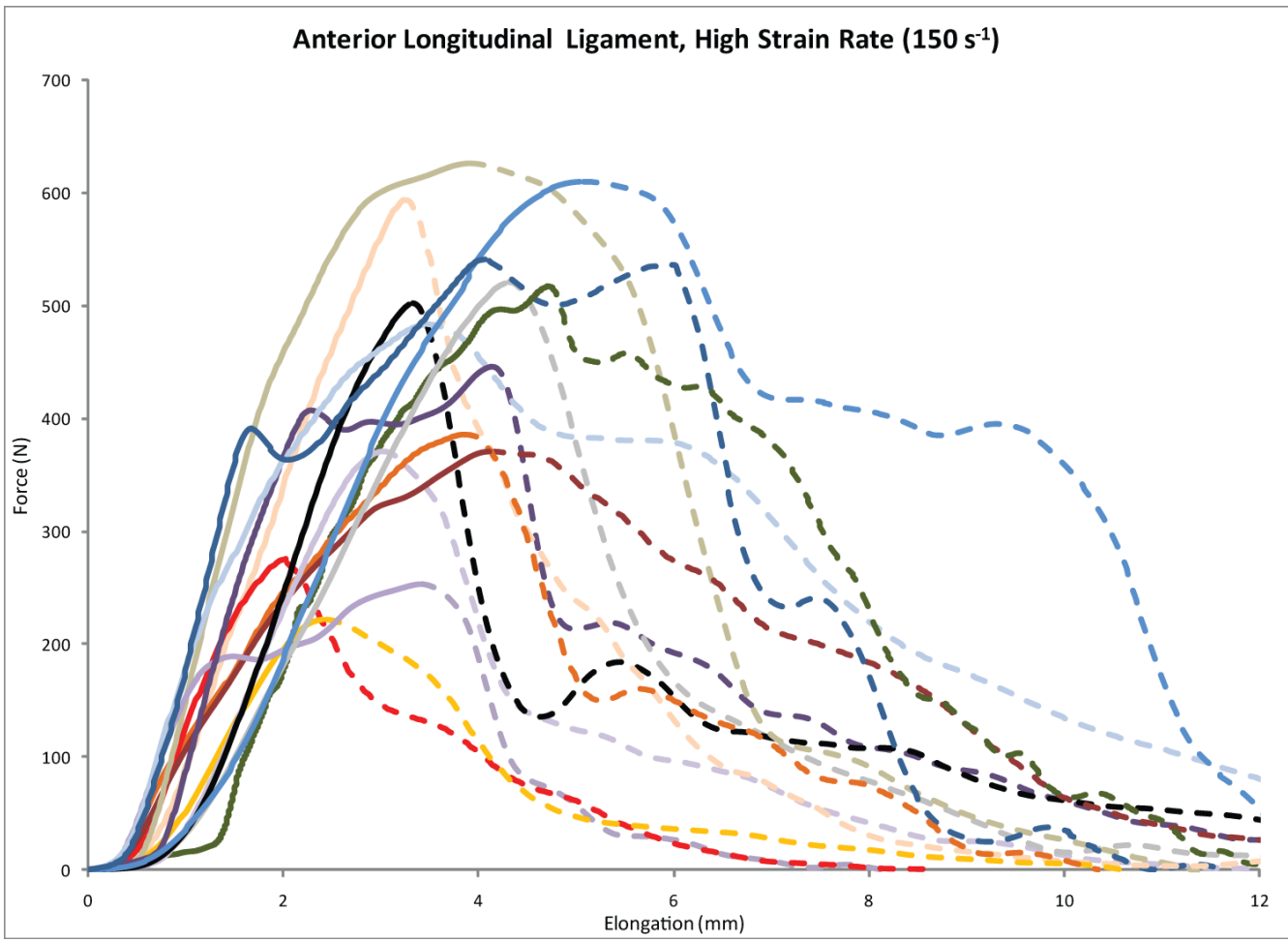


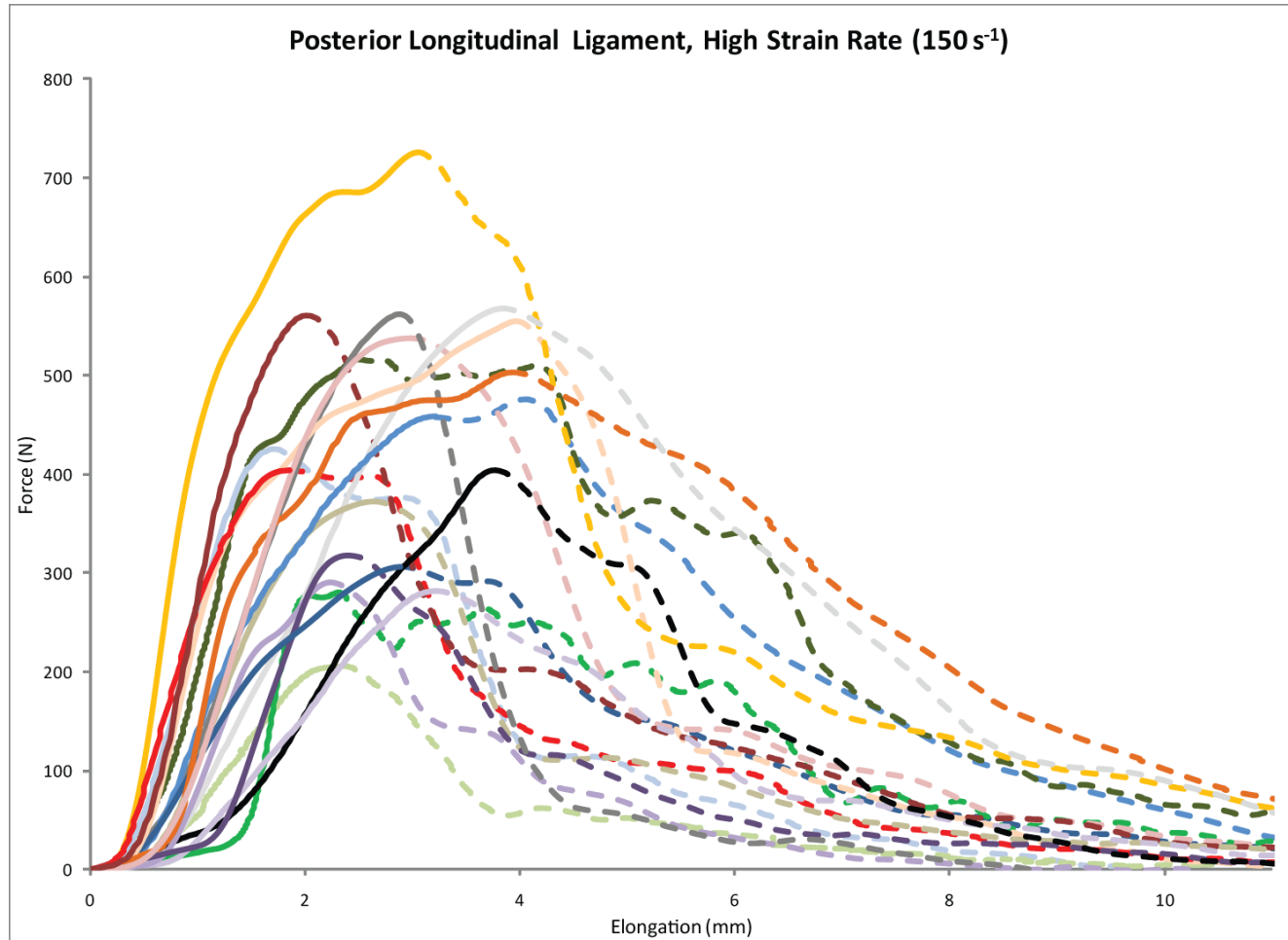


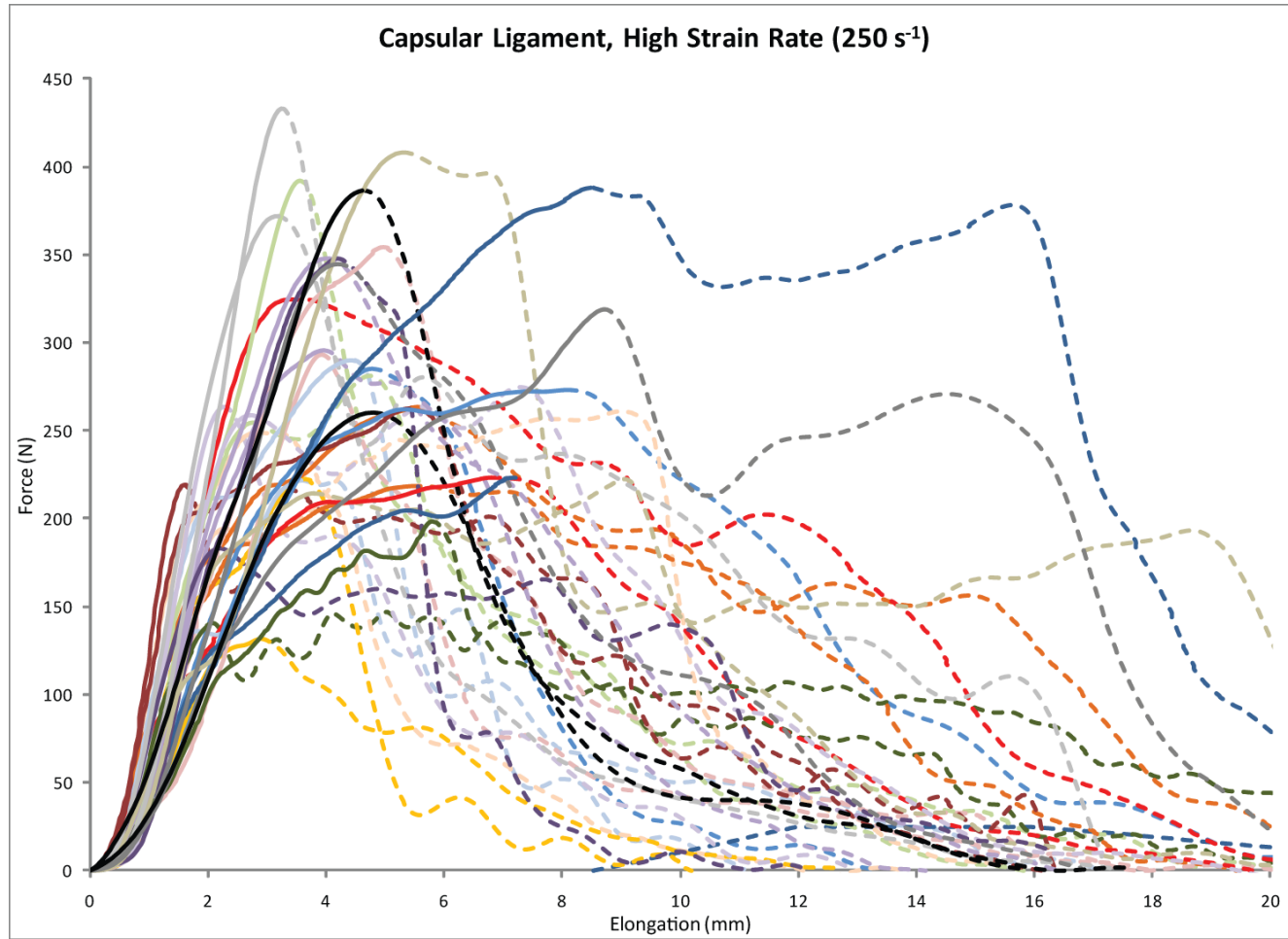


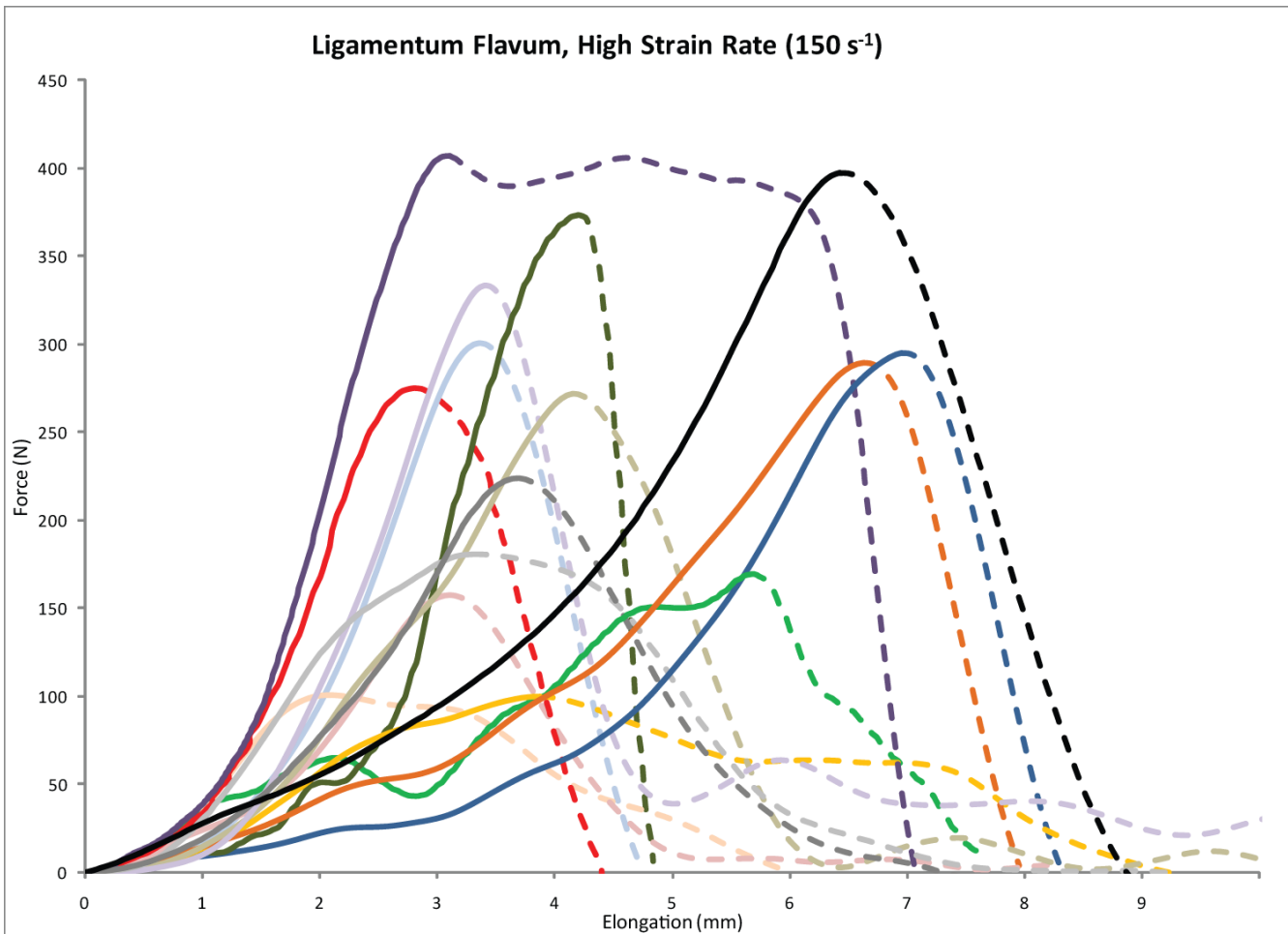


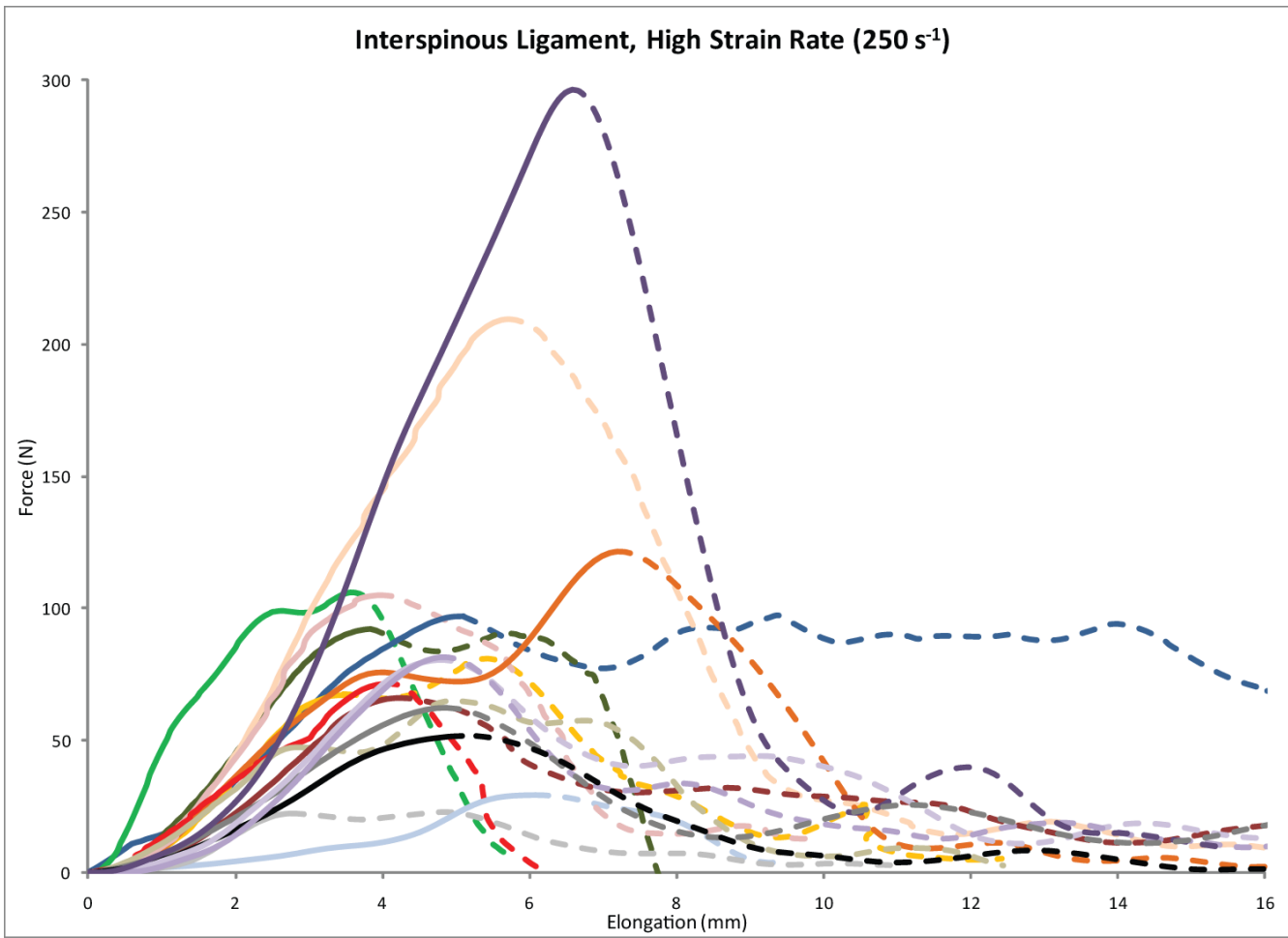


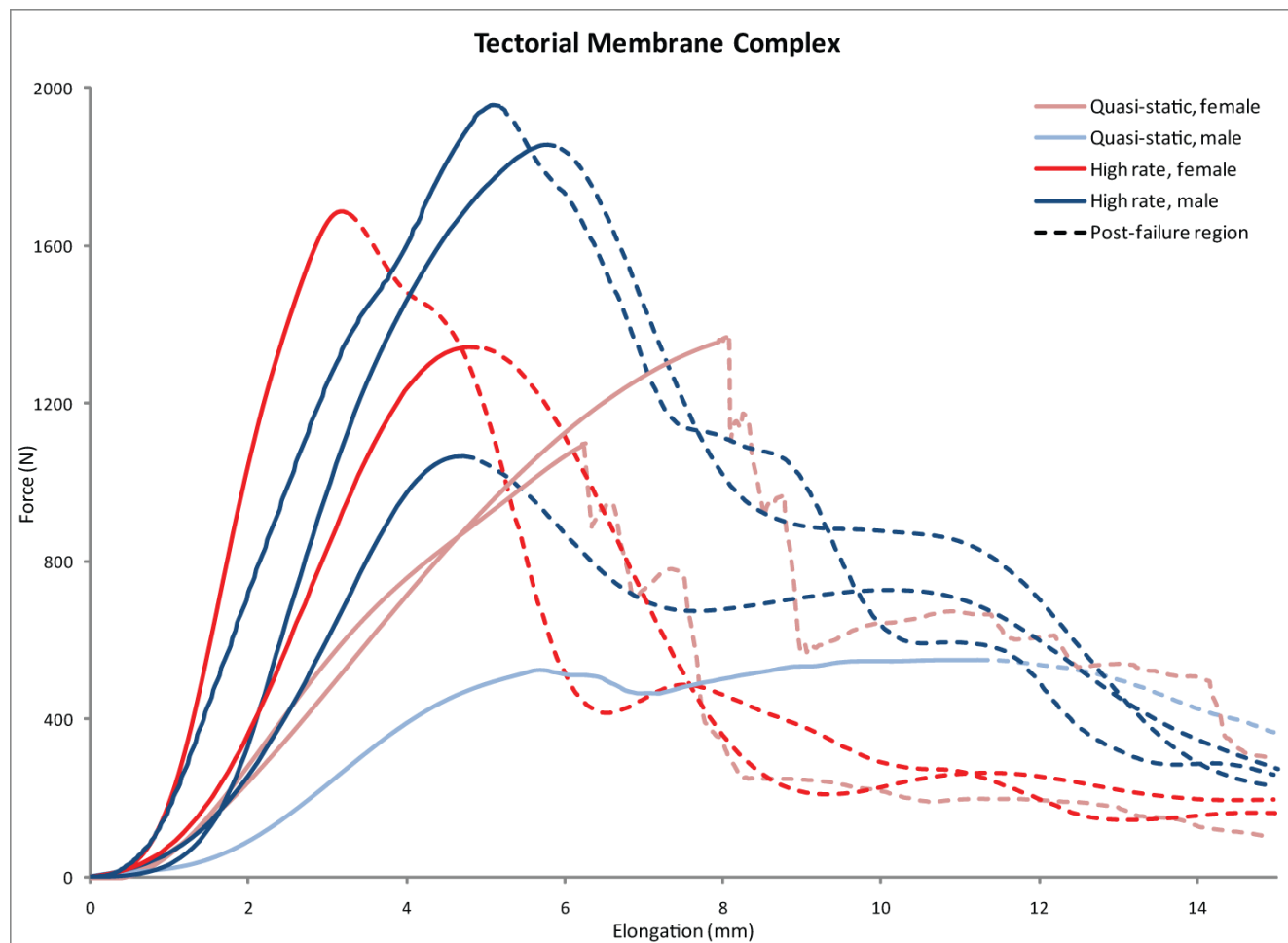


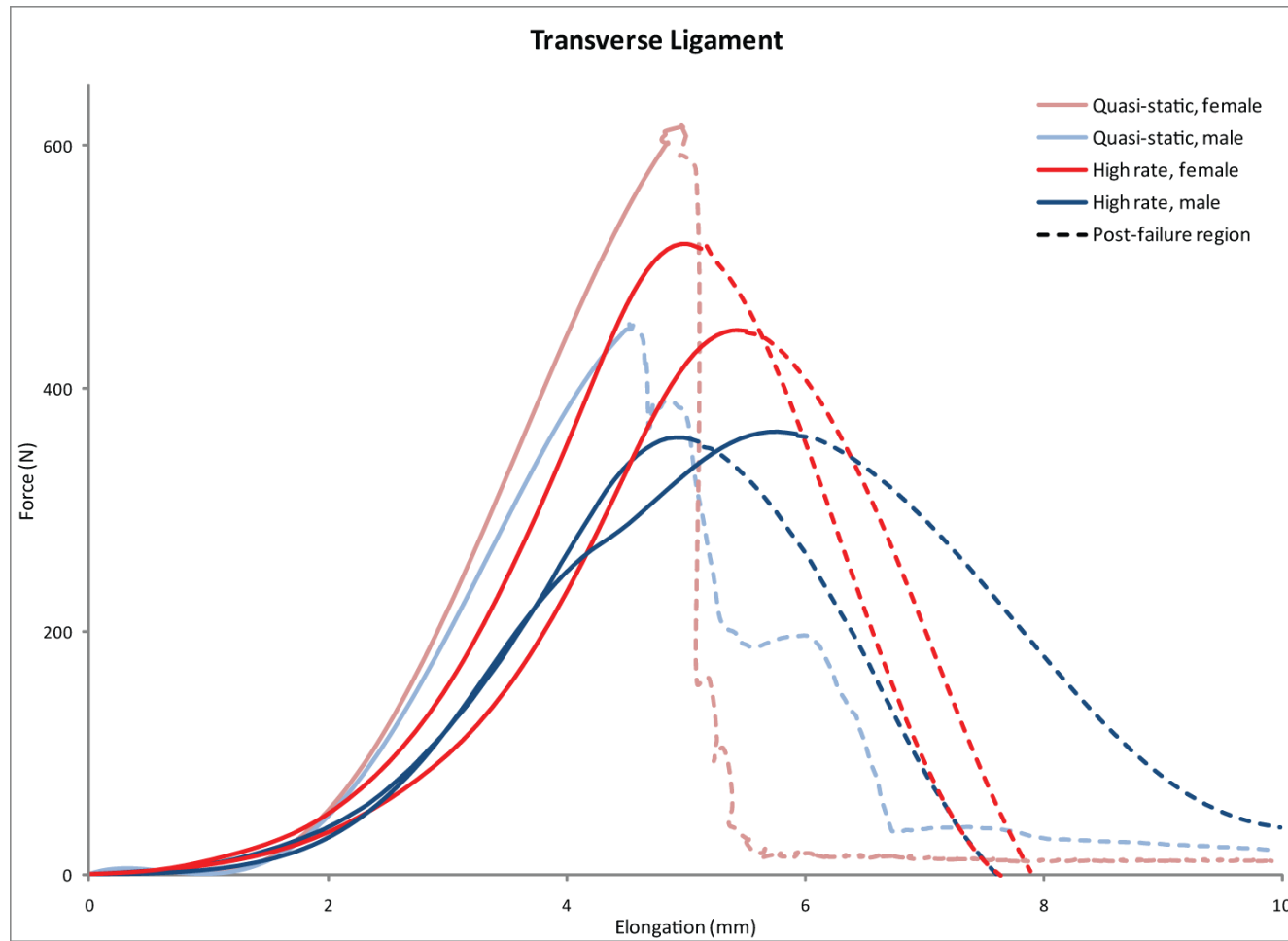


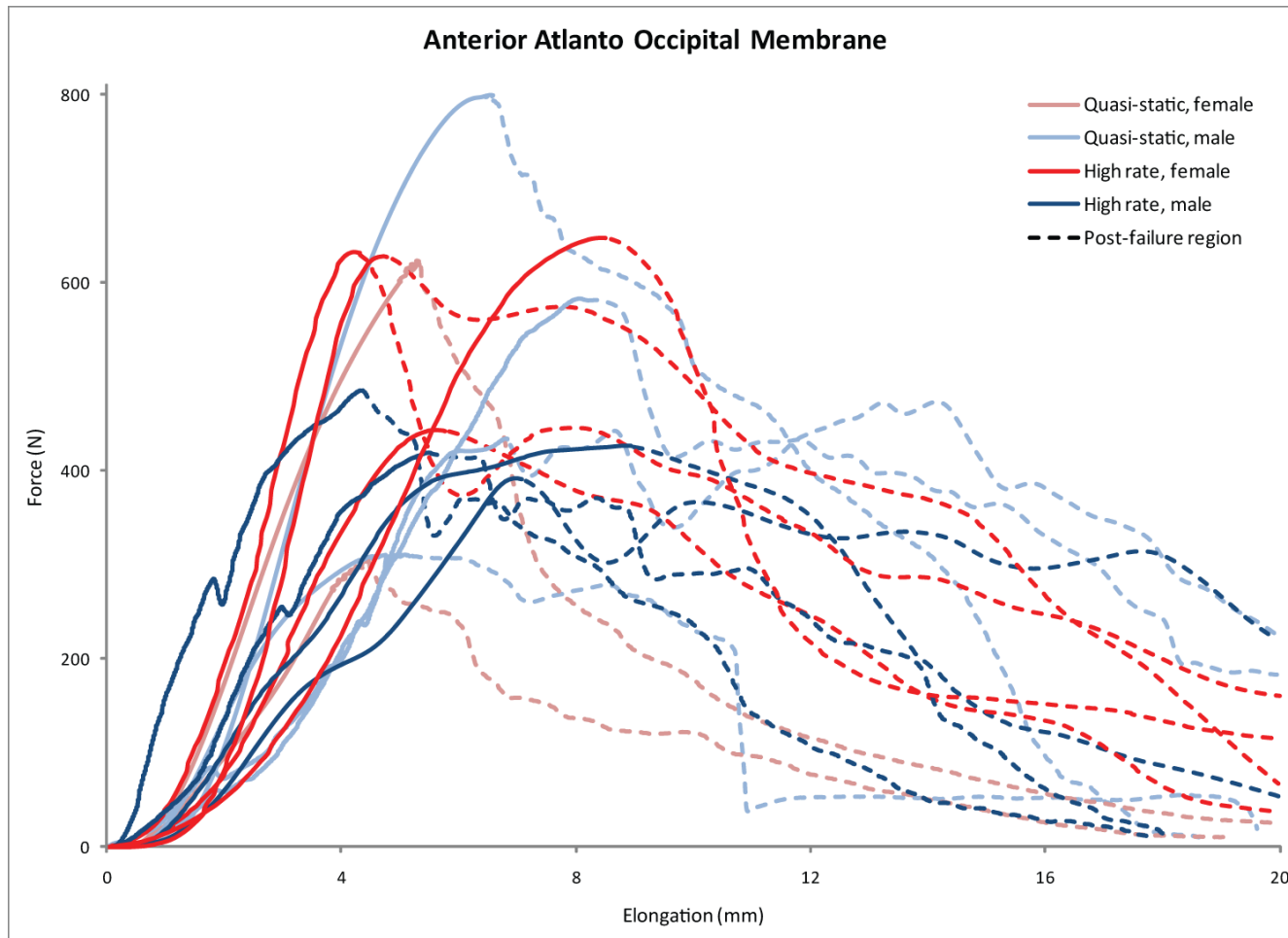


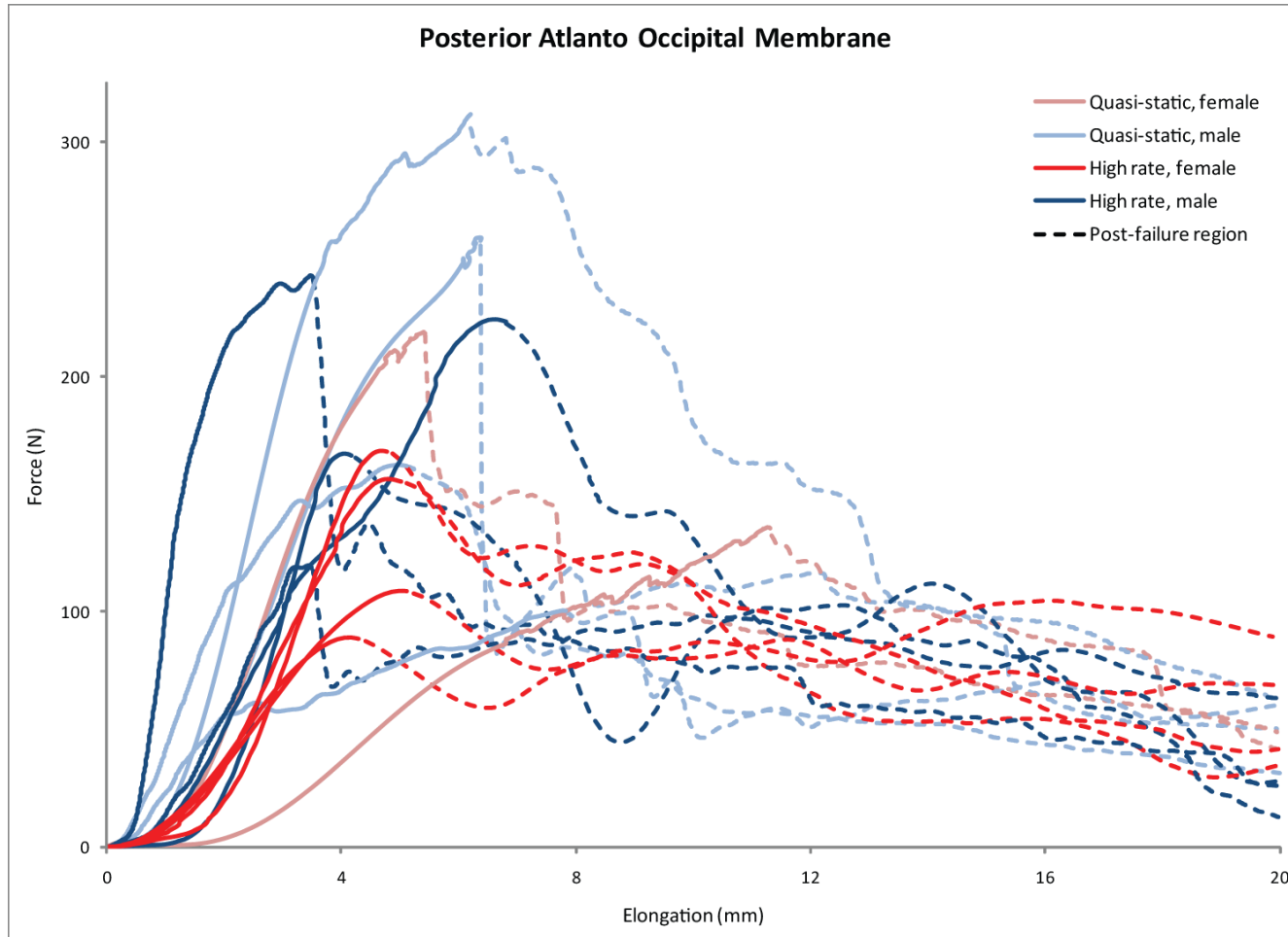


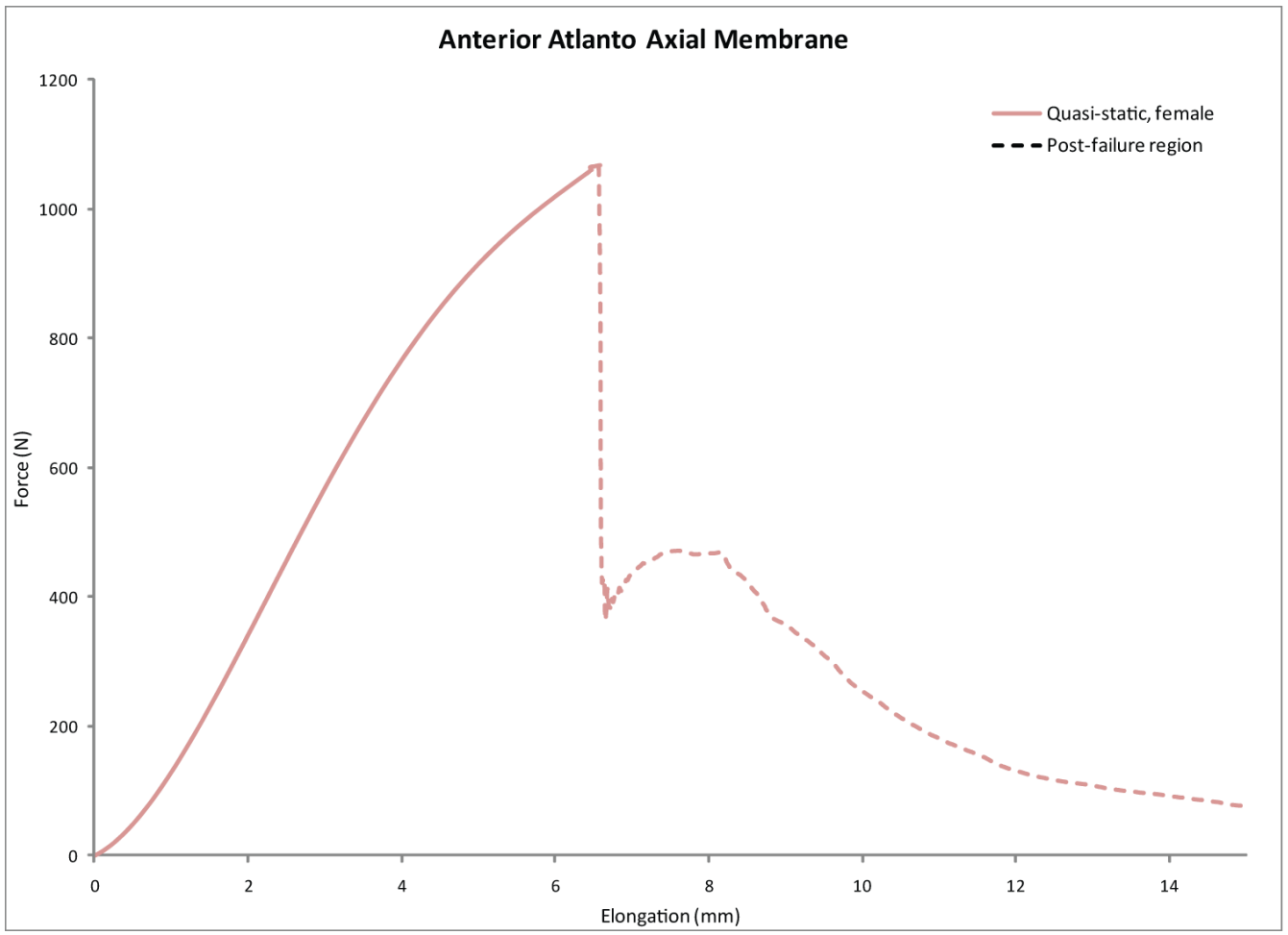


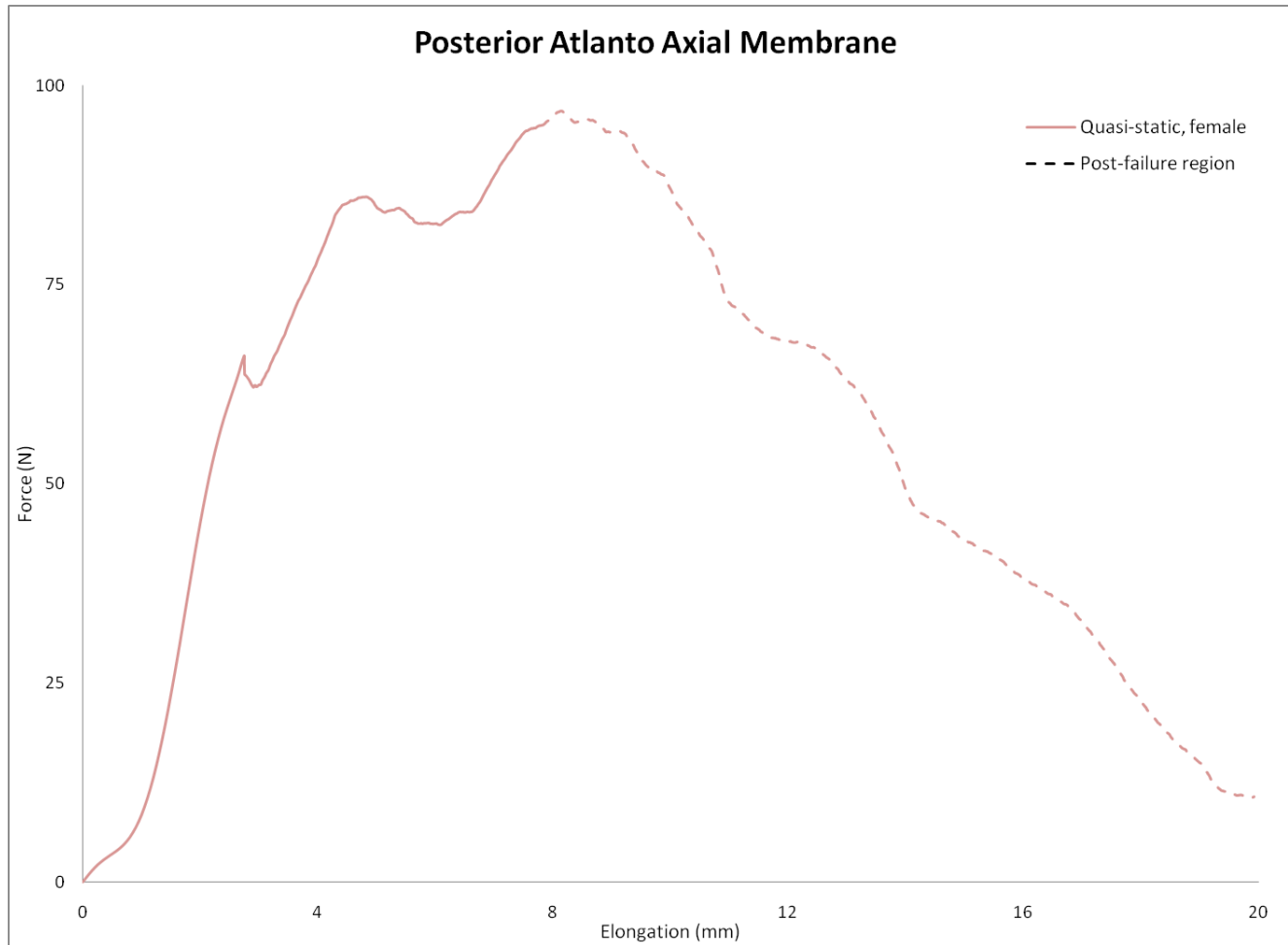












References

- Bass, C. R., Lucas, S. R., & Salzar, R. S. (2007). Failure Properties of Cervical Spinal Ligaments Under Fast Strain Rate Deformations. *Spine* , 32, E7-E13.
- Bass, C., Planchak, C., & Lucas, S. (2007). The Temperature-Dependent Viscoelasticity of Porcine Lumbar Spine Ligaments. *Spine* , 32.
- Blevins, F., Hecker, A., & Bigler, G. (1994). The Effects of Donor Age and Strain Rate on the Biomechanical Properties of Bone-Patellar Tendon-Bone Allografts. *American Journal of Sports Medicine* , 22 (3), 328-333.
- Bogduk, N., Mercer, S. (2000). Biomechanics of the Cervical Spine. I: Normal Kinematics. *Clinical Biomechanics* , 15, 633-648.
- Breig, A. (1978). Adverse Mechanical Tension in the Central Nervous System: An Analysis of Cause and Effect: Relief by Functional Neurosurgery.
- Burstein, A. H., & Frankel, V. H. (1968). The Viscoelastic Properties of Some Biological Materials. *Annals of the New York Academy of Sciences: Materials in Biochemical Engineering* , 146, 158-165.
- Cappon H, Ratingen van M, Wismans J, Hell W, Lang D, Svensson M (2003). Whiplash injuries, not only a problem in rear-end impacts. *ESV Conference, Nagoya, Japan*, 1-9.
- Chandrashekar, N., Hashemi, J., Slauterbeck, J., & Beynon, B. (2008). Low-load behaviour of the patellar tendon graft and its relevance to the biomechanics of the reconstructed knee. *Clinical Biomechanics* , 23, 918-925.
- Chandrashekar, N., Hashemi, J., Slauterbeck, J., & Beynon, B. (2008). Low-load behaviour of the patellar tendon graft and its relevance to the biomechanics of the reconstructed knee. *Clinical Biomechanics* , 23, 918-925.
- Chang, H., Gilbertson, L., Goel, V., Winterbottom, J., Clark, C., & Patwardhan, A. (1992). Dynamic Response of the Occipito-Atlanto-Axial (C0-C1-C2) Complex in Right Axial Rotation. *Journal of Orthopaedic Research* , 10, 446-453.

- Chazal, J., Tanguy, A., & Bourges, M. (1985). Biomechanical Properties of Spinal Ligaments and a Histological study of the Supraspinal Ligament in Traction. *Journal of Biomechanics* , 18 (No. 3), 167-176.
- Cowin, S. C., & Doty, S. B. (2007). *Tissue Mechanics*. New York: Springer Science.
- DeWit, J., & Cronin, D. (2010). Cervical spine segment finite element model validation and verification at traumatic loading levels for injury prediction. International IRCOBI Conference. Waterloo, ON.
- Di LulloDagger, G., Sweeny, S., & Korkko, J. (2002). Mapping the Ligand-binding Sites and Disease-associated Mutations on the Most Abundant Protein in the Human, Type I Collagen. *Journal of Biological Chemistry* , 277 (6).
- Dvorak, J., Froehlich, D., Penning, L., Baumgartner, H., & Panjabi, M. (1988). Functional Radiographic Diagnosis of the Cervical Spine: Flexion/Extension. *Spine* , 13, 748-755.
- Dvorak, J., Schneider, E., Saldinger, P., & Rahn, B. (1988). Biomechanics of the Craniocervical Region: The Alar and Transverse Ligaments. *Journal of Orthopaedic Research* , 6 (3), 452-461.
- Ferrario, V., Sforza, C., Serrao, G., Grassi, G., & Mossi, E. (2002). Active Range of Motion of the Head and Cervical Spine: A Three-Dimensional Investigation in Healthy Young Adults. *Journal of Orthopaedic Research* , 20, 122-129.
- Fice, J. (2010). Numerical Modeling of Whiplash Injury. M.A.Sc. Thesis .
- Fice, J., Cronin, D., & Panzer, M. (2009). Investigation of Facet Joint Response Under Rear Impact Conditions Using FE Model of the Cervical Spine. Enhanced Safety of Vehicles Conference. Waterloo, ON.
- Frisen, M., Magi, M., Sonnerup, L., & Viidik, A. (1969). Rheological Analysis of Soft Collagenous Tissue, Part 1: Theoretical Considerations. *Journal of Biomechanics* , 2, 13-20.
- Fung, Y.-C. (1993). *Biomechanics: Mechanical Properties of Living Tissues* (2nd Edition ed.). New York: Springer.

- Goel, V. K., Clark, C. R., Gallaes, K., & Liu, Y. K. (1988). Moment-Rotation Relationships of the Ligamentous Occipito-Atlanto-Axial Complex. *Journal of Biomechanics* , 21 (8), 673-680.
- Gray, H. (1918). *Anatomy of the Human Body* (20th ed.). Philadelphia: Lea & Febiger.
- Harris, J. H., & Yeakley, J. W. (1992). Hyperextension-Dislocation of the Cervical Spine: Ligament Injuries Demonstrated by Magnetic Resonance Imaging. *The Journal of Bone and Joint Surgery* , 74-B (3), 567-570.
- Hashemi, J., Chandrashekar, N., & Slauterbeck, J. (2005). The Mechanical Properties of the Human Patellar Tendon are Correlated to its Mass Density and are Independent of Sex. *Clinical Biomechanics* , 20, 645-652.
- Hayashi, K., & Yabuki, T. (1985). Origin of the Uncus of Luschka's Joint in the Cervical Spine. *The Journal of Bone and Joint Surgery* .
- Heuer, F., Schmidt, H., Klezl, Z., Claes, L., & Wilke, H. (2007). Stepwise Reduction of Functional Spinal Structures Increase Range of Motion and Change Lordosis Angle. *Journal of Biomechanics* , 40, 271-280.
- Huang, C., Wang, V. M., Flatow, E., & Mow, V. (2009). Temperature-Dependent Viscoelastic Properties of the Human Supraspinatus Tendon. *Journal of Biomechanics* , 42, 546-549.
- Iida, T., Abumi, K., Kotani, Y., & Kaneda, K. (2002). Effects of Aging and Spinal Degeneration on Mechanical Properties of Lumbar Supraspinous and Interspinous Ligaments. *The Spine Journal* , 2, 95-100.
- Ito, S., Ivancic, P., Panjabi, M., & Cunningham, B. (2004). Soft Tissue Injury Threshold During Simulated Whiplash: A Biomechanical Investigation. *Spine* , 29 (9), 979-987.
- Ivancic, P. C., Coe, M. P., Ndu, A. B., & al, E. (2007). Dynamic mechanical properties of intact human cervical spine ligaments. *The Spine Journal* , 7, 659-665.
- Ivancic, P., Panjabi, M., Tominaga, Y., & Malcolmson, G. (2006). Predicting Multiplanar Cervical Spine Injury Due to Head-Turned Rear Impacts Using IV-NIC. *Traffic Injury Prevention* , 7, 264-275.

- Kanis, J. A., Melton, I. J., Christiansen, C., Johnston, C., & Khaltayev, N. (1994). Perspective: The Diagnosis of Osteoporosis. *Journal of Bone and Mineral Research* , 9 (8), 1137-1141.
- Kastelic, J., Galeski, A., & Baer, E. (1978). The Multicomposite Structure of Tendon. *Connective Tissue Research* , 6, 11-23.
- Kirby, M. C., Sikoryn, T. A., Hukins, D. W., & Aspden, R. M. (1989). Structure and Mechanical Properties of the Longitudinal Ligaments and Ligamentum Flavum of the Spine. *Journal of Biomedical Engineering* , 11, 192-196.
- Kotani, Y., McNulty, P., & Abumi, K. (1998). The role of Anteromedial Foraminotomy and the Uncovertebral Joints in the Stability of the Cervical Spine: A Biomechanical Study. *Spine* , 23 (14).
- Kumaresan, S., Yoganandan, N., & Pintar, F. (1999). Finite element analysis of the cervical spine: a material property sensitivity study. *Clinical Biomechanics* , 14, 41-53.
- Lind, B., Sihlbom, H., Nordwall, A., & Malchau, H. (1989). Normal Ranges of Motion of the Cervical Spine. *Archives of Physical Medicine and Rehabilitation* , 70, 692-695.
- Lucas, S. R., Bass, C. R., Crabdall, J. R., Kent, R. W., Shen, F. H., & Salzar, R. S. (2009). Viscoelastic and Failure Properties of Spine Ligament Collagen Fascicles. *Biomechanics and Modeling in Mechanobiology* , 8, 487-498.
- Lucas, S., Bass, C., Salzar, R., Oyen, M., Planchak, C., Ziemba, A. et al. (2008). Visoelastic Properties of the Cervical Spinal Ligaments Under Fast Strain-Rate Deformations. *Acta Biomaterialia* , 4 (1), 117-125.
- McKinley, M., & O'Loughlin, V. D. (2008). *Human Anatomy* (2nd Edition ed.). New York: McGraw-Hill.
- Milz, S., Schluter, T., Putz, R., Moriggl, B., Ralphs, J., & Benjamin, M. (2001). Fibrocartilage in the Transverse Ligament of the Human Atlas. *Spine* , 26 (16), 1765-1771.
- Moon, D., Woo, S., Takakura, Y., Gabriel, M., & Abramowitch, S. (2006). The Effects of Refreezing on the Viscoelastic and Tensile Properties of Ligaments. *Journal of Biomechanics* , 39, 1153-1157.

- Moore, K. L., & Dalley, A. F. (1999). *Clinically Oriented Anatomy* (Fourth ed.). Lippincott Williams & Wilkins.
- Moroney, S., Schultz, A., Miller, J., & Andersson, G. (1988). Load-Displacement Properties of Lower Cervical Spine Motion Segments. *Journal of Biomechanics* , 21 (9), 769-779.
- Myklebust, J., Pintar, F., & Yoganandan, N. (1988). Tensile Strength of Spinal Ligaments. *Spine* , Volume 13 (5), 526-531.
- Nachemson, A., & Evans, J. (1968). Some Mechanical Properties of the Third Human Lumbar Interlaminar Ligament (Ligamentum Flavum). *Journal of Biomechanics* , 1, 211-220.
- Nakagawa, H., Mikawa, Y., & Watanabe, R. (1994). Elastin in the Human Posterior Longitudinal Ligament and Spinal Dura: A Histological and Biochemical Study. *Spine* , 19, 2164-2169.
- Neumann, P., Ekstrom, L., Keller, T., Perry, L., & Hansson, T. (1994). Aging, Vertebral Density, and Disc Degeneration Alter the Tensile Stress-Strain Characteristics of the Human Anterior Longitudinal Ligament. *Journal of Orthopaedic Research* , 12 (1), 103-112.
- Neumann, P., Keller, T., Ekstrom, L., & Hansson, T. (1994). Effect of Strain Rate and Bone Mineral on the Structural Properties of the Human Anterior Longitudinal Ligament. *Spine* , 19 (2), 205-211.
- Neumann, P., Keller, TS, Ekstrom, L., Perry, L., Hannon, T. et al. (1992). Mechanical Properties of the Human Lumbar Anterior Longitudinal Ligament. *Journal of Biomechanics* , 25 (10), 1185-1194.
- Nightingale, R., Chancey, V., Ottaviano, D., Luck, J., Tran, L., Prange, M. et al. (2007). Flexion and Extension Structural Properties and Strengths for Male Cervical Spine Segments. *Journal of Biomechanics* , 40, 535-542.
- Nightingale, R., Winkelstein, B., Knaub, K., Richardson, W., Luck, J., & Myers, B. (2002). Comparative Strengths and Structural Properties of the Upper and Lower Cervical Spine in Flexion and Externsion. *Journal of Biomechanics* , 35, 725-732.
- Noyes, F., & Grood, E. (1976). The Strength of the Anterior Cruciate Ligament in Humans and Rhesus Monkeys. *The American Journal of Bone and Joint Surgery* , 58 (8), 1074-1082.

- Oza, A., Vanderby, R., & Lakes, R. (2006). Creep and Relaxation in Ligament: Theory, Methods and Experiment. In G. Holzapfel, & R. Ogden, *Mechanics of Biological Tissue* (pp. 379-397). Springer Science.
- Panjabi, M. M., Crisco III, J. J., Lydon, C., & Dvorak, J. (1998). The Mechanical Properties of Human Alar and Transverse Ligaments at Slow and Fast Extension Rates. *Clinical Biomechanics* , 13 (2), 112-120.
- Panjabi, M., Cholewicki, J., Nibu, K., & Babat, L. D. (1998). Simulation of Whiplash Trauma Using Whole Cervical Spine Specimens. *Spine* , 23 (1), 17-24.
- Panjabi, M., Duranceau, J., Goel, V., Oxland, T., & Takata, K. (1991). Cervical Human Vertebrae Quantitative Three-Dimensional Anatomy of the Middle and Lower Regions. *Spine* , 16 (8), 861-869.
- Panjabi, M., Goel, V., & Takata, K. (1981). Physiologic Strains in the Lumbar Spinal Ligaments: An in vitro Biomechanical Study. *Spine* , 7 (3), 192-203.
- Panjabi, M., Oxland, T., & Parks, E. (1991). Quantitative Anatomy of Cervical Spine Ligaments. Part II. Middle and Lower Cervical Spine. *Journal of Spinal Disorders* , 4 (3), 277-285.
- Panjabi, M., Pearson, A., Ito, S., Ivancic, P., & MPhil, G. (2004). Cervical Spine Ligament Injury During Simulated Frontal Impact. *Spine* , 29 (21), 2395-2403.
- Panjabi, M., White III, A., & Johnson, R. (1975). Cervical Spine Mechanics as a Function of Transection of Components. *Journal of Biomechanics* , 8, 327-336.
- Panzer, M. B. (2006). Numerical Modelling of the Human Cervical Spine in Frontal Impact. University of Waterloo, MASC Thesis , 248.
- Pearson, A., Panjabi, M., Ivancic, P., Ito, S., & Cunningham, B. (2005). Frontal Impact Causes Ligamentous Cervical Spine Injury. *Spine* , 30 (16), 1852-1858.
- Penning, L., & Wilmink, J. (1987). Rotation of the Cervical Spine. A CT Study in Normal Subjects. *Spine* , 12, 732-738.
- Pintar, F. A. (1986). The Biomechanics of Spinal Elements, Ph.D. Thesis. Marquette University Graduate School, Milwaukee.

- Pintar, F. A., Yoganandan, N., Voo, L., Cusick, J., Maiman, D., & Sances, A. (1995, November). Dynamic Characteristics of the Human Cervical Spine. SAE Conference , 195-202.
- Pintar, F., Yoganandan, N., & Voo, L. (1998). Effect of Age and Loading Rate on Human Cervical Spine Injury Threshold. *Spine* , 23 (18), 1957-1962.
- Pintar, F., Yoganandan, N., Myers, T., Elhagediab, A., & Sances, A. (1992). Biomechanical Properties of Human Lumbar Spine Ligaments. *Journal of Biomechanics* , 25 (11), 1351-1356.
- Przybylski, G. J., Carlin, G., Patel, P., & Woo, S. (1996). Human Anterior and Posterior Cervical Longitudinal Ligaments Possess Similar Tensile Properties. *Journal of Orthopaedic Research* , 14, 1005-1008.
- Puttlitz, C. (1999). A Biomechanical Investigation of the Craniovertebral Junction. Ph.D. Thesis .
- Reuber, M., Schultz, A., Denis, F., & Spencer, D. (1982). Bulging of lumbar intervertebral disks. *Journal of Biomechanical Engineering* , 3 (104), 187.
- Robertson, A., Branfoot, T., Barlow, I., & Giannoudis, P. (2002). Spinal Injury Patterns Resulting from Car and Motorcycle Accidents. *Spine* , 27 (24), 2825-2830.
- Saldinger, P., Dvorak, J., Rahn, B., & Perren, S. (1990). Histology of the Alar and Transverse Ligaments. *Spine* , 15 (4), 257-261.
- Shea, M., Edwards, W., White, A., & Hayes, W. (1991). Variations of Stiffness and Strength Along the Human Cervical Spine. *Journal of Biomechanics* , 24 (2), 95-107.
- Shim, V., Liu, J., & Lee, V. (2005). A Technique for Dynamic Tensile Testing of Human Cervical Spine Ligaments. *Experimental Mechanics* , 46, 77-89.
- Silverthorn, D. U. (2010). *Human Physiology: An Integrated Approach*.
- StatSoft, Inc. (2010). *Electronic Statistics Textbook*. Tulsa, OK.
- Stemper, B., Yoganandan, N., & Pintar, F. (2003). Gender Dependent Cervical Spine Segmental Kinematics During Whiplash. *Journal of Biomechanics* , 36, 1281-1289.

Stemper, B., Yoganandan, N., Pintar, F., & Rao, R. (2006). Anterior Longitudinal Ligament Injuries in Whiplash May Lead to Cervical Instability. *Medical Engineering & Physics* , 28, 515-524.

Tkaczuk, H. (1968). Tensile Properties of Human Lumbar Longitudinal Ligaments. *Acta Orthopaedica Scandinavica* , Suppl. 115.

Tominaga, Y., Ndu, A., Coe, M., Valenson, A., Ivancic, P., Ito, S. et al. (2006). Neck Ligament Strength is Decreased Following Whiplash Trauma. *BioMed Central Musculoskeletal Disorders* , 7 (103).

Troyer, K. L., & Puttlitz, C. M. (2011). Human Cervical Spine Ligaments Exhibit Fully Nonlinear Viscoelastic Behavior. *Acta Biomaterialia* , 7 (2), 700-709.

Van Ee, C. A., Nightingale, R. W., Camacho, D. L., & Chancey, V. C. (2000). Tensile Properties of the Human Muscular and Ligamentous Cervical Spine. *44th Stapp Car Crash Conference* , 44, 85-102.

Van Mameren, H., Drukker, J., Sanches, H., & Beursgens, J. (1990). Cervical Spine Motion in the Sagittal Plane (I) Range of Motion of Actually Performed Movements, an X-Ray Cinematography Study. *European Journal of Morphology* , 28 (1), 47-68.

Vernon-Roberts, B., & Pirie, C. (1973). Healing Trabecular Microfractures in the Bodies of Lumbar Vertebrae. *Annals of the Rheumatic Disease* , 32, 406-412.

Viejo-Fuertes, D., Liguoro, D., Rivel, J., Midy, D., & Guerin, J. (1998). Morphologic and Histologic Study of the Ligamentum Flavum in the Thoraco-Lumbar Region. *Surgical and Radiologic Anatomy* , 20 (3), 171-176.

Viidik, A. (1973). Functional Properties of Collagenous Tissues. *International Review of Connective Tissue Research* , 6, 127-215.

Webb, J., Broughton, R., McSweeney, T., & Park, W. (1976). Hidden Flexion Injury of the Cervical Spine. *The Journal of Bone and Joint Surgery* , 58-B (3).

White, A. A., & Panjabi, M. M. (1990). *Clinical Biomechanics of the Spine* (2nd Edition ed.). Philadelphia: Lippincott Company.

- Winer, B. J. (1962). *Statistical Principles in Experimental Design*. New York: McGraw-Hill.
- Woo, S., Johnson, G., & Smith, B. (1993). Mathematical Modeling of Ligaments and Tendons. *Transactions of the ASME* , 115, 468-473.
- Woo, S., Orlando, C., Camp, J., & Akeson, W. (1986). Effects of Postmortem Storage by Freezing on Ligament Tensile Behaviour. *Journal of Biomechanics* , 19 (5), 399-404.
- Yoganandan, N., Haffner, M., Maiman, D., Nichols, H., Pintar, F., Jentzen, J. et al. (1989, October). Epidemiology and Injury Biomechanics of Motor Vehicle Related Trauma to the Human Spine. *SAE Trans* , 1790-1807.
- Yoganandan, N., Kumaresan, S., & Pintar, F. (2001). Biomechanics of the Cervical Spine Part 2. Cervical Spine Soft Tissue Responses and Biomechanical Modeling. *Clinical Biomechanics* , 16, 1-27.
- Yoganandan, N., Kumaresan, S., & Pintar, F. (2000). Geometric and Mechanical Properties of Human Cervical Spine Ligaments. *Journal of Biomechanical Engineering* , 122, 623-629.
- Yoganandan, N., Maiman, D., Pintar, F., Ray, G., Myklebust, J., Sances, A. J. et al. (1988). Microtrauma in the Lumbar Spine: A Cause of Low Back Pain. *Neurosurgery* , 23 (2), 162-168.
- Yoganandan, N., Pintar, F., & Butler, J. (1989). Dynamic Response of Human Cervical Spine Ligaments. *Spine* , 14 (10), 1102-1110.
- Yoganandan, N., Pintar, F., & Kumaresan, S. (1998). Biomechanical Assessment of Human Cervical Spine Ligaments. *42nd Stapp Car Crash Conference Proceedings*, (pp. 337-346). Tempe, AZ.
- Yong-Hing, K., Reilly, J., & Kirkaldy, W. (1976). The Ligamentum Flavum. *Spine* , 1, 227-234.